Developing a Geological Disposal Facility in the UK

Lucy Bailey

Head of Research Support Office, RWM

Radioactive Waste Management

Working together to protect the future

Introduction

Lucy Bailey

Head of RWM Research Support Office

- Fellow of the UK Institute of Physics
- 30 years' experience in geological disposal
- Led development of UK generic Disposal System Safety Case
- Expert peer reviewer of international safety cases
- Leading roles in NEA, IAEA and EC projects
- IAEA missions to Chernobyl, Dec 2018; China, March 2021
- Over 40 publications covering the safety case and other technical and societal aspects of geological disposal
- Chair of the OECD-NEA Integration Group for the Safety Case (IGSC) since October 2015
- Working with UK universities to deliver the academic research to underpin safe geological disposal

RWM’s mission:

To build a Geological Disposal Facility as a permanent solution for the UK’s higher activity waste, where there is a suitable site and a willing community.

Communities are at the heart of the siting process and no community will get a GDF without a demonstration of its willingness to host one.

Safety is also at the heart of all we do. We will not build a GDF unless we are confident of its safety. This requires a lot of scientific & engineering expertise

What will go into a GDF?

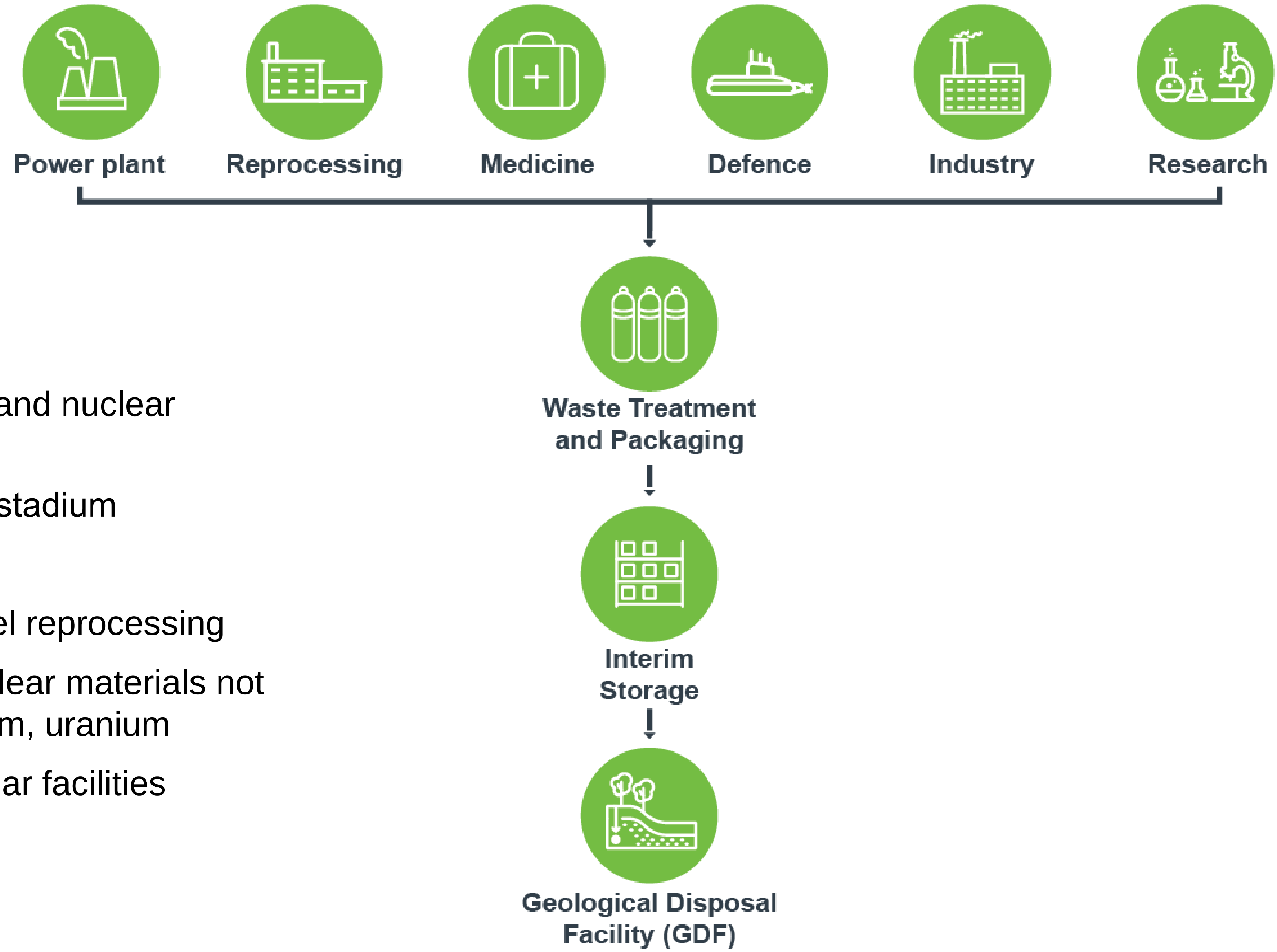

- Around 750,000 m^3 of radioactive waste and nuclear materials will be sent to a GDF
- That's roughly ¾ of the size of Wembley stadium
- Most of this volume is ILW and LLW
- Also includes vitrified HLW from spent fuel reprocessing
- GDF also designed to accommodate nuclear materials not yet defined as waste: spent fuel, plutonium, uranium
- Includes potential wastes from new nuclear facilities

The UK Radioactive Waste Inventory:
https://ukinventory.nda.gov.uk/

The GDF multi-barrier concept

A Geological Disposal Facility uses a combination of engineered and natural barriers that work together to isolate and contain radioactive waste.

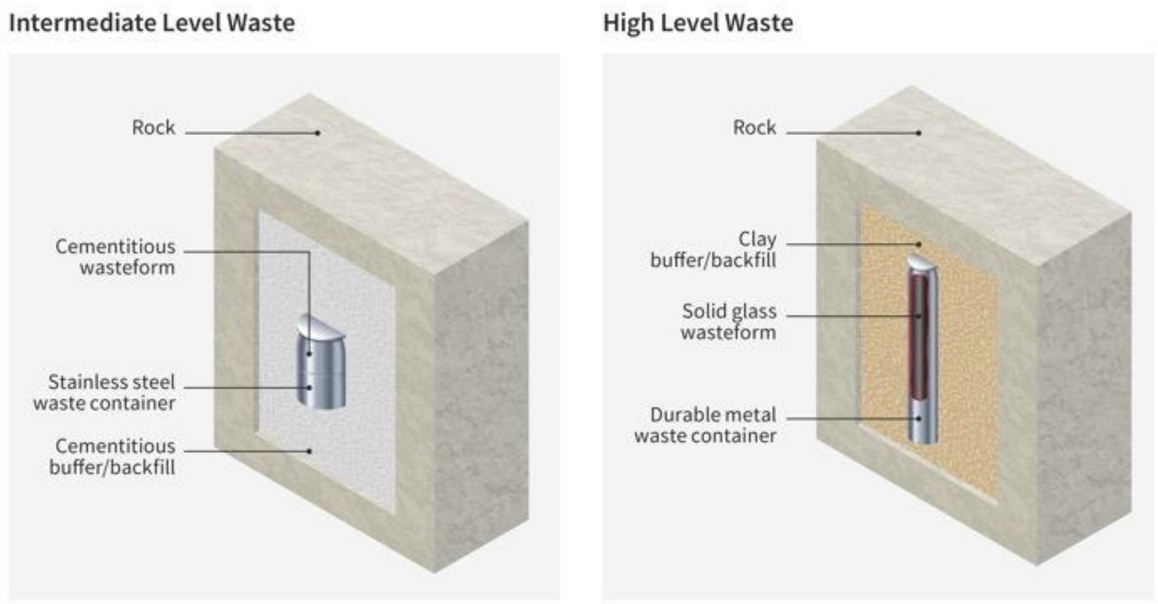

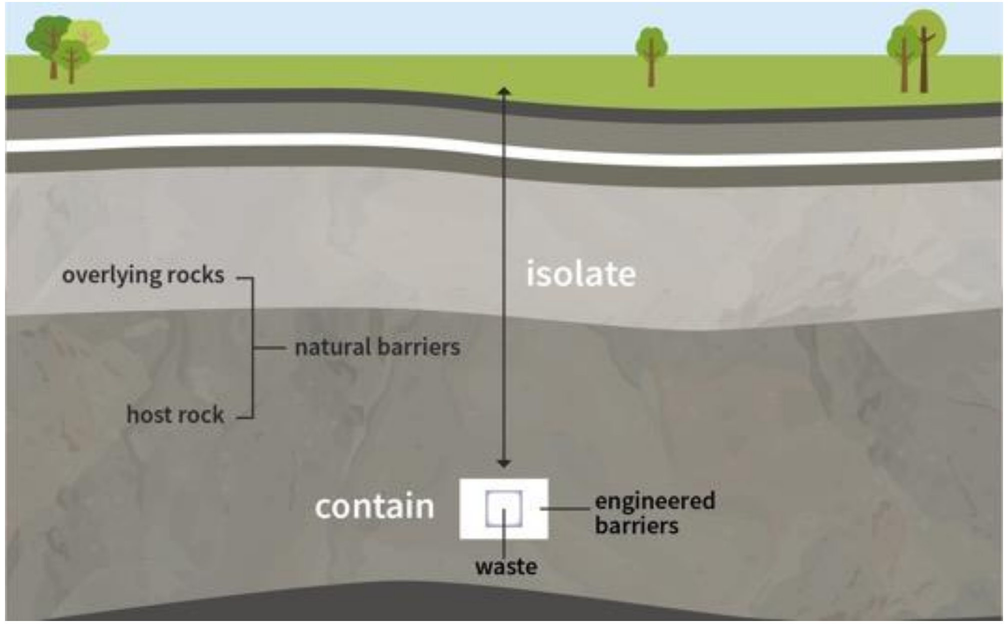

Multi-factor Safety Case

Multi-barrier + **Multiple lines of reasoning**

Safety functions

- Wasteform limits release rate
- Waste package provides containment
- Backfill limits release rate
- Geological barrier isolates and contains

Intrinsic safety

Safety arguments

- Research understanding
- Insight understanding
- Natural analogue studies
- Total system modelling

Safety assurance

Safety Case

Research at RWM

- RWM is investing in research, established Research Support Office
- Long-term **strategic** relationships with UK universities
- Better aligned academic research addressing **RWM needs**, with stronger delivery-focus
- Increased **engagement** with world-class cutting edge science
- A better co-ordinated **community** of RWM funded researchers
- A sustained and enhanced **multi-disciplinary capability** through collaborative long-term relationships
- Building the RWM team….

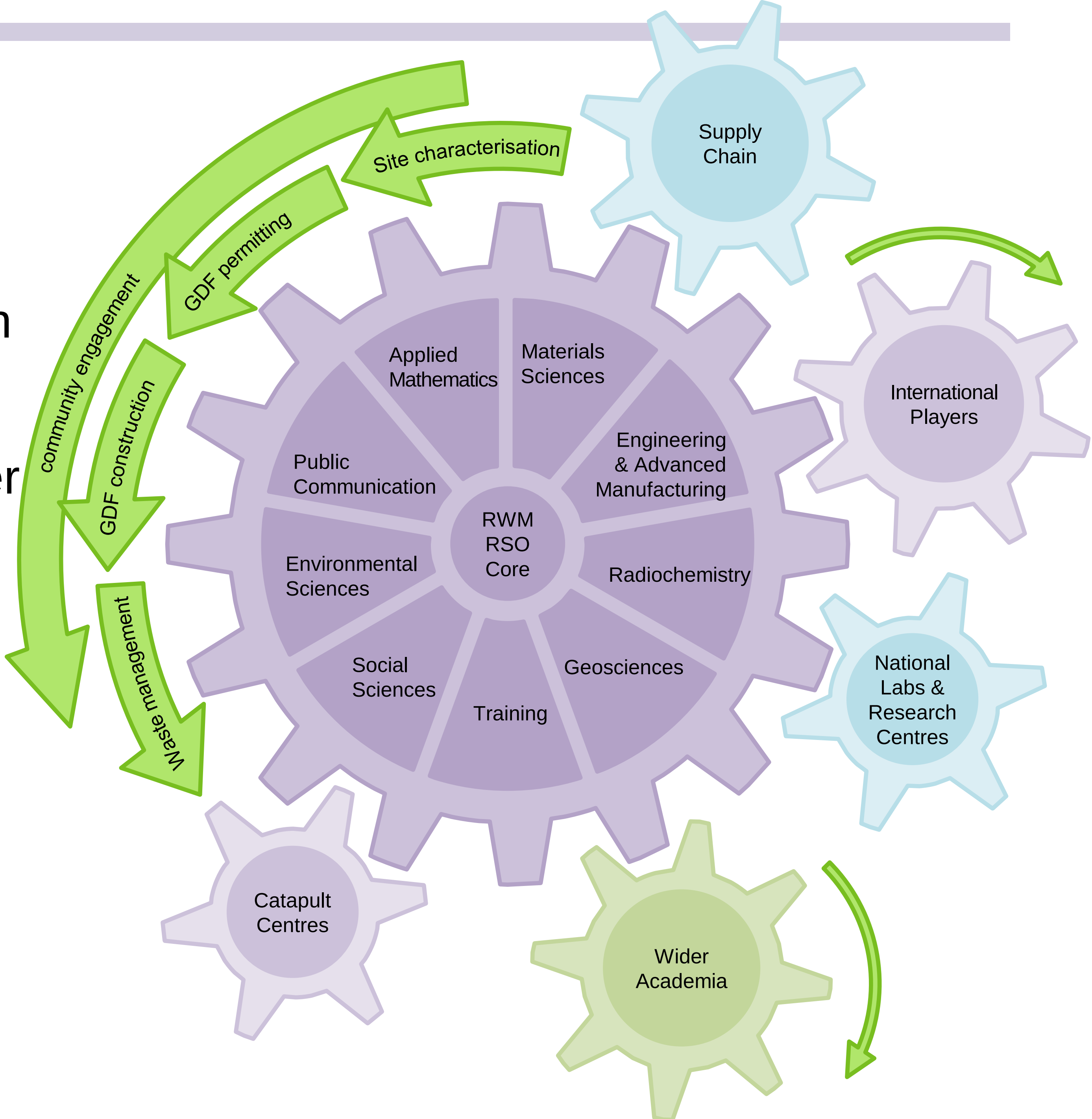

Policy for GDF delivery

Local community consent is at the heart of the GDF delivery process and is written into Government policy

- ✓ UK Government policy published 19 December 2018
- ✓ Welsh Government policy published 16 January 2019

To deliver a GDF we need:

1. appropriately packaged waste
2. a suitable site
3. a willing community

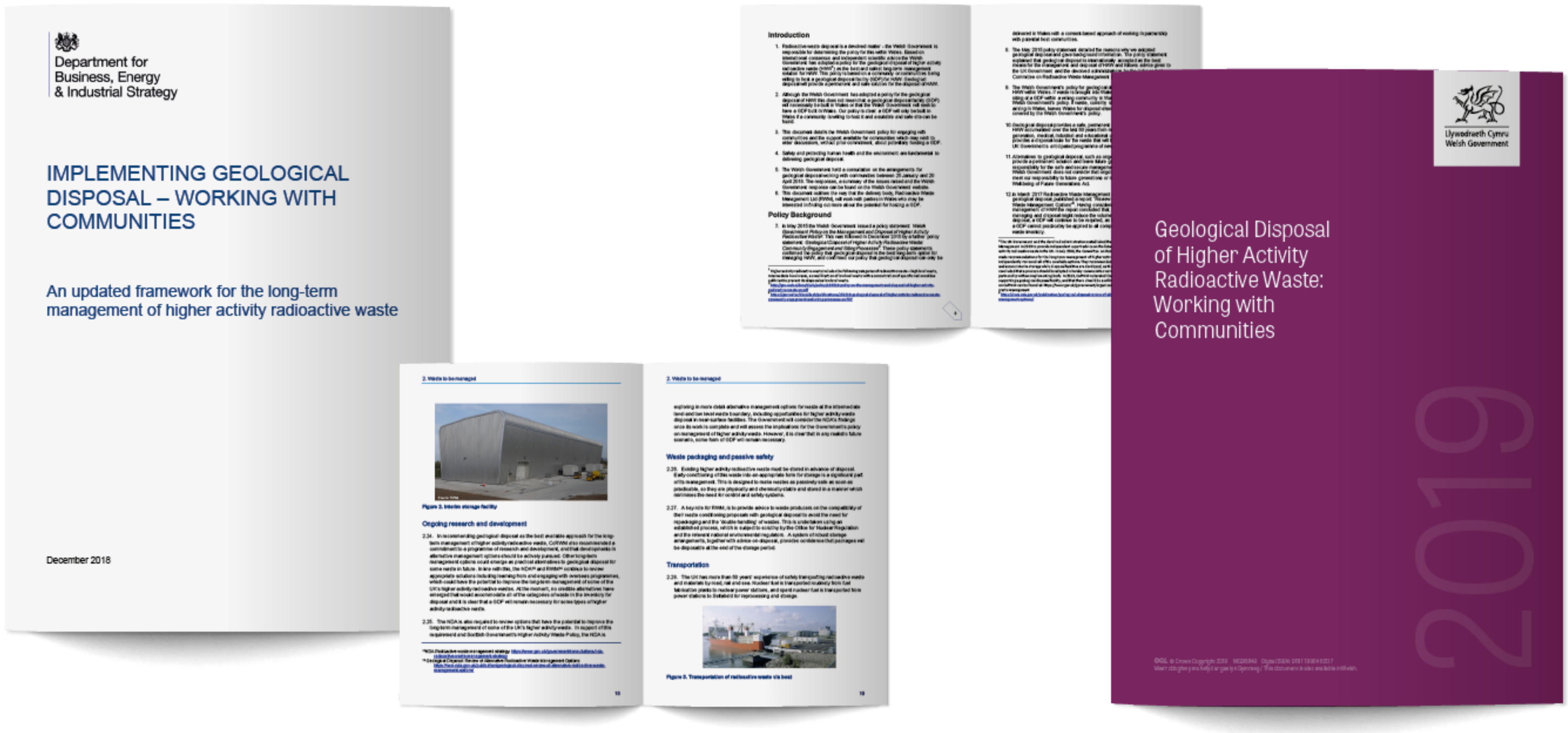

Significant economic and community benefits from hosting a GDF

Jobs and skills

Average of 550 FTEs in construction, operations, safety, logistics for over 100 years.

Peaking at +1,000 for initial 10 year construction phase.

Plus all the related jobs in the supply chain.

Infrastructure investment

Investment will flow into a community that hosts a GDF.

Community support

Local projects will benefit from Community Investment Funding. Public facilities and infrastructure will be improved over the long term.

Community investment

Initially up to

£1 million

a year per community involved in the process

This will rise up to

£2.5 million

a year per community where detailed site characterisation has taken place

Significant Additional Investment
for a host community

Siting process

Initial discussions

Any person or group of people who wish to propose an area for consideration can approach RWM for initial discussions and to find out more about geological disposal.

After agreement that the proposal merits further consideration, discussions are opened up more widely in the community.

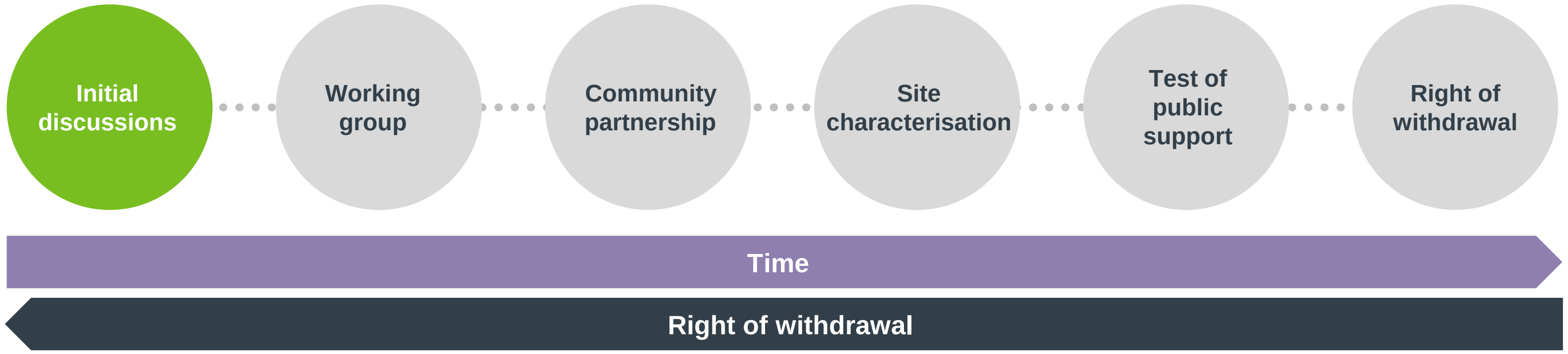

Working Group – scoping the question

The Working Group will consist of at least the Interested Party, RWM, an independent chair and facilitator.

Local authorities can be members but don't need to be.

Starts to **engage the public locally**.

Proposes a **"Search Area".**

Identifies initial membership for "Community Partnership".

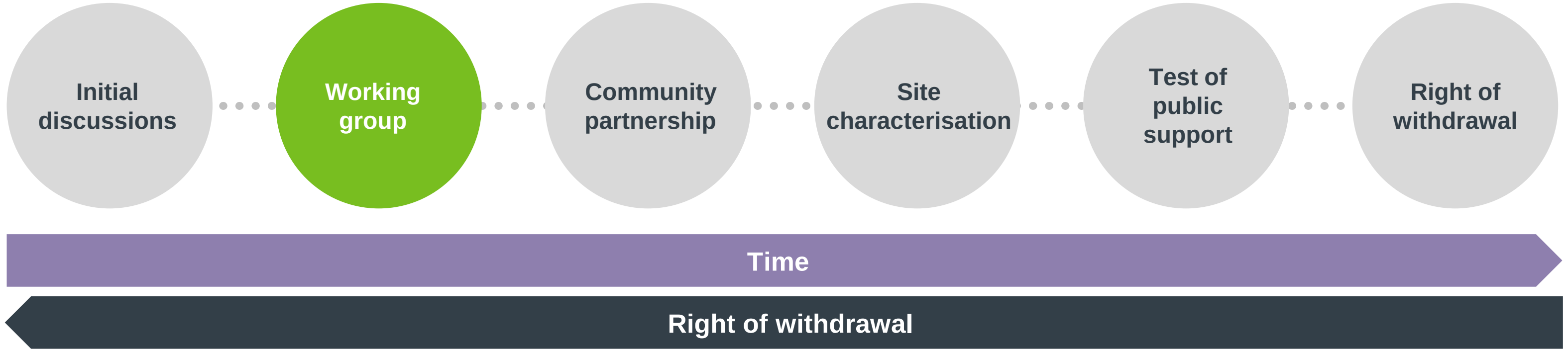

Community Partnership

After the initial “task and finish” of the Working Group, a Community Partnership is a **more enduring body**, formed of community members and organisations, RWM and at least one relevant principal local authority.

An important job for a Community Partnership is **to share information with the community** and find answers to any questions that they may have as well as **developing the community vision** for the future

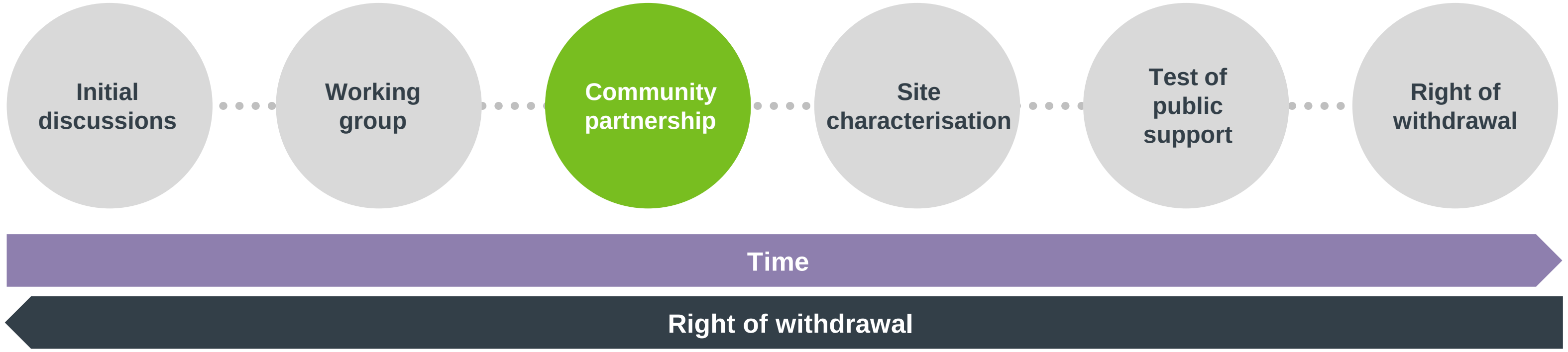

Site characterisation

Extensive site characterisation work will be required to demonstrate whether or not a specific site is suitable for a GDF, including geological investigations to develop greater understanding of the deep geological environment.

The **“Suitable Site”** part of the equation.

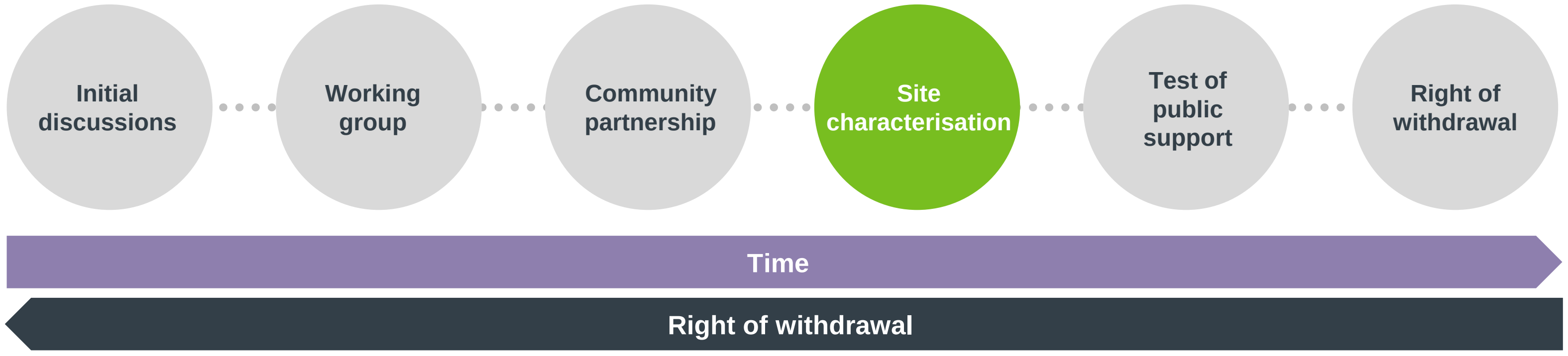

Test of public support & right of withdrawal

Before a final site is selected, the potential host community must demonstrate it is willing to host a GDF through a Test of Public Support.

The **“Willing Community”** part of the equation.

At any point, up to a Test of Public Support, a community may withdraw from the siting process.

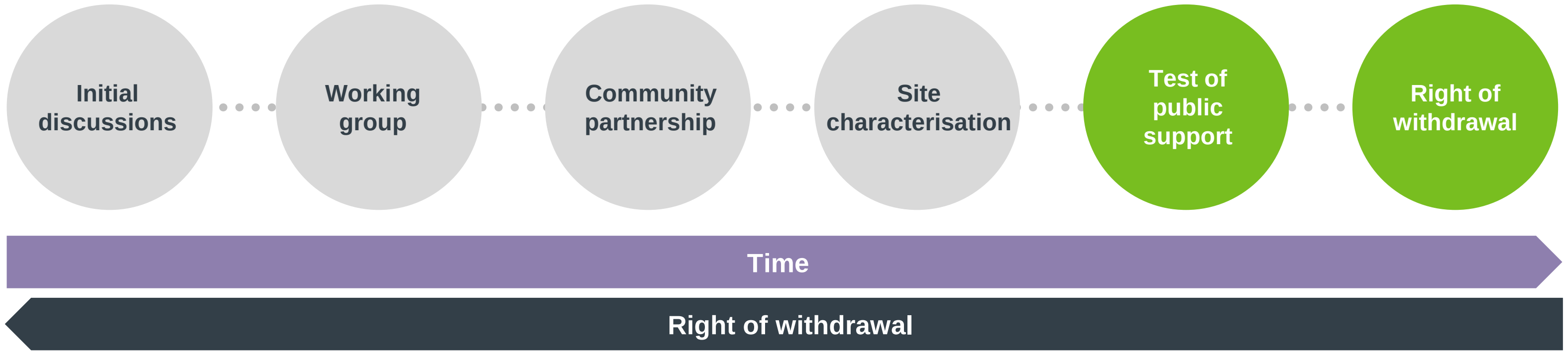

Progress with siting

A great start with launch of WGs

Very positive local headlines from
- ✓ Copeland (Nov 2020)
- ✓ Allerdale (Jan 2021)
- ✓ Theddlethorpe (Oct 2021)

The new narrative is about jobs and economic opportunities

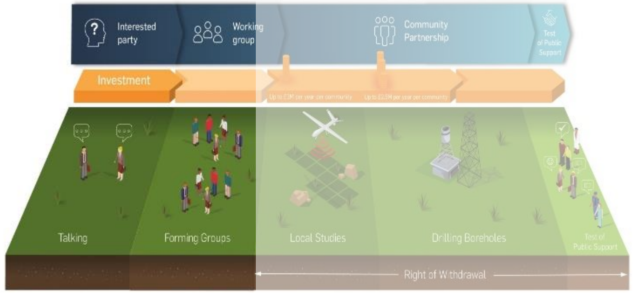

Delight as nuclear facility talks begin

By Emma Walker
emma.walker@newsquest.co.uk

REPRESENTATIVES across the county have shared their delight as the first step has officially been taken on a project that could create thousands of jobs.

Yesterday, a working group was formed to begin local engagement on whether Copeland would be a suitable location for a Geological Disposal Facility (GDF) for UK higher activity radioactive waste.

The group, which currently includes Copeland Borough Coun-

BBC Radio Cumbria
@BBC_Cumbria

Allerdale has become the second place in the country, after Copeland, to join the search to find an underground site to store high level nuclear waste. The government wants to build a Geological Disposal Facility

Assurances given over Theddlethorpe nuclear waste plans

12 October

RWM

The government agency behind the proposals has identified a potential site at a former gas terminal in Theddlethorpe, near Mablethorpe, and has released this image to show what it might look like

Copeland Working Group

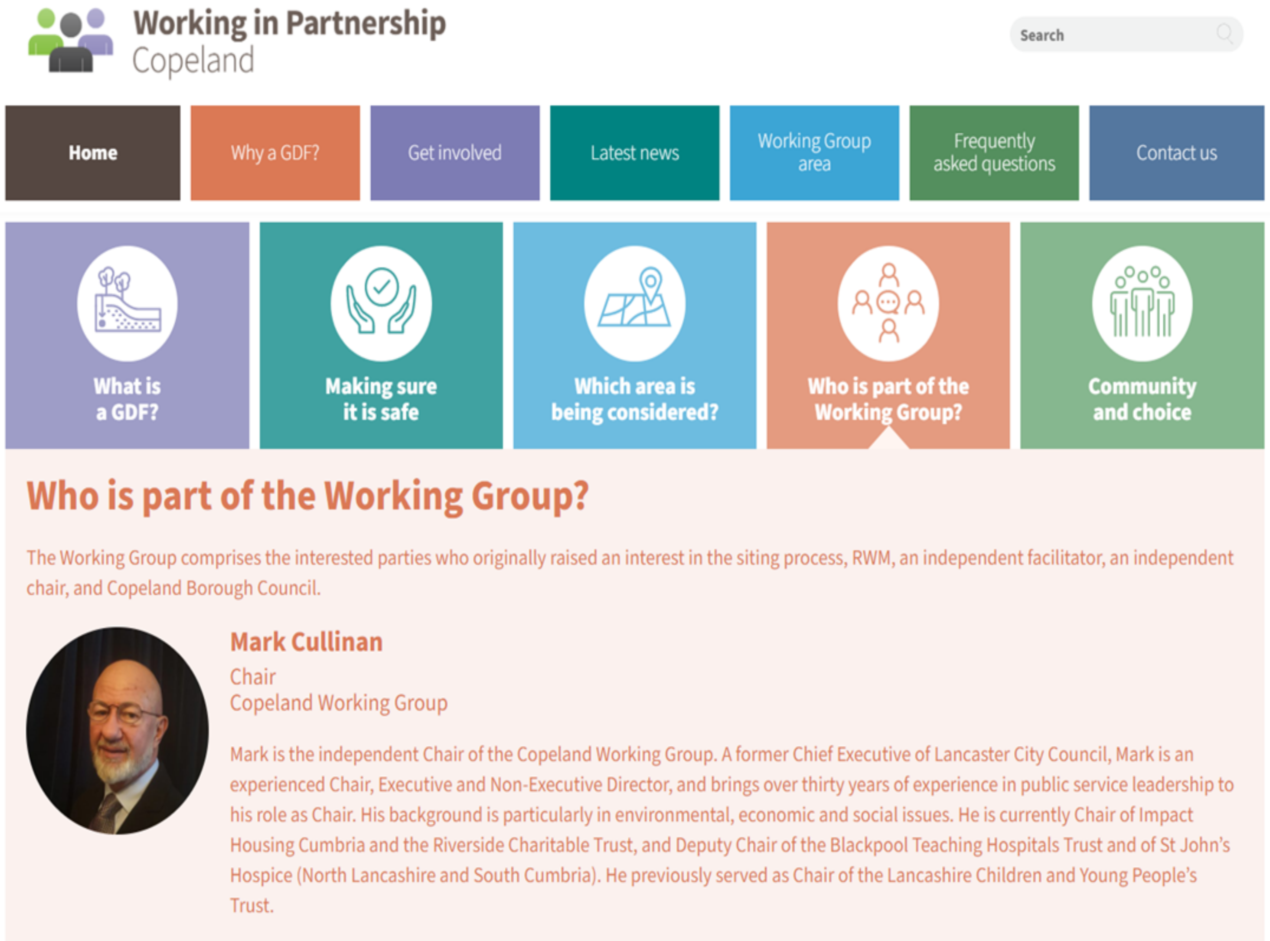

Search Areas Map

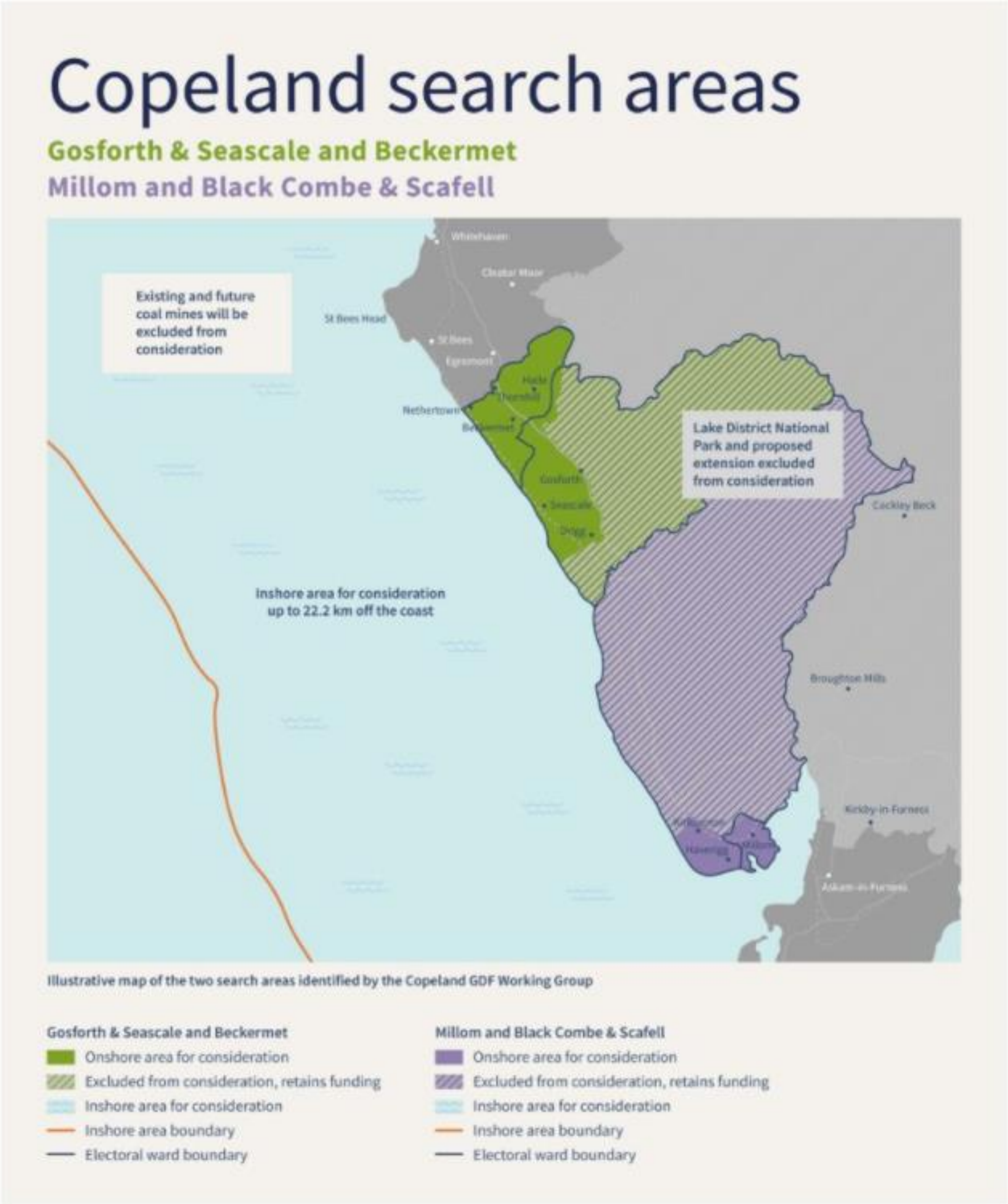

Allerdale Working Group

Working in Partnership Allerdale

Home | Resources | Get involved | Latest news | Working Group area | Frequently asked questions | Contact us

Who is on Allerdale GDF Working Group

Jocelyn Manners Armstrong
Chair
Allerdale GDF Working Group

Jocelyn is the independent Chair of the Allerdale GDF Working Group. A former member of the Yorkshire Dales National Park Authority for the past eight years, where she served as deputy Chair, Jocelyn is committed to the protection of the natural environment. Prior to this Jocelyn practiced as a corporate and commercial lawyer.

Jocelyn has also run a national legal charity, supporting refugee organisations, and served on boards of several charities, including a range of roles for Citizens Advice.

She has also previously served as a lay member of the local health group of Morecambe Bay Primary Care Trust and as an independent member of Cumbria Police Authority. Jocelyn is also Chief Executive of a business and IT consultancy supporting customers in the IT and media sectors.

Dot Kirk-Adams
Independent Facilitator

Dot is the Independent Facilitator for the Working Group. The role of the Independent Facilitator is to help ensure that discussions are constructive and that issues raised by the community are considered by the Working Group. Dot works for Community Organisers Limited, a small national charity and the membership body and training organisation for grass-roots community organising in England. Their work is all about giving people the tools to listen to their community about the things that matter to them. These conversations inspire people to join together to take action for their community and to become collectively more powerful and able to shape their future.

Dot has worked as a community organiser, trainer and facilitator for 10 years supporting communities and a range of organisations around the country to make change. She believes strongly in active listening, dialogue and supporting communities to come together to decide what should happen in their areas.

Councillor Marion Fitzgerald
Allerdale Borough Council

In Marion's role as an Executive Member of Allerdale Borough Council, she has responsibility for nuclear matters in her portfolio. Marion is a former Leader of the Council.

She said: "The Council recognises its responsibility to make sure that all of our residents have access to as much information as they need about the project and they feel that they are being listened to at the outset. Whether the GDF is eventually built here in West Cumbria or elsewhere in the country, that decision will affect Allerdale because the waste is already stored above ground in West Cumbria. That is why we decided to be involved and part of the discussion."

Genr8 North Ltd

GENR8

Genr8 North Ltd is an 'interested party' who specialise in land development and regeneration, and as a Cumbrian based company, would like the GDF programme to be given proper consideration in West Cumbria as part of future infrastructure development.

Mary Bradley
Executive Member
Cumbria Association of Local Councils (CALC)

Cumbria Association of Local Councils (CALC) is a not for profit membership organisation, representing, training and advising the parish (including town) councils of Cumbria, who form the grass roots tier of local government in England. They offer members a resource of important, operational information and facilitate communication at all levels of the parish network - district, county, regional and national.

Mary Bradley said: "CALC want to ensure that information about this controversial but important project is made available through the grass roots parish and town councils who represent the many people and communities of Allerdale. The aim will be to ensure that everyone is made aware of the chance to visit face-to-face events, as well as access information and have conversations digitally. This means we can ensure that the project fits well with the aspirations and concerns of the host community."

Search Area Map

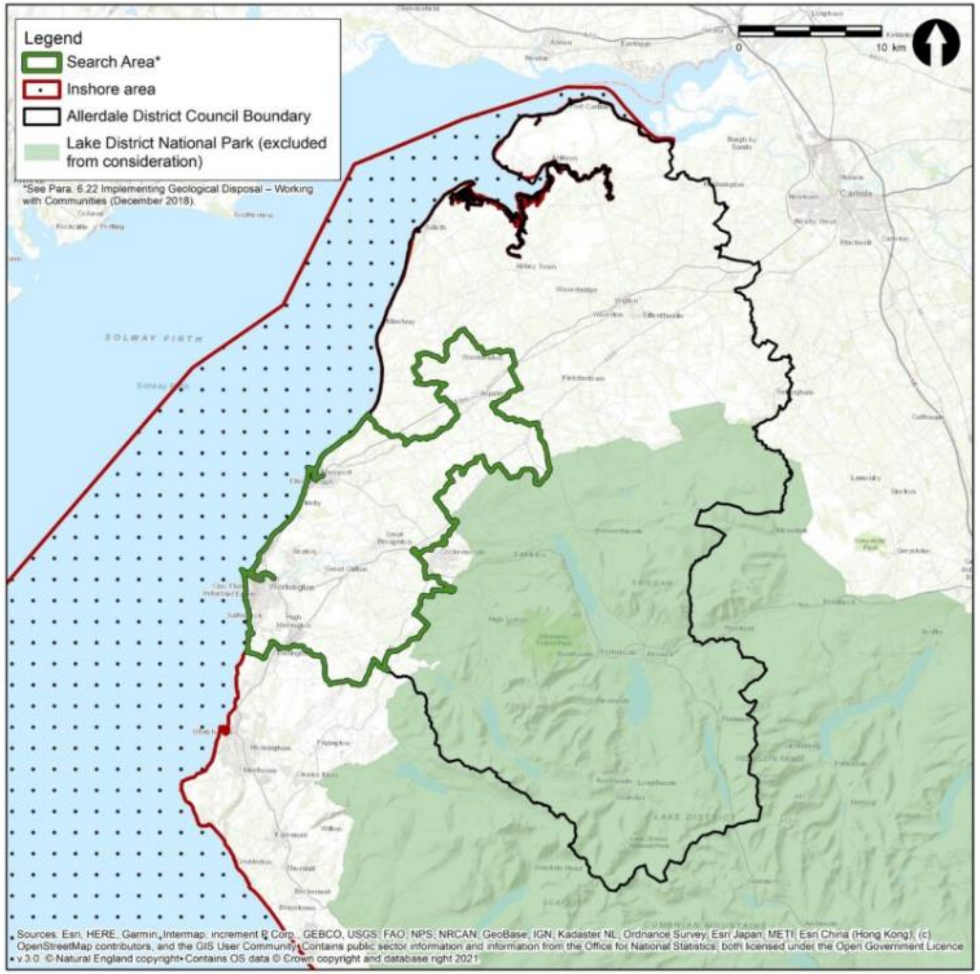

RWM Evaluation Report

Theddlethorpe Working Group

Working in Partnership Theddlethorpe

Search

Home | Resources | Get involved | Latest news | Working Group area | Frequently asked questions | Contact us

Welcome

“Establishing the Theddlethorpe GDF Working Group marks the beginning of the process of finding out if this national infrastructure project – to safely and permanently deal with some of the UK’s radioactive waste by placing it deep underground in a Geological Disposal Facility (GDF) – would be right for the area.

“This is the starting point for engaging with people in Theddlethorpe and the surrounding areas. It’s about providing information and enabling people to find out more, about hearing local issues and concerns, and making sure people’s questions get answered.

“No decisions will be made for a long time and any decision about whether to support a development will need explicit community support.

“In the months ahead, I will ensure that local people have access to information and are able to raise their views and concerns. We’re here to understand what people think about the GDF project, and look forward to meeting local people and listening to their views.”

Jon Collins, Independent Chair of Theddlethorpe GDF Working Group

Sign up

What is a GDF? | Making sure it is safe | Which area is being considered? | Who is part of the Working Group? | Community and choice

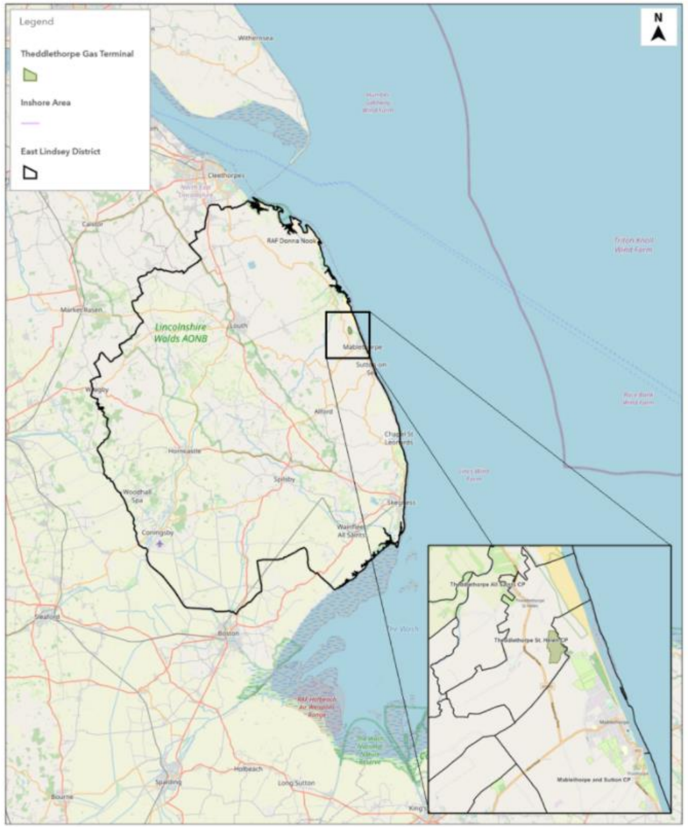

Who is on Theddlethorpe GDF Working Group

Jon Collins
Chair
Theddlethorpe GDF Working Group

Jon is the independent Chair of the Theddlethorpe GDF Working Group. He is currently a company director and freelance consultant offering advice an insight on local government and property issues. Jon previously served as a City Councillor in Nottingham for 32 years, 16 of which were as Council Leader. At various times during that period Jon chaired East Midlands Councils, Nottinghamshire’s Police Authority, was Vice-Chair of the Core Cities Group and was a member of a range of bodies including the Local Enterprise Partnership, Midland Engine and The LGA City Regions Board. Jon has also served as a Peer Councillor for both the Audit Commission and Local Government Association. Jon has also worked for an urban regeneration company, as a Local Authority communications officer, and for 20 years chaired as a volunteer, The Renewal Trust Charity.

Looking Forwards

- This is a national process
- Discussions underway in other parts of England
- We want to ensure a diversity of opportunities for the siting process

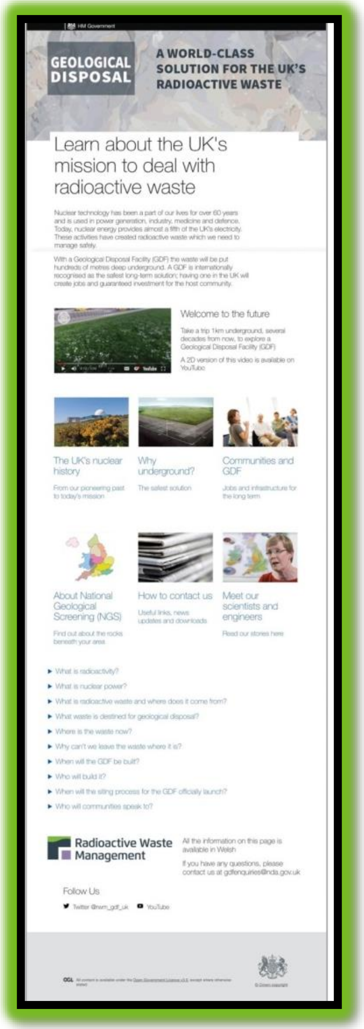

Site evaluation

Site Evaluation

The purpose of Site Evaluation:

- **Ensure a consistent and transparent approach to the evaluation of potential areas and sites.**
- **Support an appropriate level of evaluation for each potential area and site against the existing and applicable requirements.**
- **Enable RWM's future applications for permissions, including land use planning consents, environmental permits and a nuclear site licence.**
- **We recognise there are many interactions and relationships between our Siting Factors and Evaluation Considerations.**

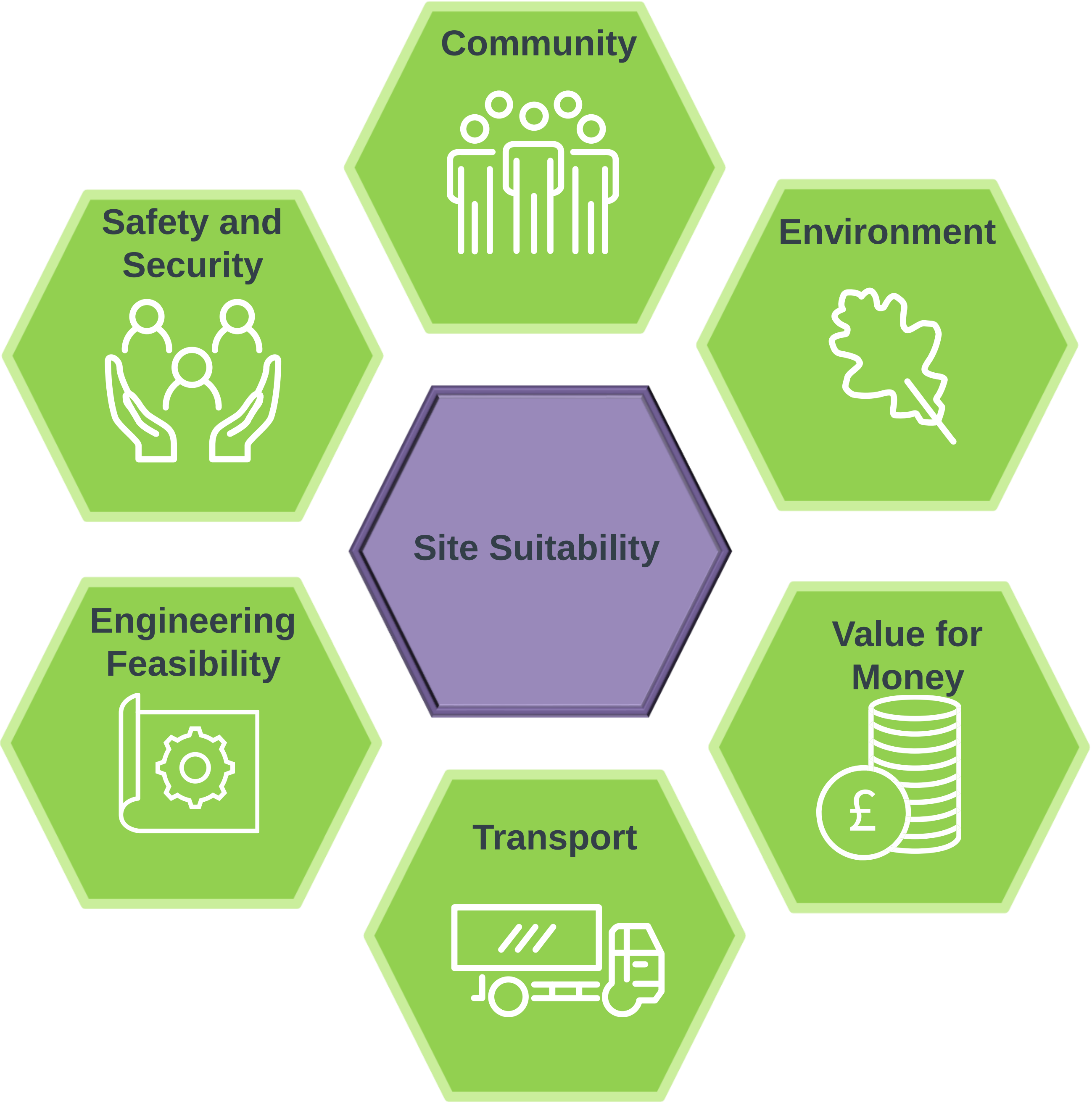

Conclusions

A GDF requires suitably packaged wastes, a suitable site and a willing community

- The first two are underpinned by safety arguments based on our research understanding
- Communities are also at the heart of the siting process - RWM is working hand in hand with local authorities and place leaders to build positive visions for the long-term future

Early but tangible progress with siting

- First Working Groups established in Copeland & Allerdale. Started the process of exploring the potential benefits of hosting a GDF in their communities, now joined by Theddlethorpe
- National process - positive discussions ongoing in range of other locations - we expect further Working Groups to form

Anticipate creation of Community Partnerships

- RWM will be able to gain more information to assess the suitability, feasibility and acceptability of alternative sites
- Site evaluation criteria have been published - RWM will work with Community Partnerships to ensure evaluations are discussed and challenges/benefits of hosting a GDF are understood.

Get in touch

To learn more about the UK’s mission to deal with radioactive waste:

Email: **gdfenquiries@nda.gov.uk**

Follow us on Twitter

@rwm_gdf_uk

@rwm_community

Visit the GDF campaign website

geologicaldisposal.campaign.gov.uk

To learn more about research opportunities:

Email: **rwm_rso@comms.manchester.ac.uk**

Visit the RSO website

research-support-office-gdf.ac.uk

Radioactive Waste Management

Working together to protect the future

Lucy.Bailey@nda.gov.uk

Transformative Science and Engineering for Nuclear Decommissioning

Radiation tolerance of high molybdenum content glass-ceramic nuclear waste

Tamás Zagyva – The University of Manchester, Dalton Cumbrian Facility

Theme 1 Integrated Waste Management

11th November 2021
Harrogate

The University of Manchester
Dalton Nuclear Institute

For a Low Carbon Future

Introduction (vitrification of POCO waste)

PhD research:

Radiation effects on nuclear waste forms: How does the crystallinity of a glass-ceramic affect radiation tolerance?

Vitrification Test Rig (VTR) samples:

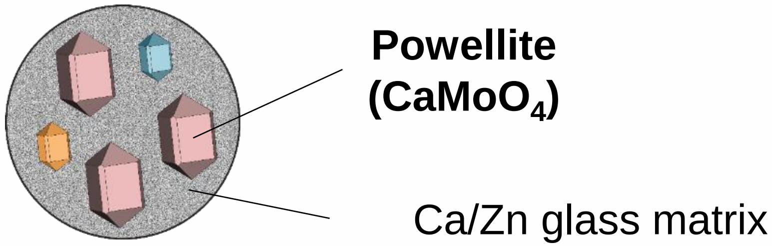

Ion irradiation experiments:

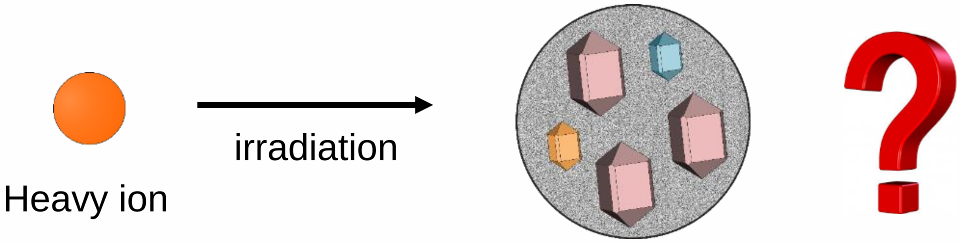

amorphisation

swelling

cracking

Crystal formation in VTR samples

– powellite – zircon – ceria-zirconia
– zincochromite – ruthenium dioxide – barium molybdate

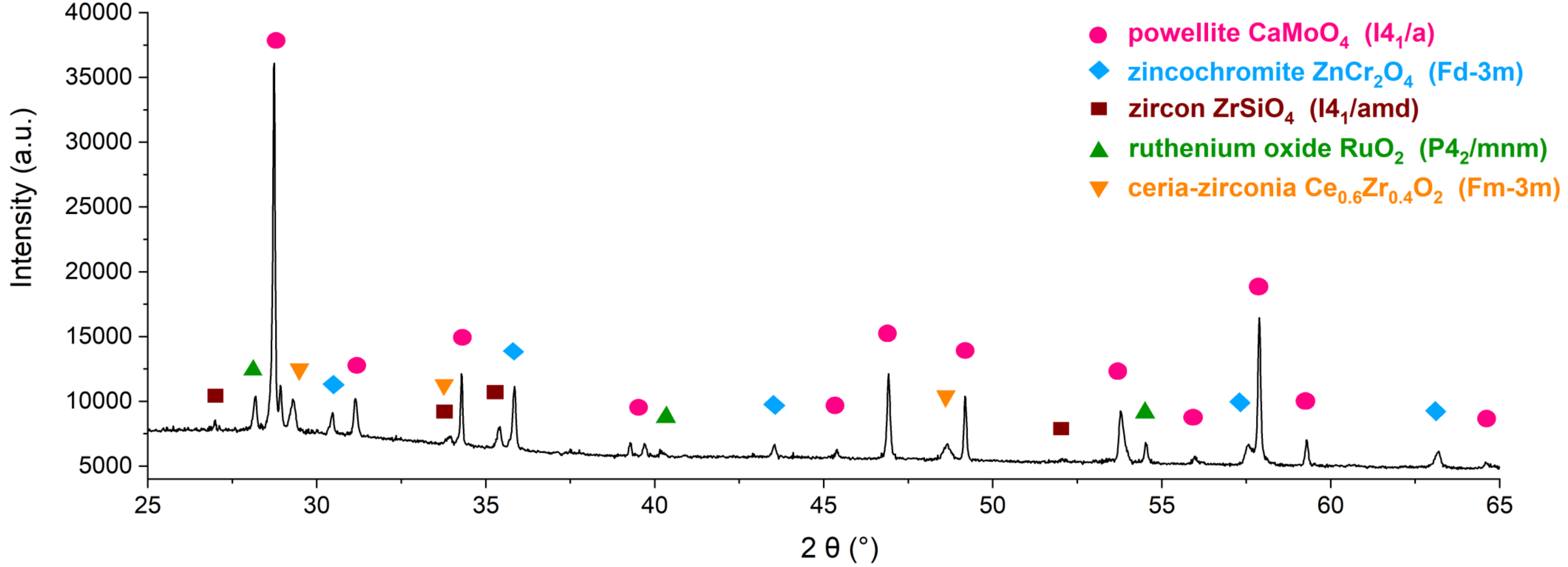

Crystal formation in VTR samples

- powellite
- zircon
- ceria-zirconia
- zincochromite
- ruthenium dioxide
- barium molybdate

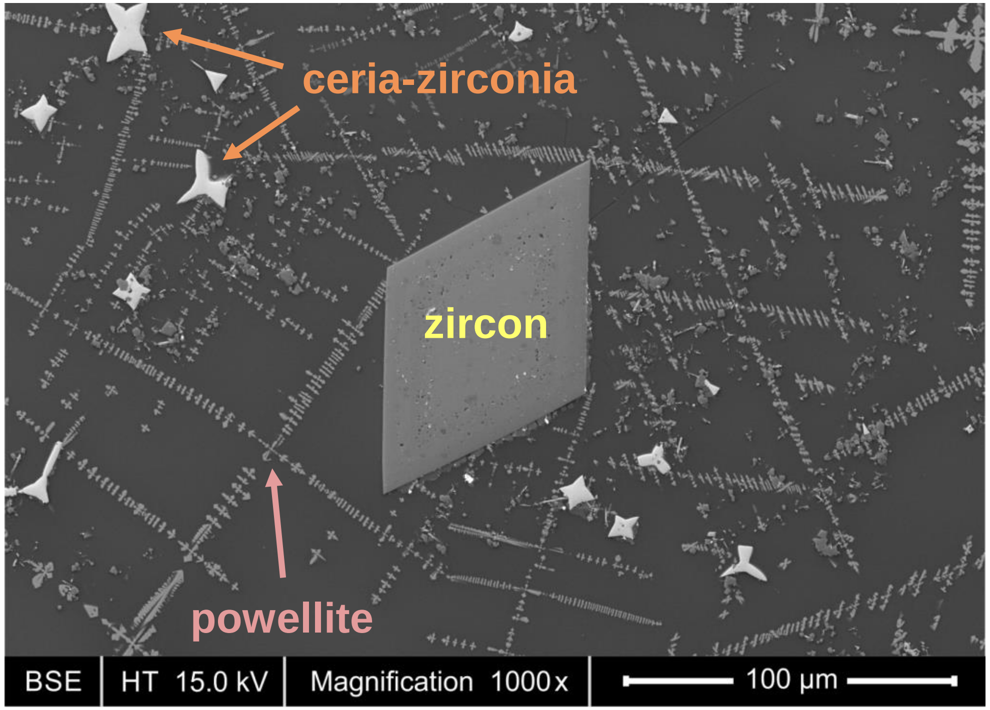

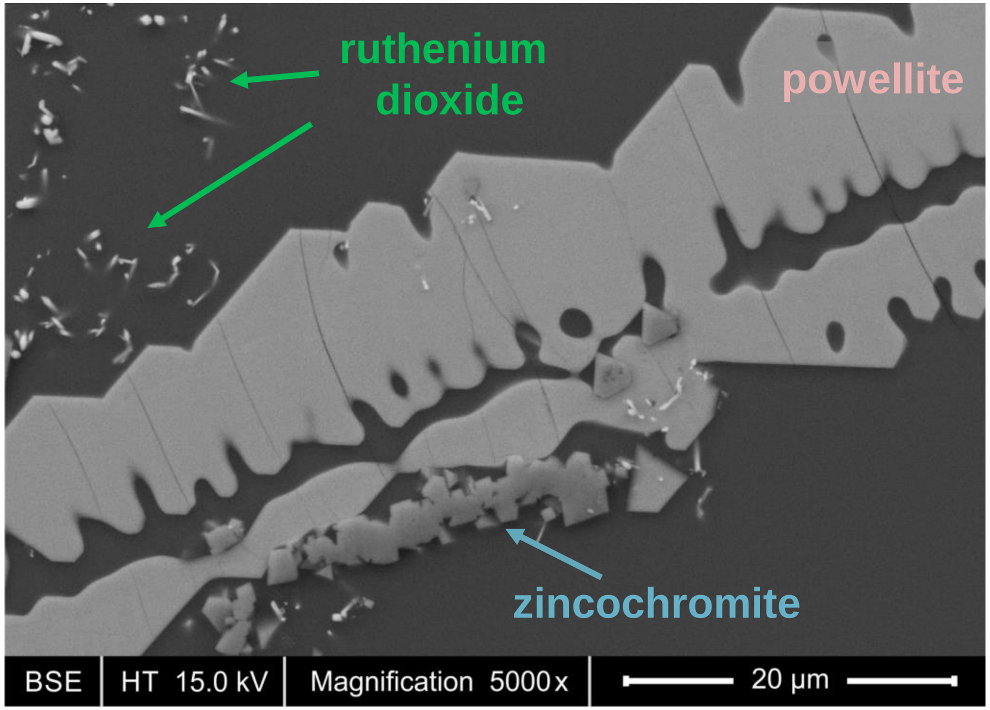

Transformative Science and Engineering for Nuclear Decommissioning

Crystal formation in VTR samples

– powellite
– zincochromite
– zircon
– ruthenium dioxide
– ceria-zirconia
– barium molybdate

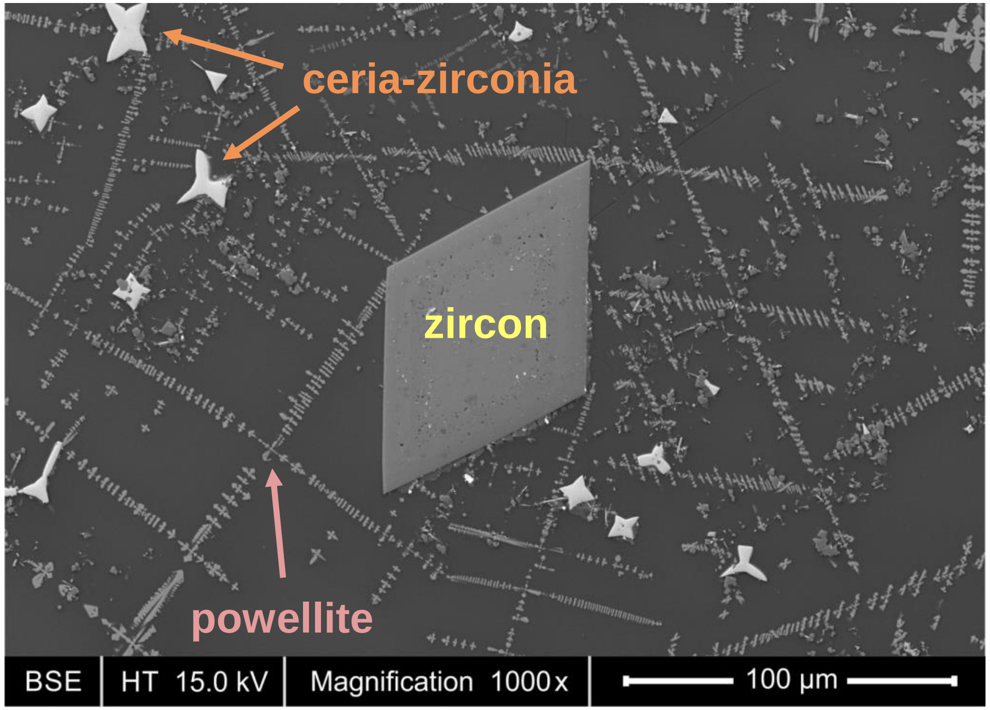

high crystallinity

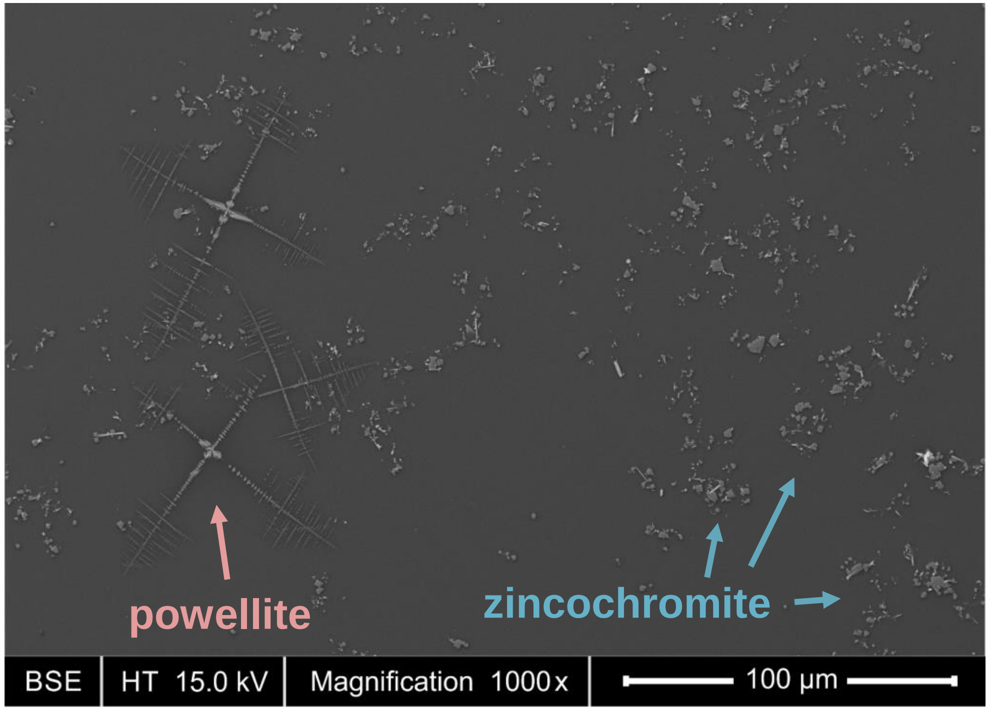

low crystallinity

Crystal formation in VTR samples

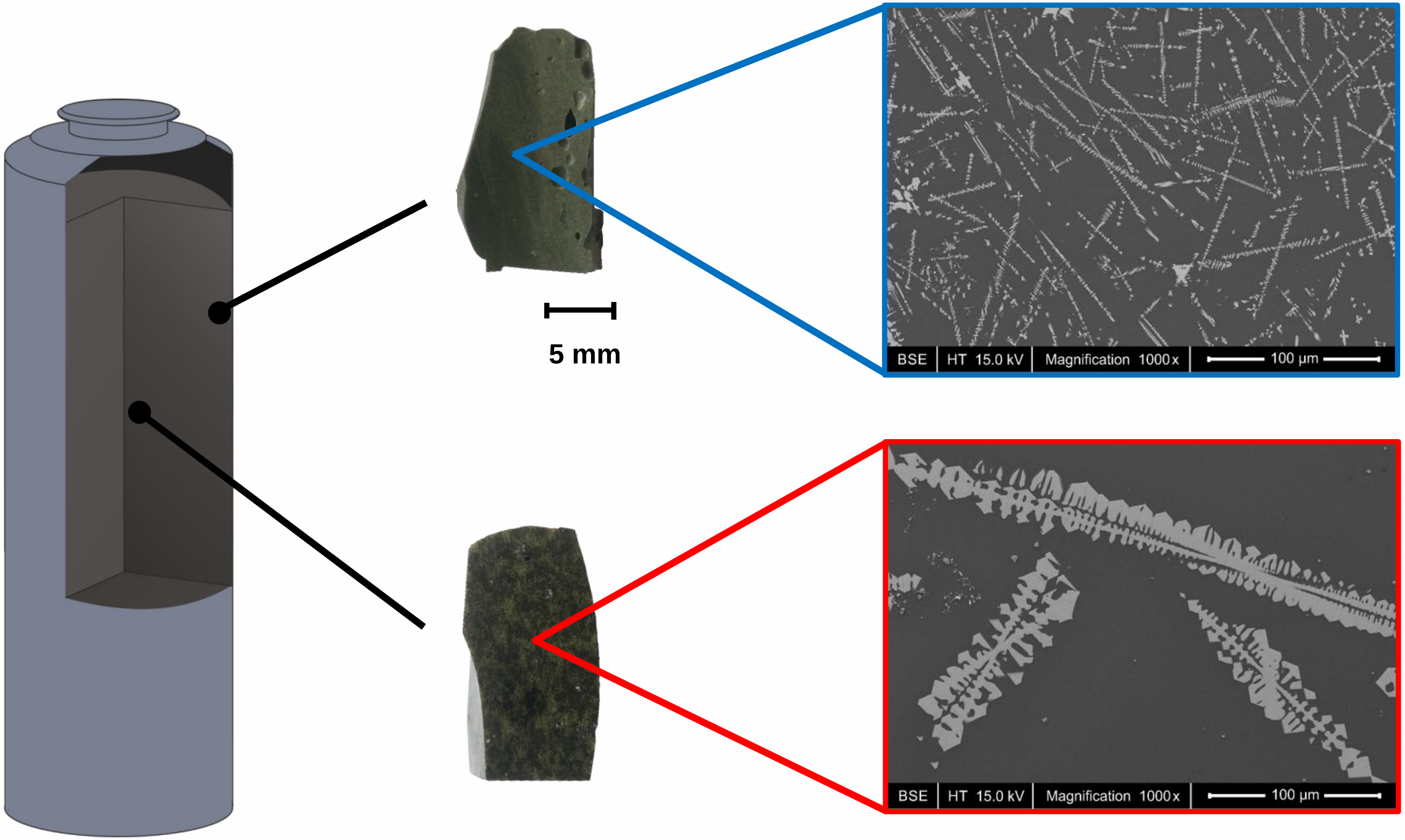

Fast cooling rate (small crystals)

Slow cooling rate (large crystals)

EPMA on powellite

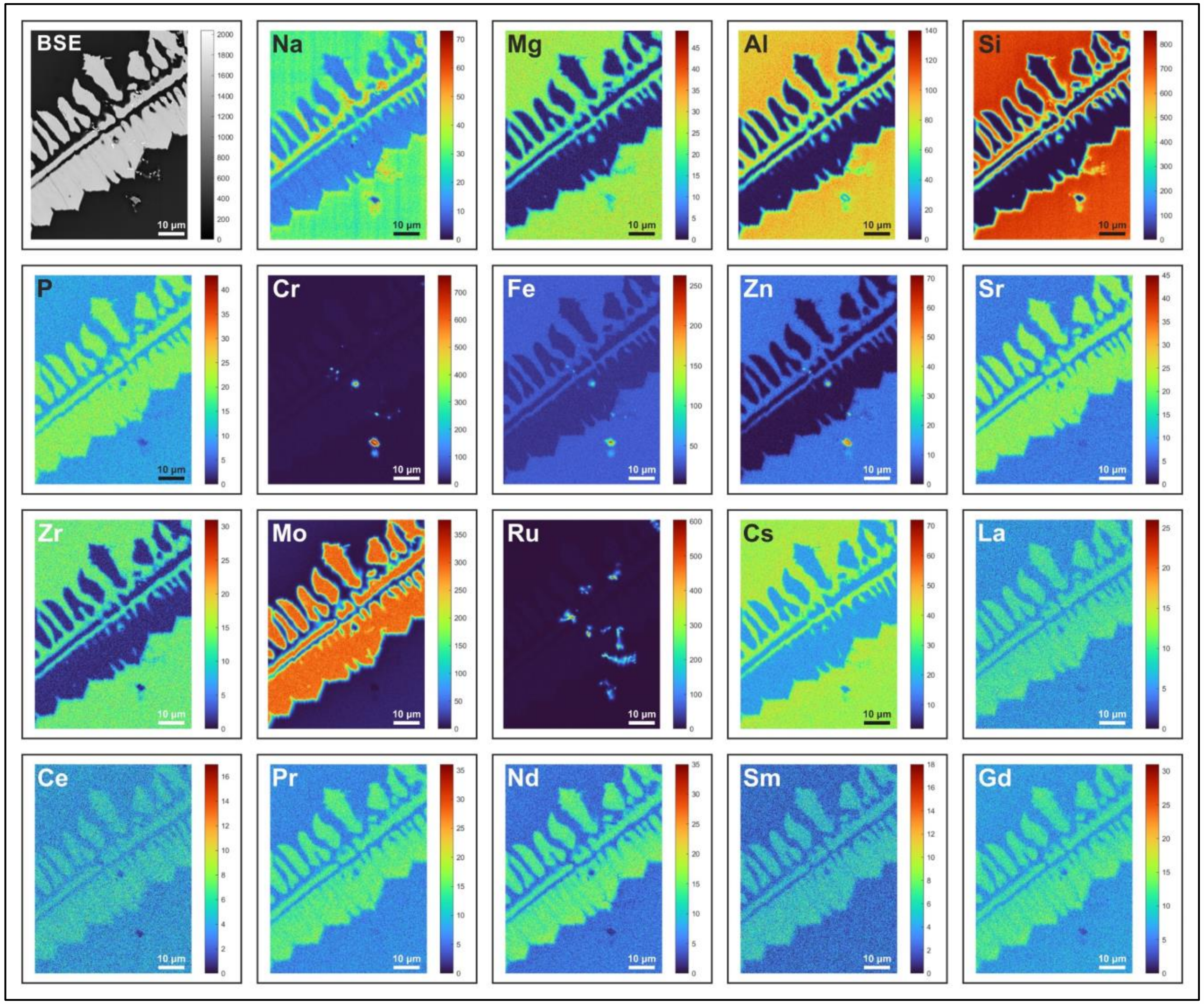

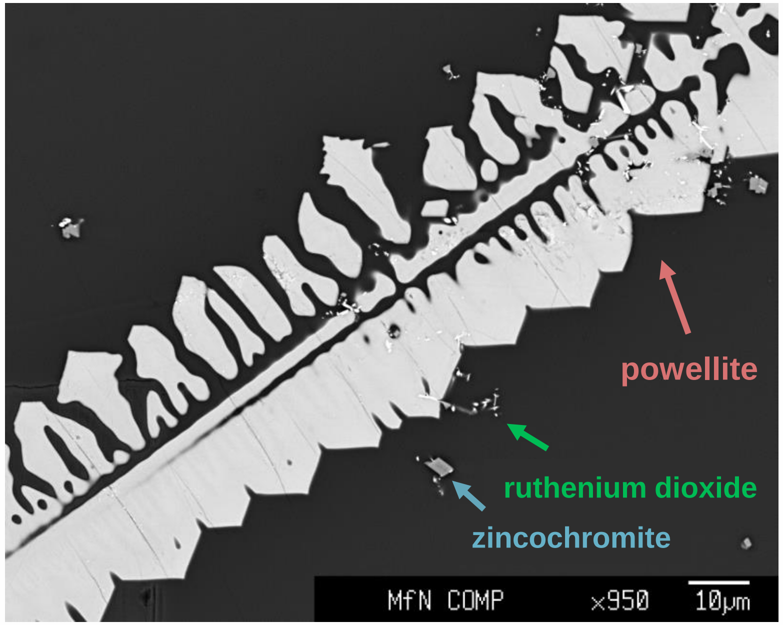

REE mainly accumulated in:
powellite, **zircon**, and **ceria-zirconia**.

Felix Kaufmann
(Museum of Natural History, Berlin)

Heavy ion irradiation experiments

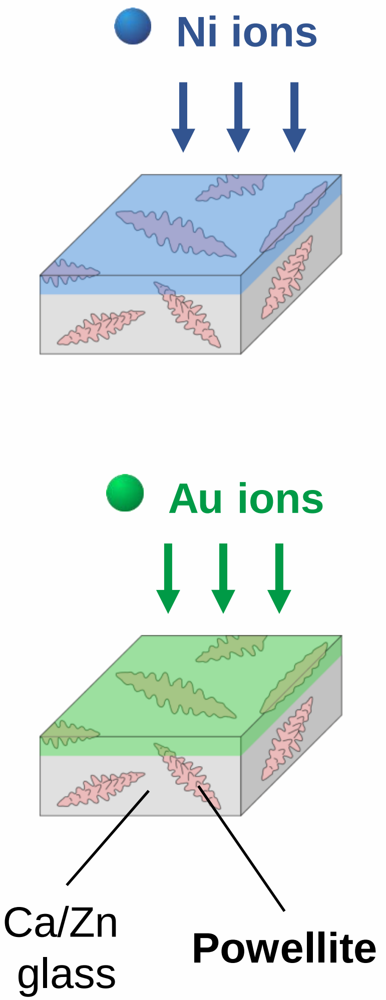

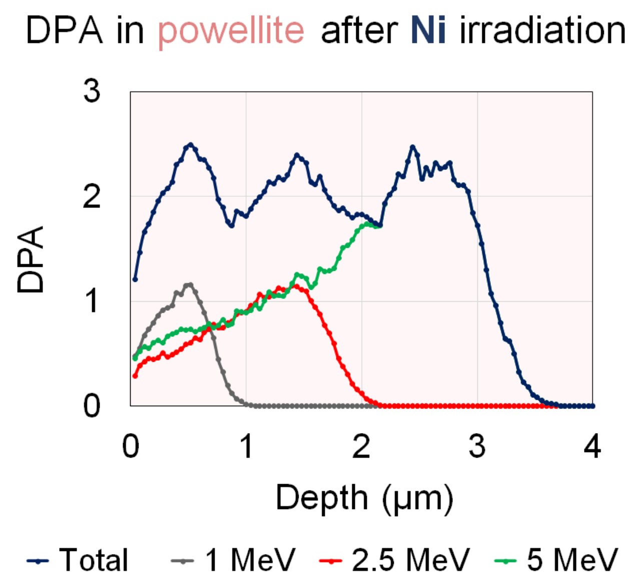

	1 MeV	2.5 MeV	5 MeV
Fluence:	6.4×10^{14}	8.2×10^{14}	1.9×10^{15}
Flux:	2.83×10^{11}	2.98×10^{11}	8.95×10^{11}

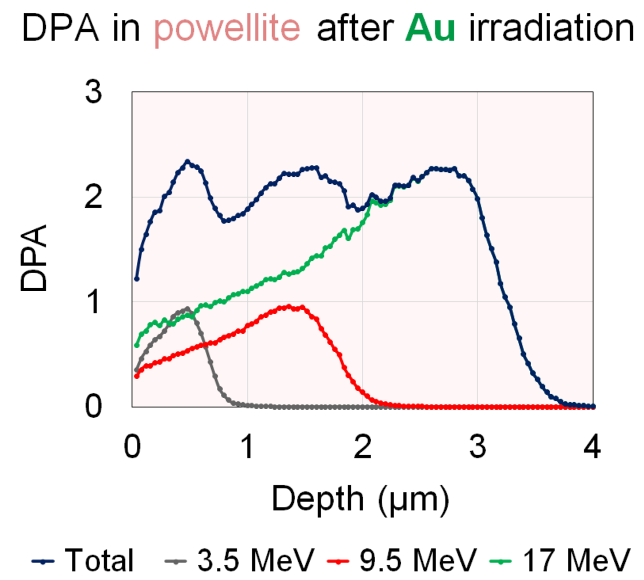

	3.5 MeV	9.5 MeV	17 MeV
Fluence:	1.5×10^{14}	2.0×10^{14}	5.64×10^{14}
Flux:	8.65×10^{10}	7.86×10^{10}	1.03×10^{11}

$$\text{Displacement per atom (DPA)} = \frac{\text{displacements (/ cm / ion)} \times \text{fluence (ion / cm}^2\text{)}}{\text{atomic density (no. atoms / cm}^3\text{)}}$$

Swelling of powellite

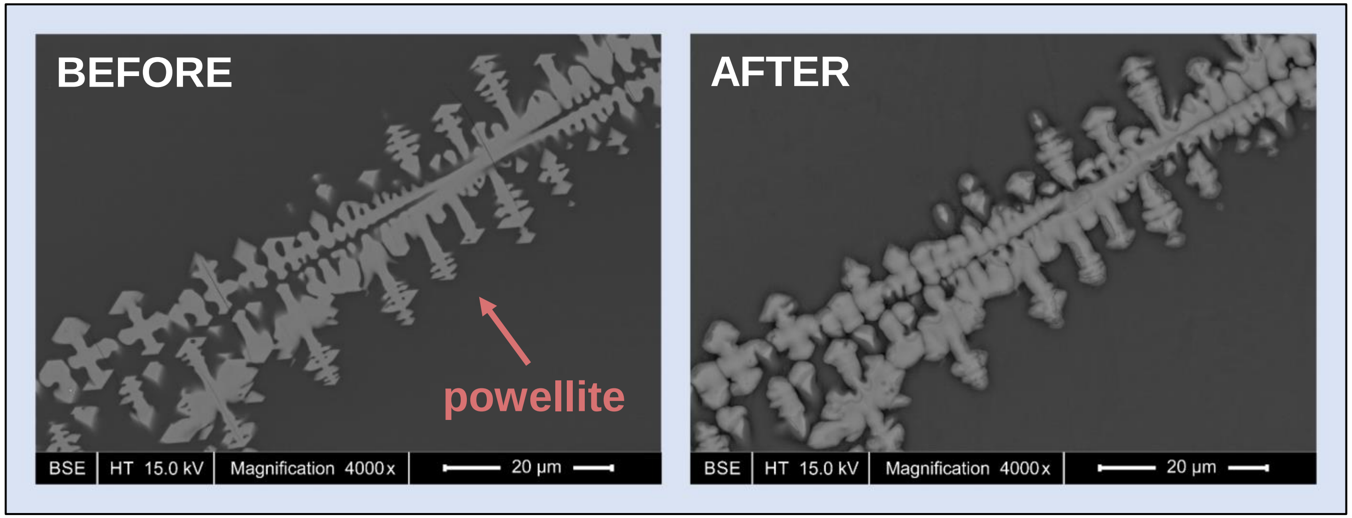

Ni ions

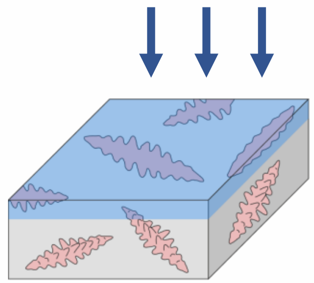

considerable swelling

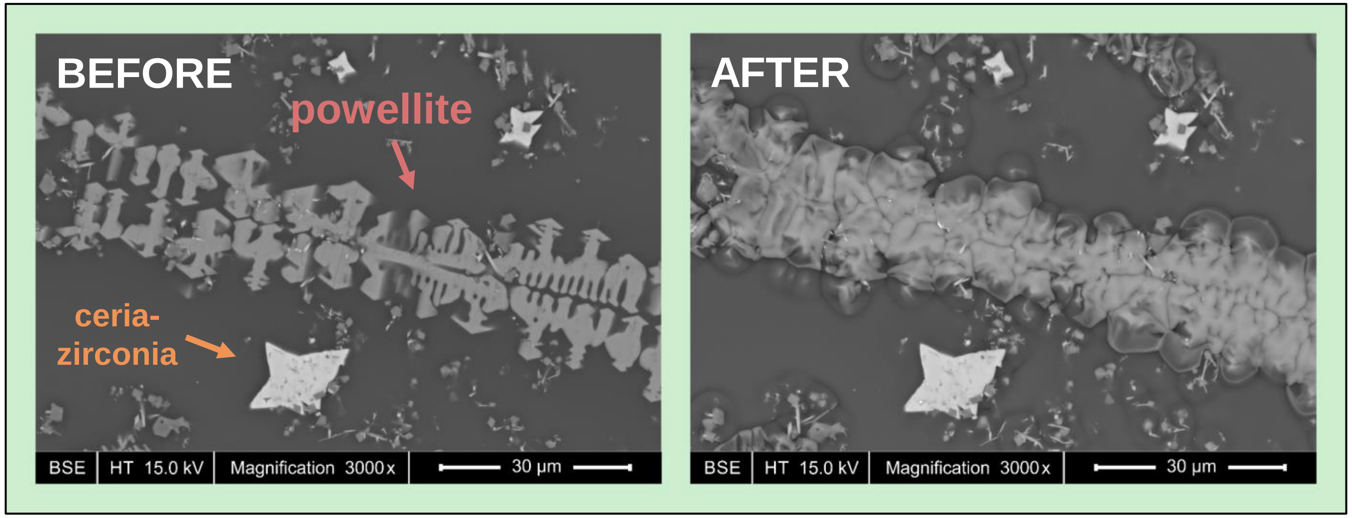

Au ions

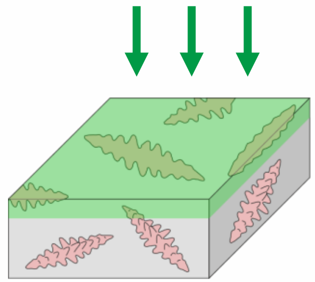

extreme swelling

Swelling of zircon

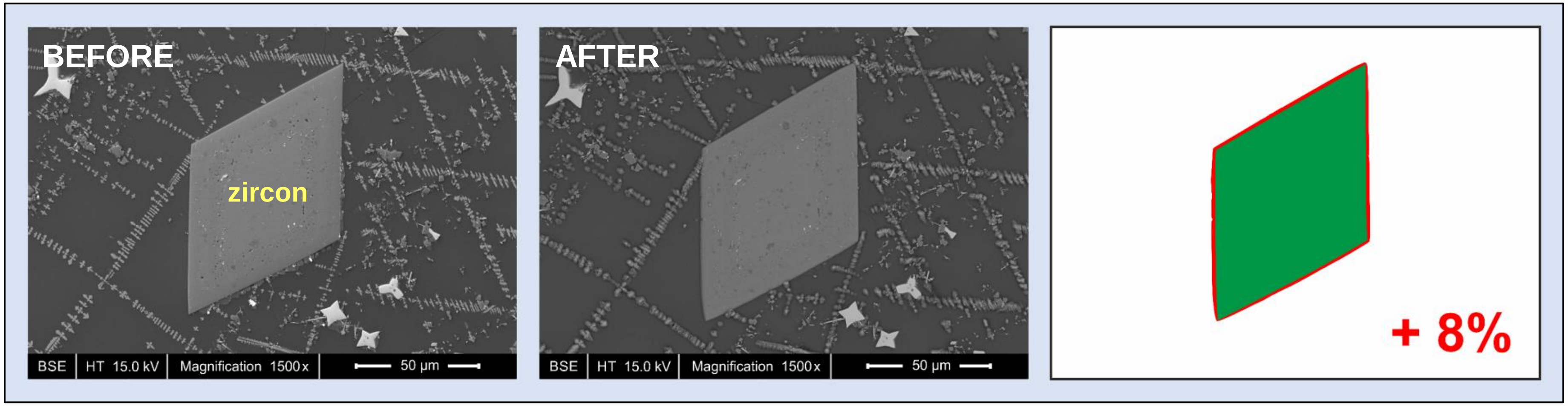

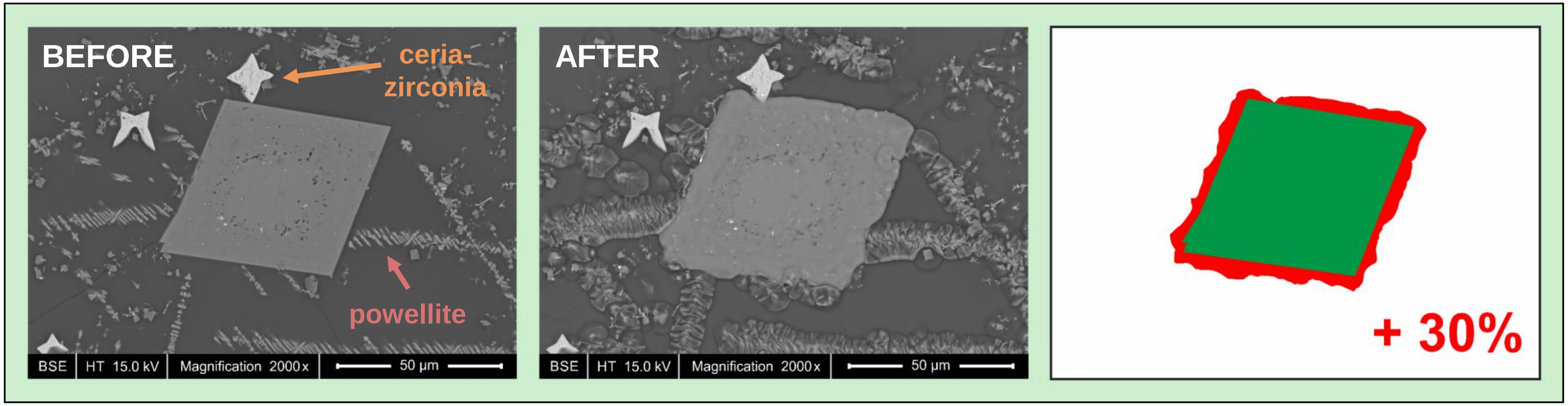

considerable swelling after **Ni** irradiation

extreme swelling after **Au** irradiation

Amorphisation of crystals after Ni irradiation (EBSD analysis)

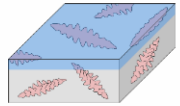

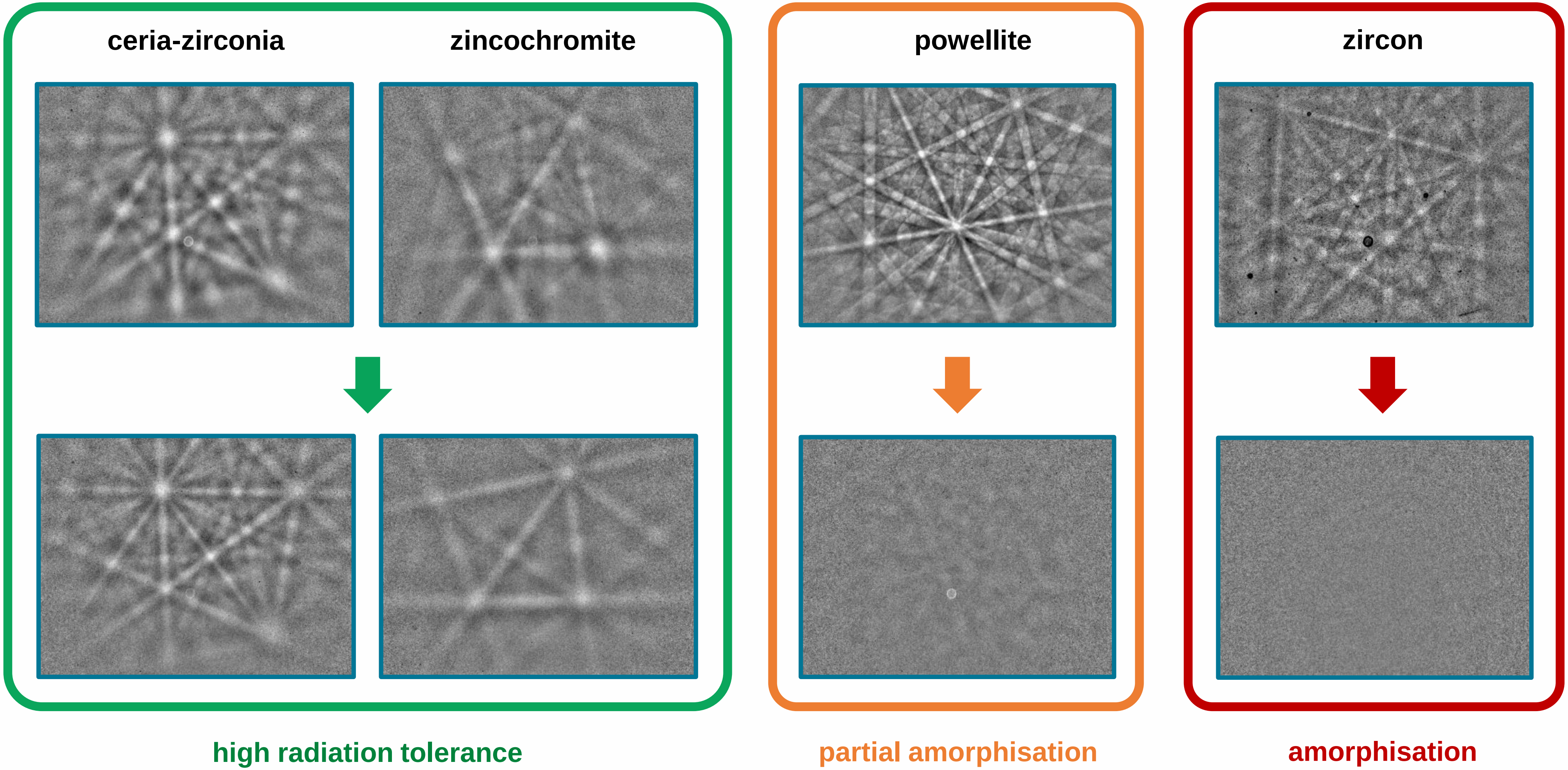

The surface was polished with **0.02 µm** alumina suspension (then coated with **~ 5 nm thick carbon**).

Amorphisation of crystals after Au irradiation (EBSD analysis)

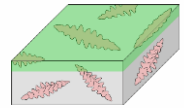

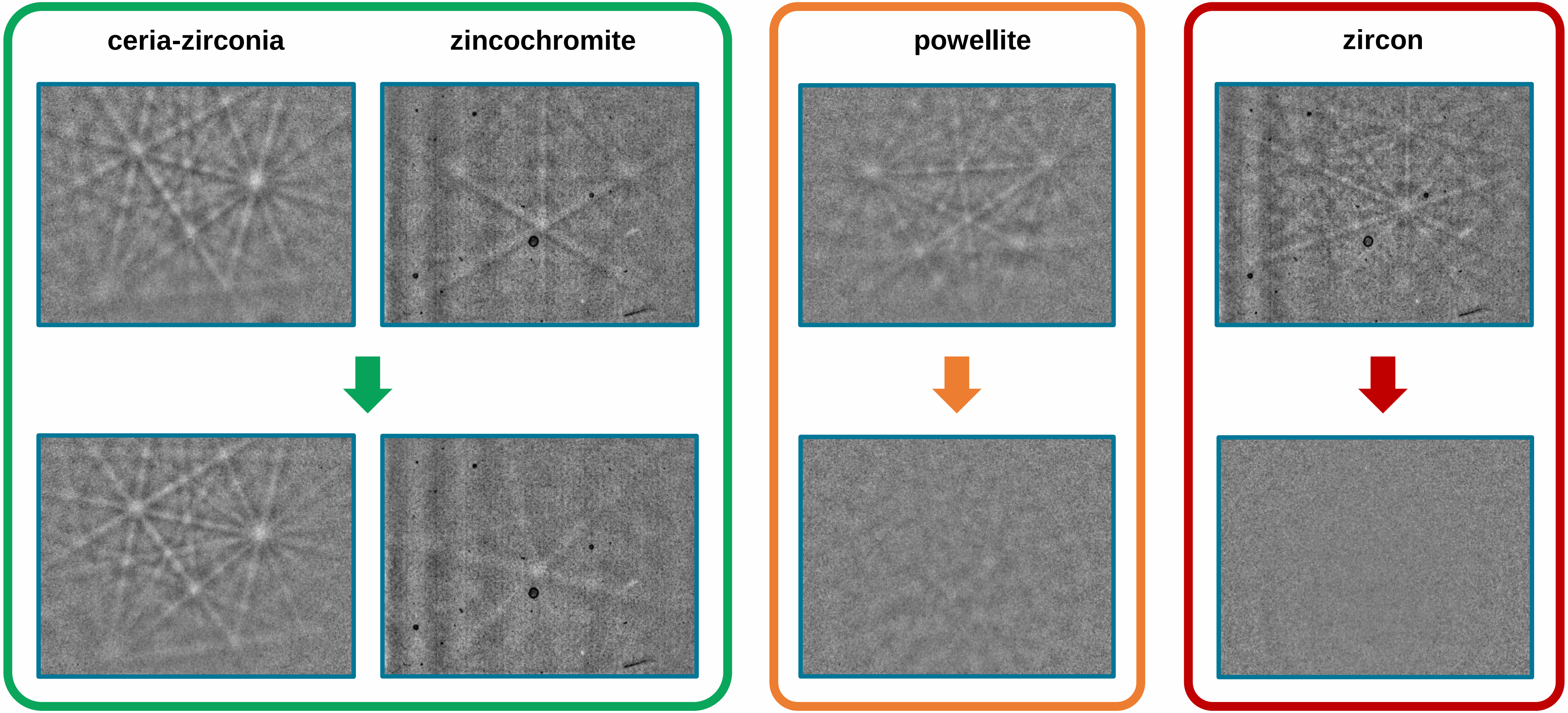

high radiation tolerance | partial amorphisation | amorphisation

The surface was polished with **0.1 µm** alumina suspension (then coated with **~ 0.9 nm thick gold**).

WHY IS IT IMPORTANT

WHY IS IT NEW?

Ni and Au irradiation results on powellite

Wang 2013

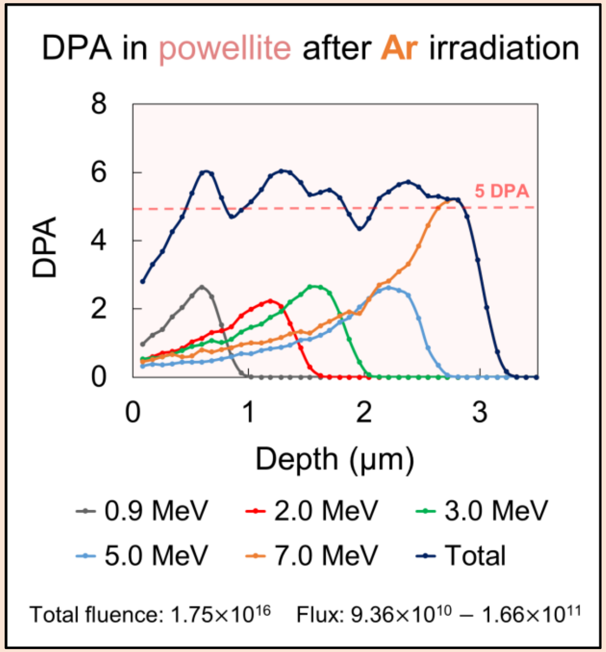

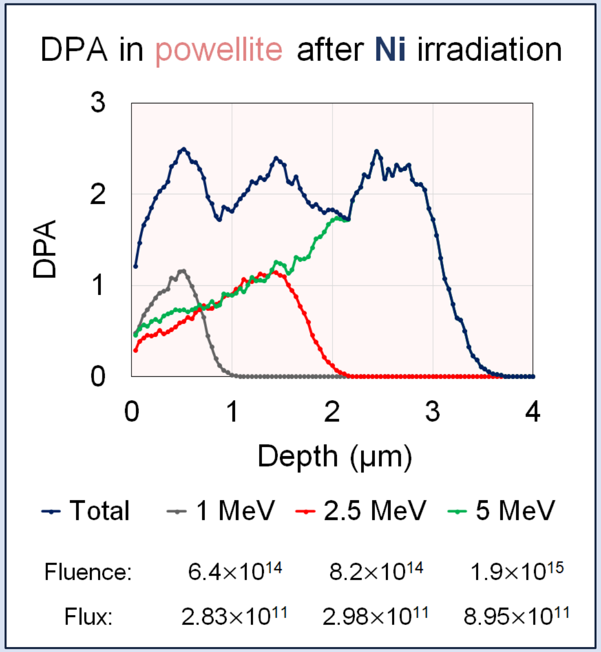

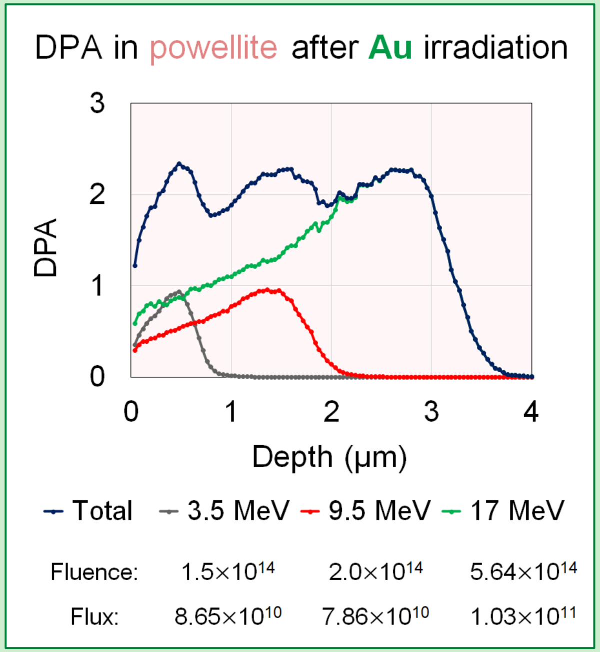

5.0 dpa
remained crystalline
minimal swelling (~ 5%)

2.0 dpa
became amorphous
considerable swelling

2.0 dpa
became amorphous
extreme swelling

Transformative Science and Engineering for Nuclear Decommissioning

WHY IS IT IMPORTANT

WHY IS IT NEW?

Ni and Au irradiation results on powellite

Wang 2013

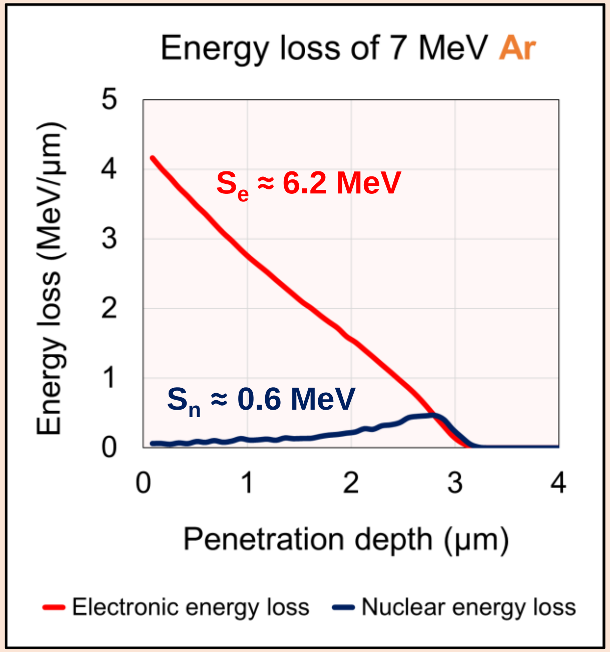

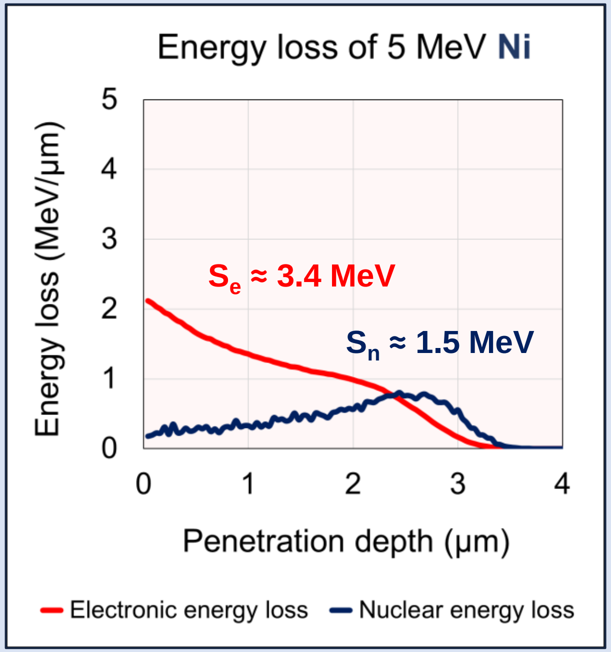

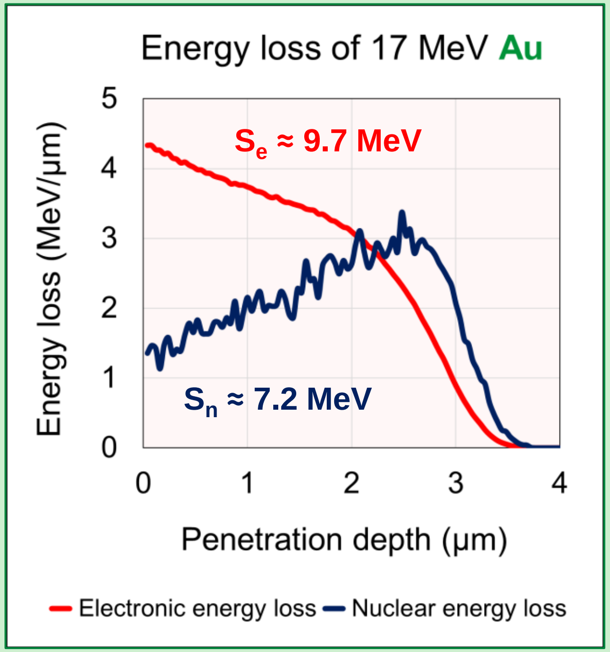

5.0 dpa	2.0 dpa	2.0 dpa
remained crystalline	became amorphous	became amorphous
minimal swelling (~ 5%)	considerable swelling	extreme swelling

$S_n/S_e \approx$ **0.10** < $S_n/S_e \approx$ **0.44** < $S_n/S_e \approx$ **0.74**

Cracking in VTR samples

– horisontal cracking inside large powellite crystals

– cracking of glass around large zircon crystals

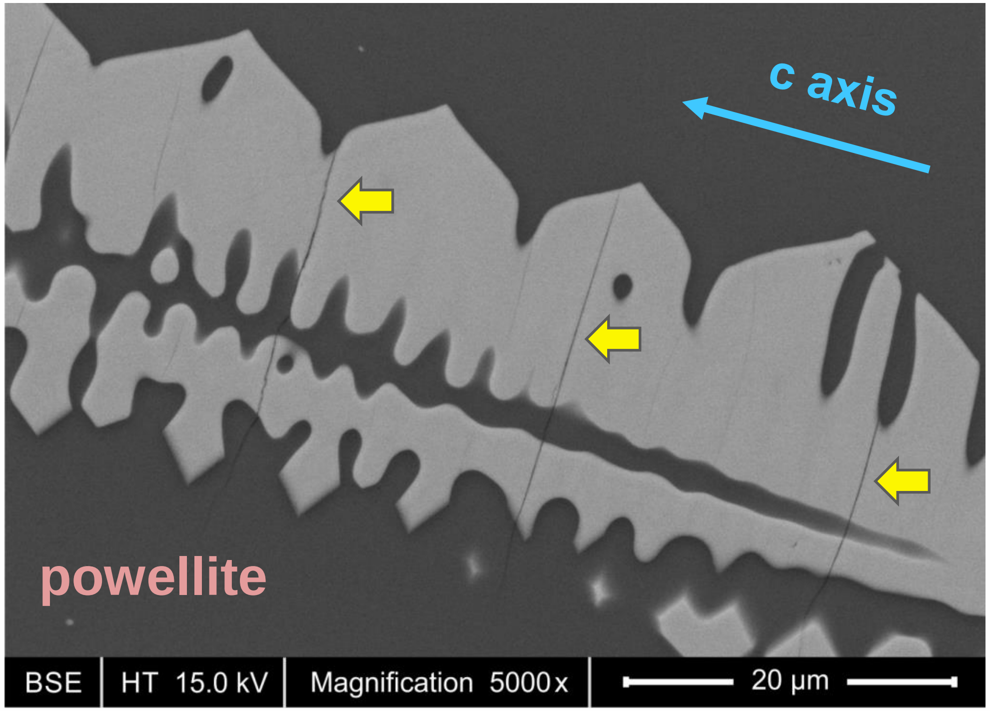

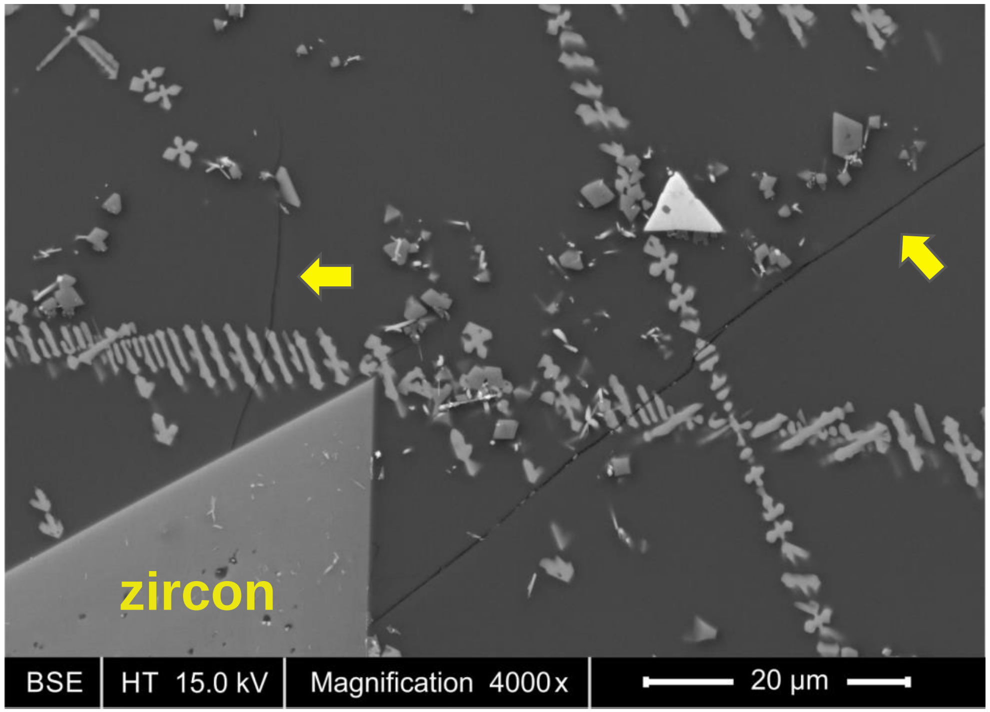

TEC $(\times 10^{-6}/°C)$**:** $\alpha_a = 13.5$ $\alpha_c = 22.8$ [2] $\alpha_a = 3.4$ $\alpha_c = 5.6$ [3]

[2] Bayer at al. 1971; [3] Achary et al. 2006

Cracking in VTR samples

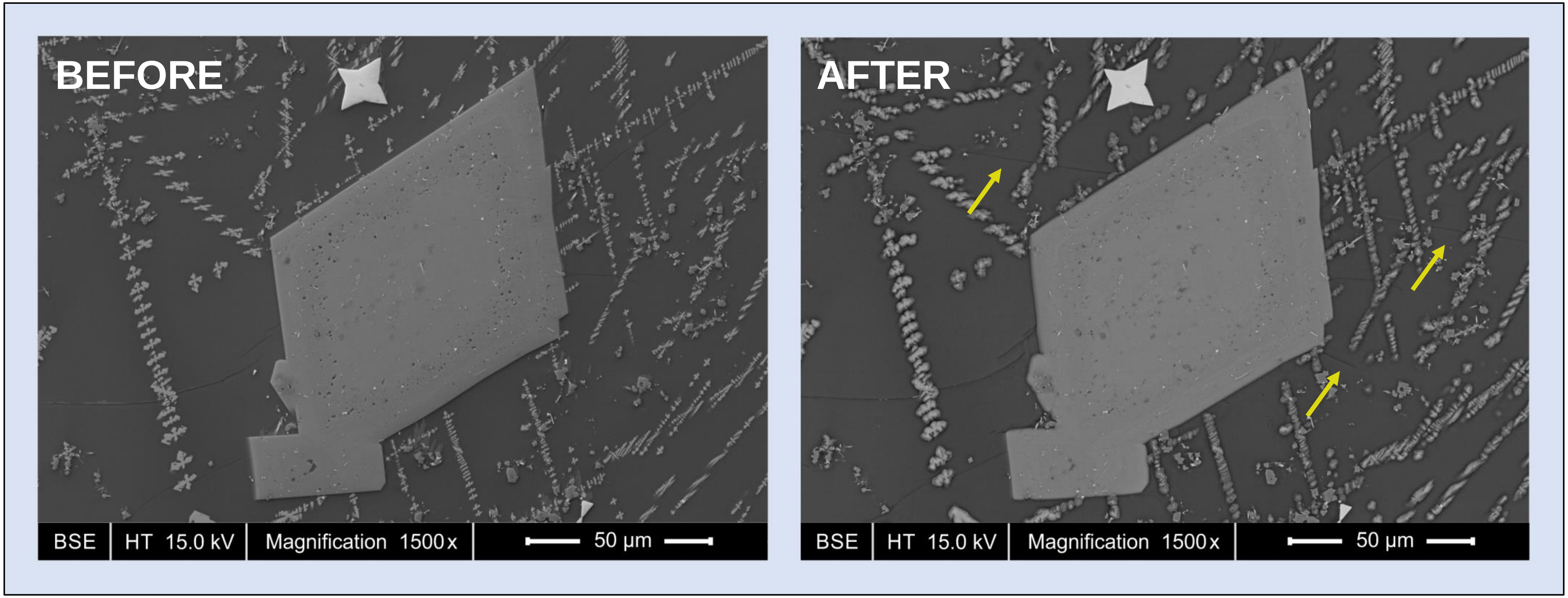

Formation of new cracks around zircon after Ni irradiation.

Summary

- Swelling and amorphisation of **powellite** and **zircon** crystals after **Ni** and **Au** irradiation.

- Amorphisation of **powellite** and **zircon** crystals (accompanied by volume change and cracking) might lead to a higher radionuclide leaching rate to the environment.

Next steps

- In-situ TEM, GIXRD, profilometry

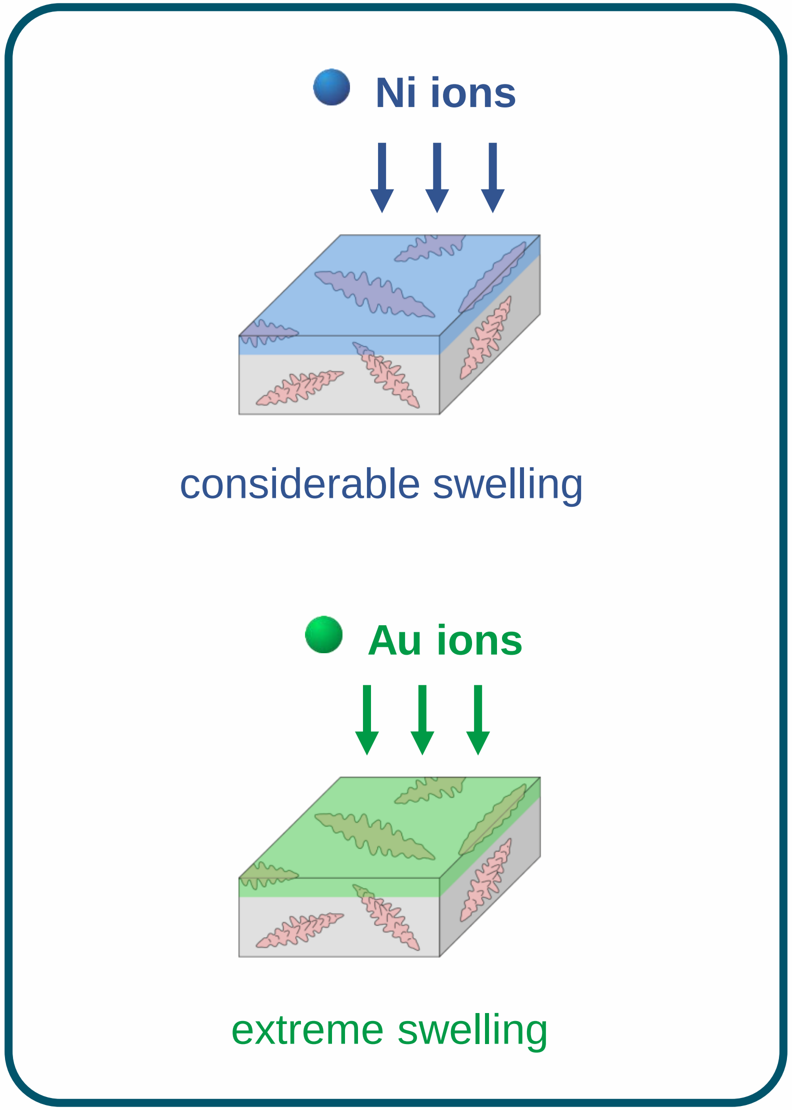

Summary

- Swelling and amorphisation of **powellite** and **zircon** crystals after **Ni** and **Au** irradiation.

- Amorphisation of **powellite** and **zircon** crystals (accompanied by volume change and cracking) might lead to a higher radionuclide leaching rate to the environment.

Next steps

- In-situ TEM, GIXRD, profilometry

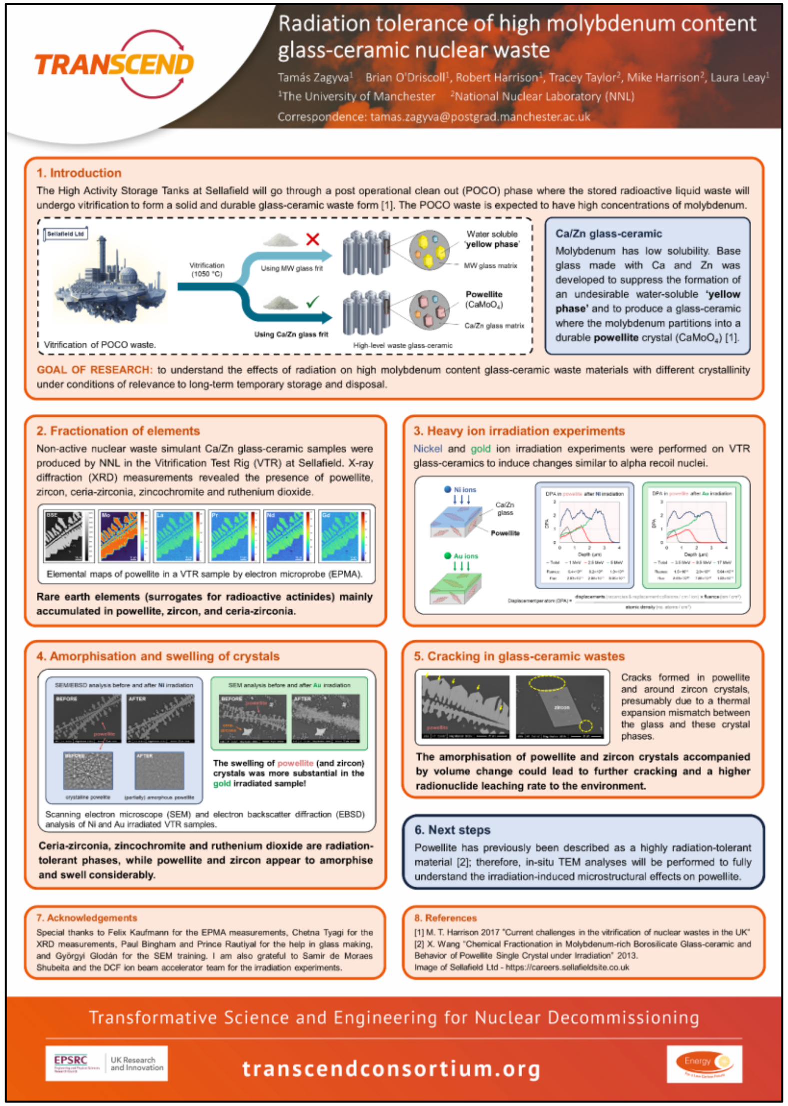

References

Articles:

[1] Wang “Chemical Fractionation in Molybdenum-rich Borosilicate Glass-ceramic and Behavior of Powellite Single Crystal under Irradiation” 2013.

[2] Bayer at al. ”Thermal expansion of ABO4- compounds with zircon and scheelite structures” 1971.

[3] Achary et al. “High temperature crystal chemistry and thermal expansion of synthetic powellite (CaMoO4): A high temperature X-ray diffraction (HT XRD) study” 2006.

Images:

Radioactive Waste Management https://www.gov.uk/guidance/why-underground#the-science-files

FAVPNG https://favpng.com/

TRANSCEND

Transformative Science and Engineering for Nuclear Decommissioning

Thank you for the help!

Brian O'Driscoll
Robert Harrison
Laura Leay

Tracey Taylor
Mike Harrison

NATIONAL NUCLEAR LABORATORY

Felix Kaufmann
Paul Bingham
Prince Rautiyal
Györgyi Glodán
Chetna Tyagi
Samir de Moraes Shubeita

Special thanks for the support from National Nuclear Laboratory.

NATIONAL NUCLEAR LABORATORY

Thank you

Contact Details
tamas.zagyva@postgrad.manchester.ac.uk

TRANSCEND

Transformative Science and Engineering for Nuclear Decommissioning

Assessing the strength of biomineral strategies for concrete repairs

Thanos Karampourniotis, University of Strathclyde

Theme 2: Site Decommissioning and Remediation

email: athanasios.karampourniotis@strath.ac.uk

Supervisors:

Professor Rebecca Lunn[1] , Dr. Enrico Tubaldi[2], Dr. Grainne El Mountassir[3]

[1,2,3] Department of Civil and Environmental Engineering, Faculty of Engineering, University of Strathclyde, Glasgow, United Kingdom

University of Strathclyde Glasgow

cavendish nuclear

Energy For a Low Carbon Future

11 November 2021

STRUCTURES IN THE UK ARE AGEING

- Many structures in the United Kingdom are past their original design life which can affect the safety of the people using them.
- According to a report published in 2014 by the **Department for Communities and Local Government**, approximately 20% of the English housing stock was built before 1919 and only 24% was built after 1980.
- Many of these structures are in need of constant maintenance to ensure that they provide both safety and functionality.

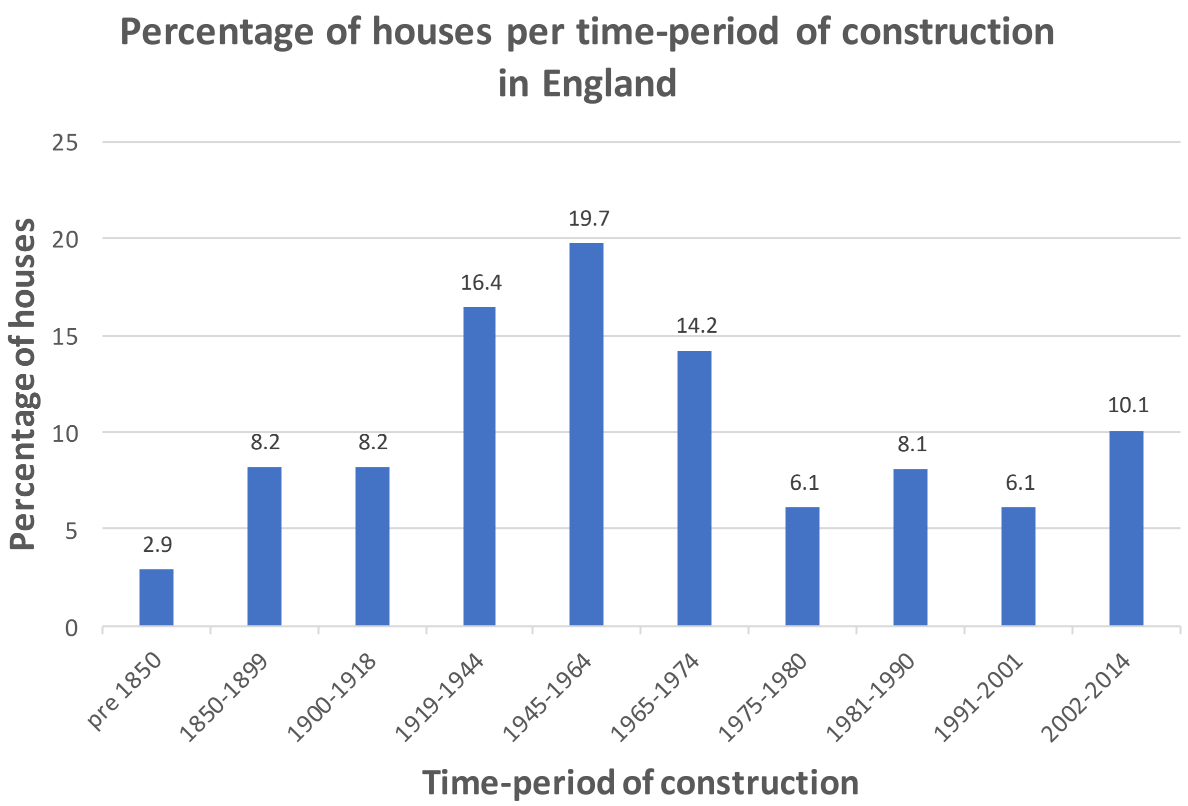

Sources: *Department for Communities and Local Government (DCLG), ''English housing survey 2014 to 2015: housing stock report'' and ''2001 English House Condition Survey''*

TRANSCEND

Transformative Science and Engineering for Nuclear Decommissioning

NUCLEAR POWER STATIONS IN THE UK

- Almost all of the UK's nuclear power stations were built from late 1970 to late 1980, with most of them closing by 2030.
- Considering both the age and the harsh environmental conditions that these assets are exposed to, the degradation and cracking of concrete in these sites can be of significant importance for their structural integrity.
- We have to guarantee the safety of the structures, until the decommissioning process is completed.

*Hinkley B power station, **Source:** www.itv.com*

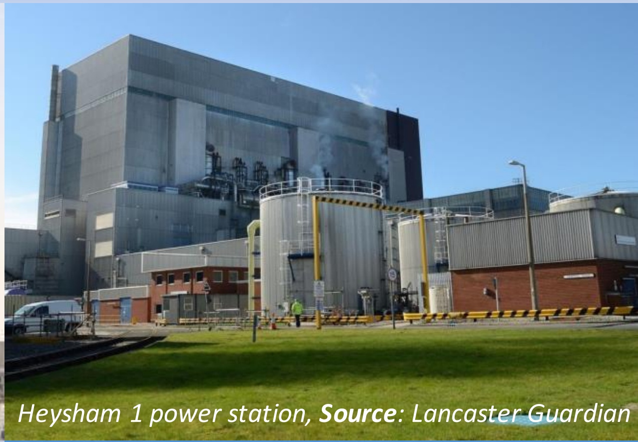

*Heysham 1 power station, **Source**: Lancaster Guardian*

*Hunterston B power station, **Source**: Sky news*

*Dungeness B power station, **Source**: BBC*

GLOBAL CONCRETE REPAIR MORTARS MARKET SIZE

- The global market size of concrete repair mortars based on recent estimations is approximately 2.1 to 2.5 billion dollars

- The demand is expected to keep increasing at least by late 2020.

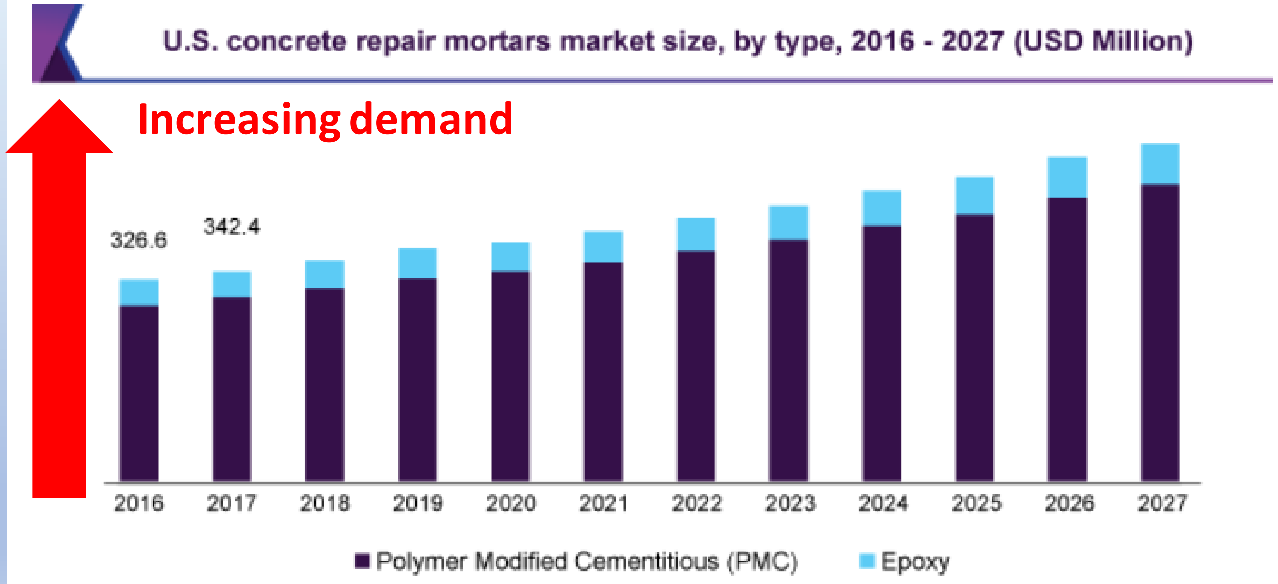

Source: *grandviewresearch.com*

TRADITIONAL CONCRETE-REPAIR STRATEGIES

Epoxy-based mortars

- They have a much greater coefficient of thermal expansion than concrete, something that can cause high shear stresses. As a result, cracks begin to form in the interface.
- They need constant periodic care and maintenance.

Cement-based mortar

- They consists of big particle size grains, resulting in poor penetration, making it ineffective when treating micro-cracking.

Source: *engineeringdiscoveries.net*

Source: *homedepot.com*

RESEARCH ON MICROBIALLY INDUCED CARBONATE PRECIPITATION

Microbially Induced Carbonate Precipitation

- A novel concrete repair method that takes advantage of bacteria like S. Pasteurii where together with a calcium source can form calcium carbonate (CaCO3).

$$CO(NH_2)_2 + 2H_2O \rightarrow 2NH_3 + H_2CO_3$$

$$2NH_3 + 2H_2O \leftrightarrow 2NH_4^{\ +} + 2OH^-$$

$$H_2CO_3 + 2OH^- \leftrightarrow HCO_3^{\ -} + H_2O + OH^-$$

$$HCO_3^{\ -} + H_2O + OH^- \leftrightarrow CO_3^{2-} + 2H_2O$$

$$Ca^{2+} + CO_3^{2-} \rightarrow CaCO_3\ (s)\ \text{(calcite precipitation)}$$

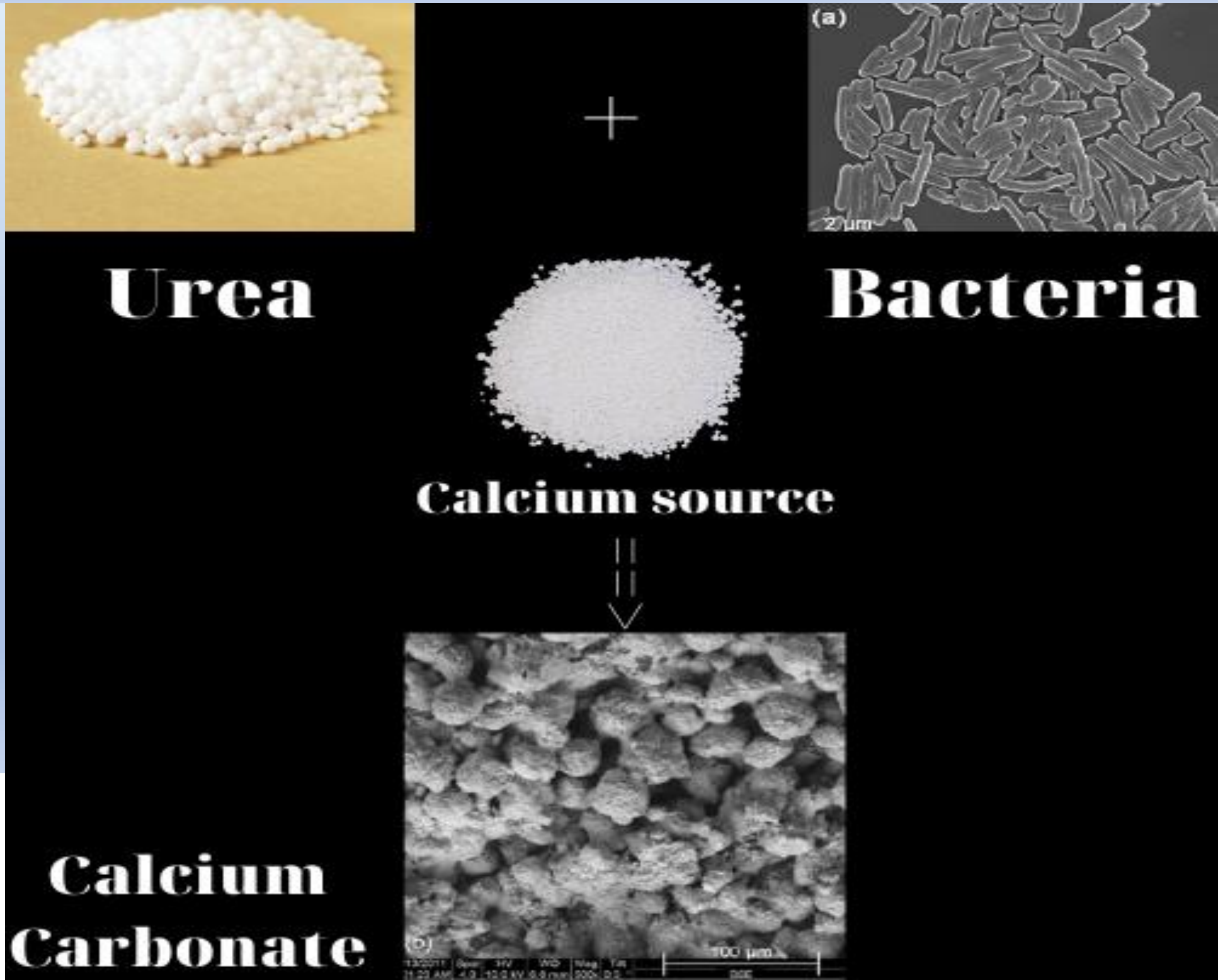

THE AIM AND OBJECTIVES OF THIS PHD ARE:

AIM

- To provide a durable repair for both micro-cracking and large cracks that lasts for decades.

OBJECTIVES

- To develop a modelling strategy, conduct experiments to validate it and show it can predict the mechanical behavior of MICP-treated concrete.
- To optimize the injection strategies that are investigated.

GRANITE CORES TREATMENT AND SHEAR TESTING

Experimental set-up

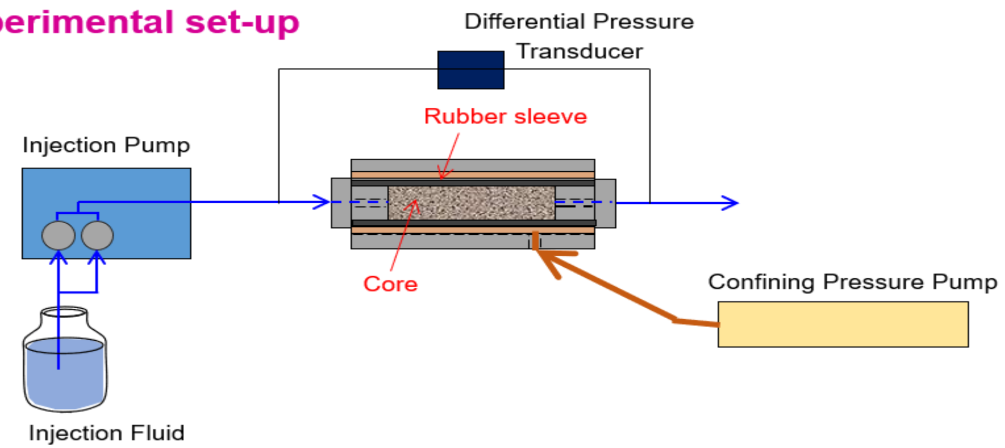

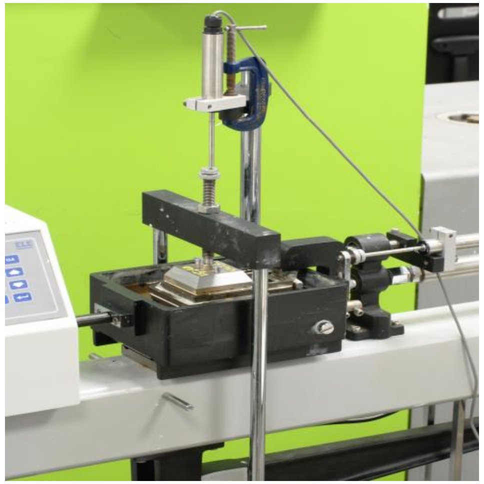

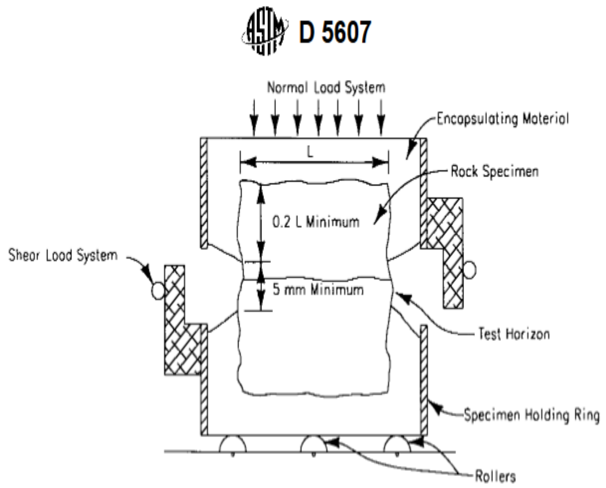

Calcite crystals bridged the fracture after the MICP treatment was implemented

THE FINITE-ELEMENTS MODEL CREATED

1. Vertical load on the top surface of the half-core.
2. Displacement rate on the second half-core.
3. Horizontal fracture.
4. Calcite distribution on half-cores' surfaces.
5. Displacement.

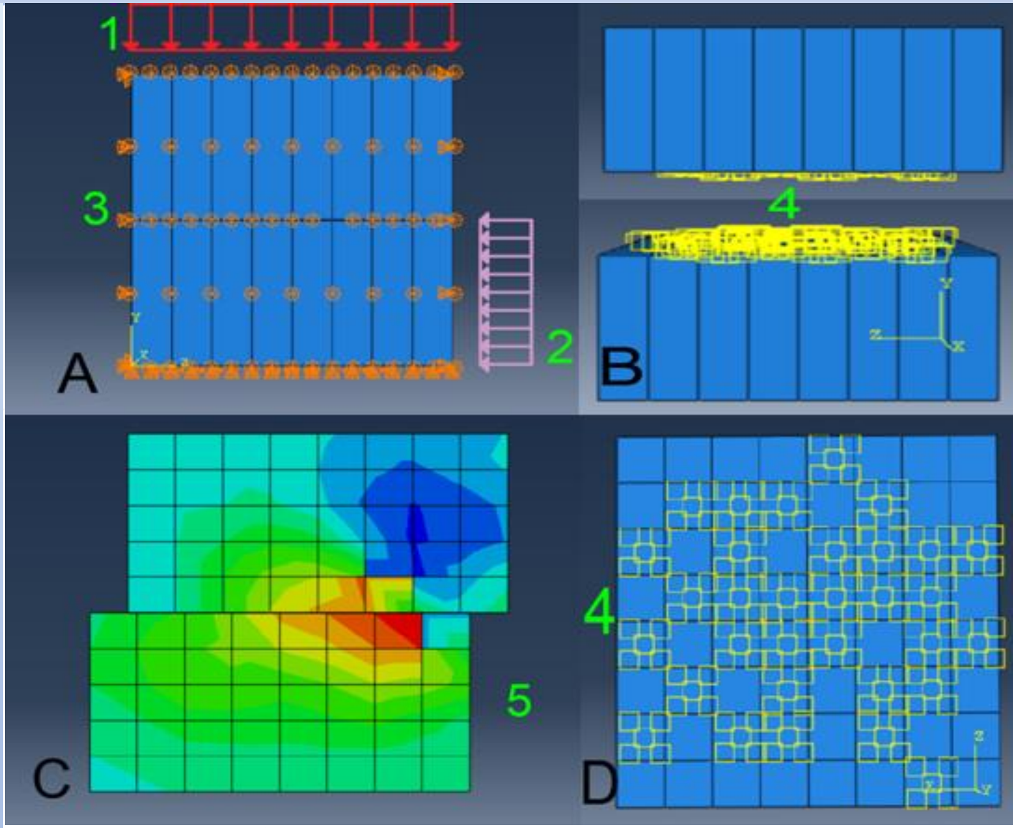

Figures A and B: Loading and boundary conditions on the rock core, consisting of two rock sections (top and bottom half). *Y-Z axes view*
Figure C: Shear stress distribution and displacement. *Y-Z axes view*
Figure D: Simulating calcite (yellow patches) as a cohesive component in different geometrical patterns on the rock's surfaces. *X-Z axes view*

MODELLING THE CONNECTED REGIONS OF THE HALF-CORES

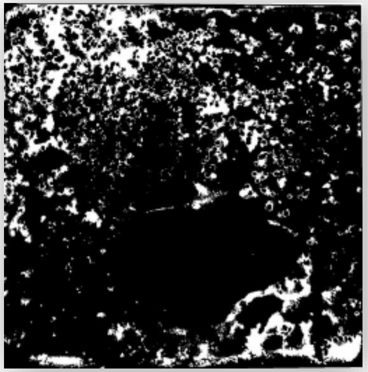

X-CT Image, FG2 Core

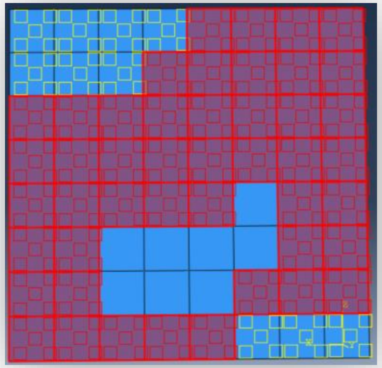

64 elements Model, FG2 Core

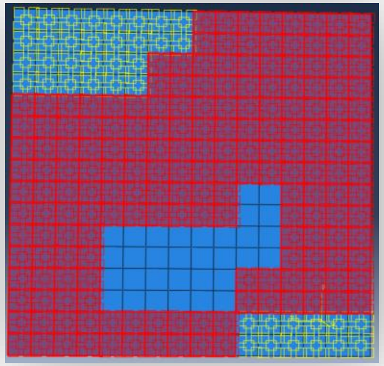

256 elements Model, FG2 Core

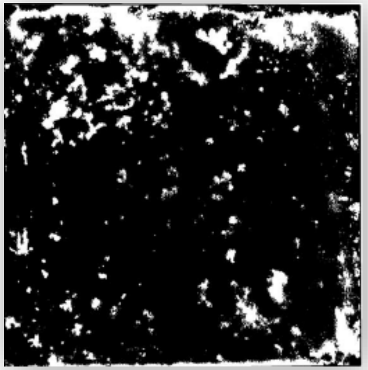

X-CT Image, FG4 Core

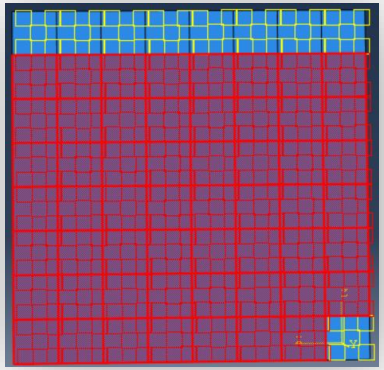

64 elements Model, FG4 Core

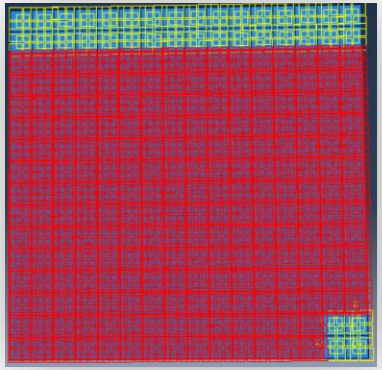

256 elements Model, FG4 Core

Yellow elements:

Cohesive behavior assigned

FG2 Core: 0.50 MPa

FG4 Core: 0.73 MPa

Red elements:

Frictional behavior assigned

CALIBRATION OF THE MODEL – MESH DEPENDENCY

FG2 Core

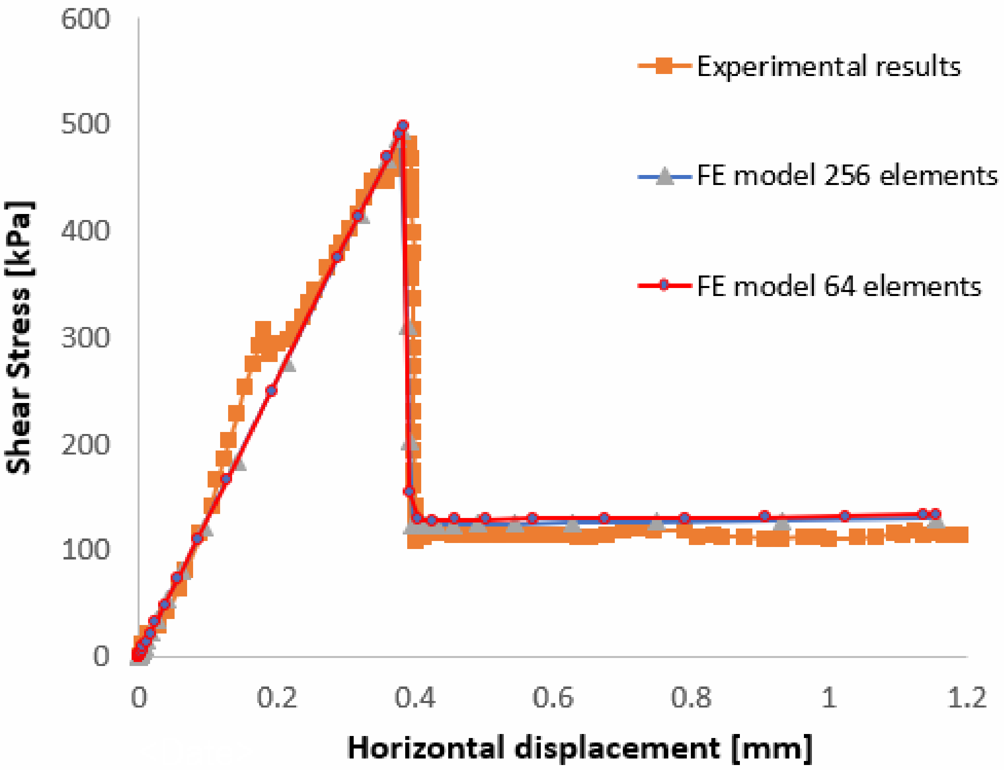

FG4 Core

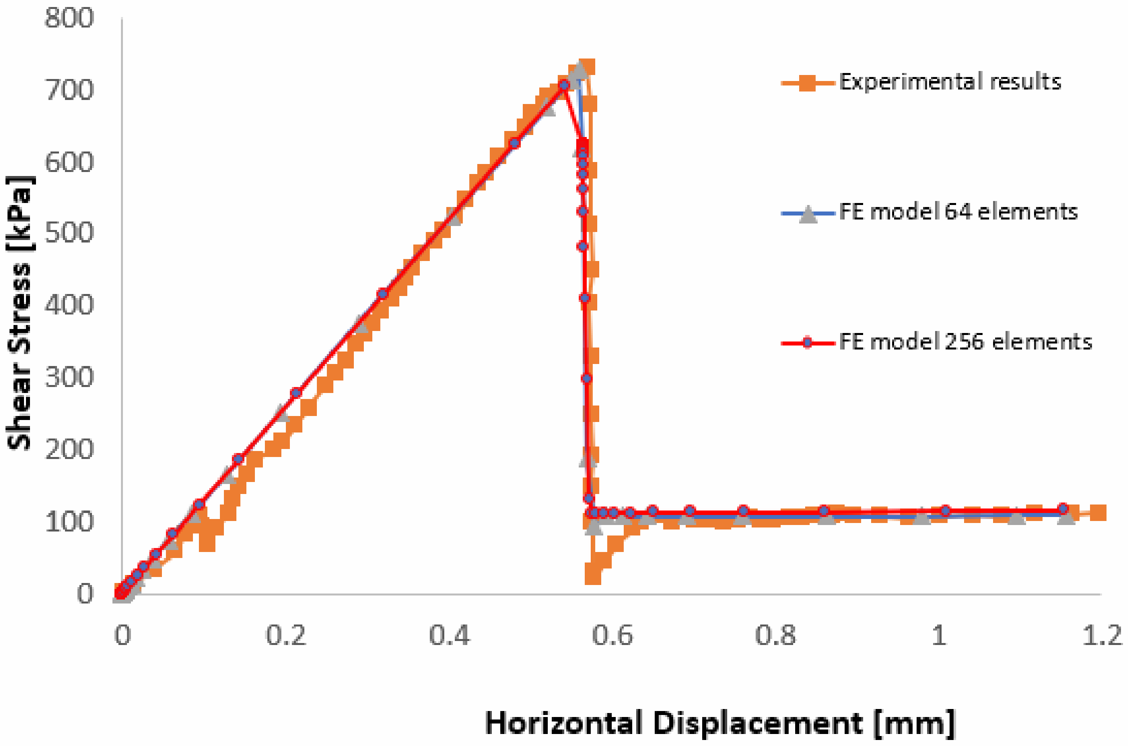

CALCITE DISTRIBUTION STRATEGIES

DIFFERENT CALCITE DISTRIBUTIONS

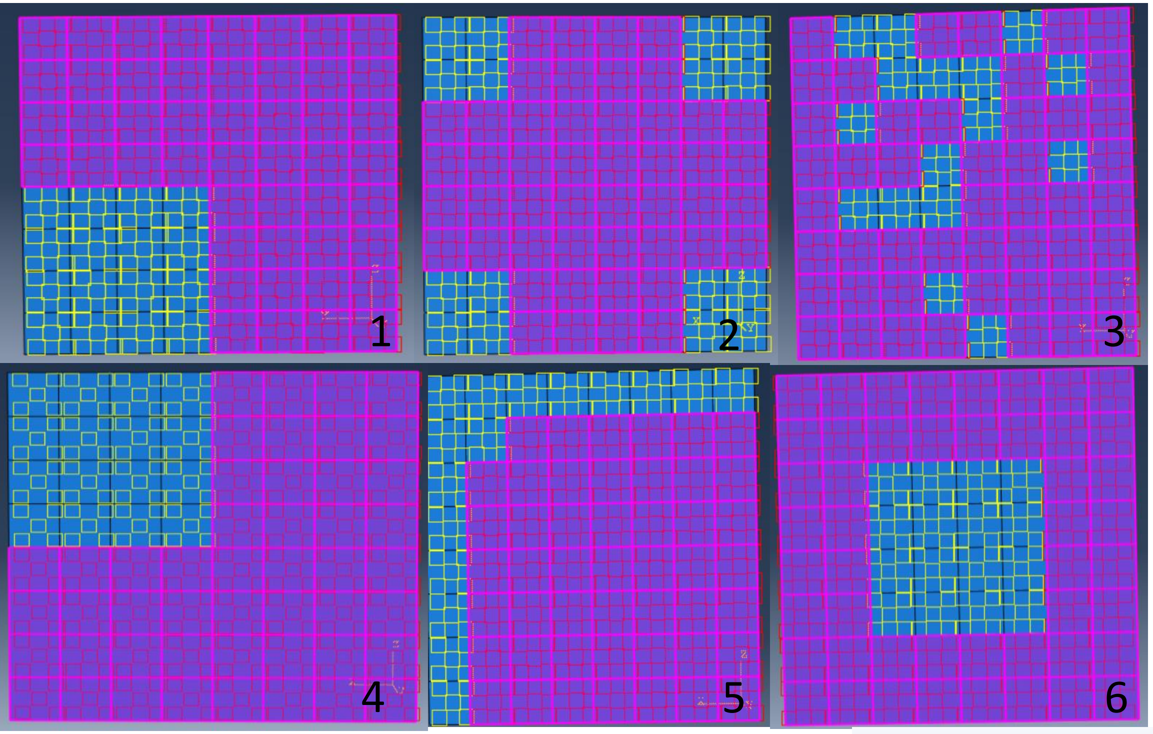

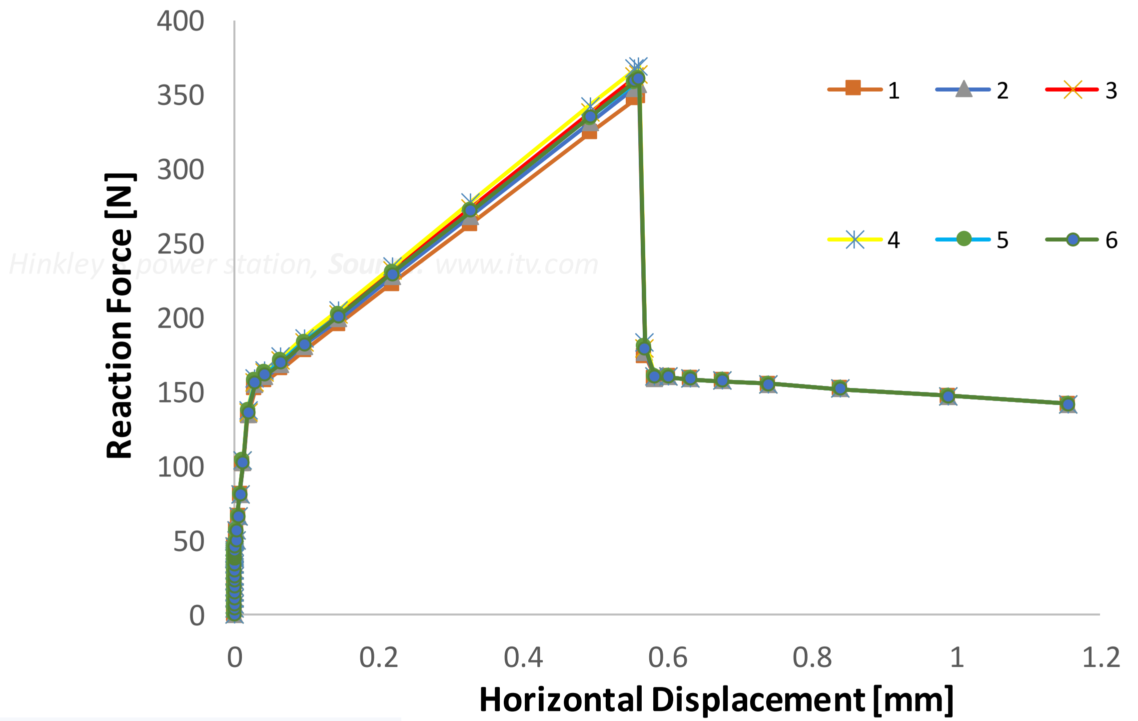

Yellow elements: Cohesive behavior assigned

Purple elements: Frictional behavior assigned

Transformative Science and Engineering for Nuclear Decommissioning

CALIBRATION OF THE MODEL – MESH DEPENDENCY

"Random distribution of calcite" models

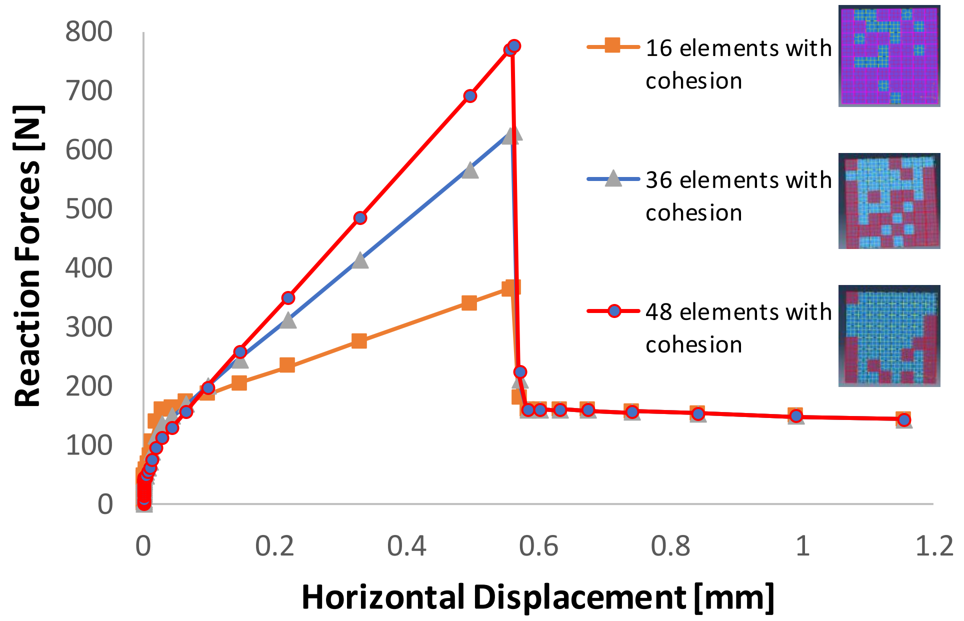

"Pillars distribution of calcite" models

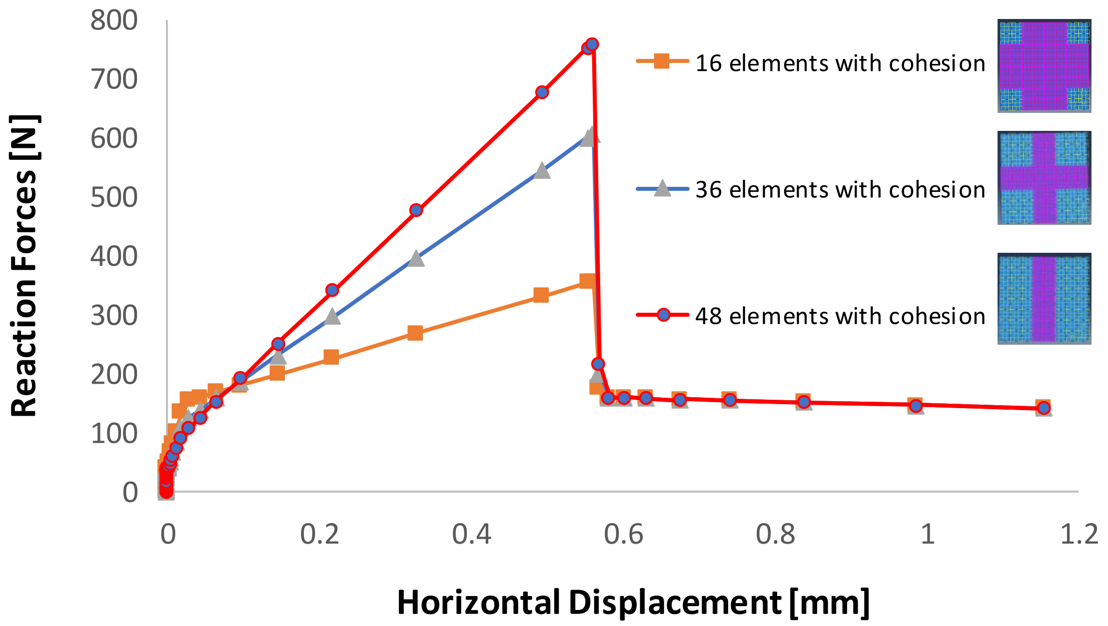

STRUCTURE OF THE EXPERIMENTS

The experiments we are developing will be used to test the FEM-model's effectiveness and validate it against the results.

3 treatment strategies:

- Glass beads only on the corners of one half-core.
- Glass beads on the corners of one half-core and patches in the middle.
- Glass beads on the corners of one half-core and in addition sand grains are used as a filler.

MICP is structured by layers that after a number of treatment cycles, bridge the initial gap between the concrete half-cores.

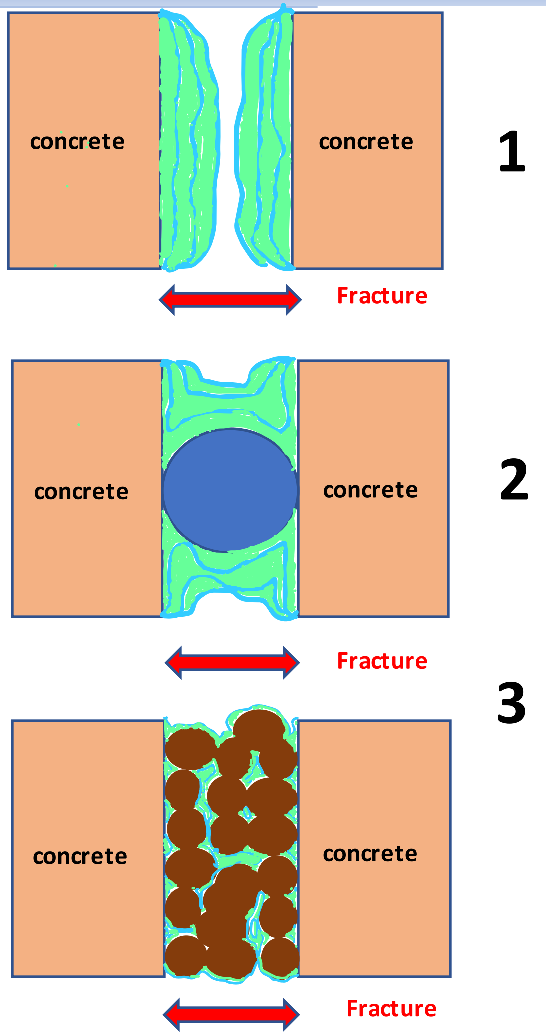

EXPERIMENTAL SETUP

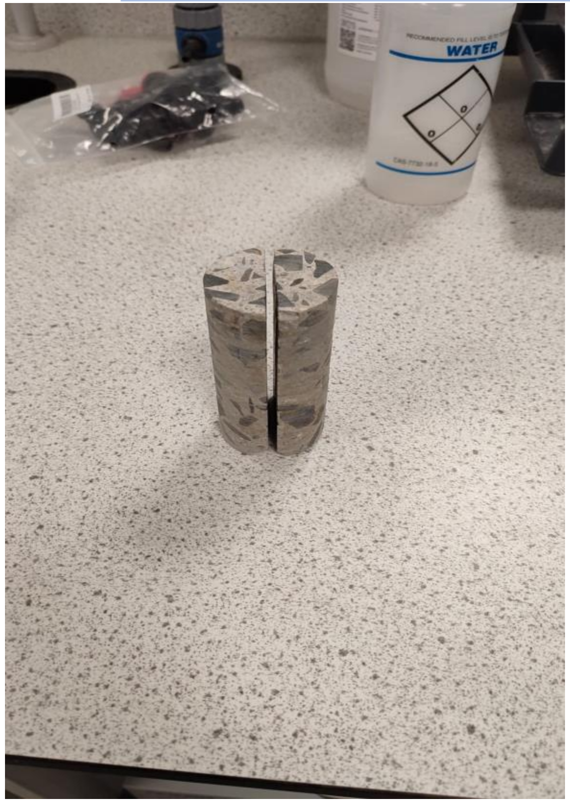

The separated half-cores

0.5mm diameter glass beads on the half-core’s surface

The half-cores wrapped together with membrane layers

EXPERIMENTAL SETUP

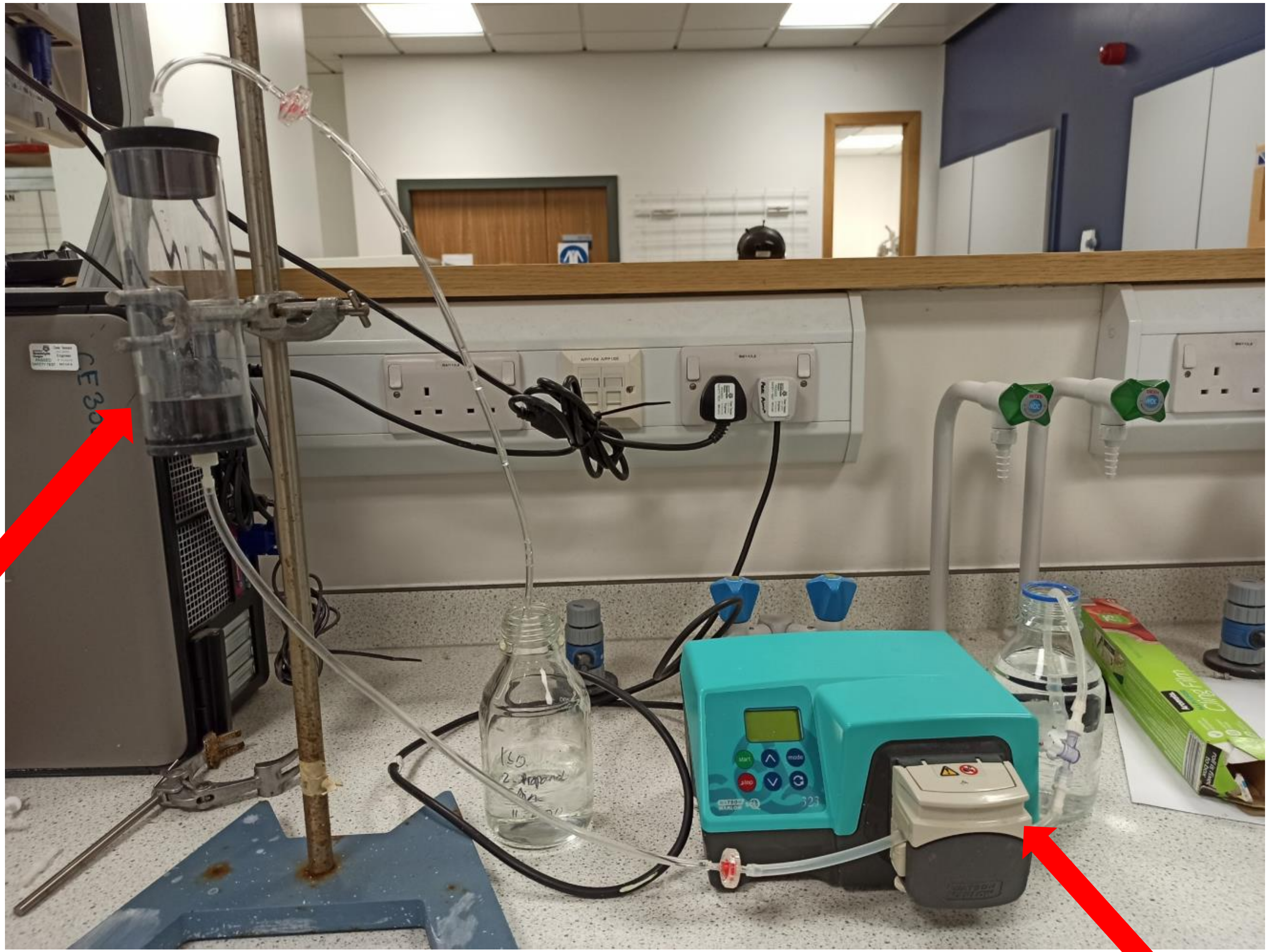

Rigid clear tube acting as core holder

Peristaltic pump

EXPERIMENTAL SETUP

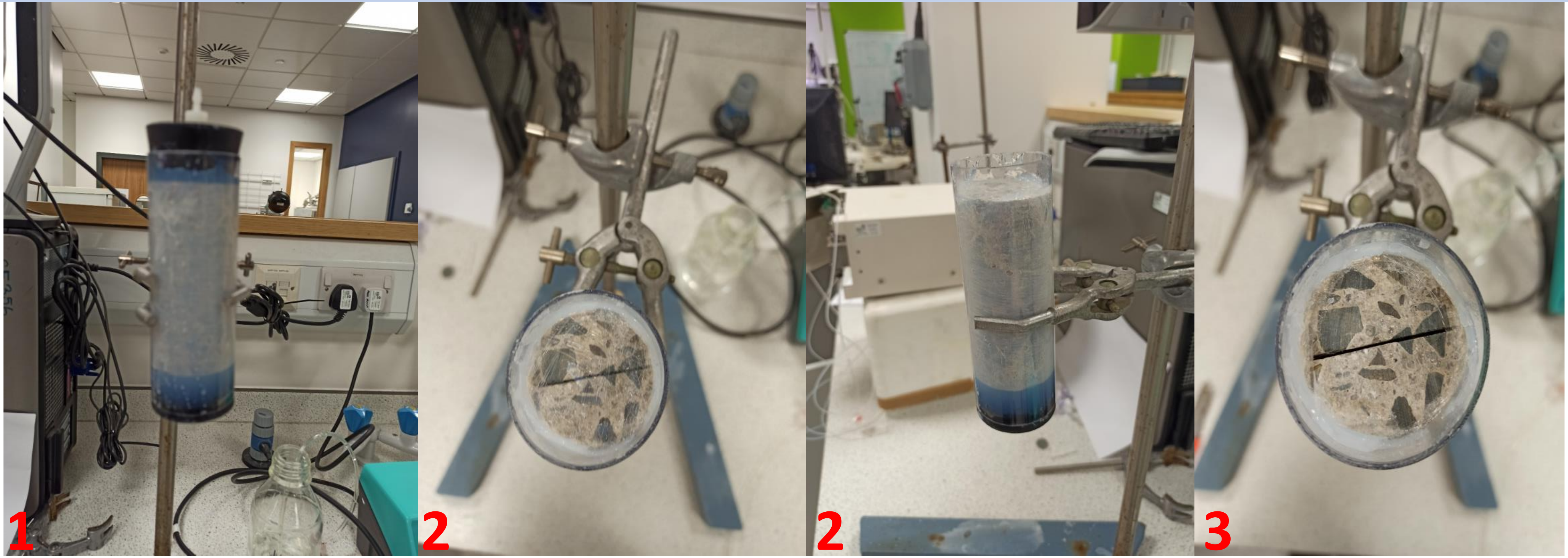

After having the wrapped half-cores immersed in colloidal silica

15 minutes after having introduced colloidal silica

After removing the top layer of membrane

EXPERIMENTAL SETUP

AFTER 15 TREATMENT CYCLES

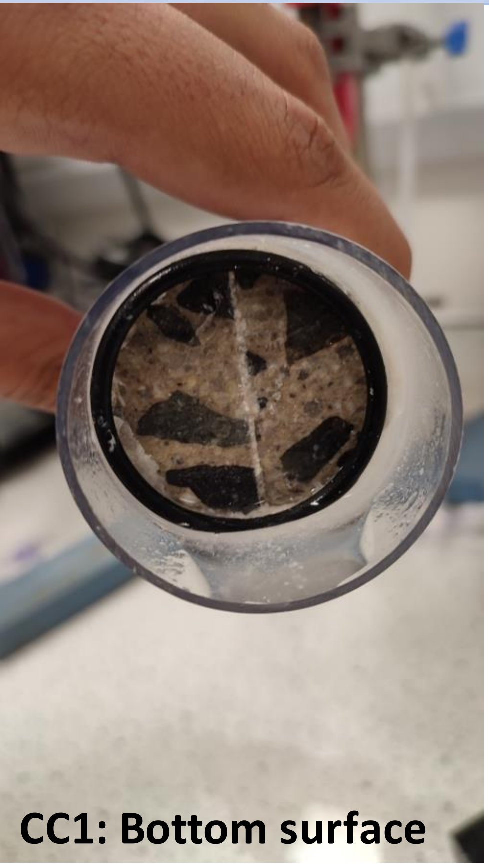

HYDRAULIC CONDUCTIVITY AFTER 15 TREATMENT CYCLES

Concrete Core 1:

Initial Hydraulic Conductivity: **0.464 mm/sec**

Hydraulic Conductivity after 15 treatment cycles: **0.0015 mm/sec**

Concrete Core 2:

Initial Hydraulic Conductivity: **0.284mm/sec**

Hydraulic Conductivity after 15 treatment cycles: **0.0009mm/sec**

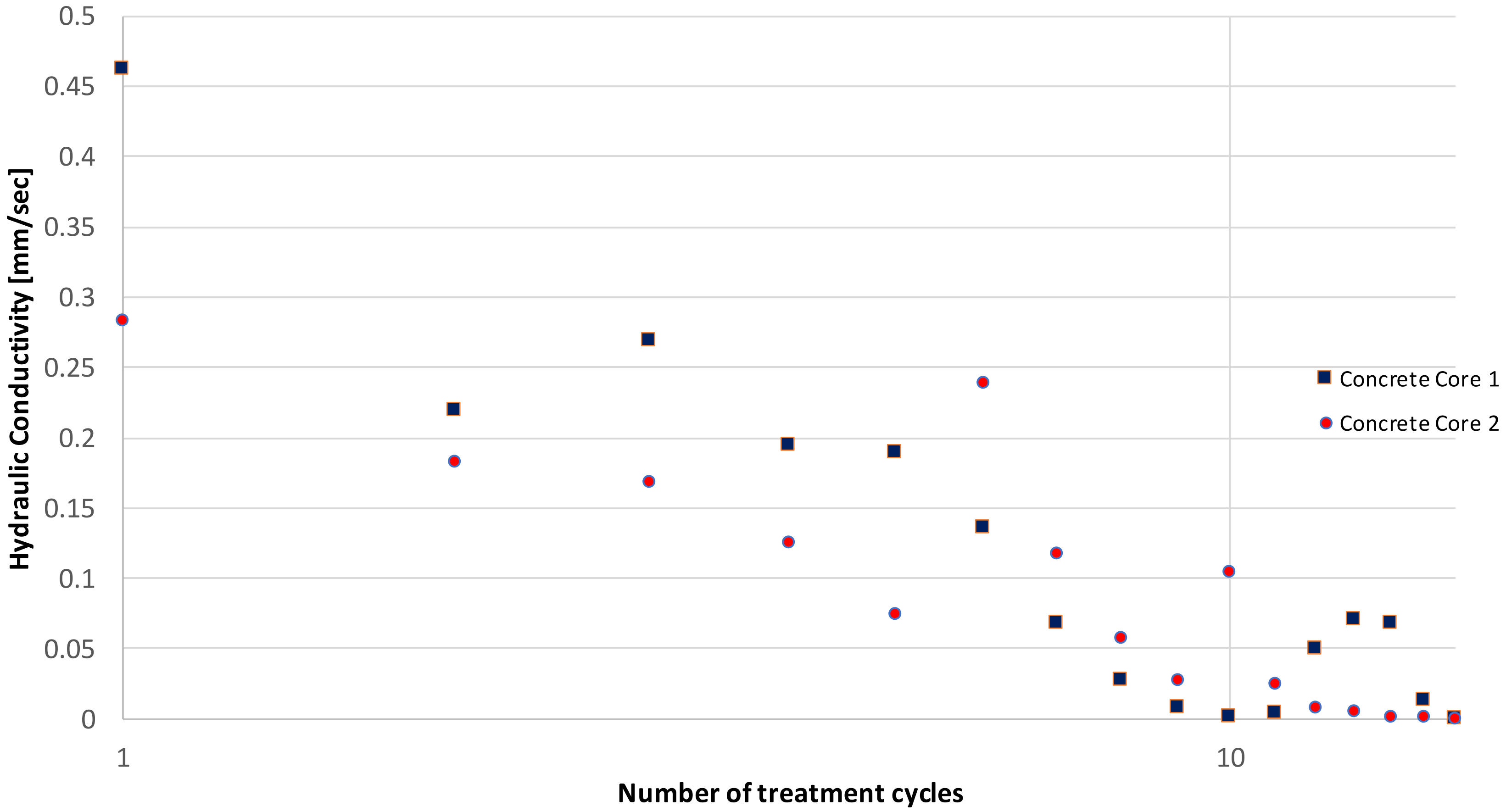

CONCLUSIONS

- A Finite Elements Model has been developed and calibrated against experimental data.

- According to the sensitivity analyzes that took place, the model shows that there is relatively little effect on the geometry of the calcite and that strength is largely governed by the size of the contact area.

- Microbially Induced Carbonate Precipitation treatments have been implemented to old artificially-cut concrete cores, exhibiting a substantial decrease in their initial Hydraulic Conductivity.

FUTURE WORK

- When all concrete cores are treated with MICP, they will be subjected to XCT scanning to evaluate the distribution of calcium carbonate in the initial fracture and the contact areas created.
- After the XCT-scanning the cores will be subjected to shear testing to assess the developed shear resistance.
- The effect of the created flow paths due to the spatial distribution of calcite on the efficiency of the repair will be also investigated.
- In later stages of this PhD, the durability of the MICP method will be examined and compared to the durability of other commercialized methods.

Thank you

e-mail: athanasios.karampourniotis@strath.ac.uk

TRANSCEND

Transformative Science and Engineering for Nuclear Decommissioning

Thin film fabrication and characterization capabilities at University of Bristol

Dr. Jacek Wąsik, University of Bristol

2nd Annual Meeting

11th November 2021
Harrogate

Energy
For a Low Carbon Future

Thin films

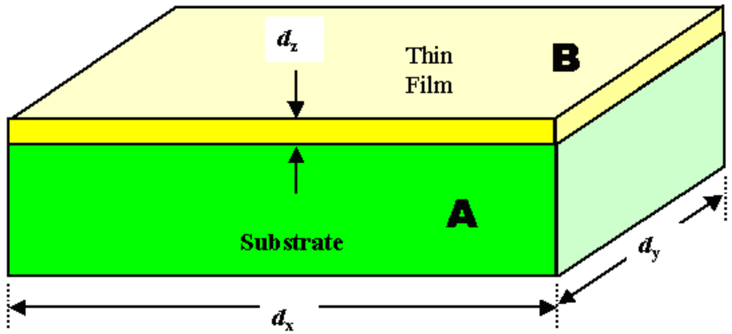

A thin film is a layer of material ranging from fractions of a nanometer (monolayer) to several micrometers in thickness.

Applications:

- magnetic recording media,
- electronic semiconductor devices,
- Integrated passive devices,
- LEDs,
- optical coatings (such as antireflective coatings),
- hard coatings on cutting tools,
- energy generation (e.g. thin-film solar cells)
- energy storage (thin-film batteries),
- pharmaceuticals (thin-film drug delivery),

- Multilayers: multiferroic materials, and superlattices that allow the study of quantum phenomena.

Applications in nuclear fuels?

Surface processes

https://www.powermag.com/exelons-byron-2-completes-first-insertion-of-westinghouse-accident-tolerant-fuel/

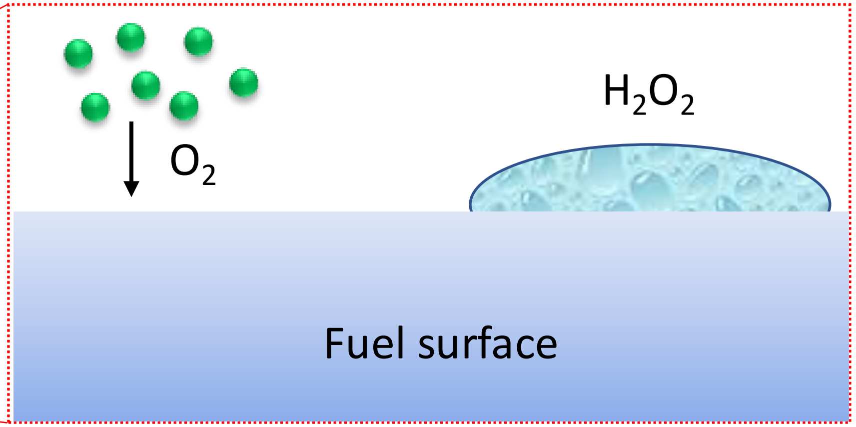

Thin films:
- Excellent representation of a material surface
- No need of a surrogate material

Advantages of thin films?

Reduced radioactivity

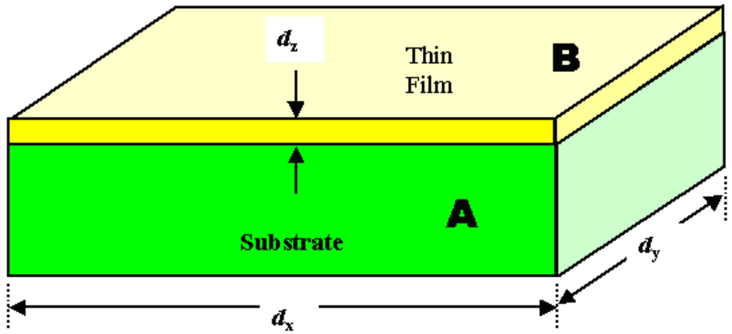

10nm x 1cm x 1cm= $1x10^{-8}m^3$

U density: 19100 kg/m^3

U mass: 19.1 µg

People ingest about 2 micrograms (µg) of natural uranium every day through food, and take in about 1.5 µg for every litter of water they drink.

We ingest almost equivalent of two samples every week!

https://www.vdh.virginia.gov/epidemiology/epidemiology-fact-sheets/uranium/

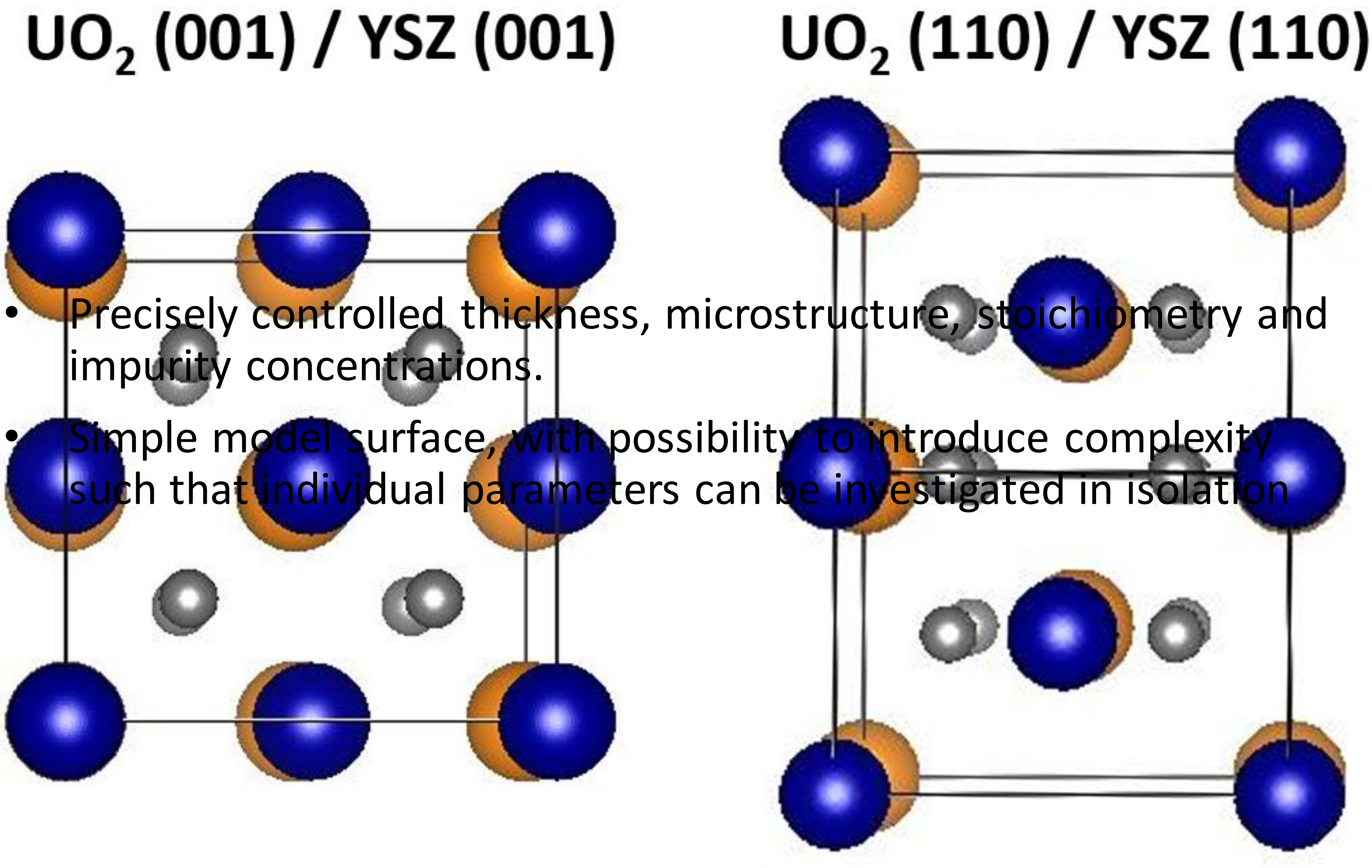

- Precisely controlled thickness, microstructure, stoichiometry and impurity concentrations.
- Simple model surface, with possibility to introduce complexity such that individual parameters can be investigated in isolation

Schematic representation of the epitaxial matches of the three principle UO2 orientations (100), (110) and (111) with (100), (110) and (111) oriented YSZ substrates. The lattice mismatch is the same in each case at 6.3%. (S. Rennie PhD Thesis)

Poly-epitaxy: columnar growth

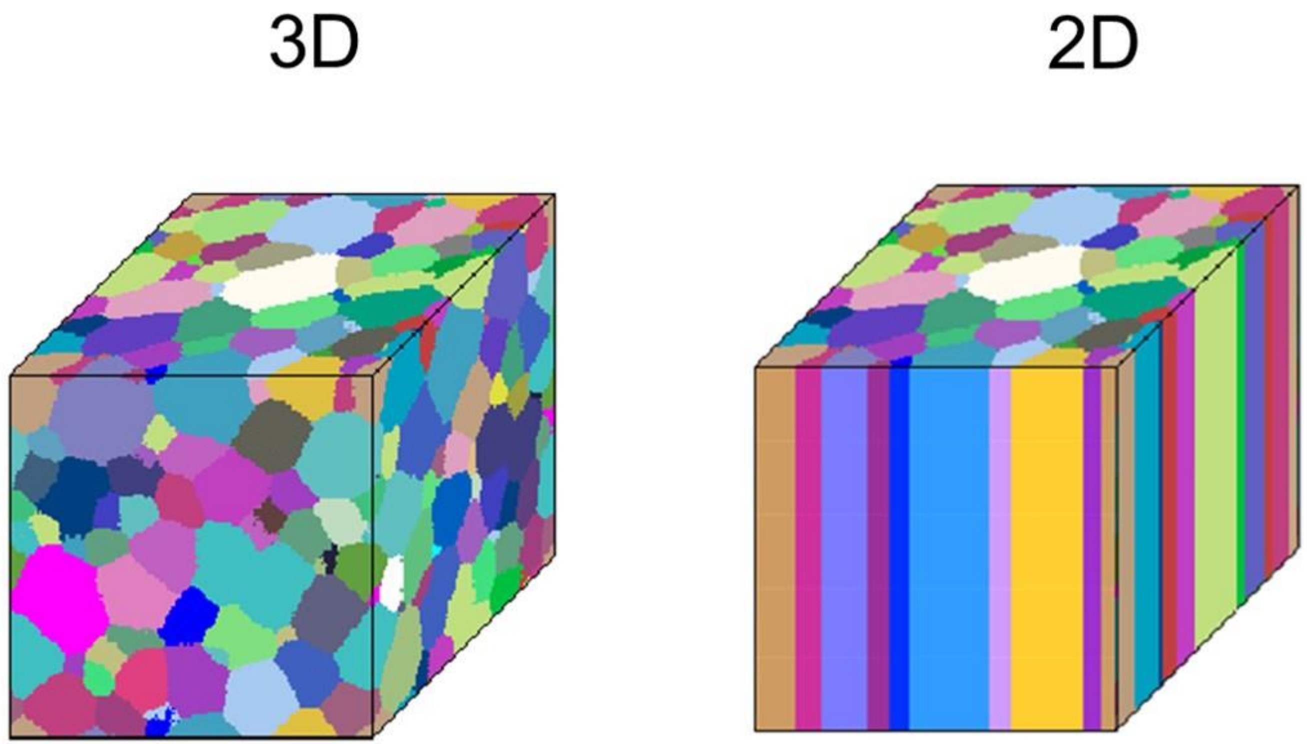

Poly-epitaxy

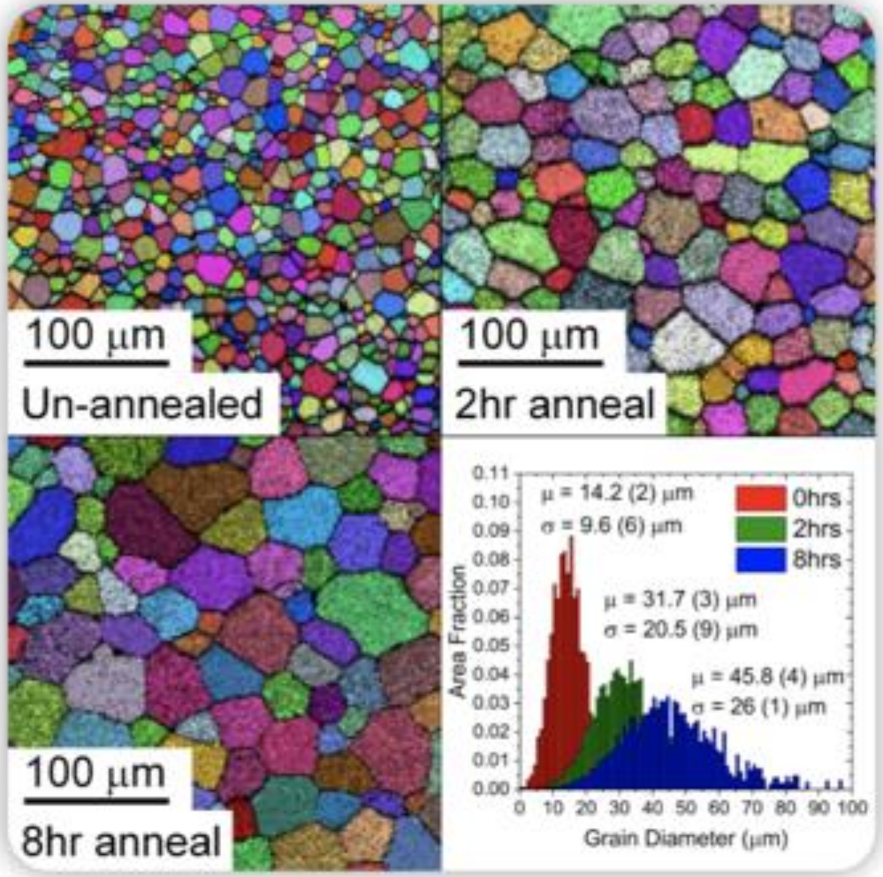

Grain size controllable by annealing in microns

Deposition rate of UO_2 ~1Å/s

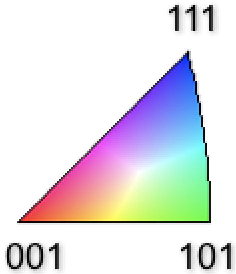

Controlled stoichiometry

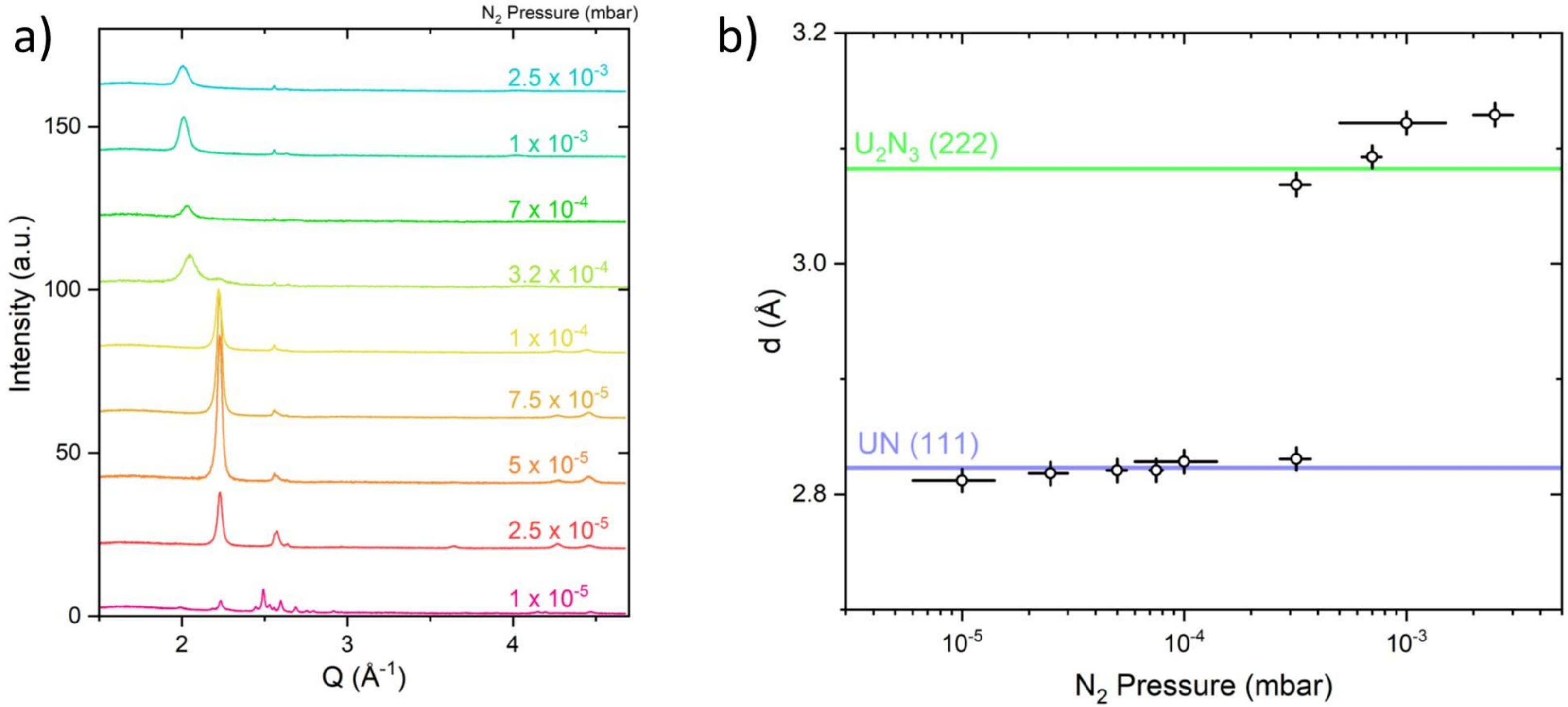

Controlled dopant level

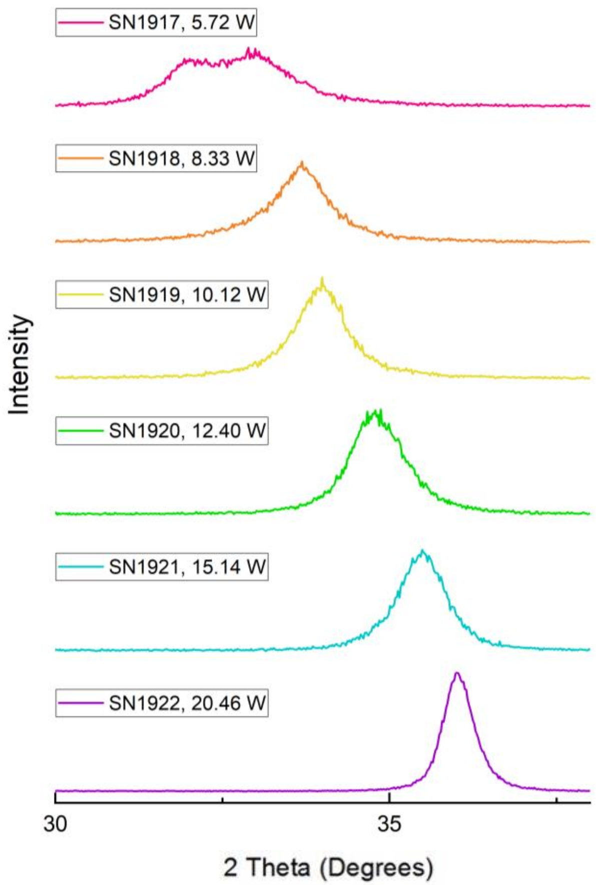

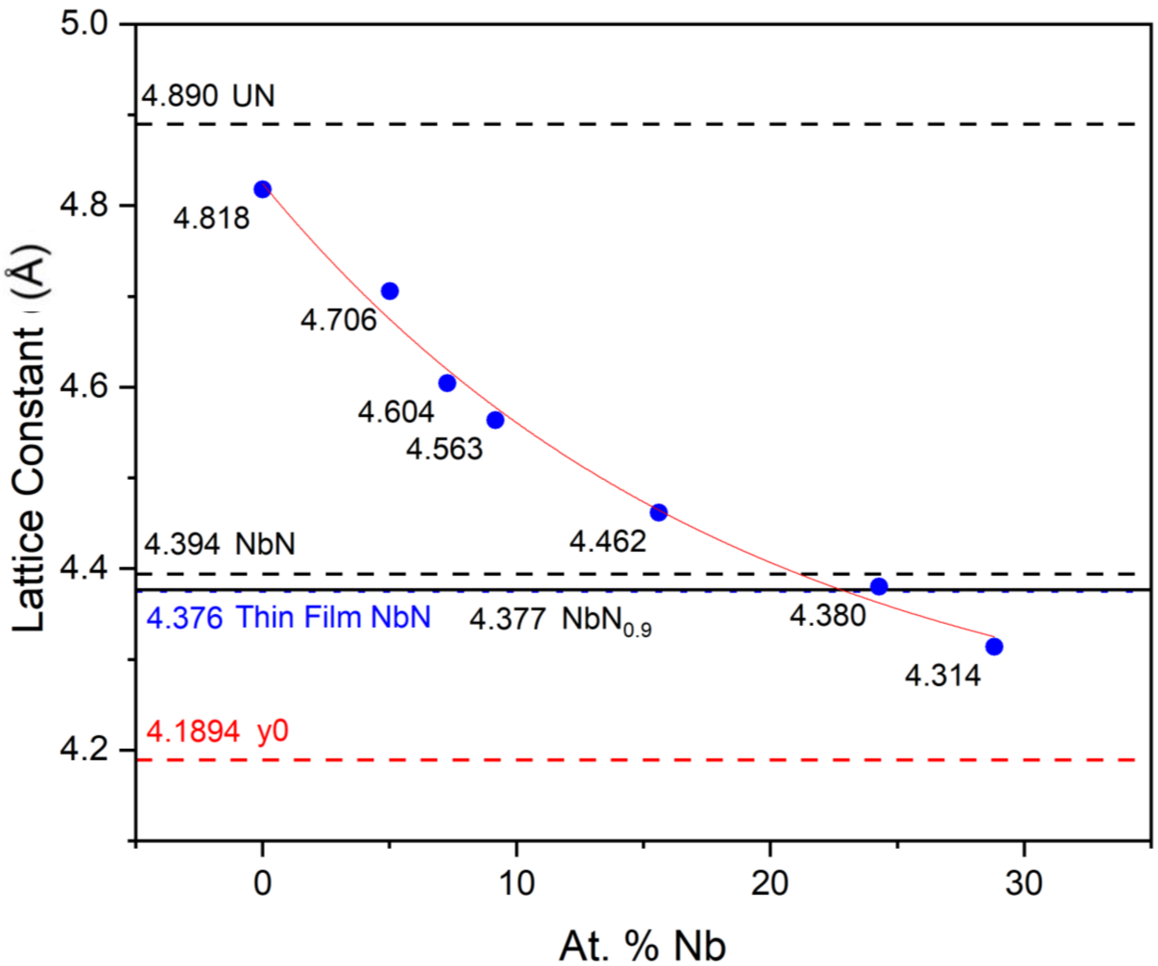

DC magnetron Deposition

- Excellent layer uniformity
- Precise thickness control
- Suitable for many materials
- Very smooth sputtered layers

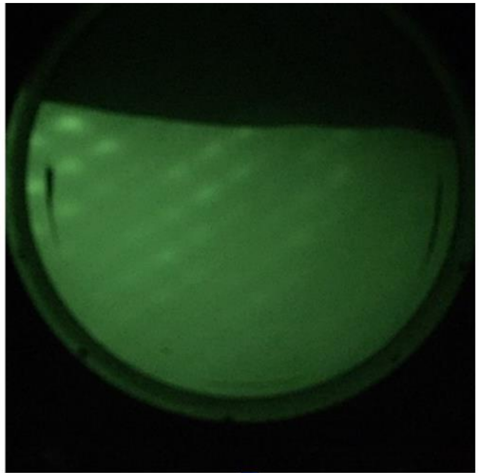

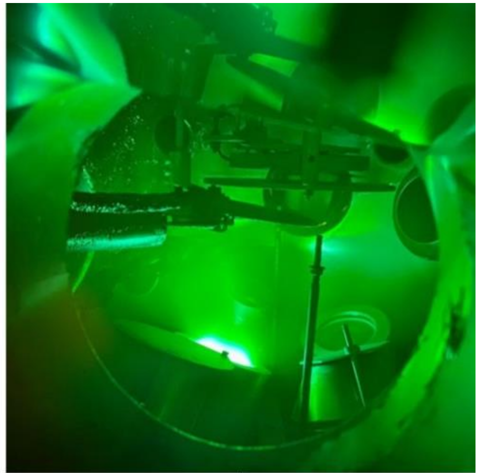

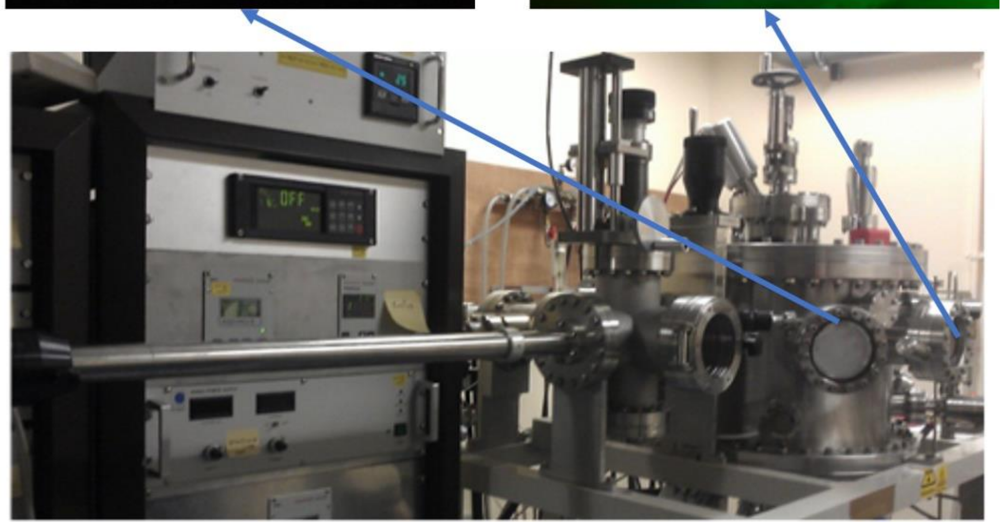

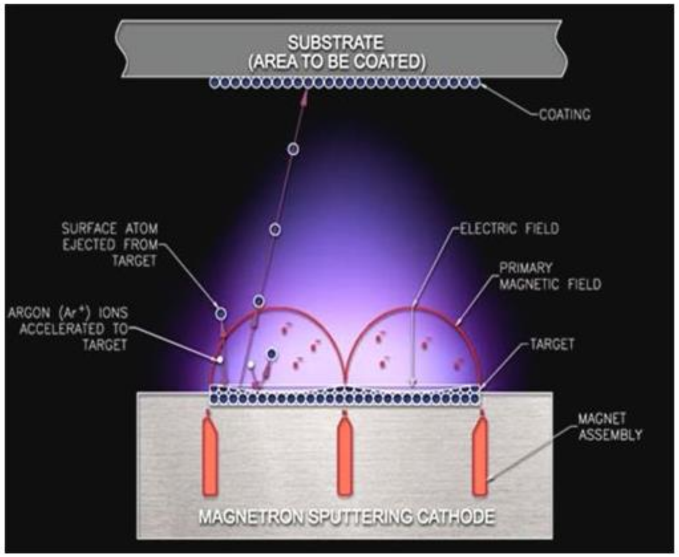

E-beam evaporator

- Higher deposition rate
- Small amounts of starting material

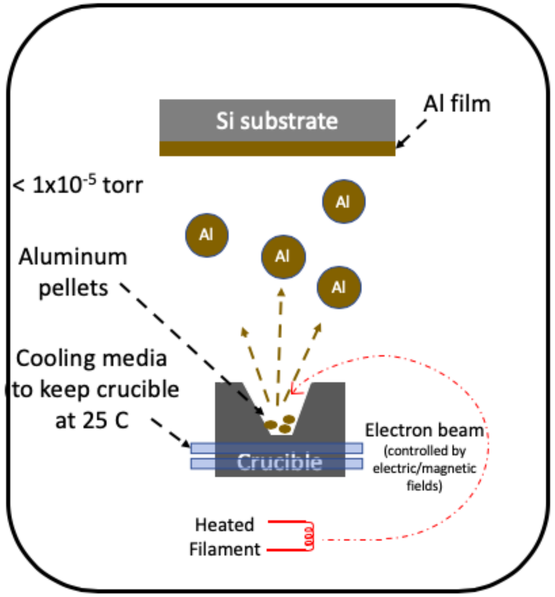

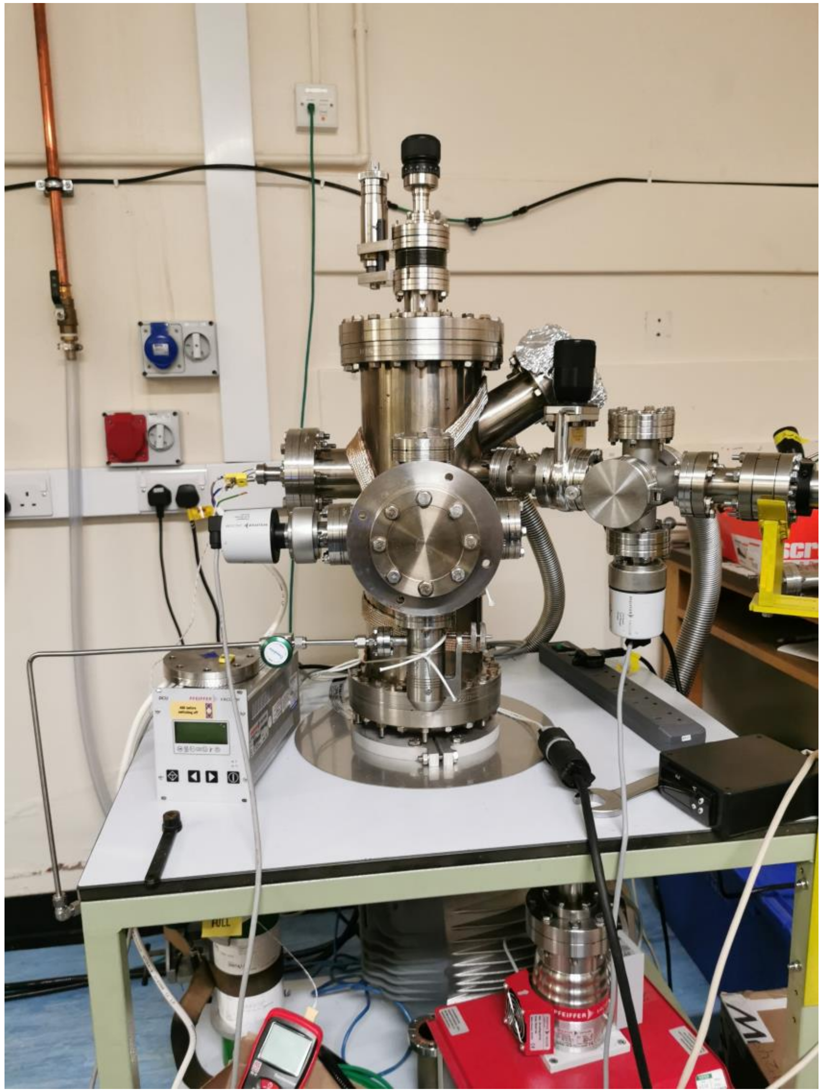

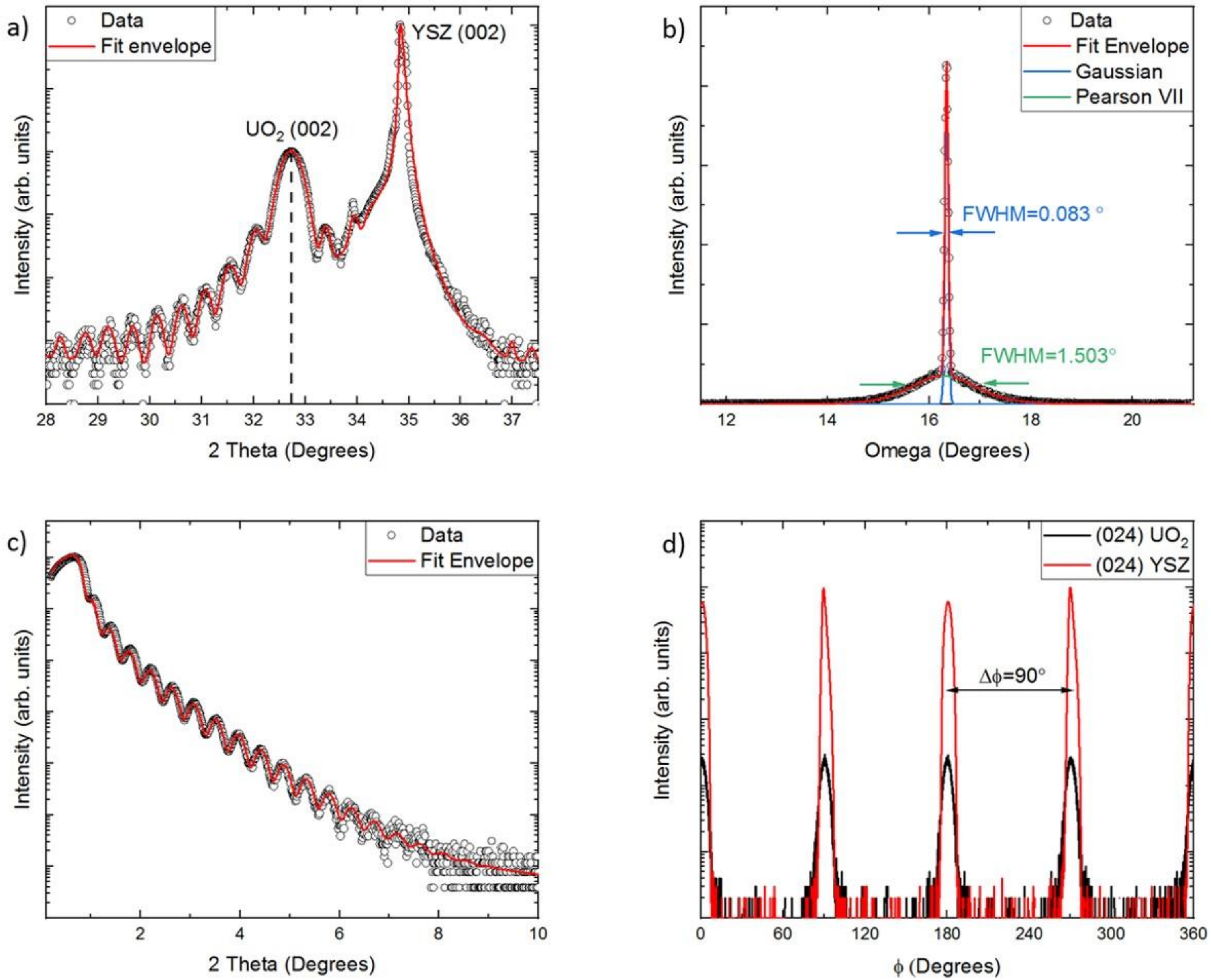
a)
Data
Fit envelope
YSZ (002)
UO_2 (002)
Intensity (arb. units)
2 Theta (Degrees)
b)
Data
Fit Envelope
Gaussian
Pearson VII
FWHM=0.083 °
FWHM=1.503°
Intensity (arb. units)
Omega (Degrees)
c)
Data
Fit Envelope
Intensity (arb. units)
2 Theta (Degrees)
d)
(024) UO_2
(024) YSZ
Δϕ=90°
Intensity (arb. units)
ϕ (Degrees)

In-situ X-ray diffraction oxidation experiment

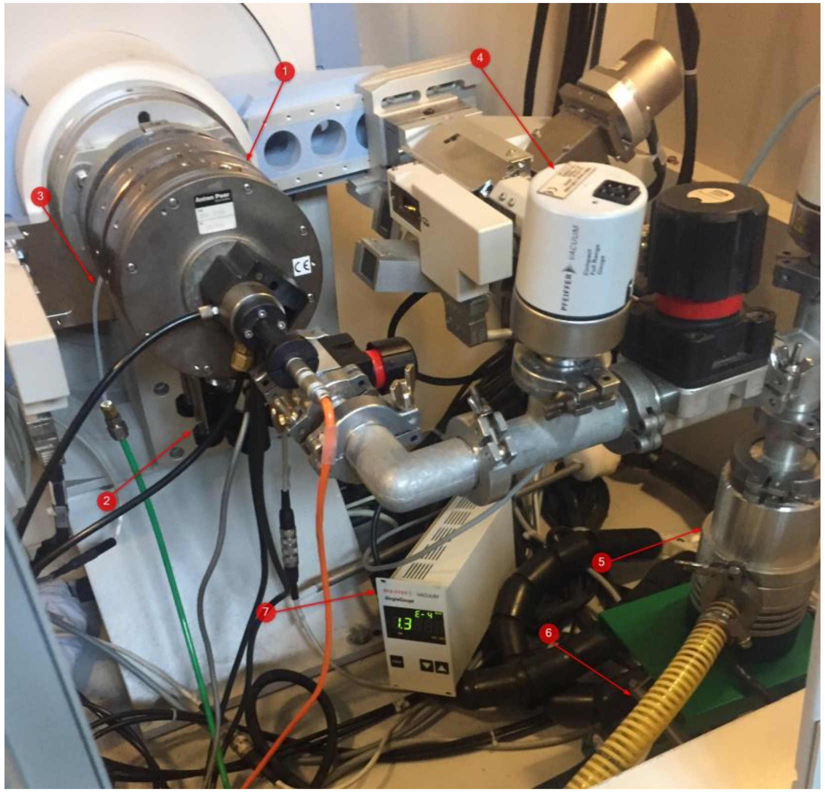

Experimental set-up

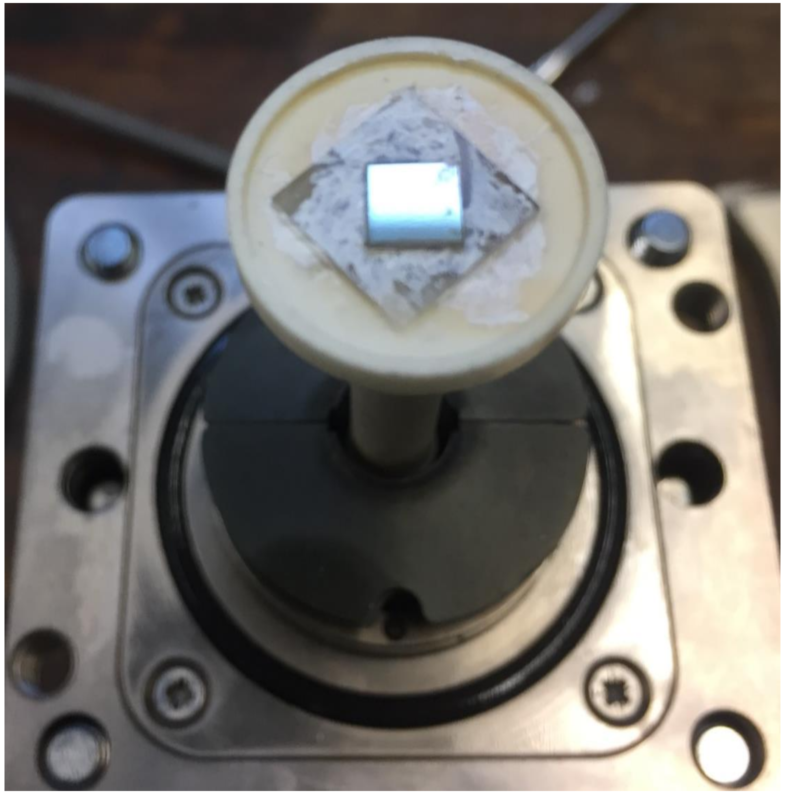

Sample stage

Crystallographic orientation

Schematic diagrams of the UO2 (0 0 1), (1 1 0) and (1 1 1) thin films as a function of dissolution over 270 s.

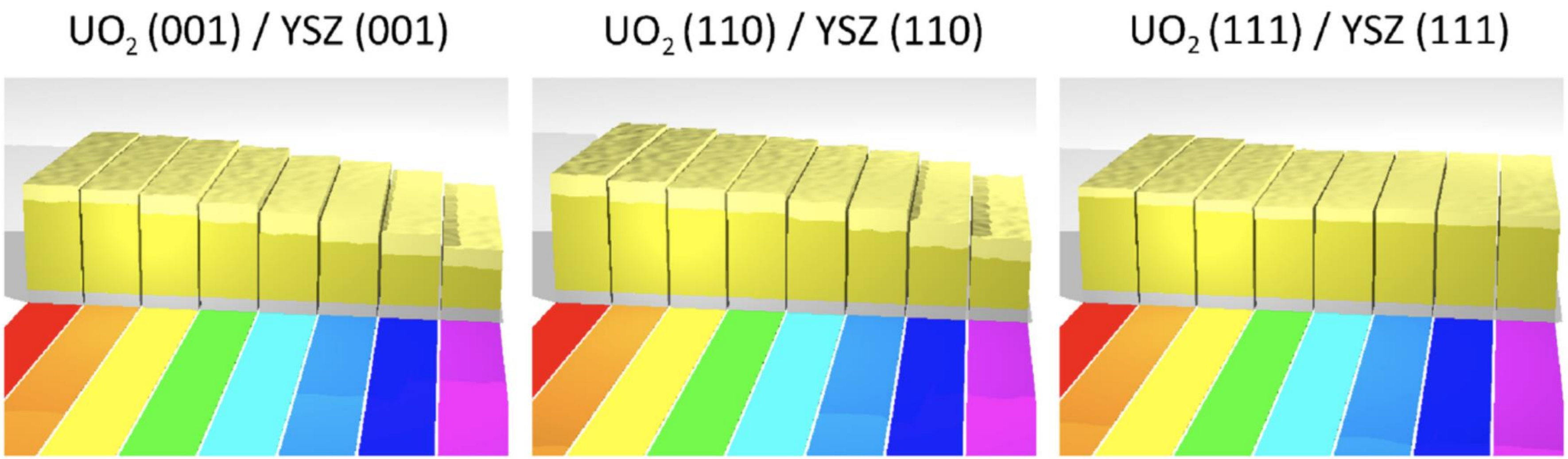

Rennie, S., Bright, E.L., Sutcliffe, J.E., Darnbrough, J.E., Burrows, R., Rawle, J., Nicklin, C., Lander, G.H. and Springell, R., 2018. The role of crystal orientation in the dissolution of UO2 thin films. *Corrosion Science*, *145*, pp.162-169.

Single crystal (111) UO_2 thin film

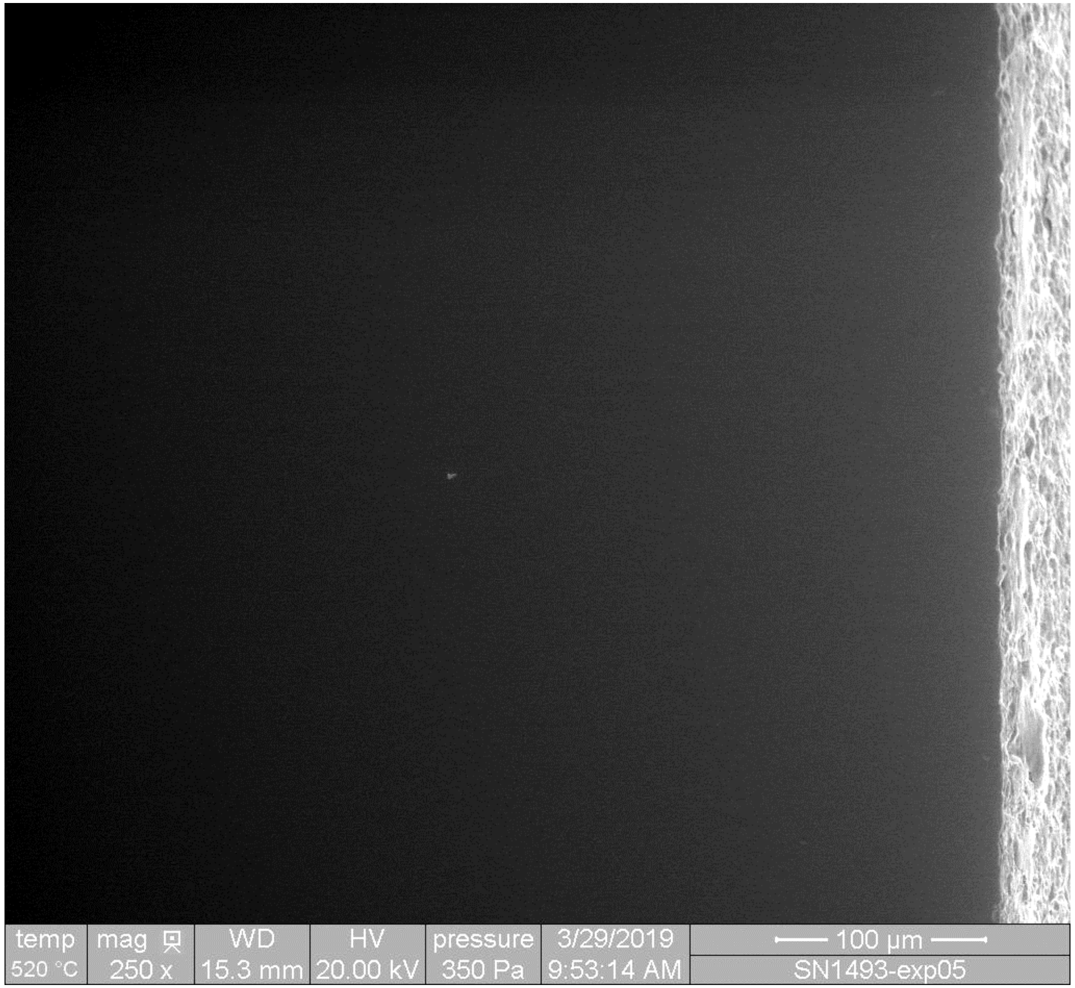

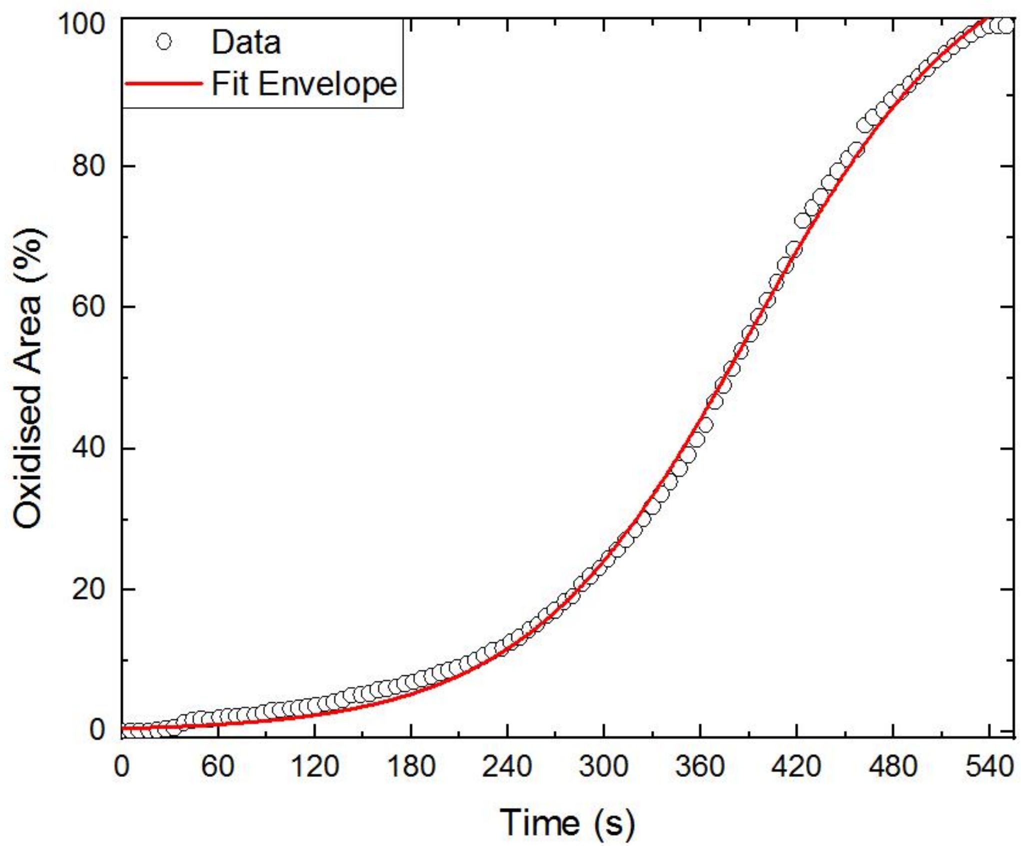

Single crystal (001) UO_2 thin film

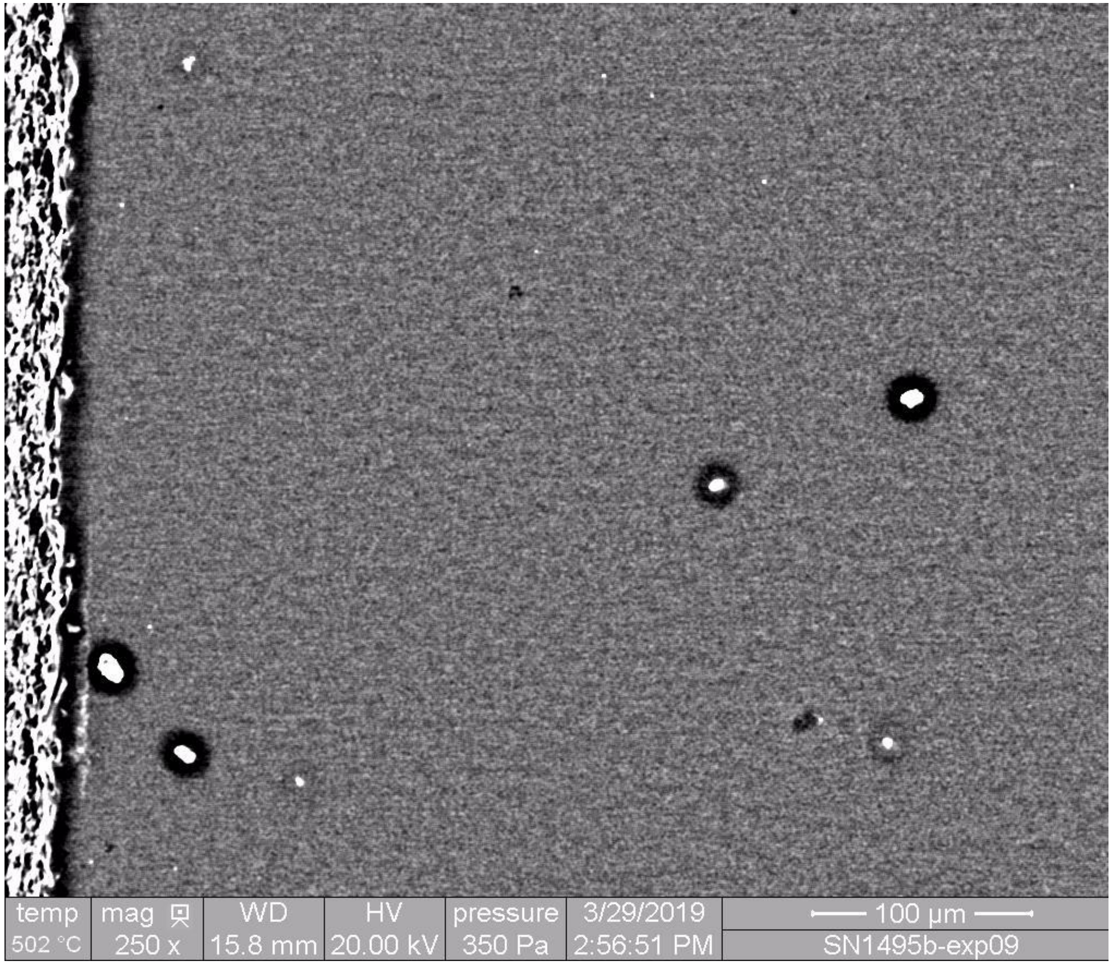

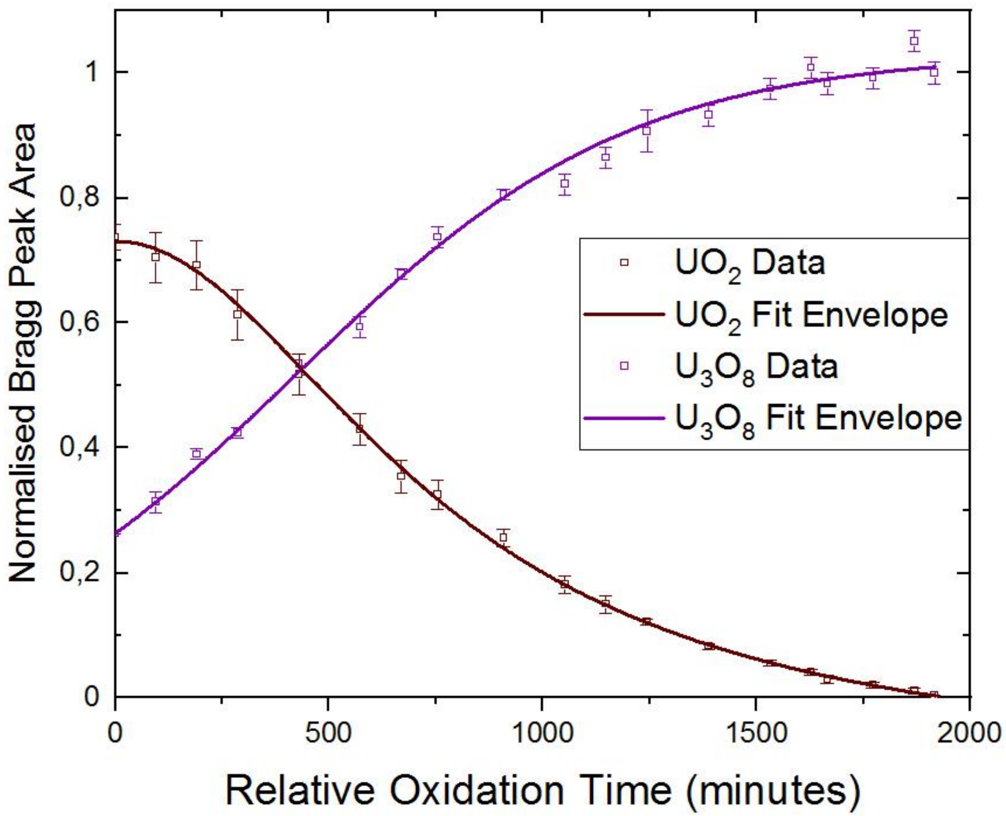

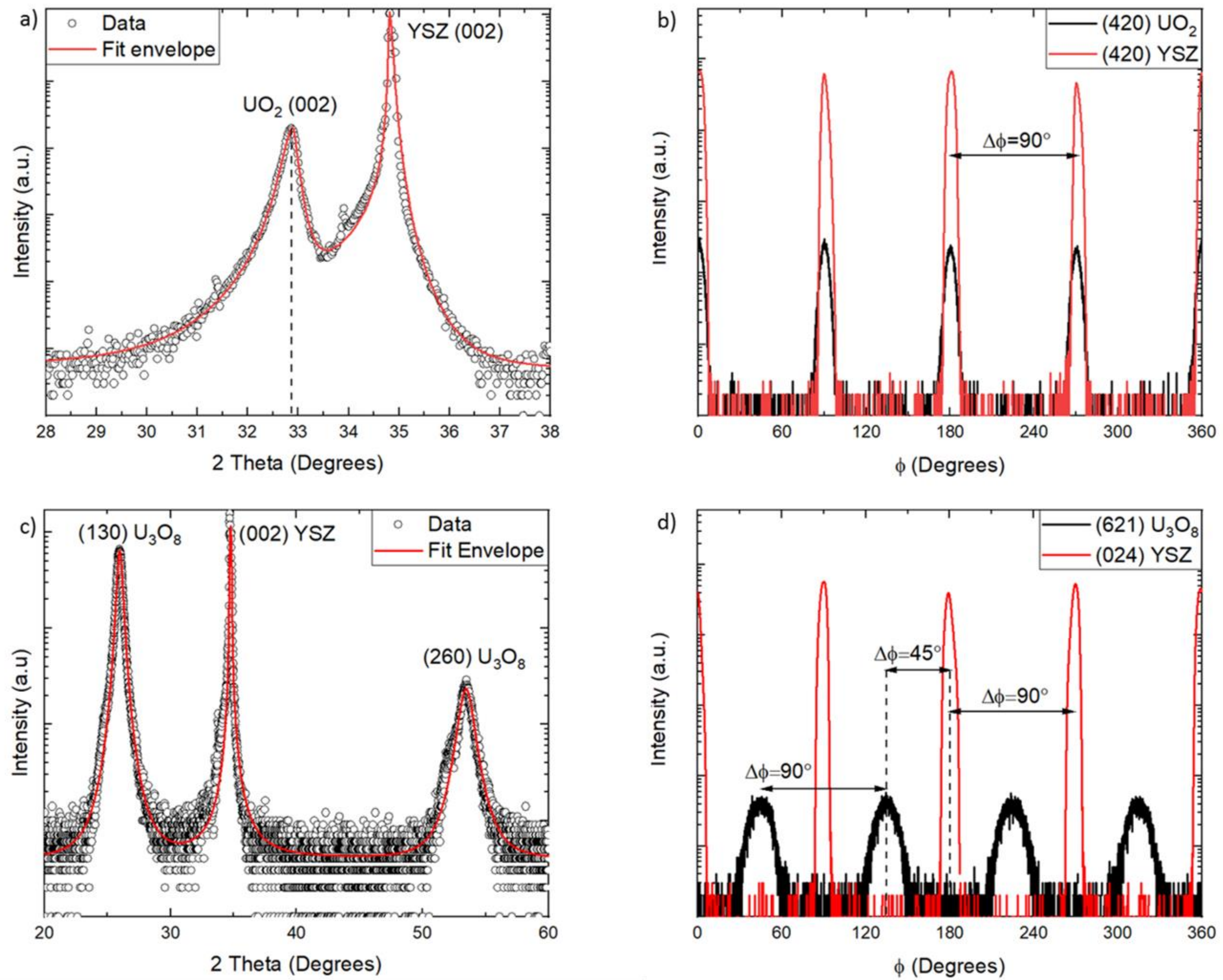

a)
Data
Fit envelope
YSZ (002)
UO2 (002)
Intensity (a.u.)
2 Theta (Degrees)
b)
(420) UO2
(420) YSZ
Δϕ=90°
Intensity (a.u.)
ϕ (Degrees)
c)
(130) U3O8
(002) YSZ
Data
Fit Envelope
(260) U3O8
Intensity (a.u)
2 Theta (Degrees)
d)
(621) U3O8
(024) YSZ
Δϕ=45°
Δϕ=90°
Δϕ=90°
Intensity (a.u.)
ϕ (Degrees)

Topotactic phase transition

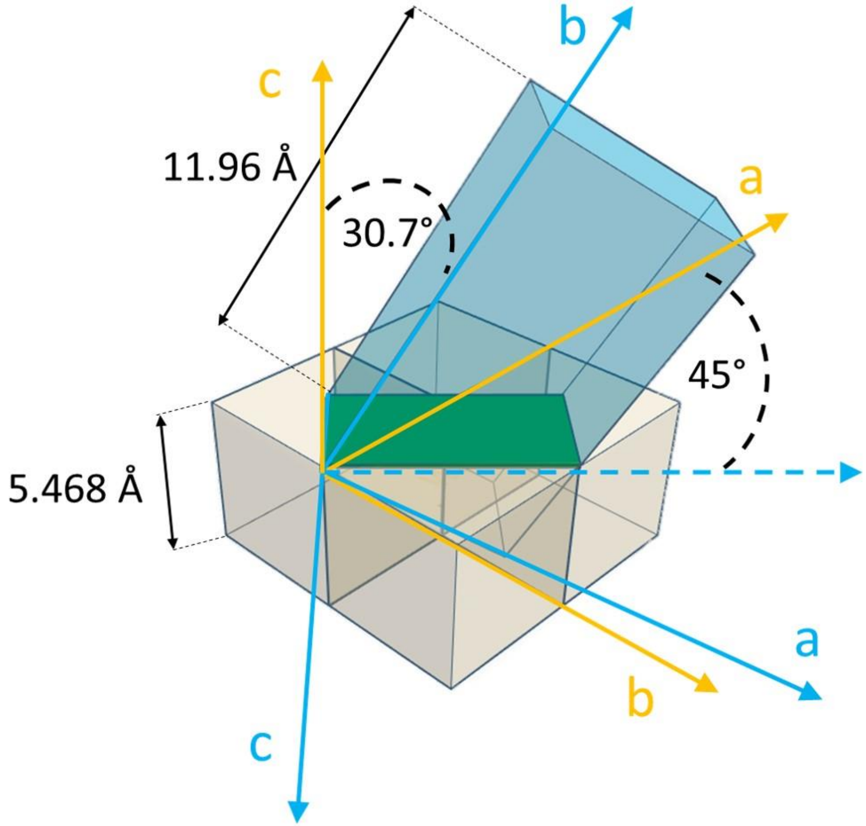

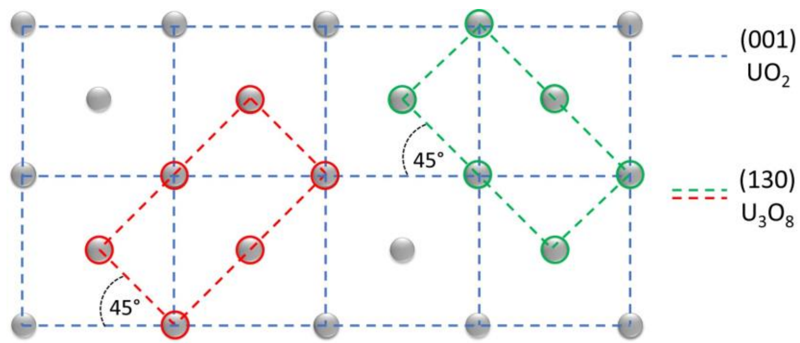

Poly-epitaxial UO_2 thin film

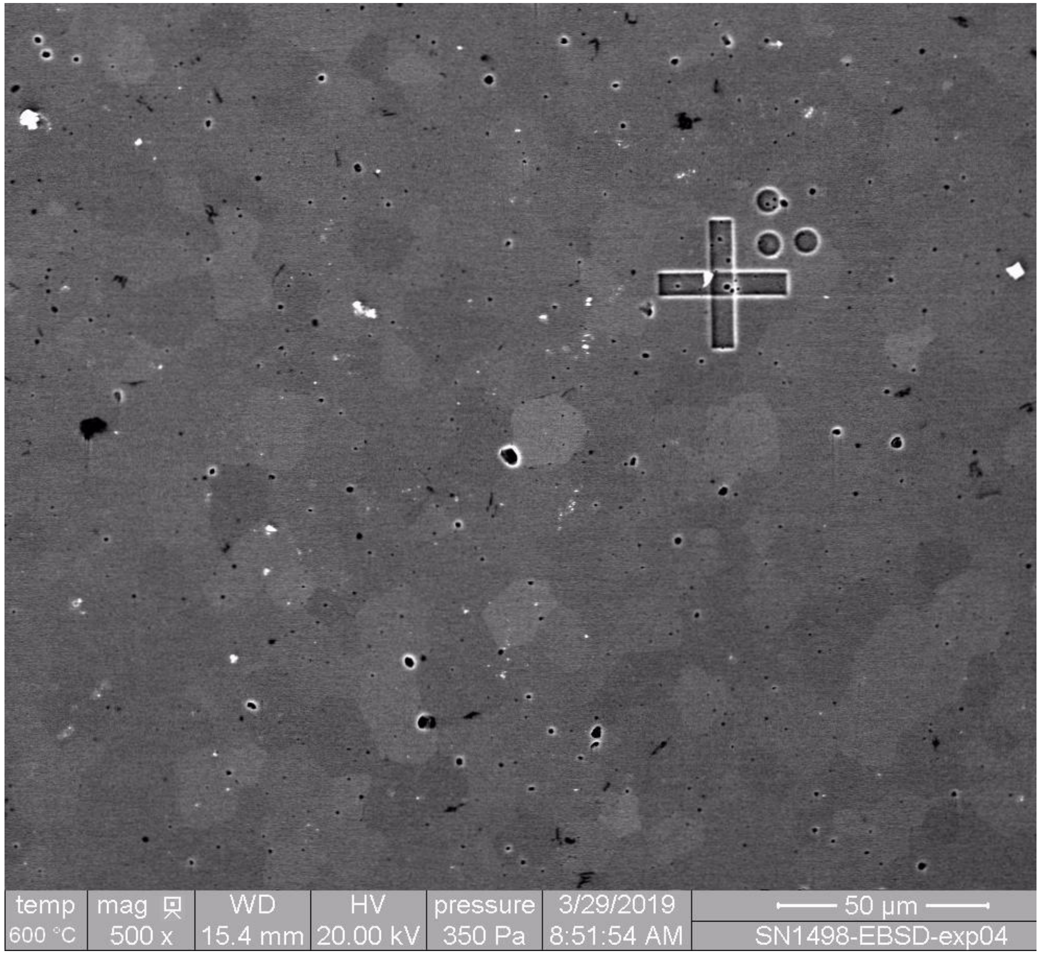

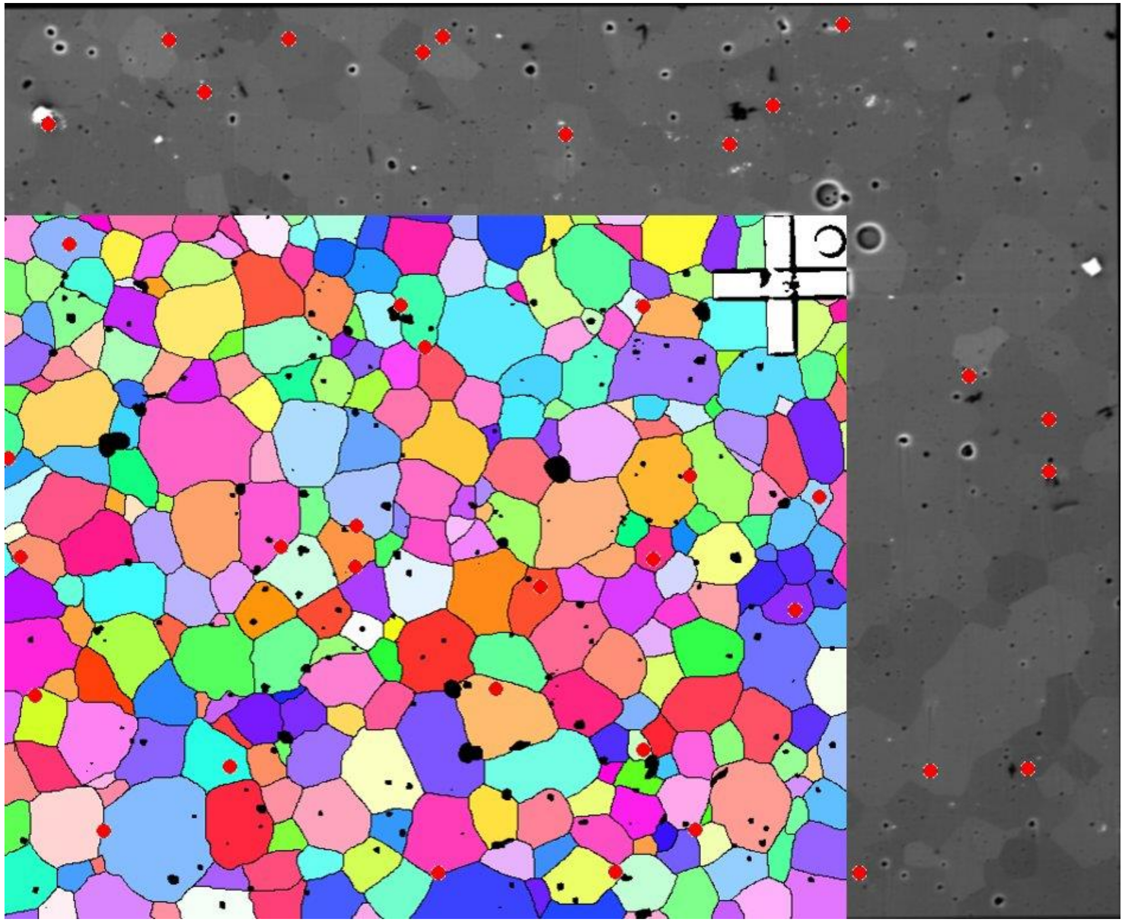

Poly-epitaxial UO_2 thin film

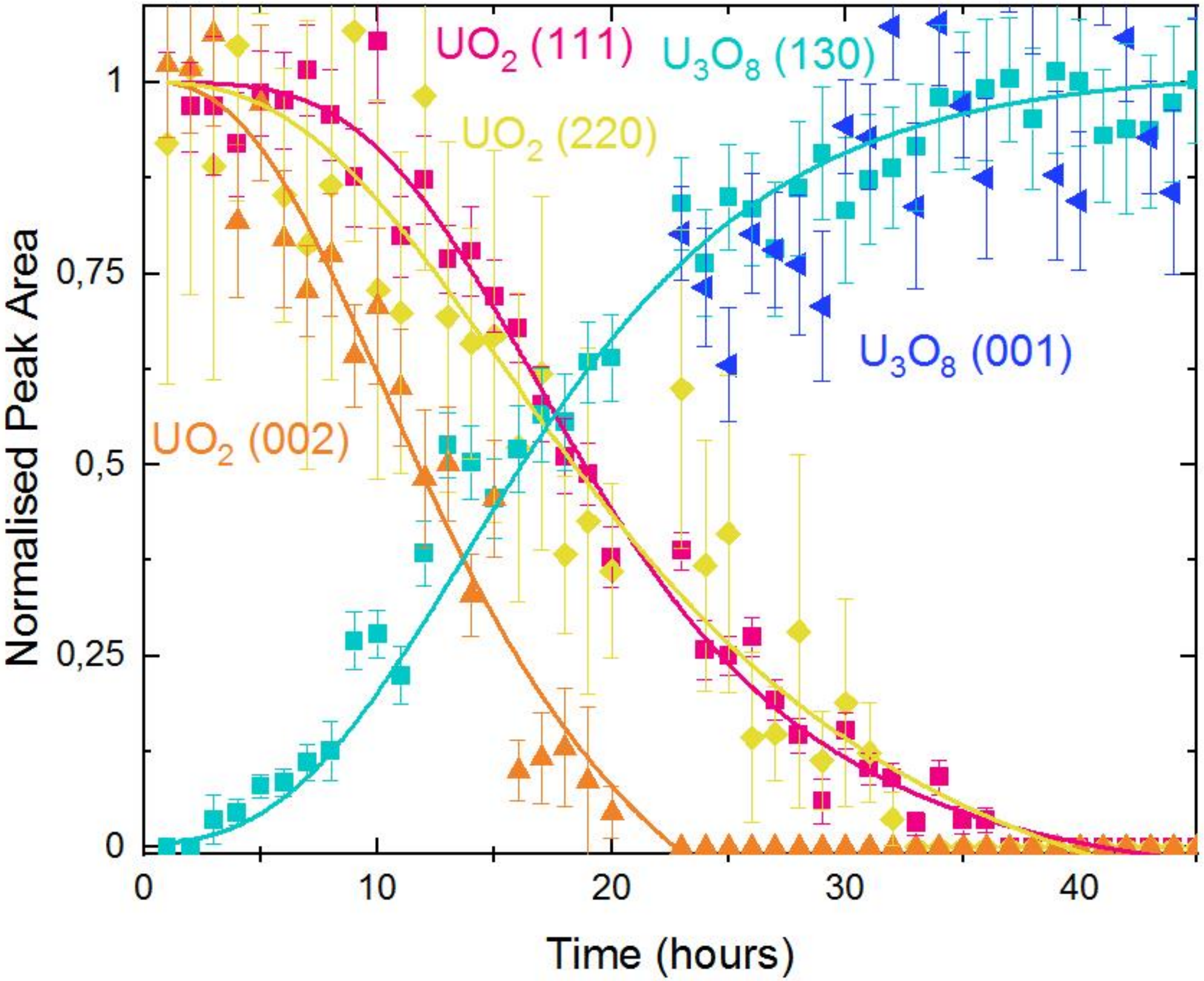

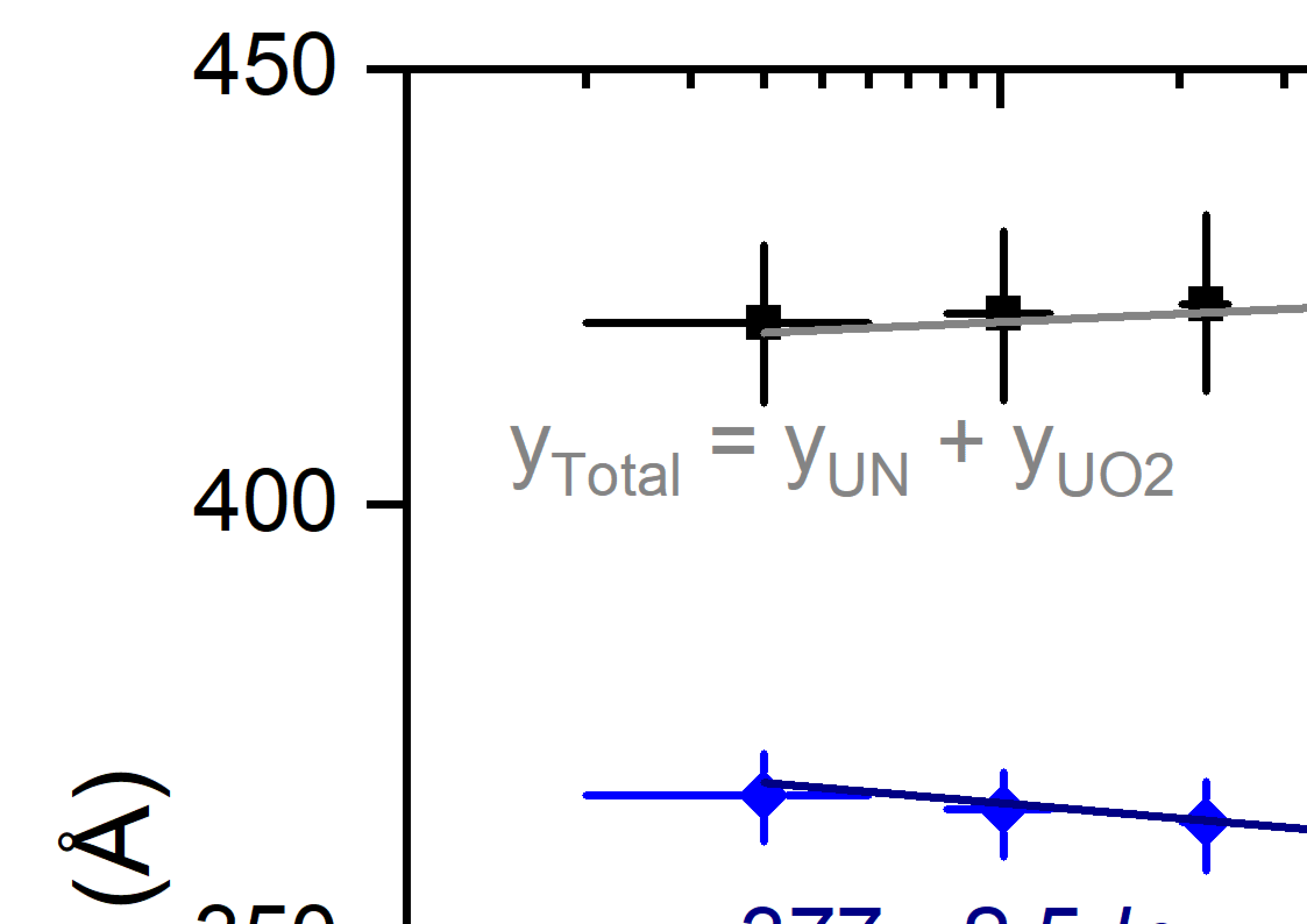

450
400
(Å)
$y_{Total} = y_{UN} + y_{UO2}$

UN corrosion

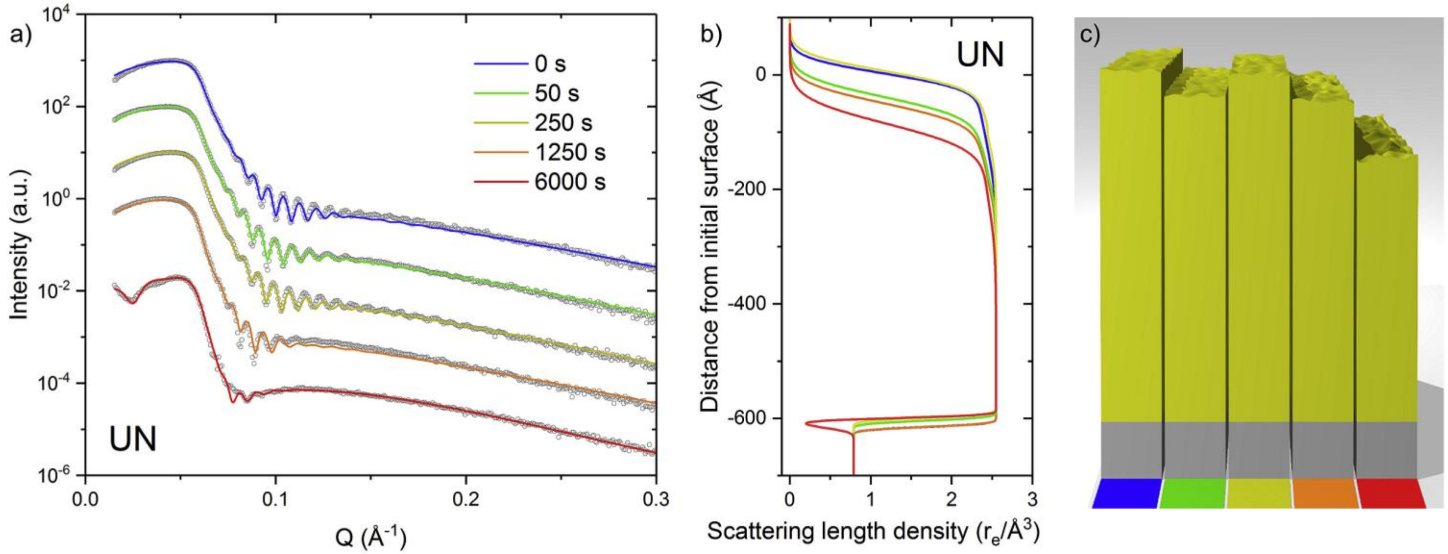

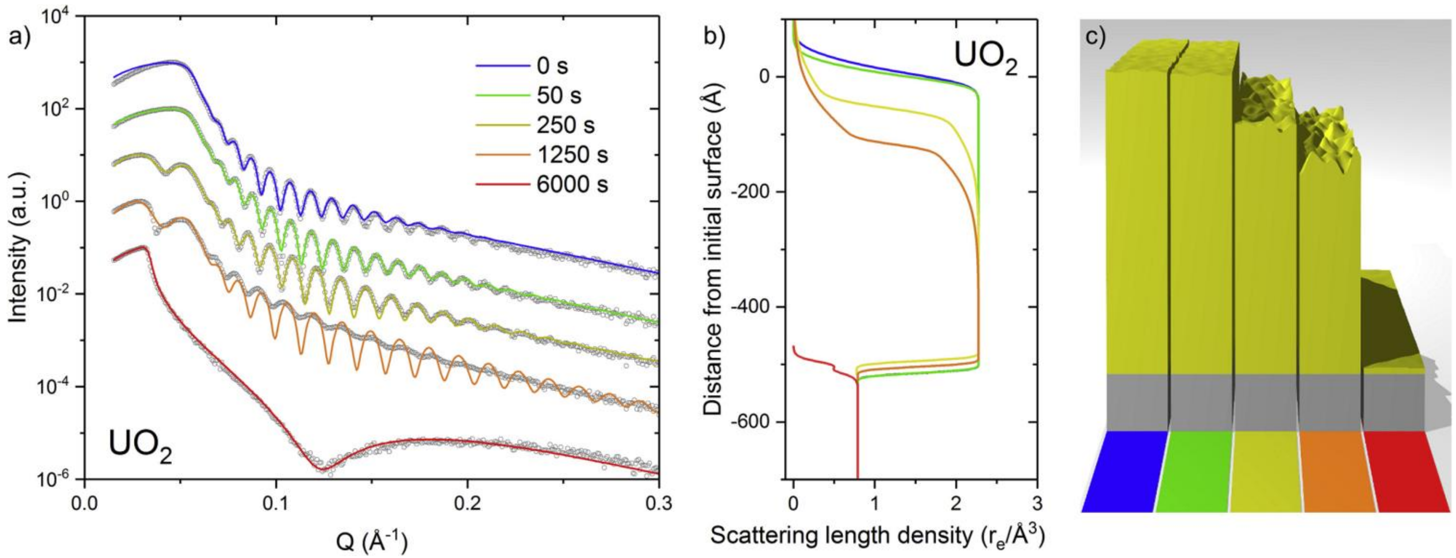

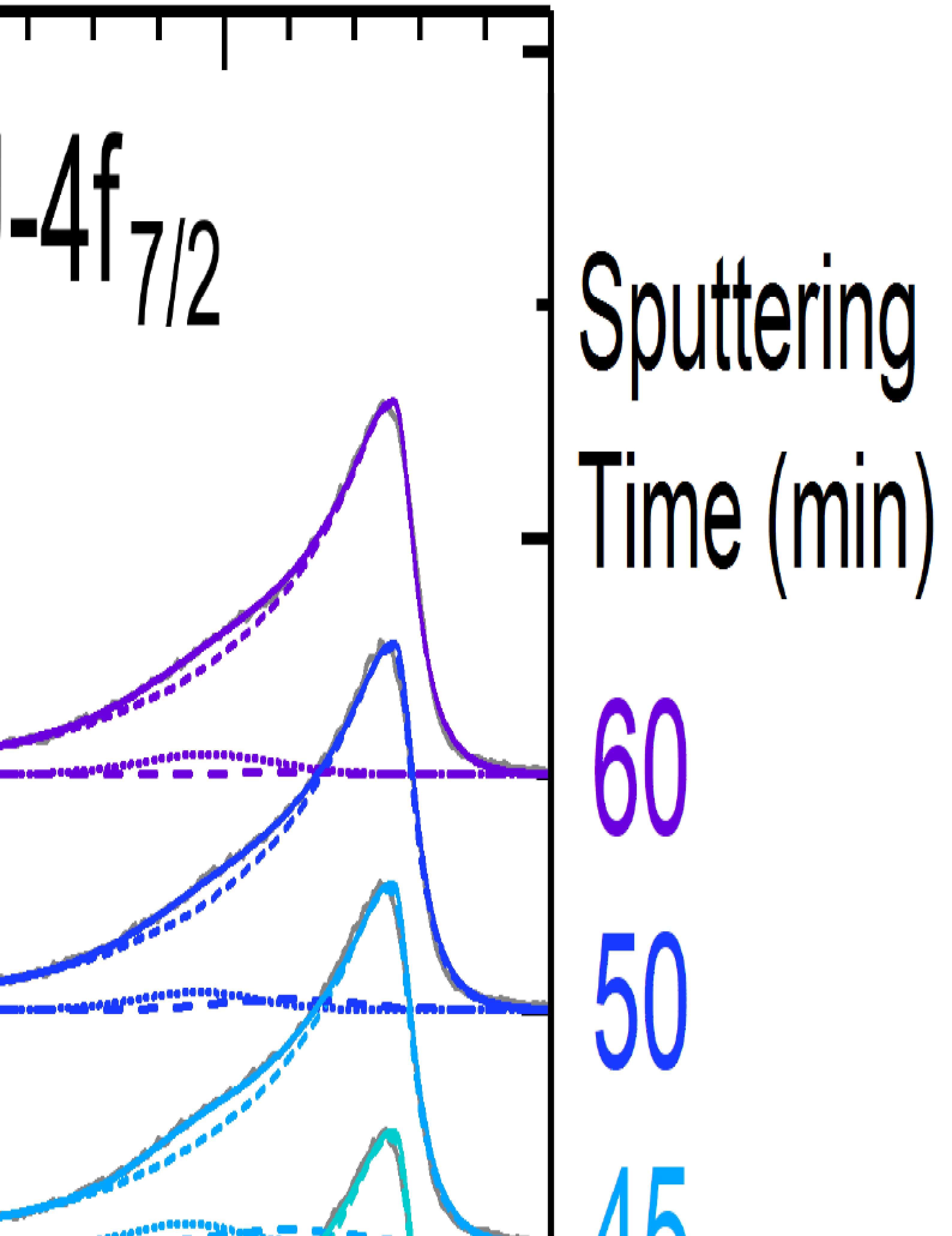

-4f7/2
Sputtering
Time (min)
60
50
45

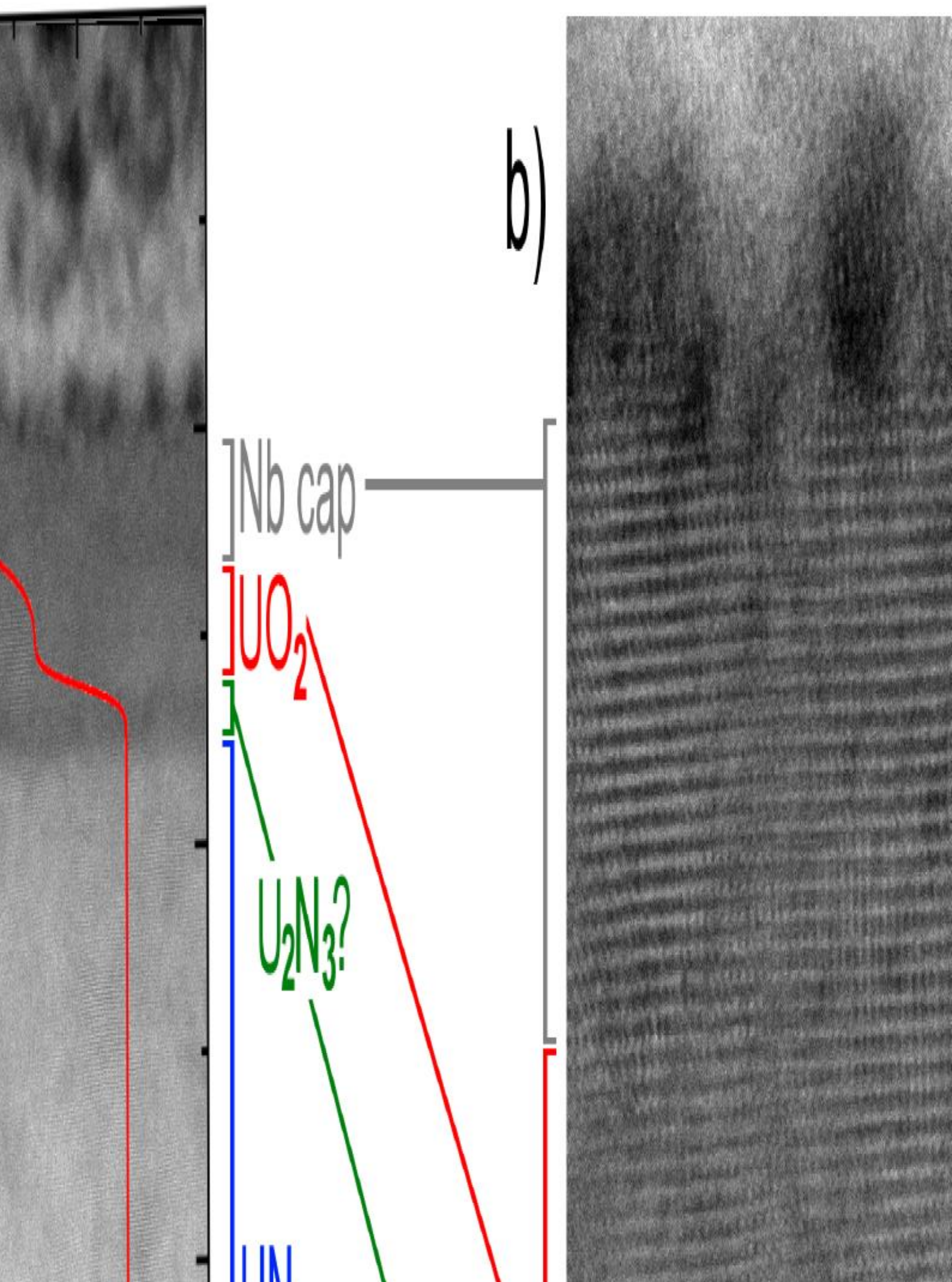

b)
Nb cap
UO_2
U_2N_3?
UN

Summary

Fabrication:

Controlled microstructure: single-crystal, polycrystalline, poly-epitaxial;

Thickness, stoichiometry, grain size, dopants

Characterization:

XRR/XRD (in-situ experiments)

XPS depth profiling

Electron and Ion microscopy (in-situ experiments)

NNUF system

In-situ deposition system with attached depth profiling XPS and environmental chamber

Facility for **R**adioactive **M**aterials **S**urfaces

FaRMS
Facility for Radioactive Materials Surfaces

FARMS

FaRMS
Facility for Radioactive Materials Surfaces

FARMS

Thank you

Jacek.Wasik@bristol.ac.uk
phrss@bristol.ac.uk

TRANSCEND

Transformative Science and Engineering for Nuclear Decommissioning

Water radiolysis on metal oxides and radiation hardness testing of experimental systems

Chris Anderson, Dalton Cumbria Facility, University of Manchester

Theme 4: Nuclear Materials

02/11/2021

Email: christopher.anderson-3@postgrad.manchester.ac.uk
Mobile: 07857420556

Who am I?

PhD student at this sunny place

Gas generation from the radiolysis of water on uranium and thorium oxides

Radiation hardness testing of experimental systems

What is water radiolysis?

Water Radiolysis = Radiolytic decomposition of water

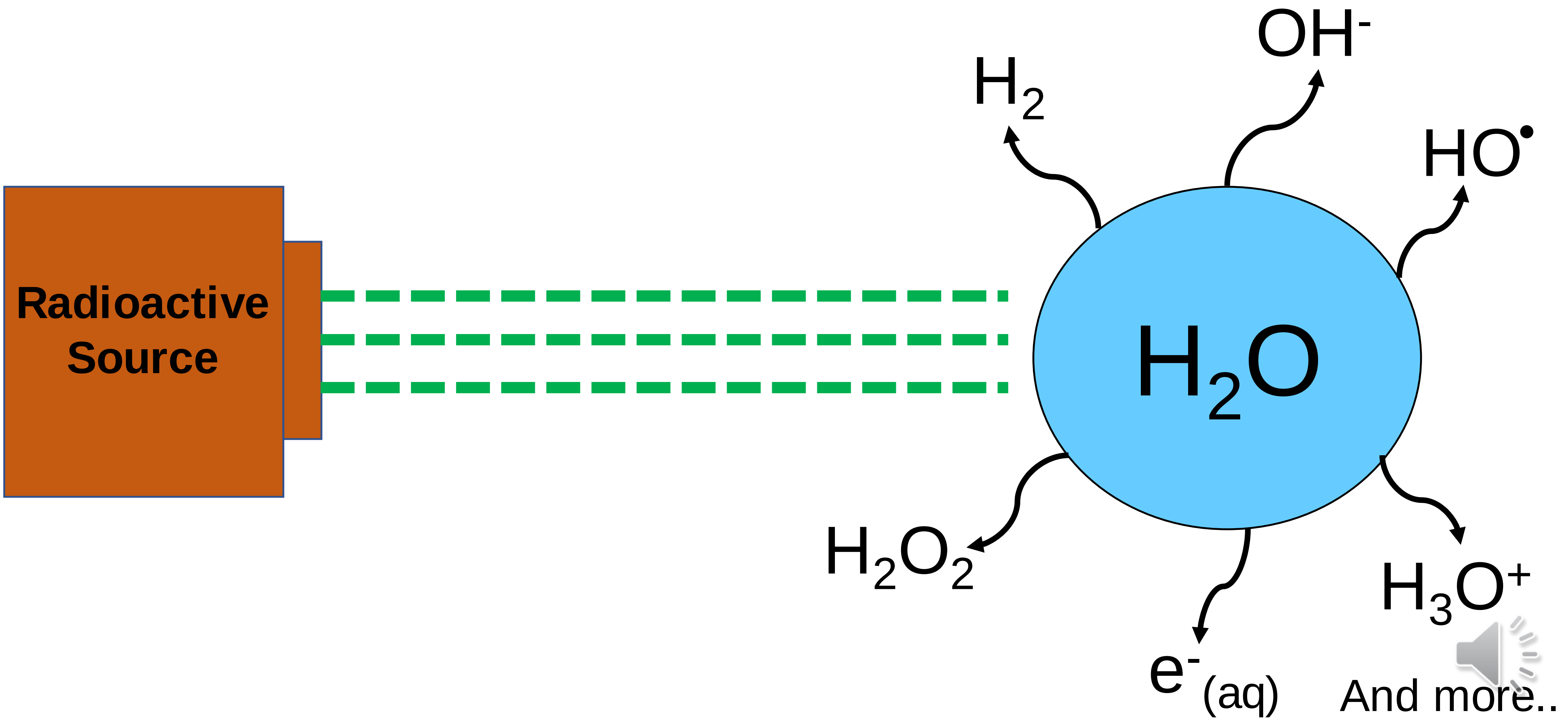

Why is it important?

The products of water radiolysis vary in desirability

For example:

The Good

Hydroxyl radicals in radiotherapy

Useful!

The Bad

H_2 is explosive..

So not great.

Not so useful!

The Confusing

Add an oxide interface for the water

Can hugely modify yields of products.. or do nothing

Transformative Science and Engineering for Nuclear Decommissioning

Adding an oxide..

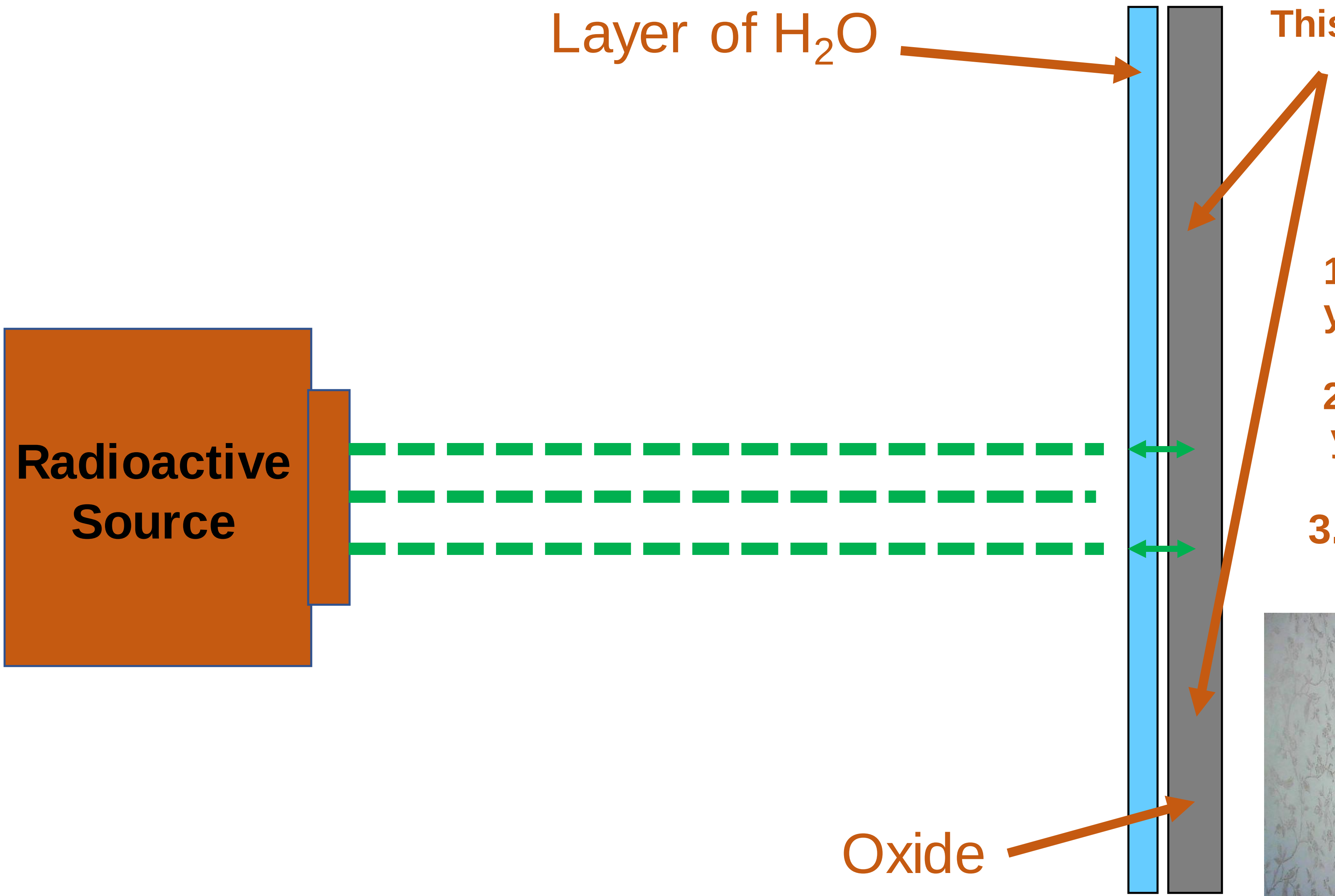

This has one of 3 effects

1. **Increases the yield of product**
2. **Decreases the yield of product**
3. **Does nothing**

How is yield determined?

Radiolysis uses “G” values to quantify yield

G values are specific to product, example: $G(H_2)$ = H_2 yield

G = Molecules produced/100 eV

More examples:

$G(H_2)$ for just H_2O = 0.45

$G(H_2)$ for water on ZrO_2 = 20-80

$G(H_2)$ for water on MnO_2 = 0.002-0.0

Why does this occur?

Nobody knows for sure!

There's plenty of suggestions →

Adsorbed water layers

"Band gap distance and resonance"

Number of binding sites for water

"Auger Electrons"

Dose rate and type of radiation

LET

"Migration of Excitons"

Crystalline phase of the oxide

"Electron hole transport"

Particle size

"Electron hole recombination"

Doping, intentional or other

"Dissociative electron attachment of low-energy electrons"

"Excess electrons and their subsequent reactions"

"Exciton migration distance"

Transformative Science and Engineering for Nuclear Decommissioning

Controlling the environment

Radiolysis experiments for $G(H_2)$ tend to be conducted within a closed system

A dependable method of live measurement during irradiation would be even more beneficial..

Solenoid valve

Filter

Sample holder

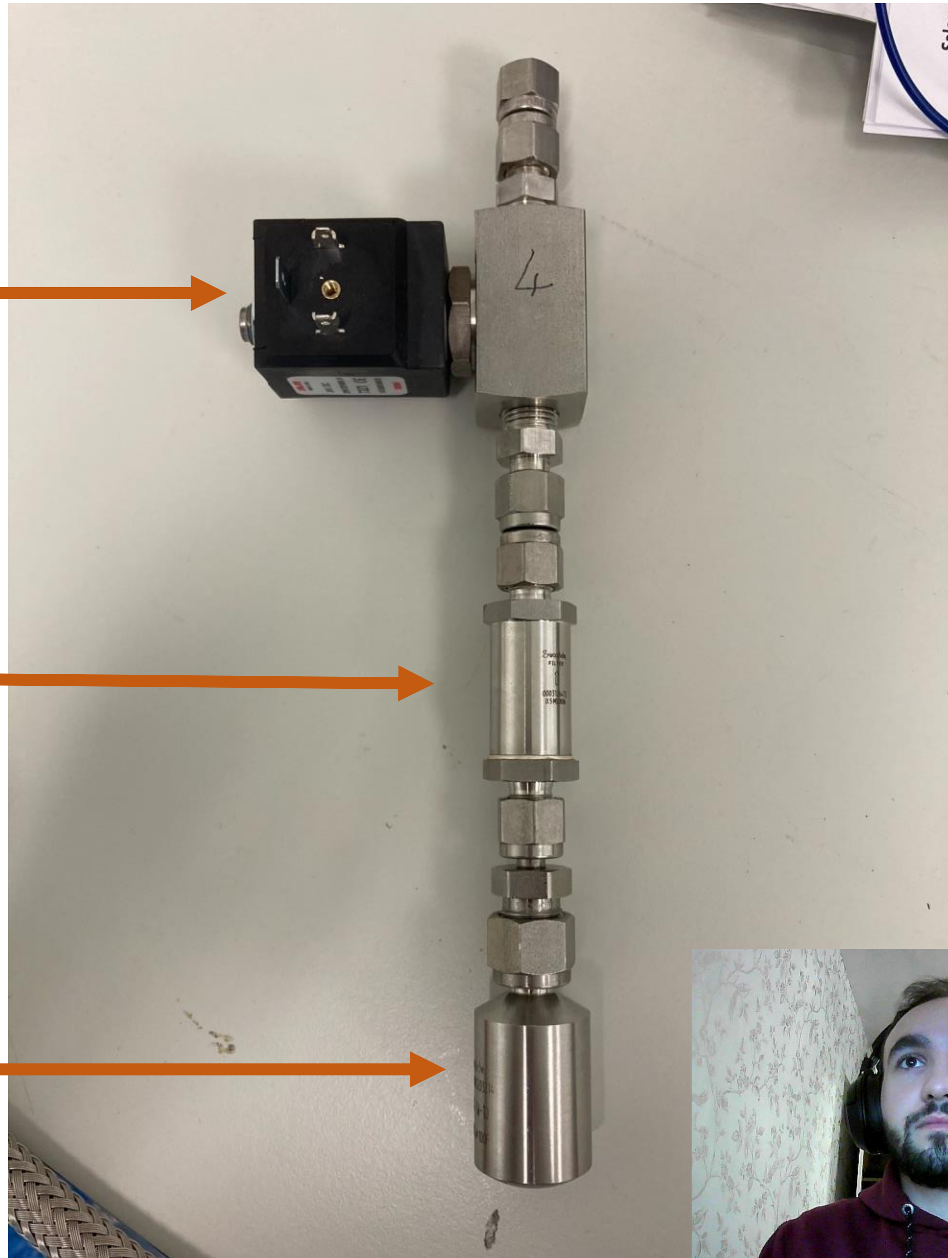

lear Decommissioning

Outside world

Radiation hardness

This apparatus uses solenoid valves

Solenoid valves are electrical components

Solenoid valves also have a seal (usually polymer)

This does too but to a lesser degree

Needs to withstand radiation

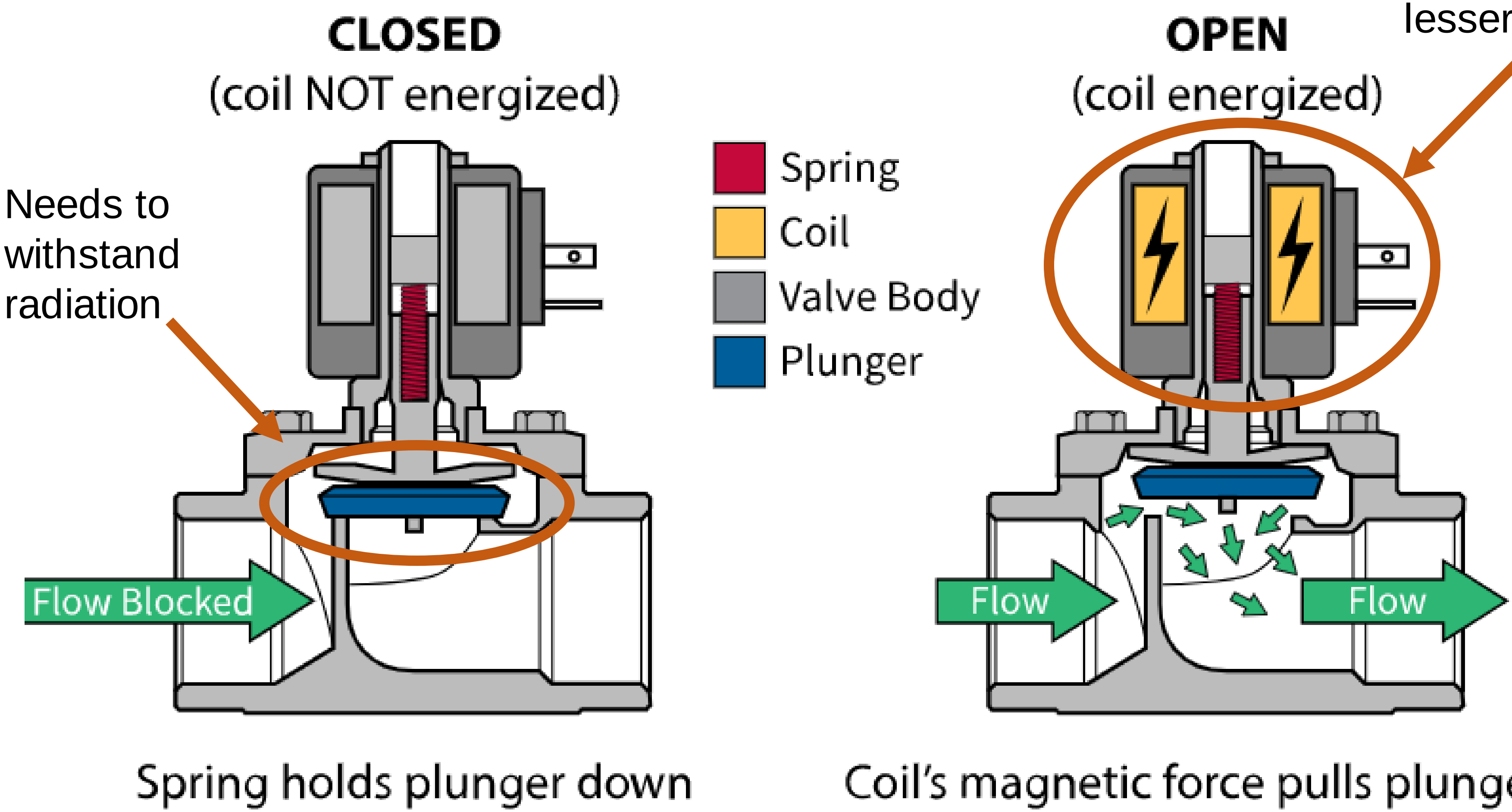

TRANSCEND

Transformative Science and Engineering for Nuclear Decommissioning

Radiation hardness – the experiment

Take 3 commercially available and affordable solenoid valves..

EPDM seal
stainless steel

NBR seal
brass

Synthetic Ruby seal
stainless steel

Radiation hardness – the experiment

For obvious reasons you can't seal fittings with PTFE tape

Copper gaskets

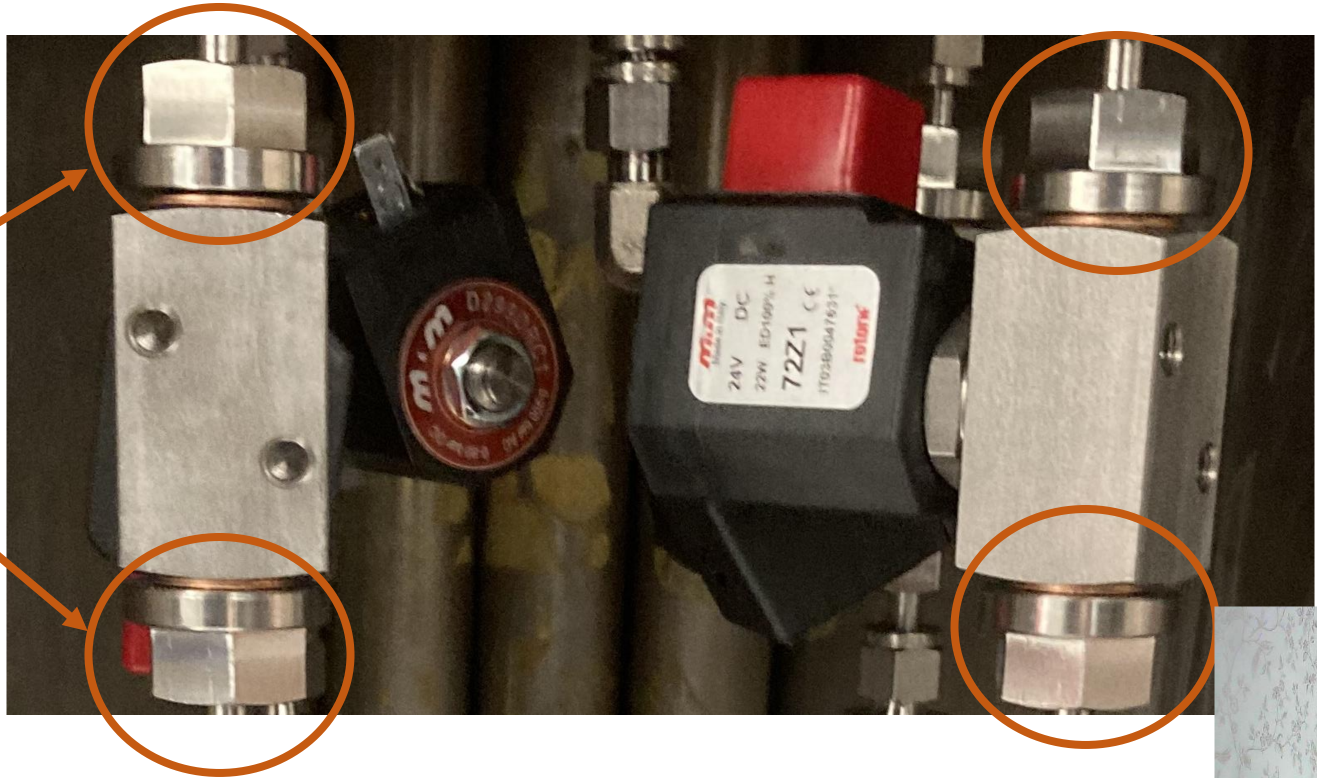

Radiation hardness – the experiment

Multiple of each valve type irradiated at 5 dose intervals and leak tested for periods of 10 minutes each

One end of the valve is attached to a gas manifold with vacuum conditions

The valve is closed and the other end is connected to nothing

If there is a leak, the pressure transducer would record this as air would travel through the damaged seal into the manifold

Pressure is recorded at each interval with the vacuum pump and then after 10 minutes

Transformative Science and Engineering for Nuclear Decommissioning

Leak test results - NBR

(Still playing with the data as much of it is relatively new)

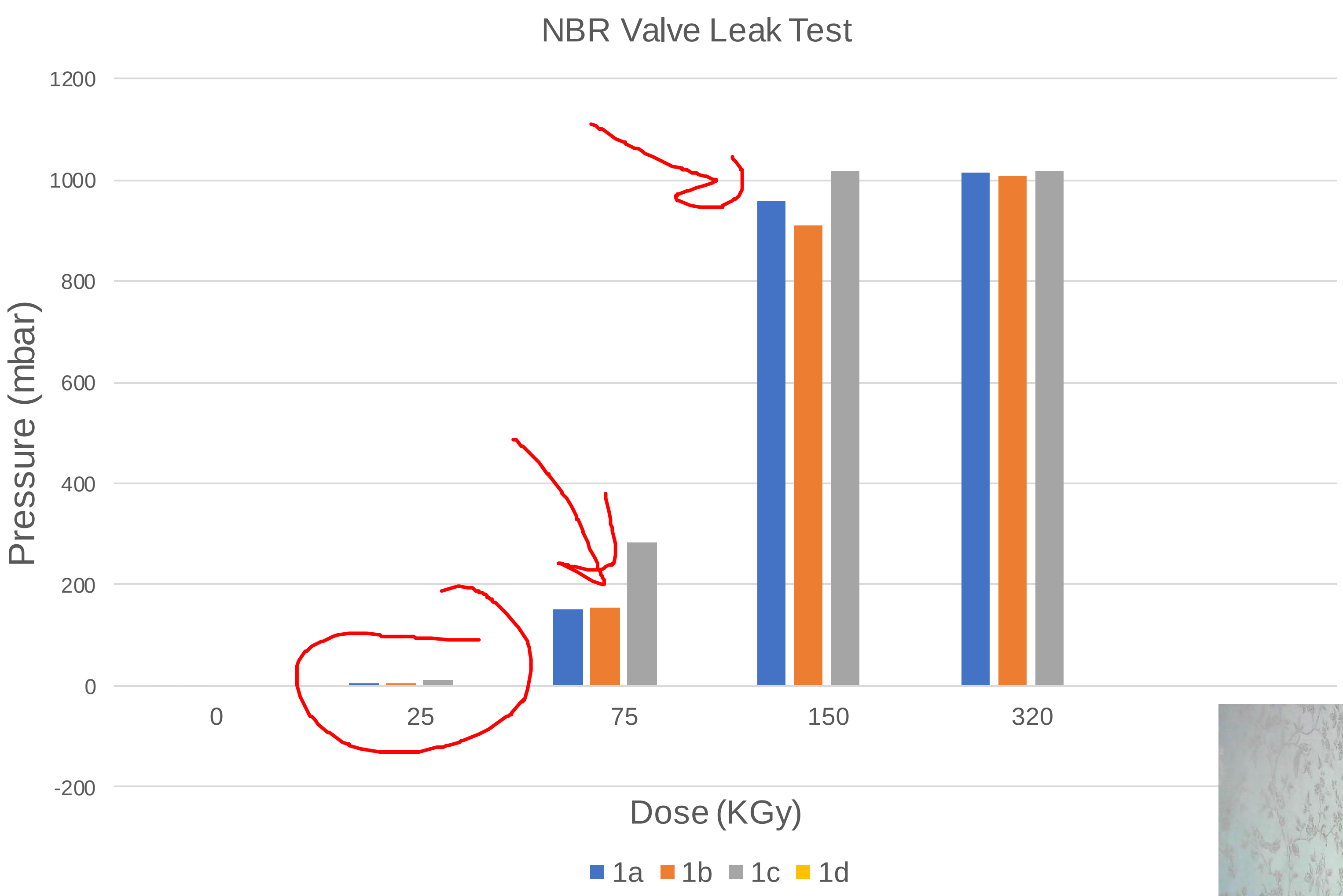

Transformative Science and Engineering for Nuclear Decommissioning

Leak test results - EPDM

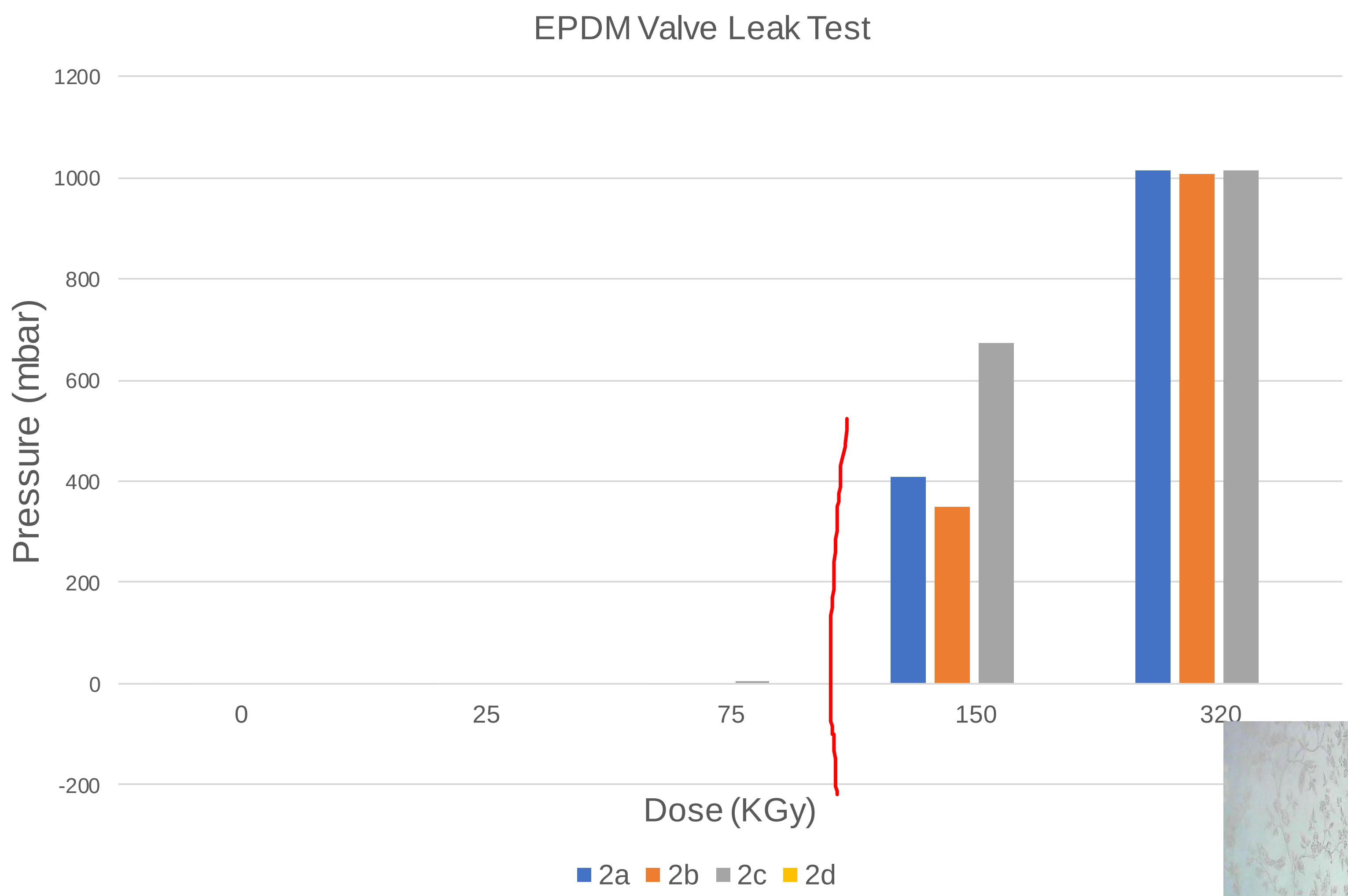

TRANSCEND

Transformative Science and Engineering for Nuclear Decommissioning

Leak test results - Ruby

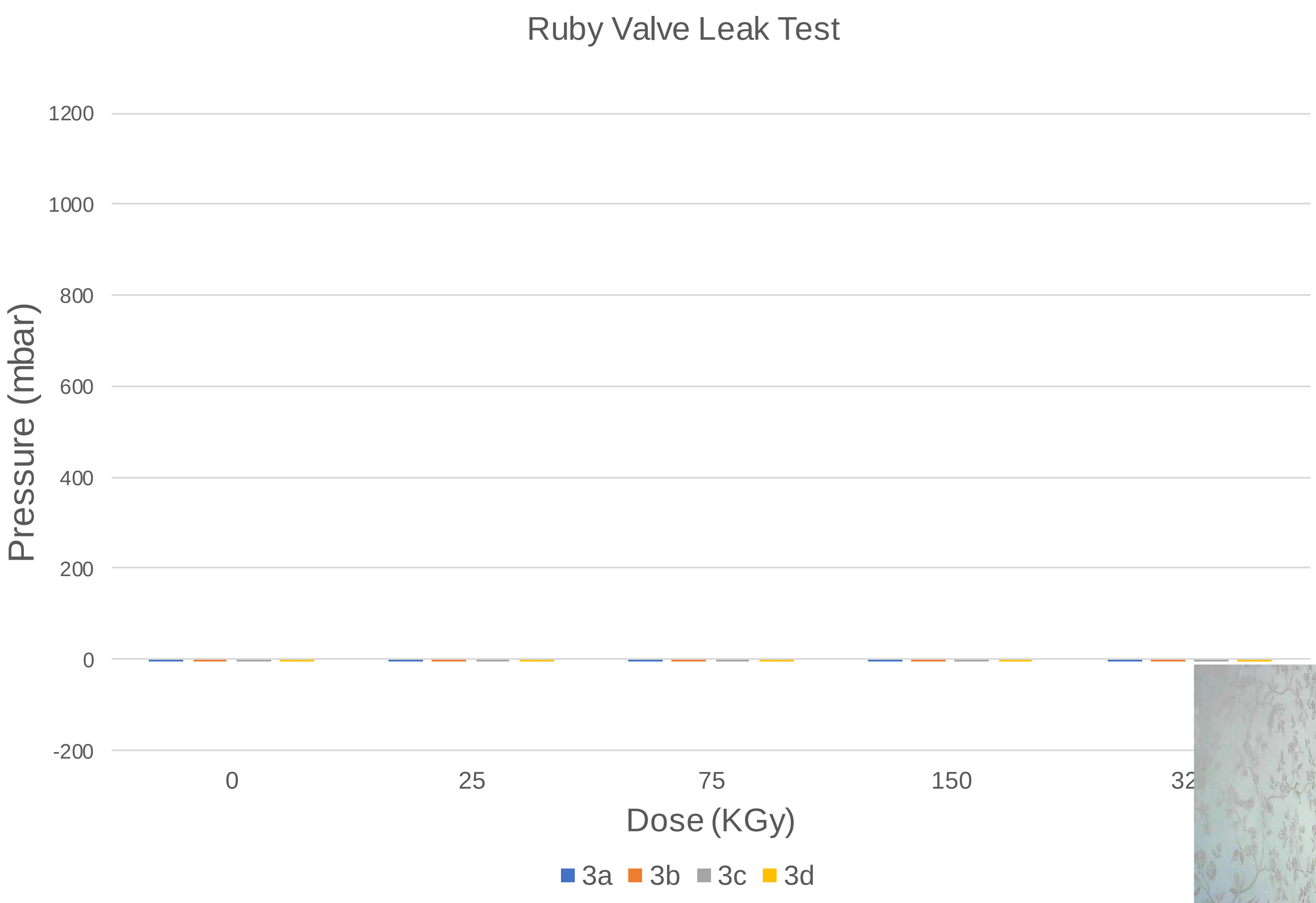

So what does this mean?

EPDM and NBR could be used for short irradiations of <25KGy..

EPDM displays more resistance than NBR, beginning to leak between 25-75KGy

Ruby seals however appear to be resistant, one valve was irradiated to 1.2 MGy and didn’t leak

The Irradiator manifold should be good for use – which is also good for industry

Also means that live gas production will be measurable and controllable whilst samples are irradiated

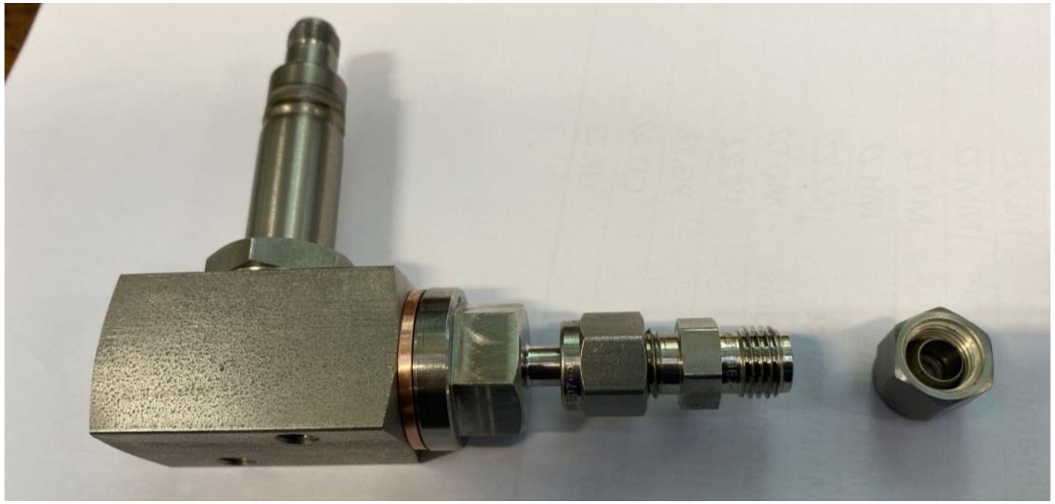

Back to radiolysis

The big oxide question?

Why do different oxides have such a varied effect on $G(H_2)$?

How to explore this

How to remedy this mystery?

First lets target a possible mechanism:

If this mechanism is true then surely only oxides with a band gap close to 5.15 eV would enhance H_2 yields significantly?

And that's correct, not all do but some still enhance

So lets did deeper

This one for example!

Band gap resonance

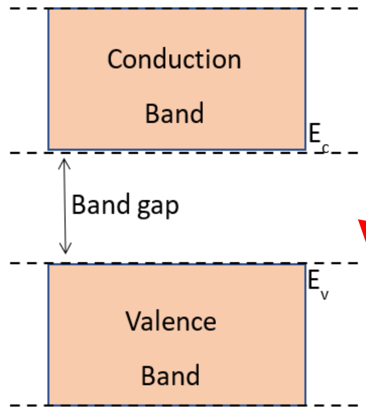

When....

Bond energy of O-H (~5.15 eV)

Matches

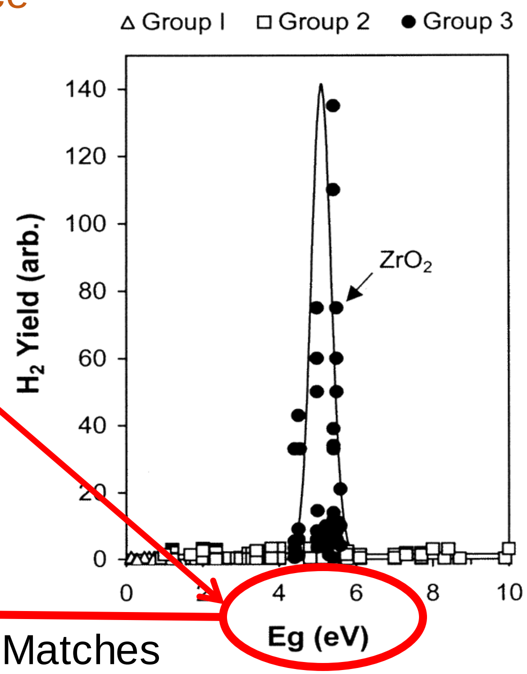

Interfacial Energy Transfer during Gamma Radiolysis of Water on the Surface of ZrO_2 and Some Other Oxides

N. G. Petrik, A. B. Alexandrov, and A. I. Vall

TRANSCEND

Transformative Science and Engineering for Nuclear Decommissioning

Modifying the Band Gap

If ZrO_2 is such an effective enhancer then lets change it's band gap

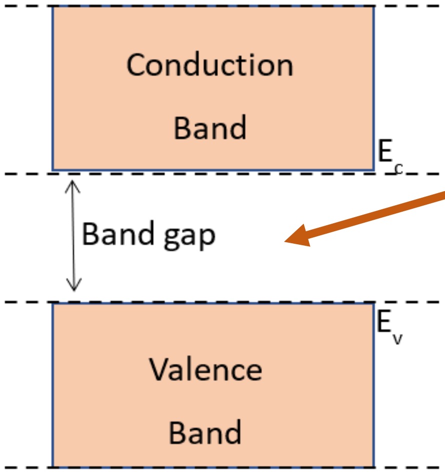

ZrO_2 nanoparticles were doped with varying quantities of Ti were synthesised in Manchester

Titanium Ions Dispersed into the ZrO_2 Matrix: Spectroscopic Properties and Photoinduced Electron Transfer

S. Livraghi, F. Olivero, M. C. Paganini,* and E. Giamello

Dipartimento di Chimica IFM, Università di Torino and NIS, Nanostructured Interfaces and Surfaces Centre of Excellence, Via P. Giuria 7, I-10125 Torino, Italy

Received: July 6, 2010; Revised Manuscript Received: September 10, 2010

So if we irradiate these samples and compare the yield against stock ZrO_2 then we'd expect the samples with more doping to experience a diminished yield

This was hoped to have been completed earlier

But the GC is haunted

And by haunted I mean it developed a leak

A leak that only sometimes leaked

And that's without touching or changing anything

So I've now swapped to Unisense gas probes

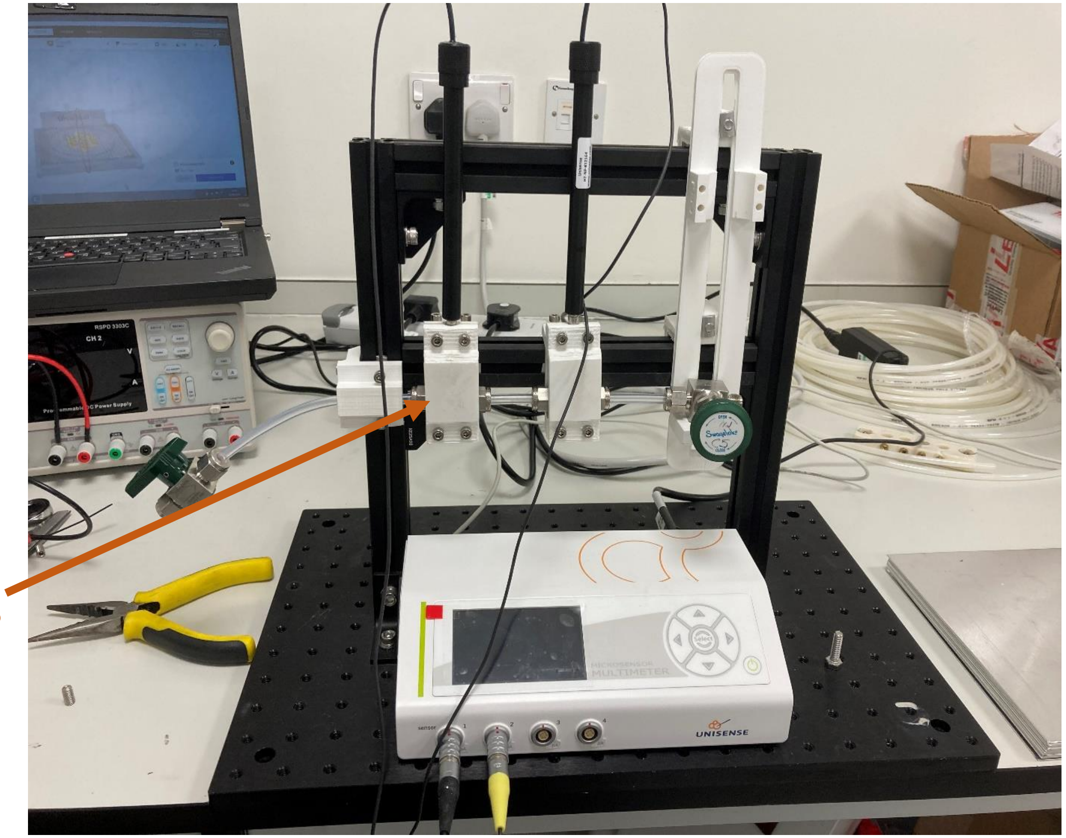

So where do we stand?

- Whilst water radiolysis is well understood:

Mechanistic processes for enhanced gaseous yields are still unknown

- Experiments to explore this are currently being undertook
- EPDM and NBR have limited capabilities when exposed to radiation
- Ruby however may provide a viable radiation hard solution for industrial and experimental needs that is both:
  - economically viable
  - commercially available

TRANSCEND

Transformative Science and Engineering for Nuclear Decommissioning

Thank you

Contact Details: christopher.anderson-3@postgrad.manchester.ac.uk
07857420556

TRANSCEND

Transformative Science and Engineering for Nuclear Decommissioning

High-fidelity simulation of behavioural modification techniques for nuclear waste transport flows

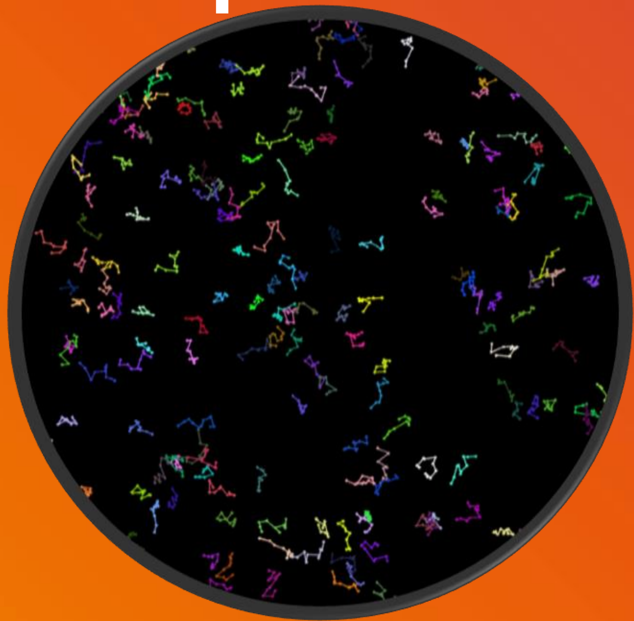

Dr. Lee Mortimer, University of Leeds

Prof. Mike Fairweather, University of Leeds

TRANSCEND ANNUAL MEETING 2021

11th November 2021
Harrogate, UK

Energy
For a Low Carbon Future

BACKGROUND

- At **Sellafield Ltd**, waste suspension sludge flows transport solid-liquid mixtures of radioactive legacy material from ponds, silos and tanks to other interim locations where they can be safely stored.

- Such retrievals are currently underway during **POCO** operations in plants such as the Pile Fuel Storage Pond, the First Generation Magnox Storage Pond and a number of associated packaging, export and encapsulation plants, and settling, decant and storage tanks.

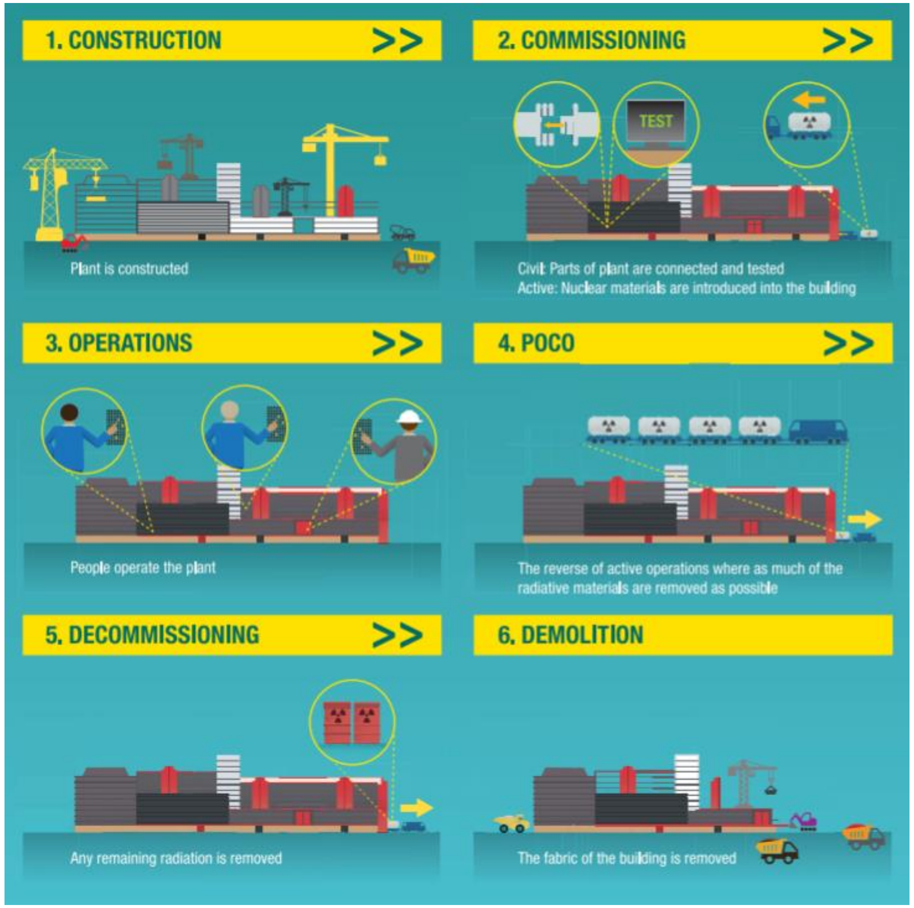

Sellafield magazine – Issue 02, 2015.

MOTIVATION

Pile fuel storage pool at Sellafield - IAEA Nuclear Energy Series No. NW-T-2.6 - Decommissioning of Pools in Nuclear Facilities, IAEA.

- However, at present these processes are executed sub-optimally and carried out with caution due to the complex nature of the wastes and a lack of understanding of their flow behaviour.

- In practice, the bulk transportive behaviour of interest associated with these activities is sensitive to the material properties and flow conditions.

- This sensitivity is capable of being exploited, however, and the modification of such quantities to obtain a desired outcome is referred to as **behavioural modification**.

MOTIVATION

- In developing such techniques, solutions can be generated to discourage or encourage waste particle agglomeration within these transport flows, ultimately controlling the extent of long-term particle migration and interaction events.

MOTIVATION

- That said, to develop beneficial behavioural modification techniques the system response to deviations in key parameters must be known. It is extremely difficult, if not impossible, to probe the effects of such variations experimentally.

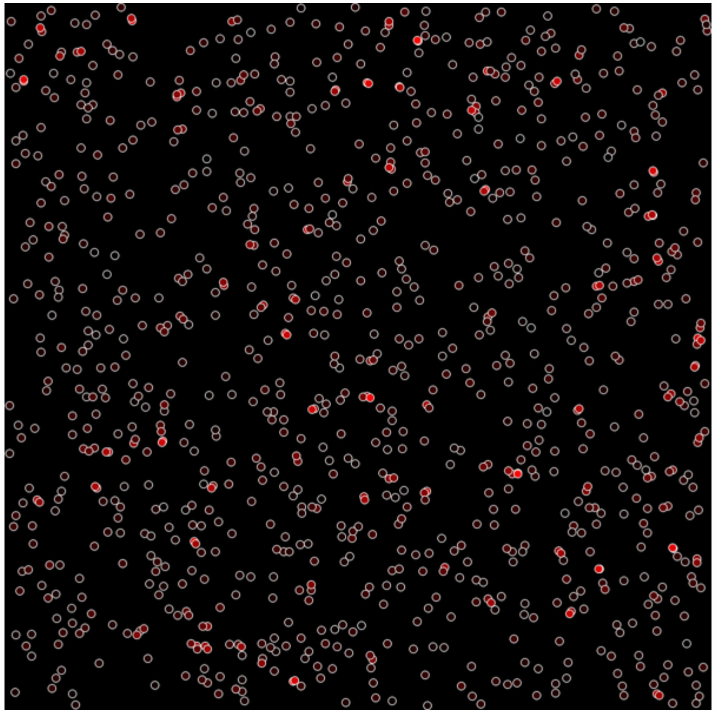

LOW HAMAKER CONSTANT

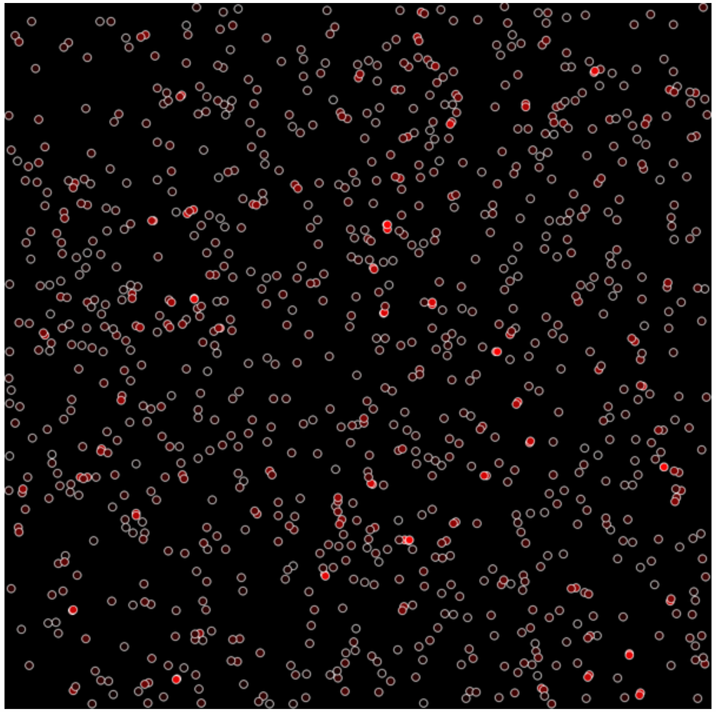

HIGH HAMAKER CONSTANT

- Computer simulations provide a means to overcome this difficulty by providing the capability to specify and explore the impact of changes to a set of precise system parameters.

MOTIVATION

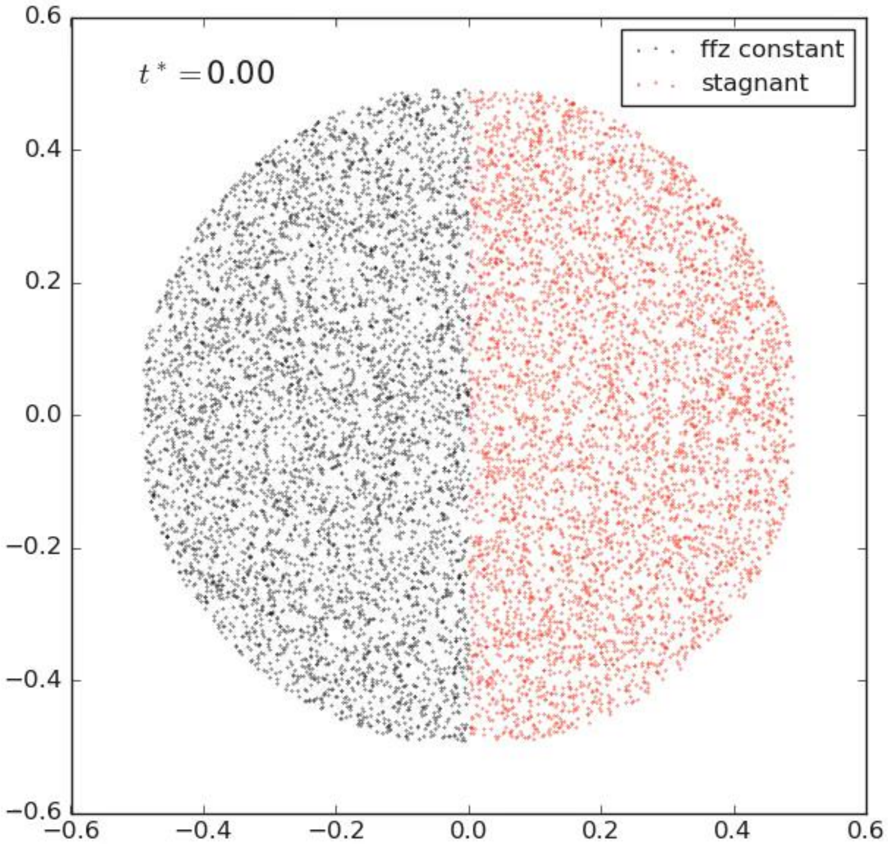

Comparison of turbulent ($Re_\tau = 720$) and stagnant ($Re_\tau = 0$) horizontal pipe flow with low density-ratio particles ($St^+ = 1.2$)

SIMULATION TECHNIQUES

- The accuracy and reliability of such calculations is based upon both the order of the discretisation techniques used for each phase, as well as the fidelity of the models used to predict the wide array of interactions between the phases.

CONTINUOUS PHASE

Direct numerical simulation (DNS)

PARTICULATE PHASE

Lagrangian particle tracking (LPT)
Immersed boundaries method (IBM

POLYMER PHASE

Finitely extensible nonlinear elastic model (FENE)

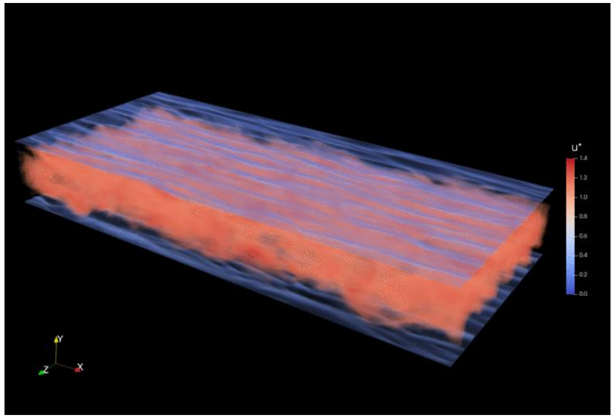

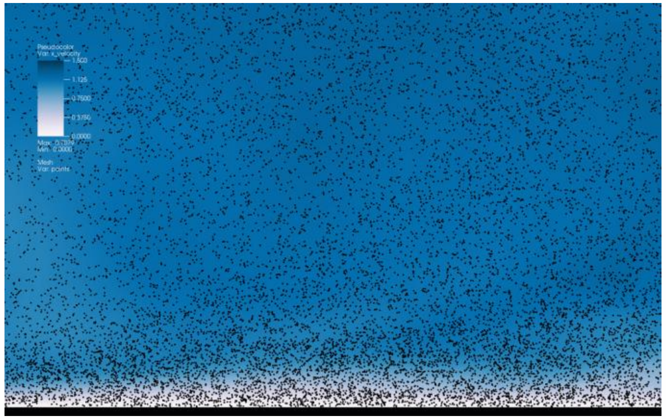

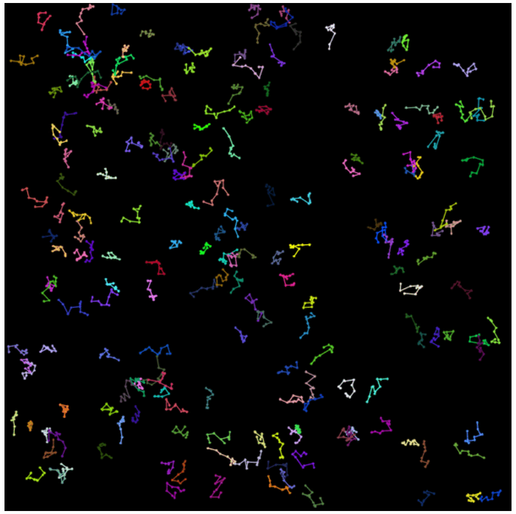

- Focus on coupling methods together to obtain a solver capable of predicting particle-fluid, particle-particle and particle-polymer interaction.

POLYMERIC FLOWS

- Polymers are chemical compounds with molecules bonded together in **long repeating chains** of monomers.
- Both **synthesized** and **naturally occurring**.
- Possess **important advantageous properties** surrounding the way in which they interact with both themselves and other materials.
- In the present case, we are interested in how they **interact** and beneficially **modify behaviour** of both the fluid and particles.

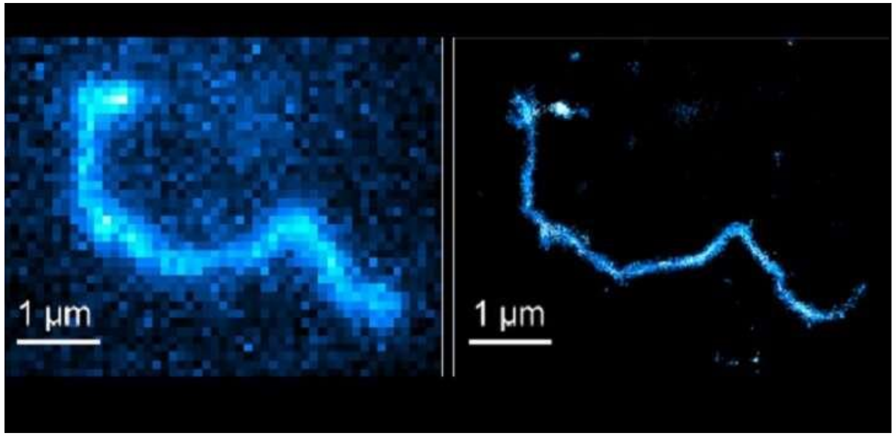

Super-resolution fluorescence microscopy of Lambda DNA.
[Abadi et al. Entangled polymer dynamics beyond reptation, *Nature Communications* (2018).]

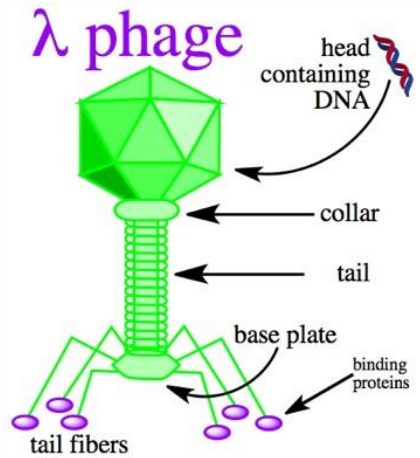

POLYMER-PARTICLE INTERACTION

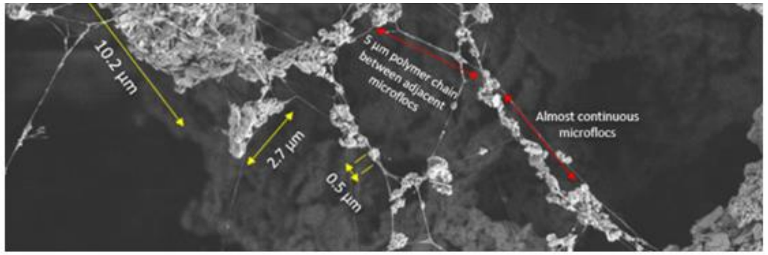

Microstructure of kaolinite floc as revealed by cryo-SEM - Sharma, S., Lin, C. L., & Miller, J. D. (2017). Multi-scale features including water content of polymer induced kaolinite floc structures. Minerals Engineering, 101, 20-29.

- Polymer flocculants **induce flocculation** by neutralizing the surface charge of the particles or by forming bridges between individual particles.

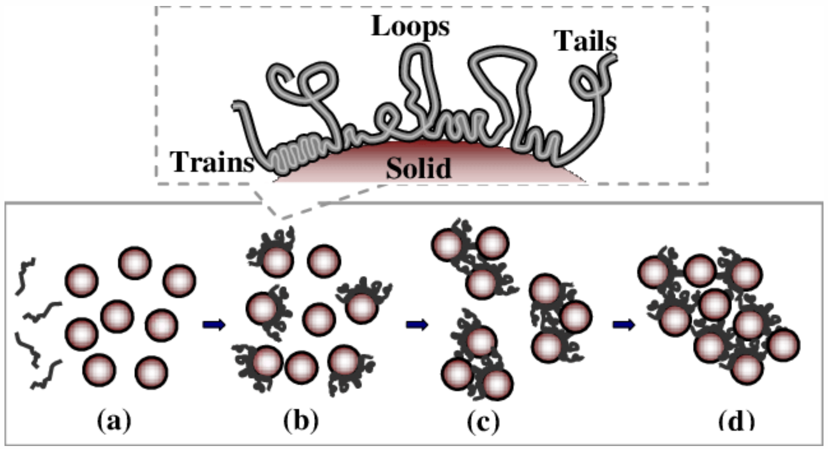

- Adsorption mechanism needs to be modelled, no current techniques available in the literature and so this needs to be developed.
- **Bridging mechanism** will hence be implicit from adsorption.
- Adsorption is determined by attachment process, **hydrophobic** or **electrostatic interaction**.
- Hence attachment mechanism upon collision will rely on **electrochemical properties** of surface of particle and the polymer charge distribution.

LANGEVIN DYNAMICS

- FENE (finitely extensible nonlinear elastic) chain model represents the polymer as a sequence of beads connected by nonlinear springs.

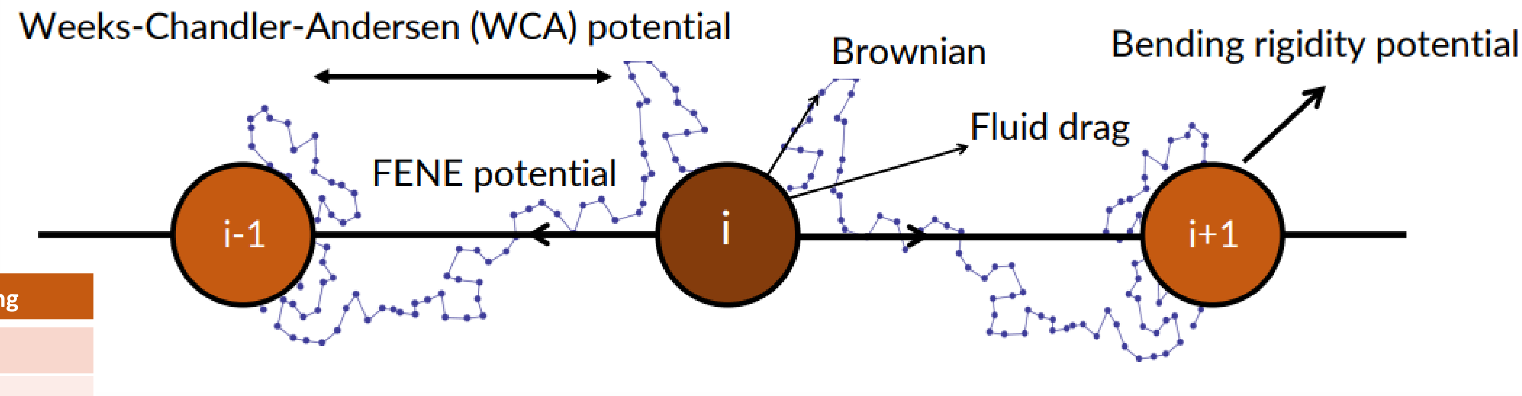

Symbol	Meaning
m	Mass
$\boldsymbol{r}$	Position
t	Time
V_i	Potential
$\boldsymbol{\eta}_i(t)$	Brownian noise
ζ	Drag coefficient
k_B	Boltzmann's constant
T	Temperature
K_{BEND}	Bending potential
θ_i	Bead angle
σ	Bead diameter
r_{ij}	Bead separation

$$\underbrace{m\frac{d^2\boldsymbol{r}_i}{dt^2}}_{\text{Inertia}} = \overbrace{-\boldsymbol{\nabla}\mathrm{V_i}}^{\text{Interaction potentials}} \underbrace{- \zeta\frac{d\boldsymbol{r}_i}{\mathrm{dt}}}_{\text{Fluid drag}} + \overbrace{\sqrt{2k_BT\zeta}\,\boldsymbol{\eta}_i(t)}^{\text{Brownian motion}}$$

$$\mathrm{V_i} = \underbrace{-\frac{K_{FENE}R_0^2}{2}\ln\left[1-\left(\frac{r_{i,i+1}}{R_0}\right)^{2}\right]}_{\text{FENE bead-spring}} + \underbrace{K_{BEND}(1+\cos\theta_i)}_{\text{Bending rigidity}} + \underbrace{1 + 4\left[\left(\frac{\sigma}{r_{ij}}\right)^{12} - \left(\frac{\sigma}{r_{ij}}\right)^{6}\right]}_{\text{WCA potential}}$$

LANGEVIN DYNAMICS

- Beads interact with particles via a shifted and truncated Lennard-Jones potential.

$$V_i = 4\epsilon\left[\left(\frac{\sigma}{r_{ij}}\right)^{12} - \left(\frac{\sigma}{r_{ij}}\right)^{6}\right] - 4\epsilon\left[\left(\frac{\sigma}{r_c}\right)^{12} - \left(\frac{\sigma}{r_c}\right)^{6}\right]$$

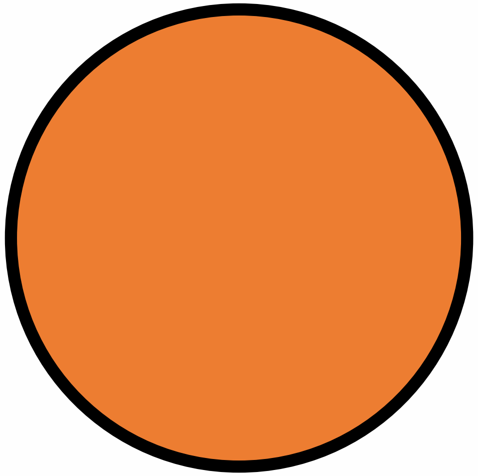

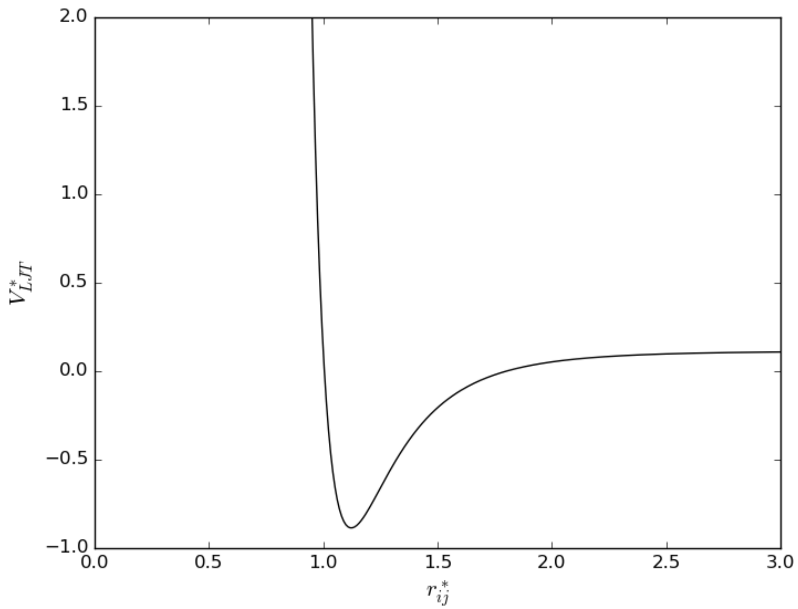

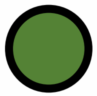

Symbol	Meaning
m	Mass
$\boldsymbol{r}$	Position
t	Time
V_i	Potential
$\boldsymbol{\eta}_i(t)$	Brownian noise
ζ	Drag coefficient
k_B	Boltzmann's constant
T	Temperature
K_{BEND}	Bending potential
θ_i	Bead angle
σ	Bead diameter
r_{ij}	Bead separation
r_c	LJT range
ϵ	LJT strength

POLYMERS UNDER EQUILIBRIUM CONDITIONS

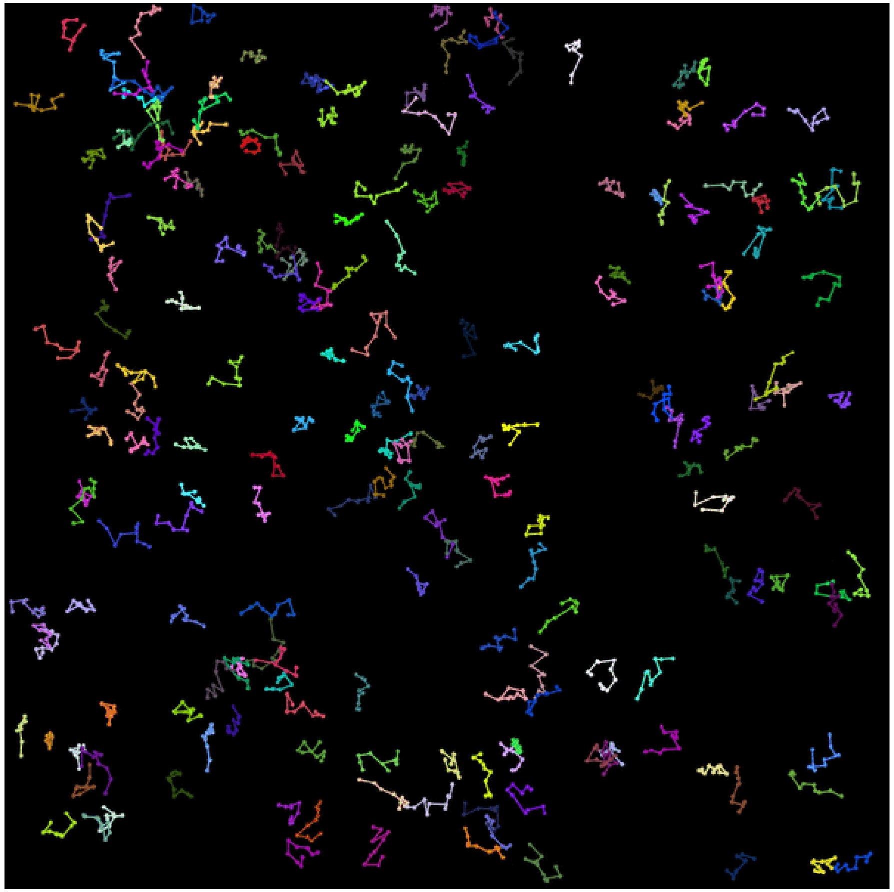

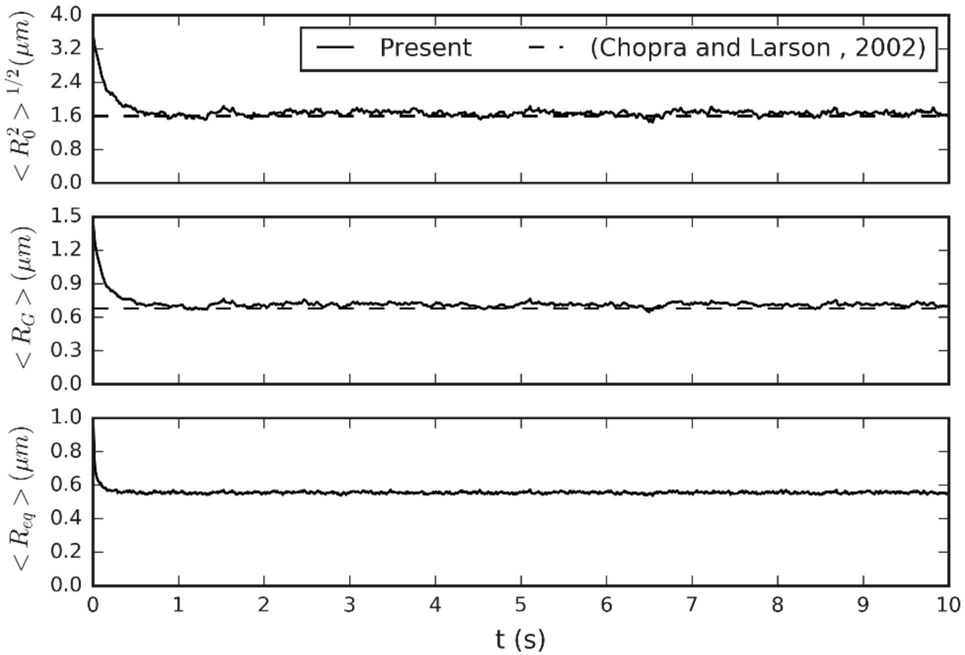

Validation data from M. Chopra and R. G. Larson, *J. Rheol.*, 2002, 46, 831–862

End-to-end distance vector

$$< R_0^2 >^{\frac{1}{2}} = \sqrt{\frac{\sum_p \left(\boldsymbol{X}_{N_B,p} - \boldsymbol{X}_{1,p}\right)^2}{N_P}}$$

Radius of gyration

$$< R_G^2 >^{\frac{1}{2}} = \sqrt{\frac{\sum_p \frac{\sum_b \left(\boldsymbol{X}_{b,p} - \boldsymbol{X}_{COM,p}\right)^2}{N_B - 1}}{N_P}}$$

Equilibrium stretch

$$< R_{eq}^2 >^{\frac{1}{2}} = \sqrt{\frac{\sum_p \frac{\sum_r \boldsymbol{R}^2}{N_B - 1}}{N_P}}$$

SHEAR FLOW VALIDATION

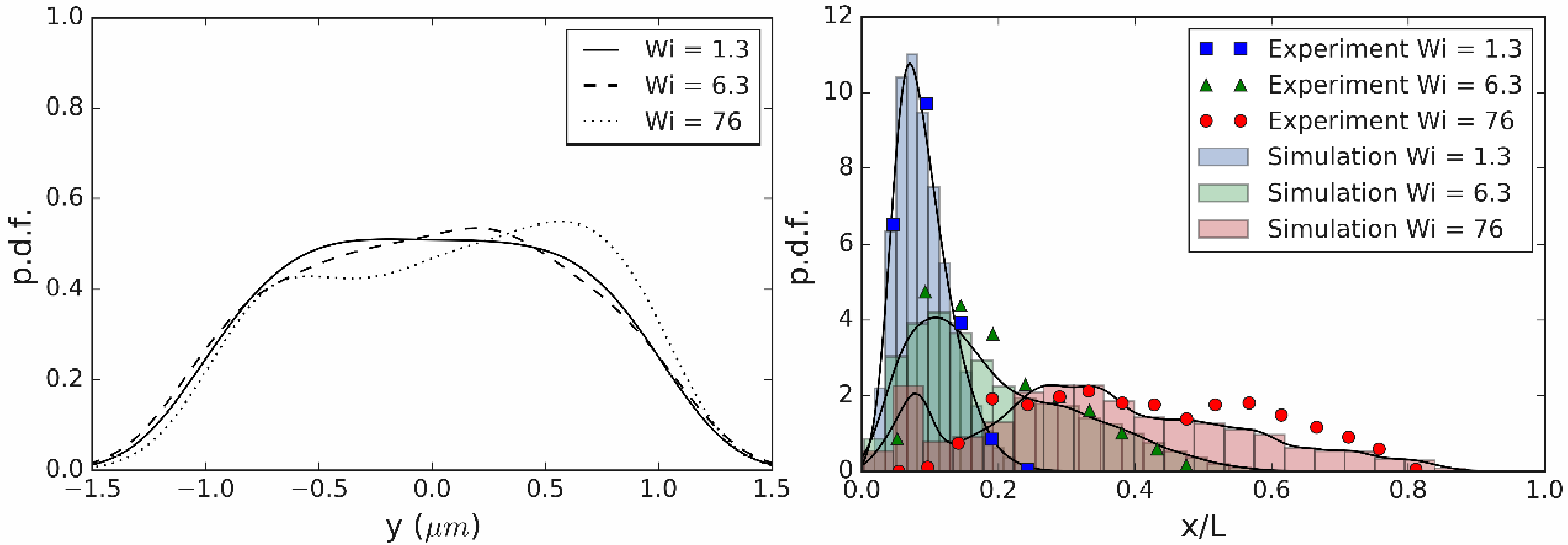

Shear flow simulation for $Wi = 1.3, 6.3$ and 76. Probability distribution functions of bead position within the domain (left) and mean polymer extension (right).

EFFECT OF BENDING POTENTIAL ON POLYMER CONFORMATION

$$N_{POL} = 200$$
$$N_{BPP} = 20$$
$$l_P = 3\sigma$$
$$\delta t = 0.01\tau$$

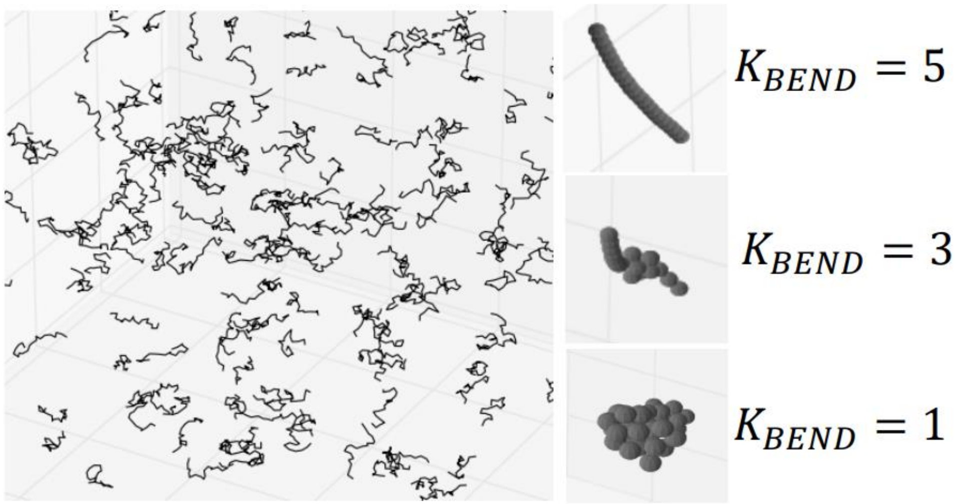

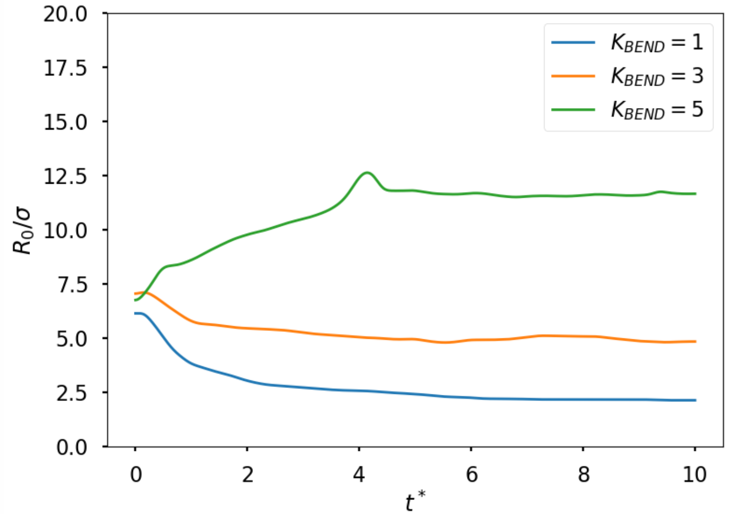

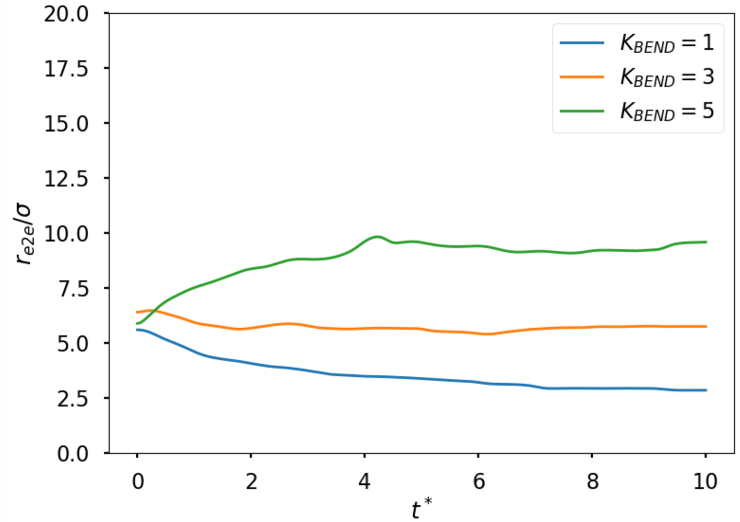

- Increased bending potential causes stronger rigidity in linear polymer conformation.
- Both mean radius of gyration (left) and end-to-end distance (right) increase with increased bending potential.
- This leads to larger collision cross section of the polymer chain with particles, leading to increased adsorption rates

EFFECT OF BENDING POTENTIAL ON POLYMER-PARTICLE COLLISIONS

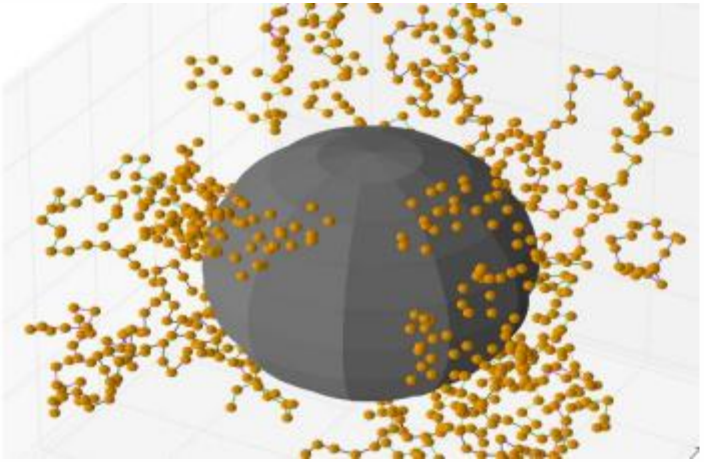

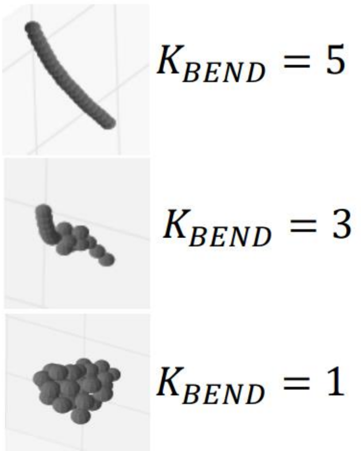

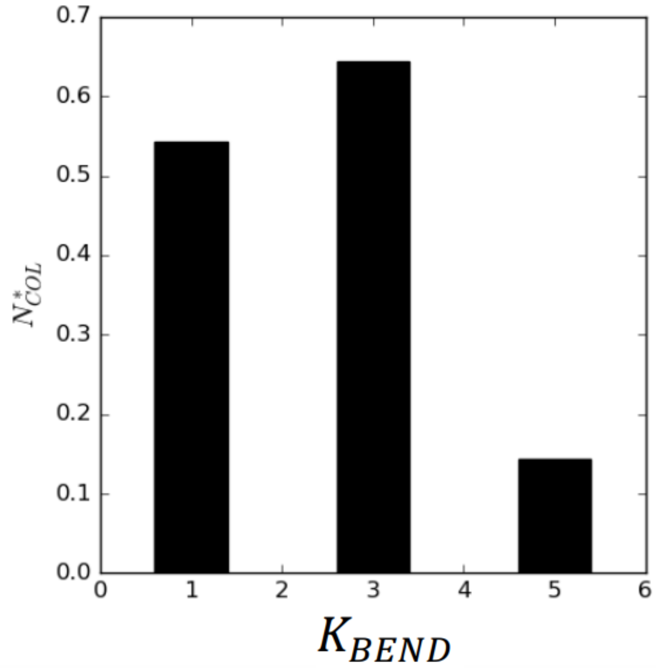

- Counting collision events between beads and a stationary sphere, medium bending rigidity leads to increased adsorption.
- The way in which the bending potential relates to chemical and mechanical properties such as ionic strength will be key to developing behavioural modification effects.

CONCLUSIONS AND FURTHER WORK

- New Langevin dynamics code, capable of predicting FENE bead-spring polymer and particle model, has been developed, implemented and validated.
- Effect of polymer conformation has been further studied, with bending potential playing an important role in the conformation of polymer chains.
- Low bending potential means particles bunch up on themselves. Higher bending potential leads to angles between beads closer to 180 degrees.
- Polymer-particle interaction mechanism through truncated Lennard-Jones potential has been implemented and tested, with preliminary simulations showing most interaction at medium potential.
- Further simulations are being performed to study the way in which polymers conform onto particles based on shear rate and ionic strength.

PUBLISHED WORK ON BEHAVIOURAL MODIFICATION

Mortimer, L. F. and Fairweather, M., 2021. Assessment of behavioral modification techniques through immersed boundary method simulation of binary particle interactions in isotropic turbulence. *Physics of Fluids.* 33 (3), 073307 doi: 10.1063/5.0049779

Mortimer, L. F. and Fairweather, M., 2020. Density ratio effects on the topology of coherent turbulent structures in two-way coupled particle-laden channel flows. *Physics of Fluids. 32* (10), 103302. doi: 10.1063/5.0017458

Mortimer L. F., Njobuenwu D. O. , Fairweather M., 2020. Agglomeration dynamics in liquid–solid particle-laden turbulent channel flows using an energy-based deterministic approach. *Physics of Fluids.* 32 (4) doi: 10.1063/5.0001596

Mortimer L. F., Njobuenwu D. O. , Fairweather M., 2019. Near-wall dynamics of inertial particles in dilute turbulent channel flows. *Physics of Fluids. 31 (6)* 063302 doi:10.1063/1.5093391

ACKNOWLEDGEMENTS

This work is supported by a UK Engineering and Physical Sciences Research Council grant at the University of Leeds from the TRANSCEND (Transformative Science and Engineering for Nuclear Decommissioning) project.

Engineering and Physical Sciences Research Council

Thank you for your attention!

Dr. Lee Mortimer
PhD, MPhys (Hons)
Research Fellow
Office 2.22 Chemical and Process Engineering Building
School of Chemical and Process Engineering
University of Leeds
l.f.mortimer@leeds.ac.uk

Transformative Science and Engineering for Nuclear Decommissioning

Thank you

&

Questions?

Dr. Lee Mortimer
PhD, MPhys (Hons)
Research Fellow
Office 2.22 Chemical and Process Engineering Building
School of Chemical and Process Engineering
University of Leeds
l.f.mortimer@leeds.ac.uk

Transformative Science and Engineering for Nuclear Decommissioning

Advanced Blind-Tube Instrument for Characterisation of Underground Sources

Soraia Elísio[1] (s.elisio@lancaster.ac.uk);
Malcolm J. Joyce[1] (m.joyce@lancaster.ac.uk);
James Graham[2] (james.graham@uknnl.com);
Barrie Greenhalgh[3] (barrie.greenhalgh@sellafieldsites.com)

[1]Department of Engineering, Lancaster University

[2]National Nuclear Laboratory Ltd., Central Laboratory, Sellafield

[3]Radiometric Systems Group, Sellafield Ltd., Site Management Centre, Sellafield

Content

1. Motivation
2. Radiation assessment using in-ground assets:
   - Routine sampling practice
   - In-situ deployments
3. Research focus & Challenges
4. The concept: Blind-tube radiometric probe
5. The blind-tube test bed
6. Laboratory experiments:
   - Gamma detection performance
   - ^{137}Cs + ^{90}Sr Assessment in blind-tubes
7. Conclusion & Future work

Motivation

- Whilst interim storage of waste in ponds and silos is widespread, many older facilities were not designed to modern building standards, and some have leaked.

- The resulting migratory, radioactive plumes in the ground pose a risk to groundwater, surface water receptors and subsequently public health and the environment.

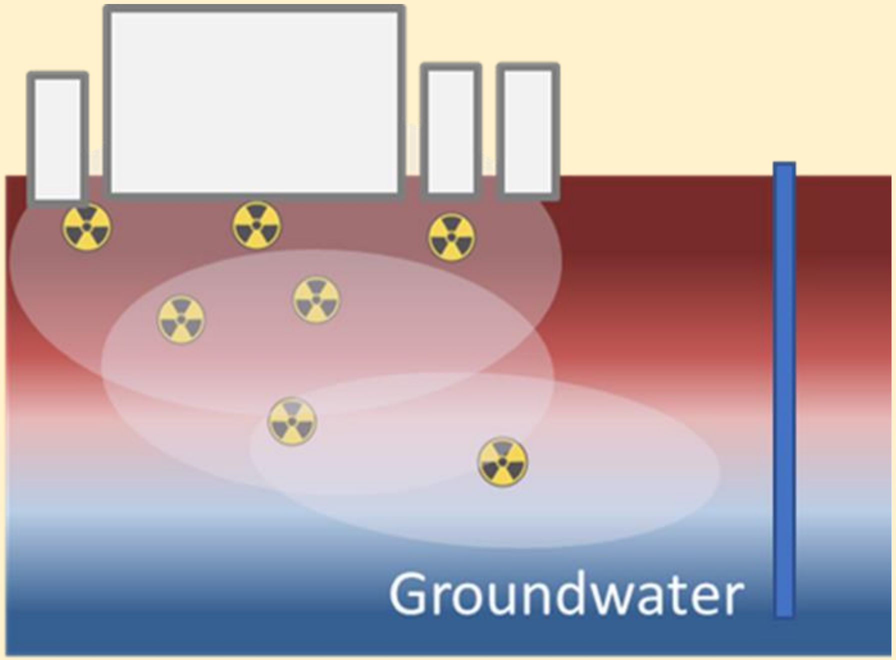

Simplified representation of underground leak and monitoring in-ground asset.

Radiation assessment using in-ground assets

- Routine sampling practice:

Groundwater monitoring at Sellafield:
Annual data review, 2016

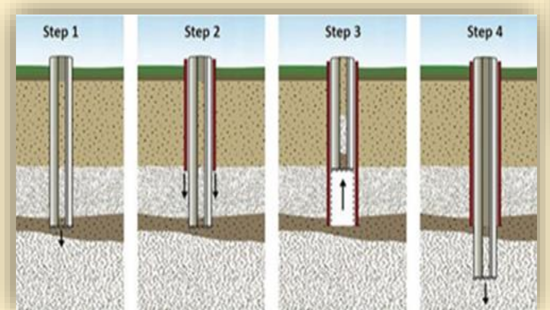

www.hbpw.co.uk/drilling-at-the-speed-of-sound/

- Soil
- Groundwater

- Samples are processed and analysed in laboratory.

Positive aspects:

- Specialized instruments are available.
- Techniques employed to separate and purify radionuclides.
- Quantitative identification of α, β, or γ emitting radionuclides.

Limitations:

- Restricted sample volumes.
- Secondary wastes produced.
- Laborious, time consuming and expensive techniques.
- Radiological risk to workers.

Radiation assessment using in-ground assets

- In-situ deployments:

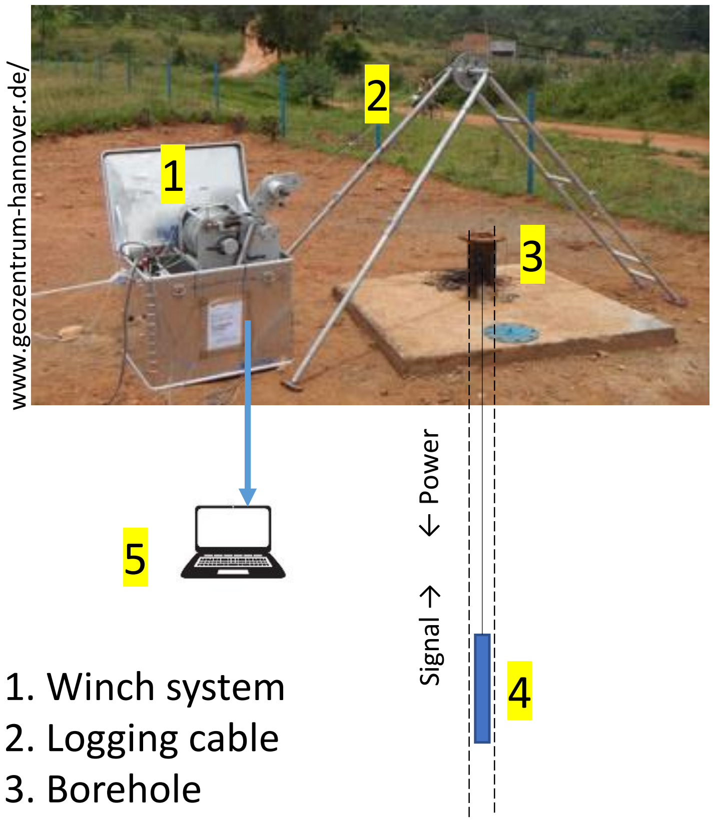

1. Winch system
2. Logging cable
3. Borehole
4. Logging probe
5. Data logger

Radiometric logging probes

Sensor → Gamma-ray detector

Geiger-Muller counter (GM)

Bismuth germanate scintillator (BGO)

Sodium-iodide scintillator (NaI:Tl)

Portable high-purity germanium detector (HPGe)

Radiation a… …round assets

- In-situ deployments:

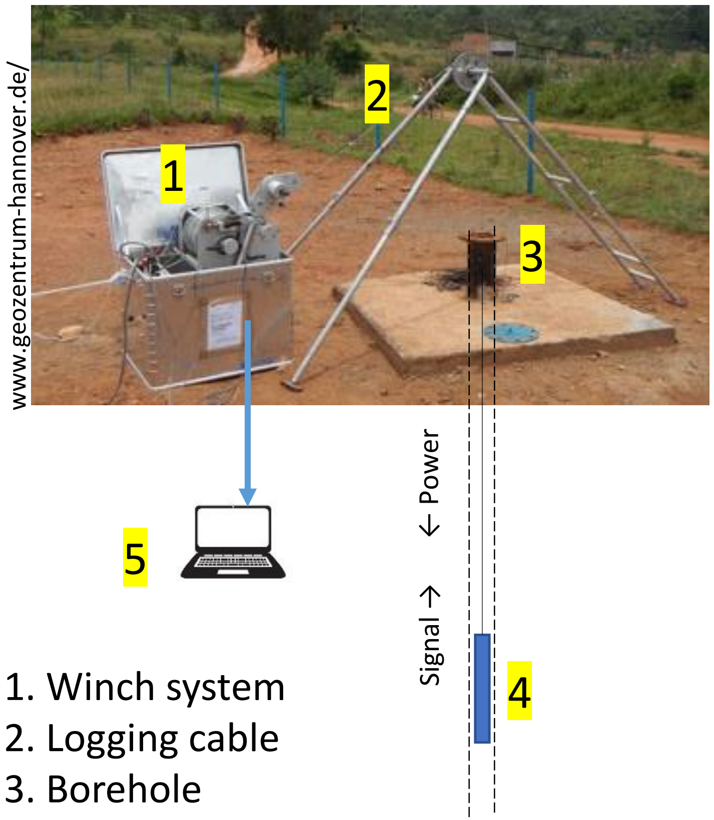

1. Winch system
2. Logging cable
3. Borehole
4. Logging probe
5. Data logger

…g probes

…y detector

…er (GM)

…llator (BGO)

…tor (NaI:Tl)

…n detector (HPGe)

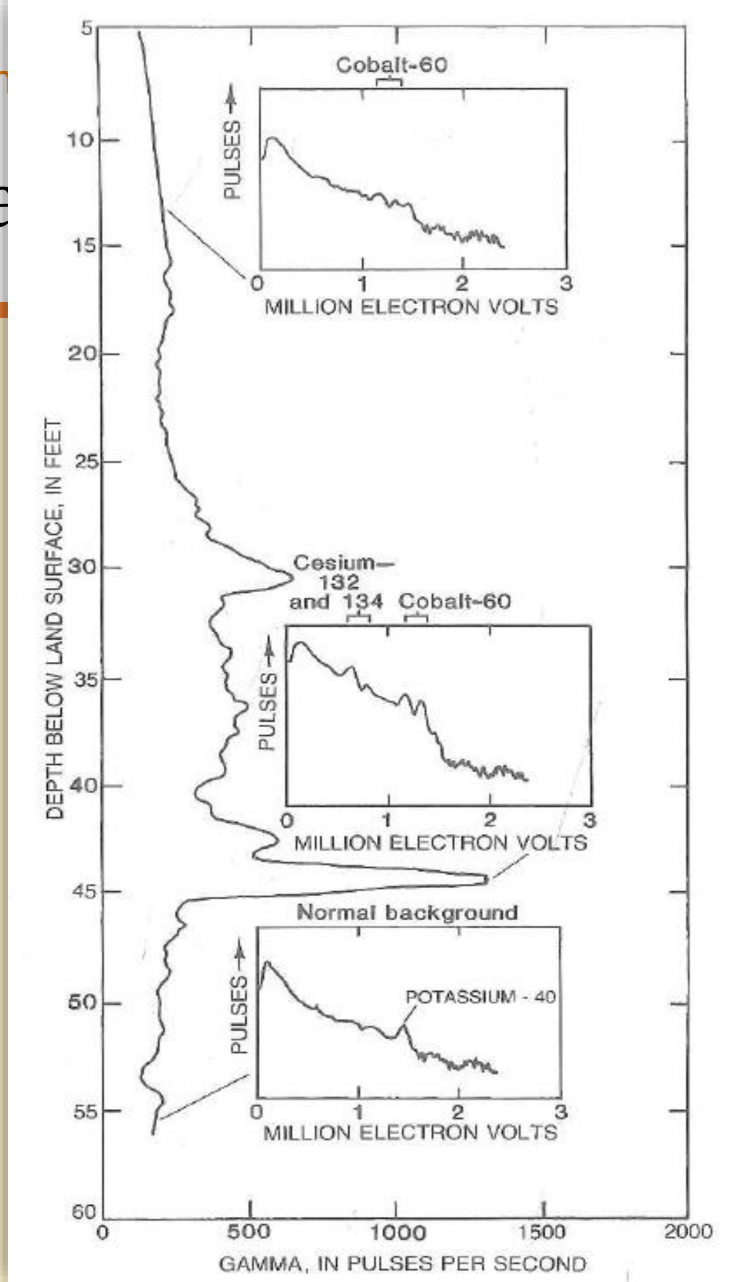

Gamma logging record from borehole survey at Maxey Flats site (US)

Ref. W. Scott Keys (1997) A practical guide to borehole geophysics in environmental investigations

Radiation assessment using in-ground assets

- In-situ deployments:

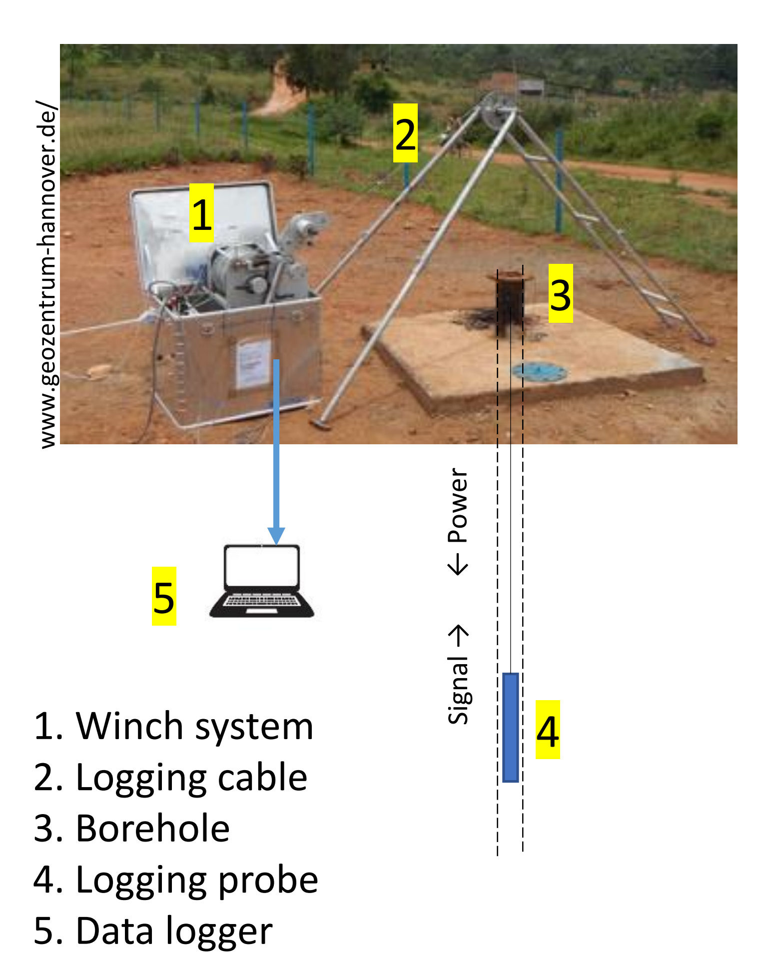

Positive aspects:

- Continuous, real-time assessment of vertical soil profiles.
- Less intrusive approach.
- Volume of investigation larger than the borehole size.

Limitations:

- Need to drill and install ground assets.
- Limiting penetration power of radioactivity in matter.
- <u>Significant challenge to detect α and β emitting radionuclides.</u>
- <u>Intrinsic limitations of available logging probes.</u>

Research focus & Challenges

- Radiological surveillance at Sellafield site:

Focus: Liquor from the Magnox Swarf Storage silos (MSSS) have leaked into the ground contaminated the land below the silo.

Additional challenges:

- Operational infrastructure and deployment constraints.
- Device has to be deployed in the existing in-ground assets:
  - Narrow carbon steel blind-tubes (ID 7 cm)
- The radioactivity fingerprint in the soil is believed to be dominated by caesium-137 and strontium-90.
- Doses involved can be significant:
  - Non-isotopic specific dose rate < 1 Gy/h

GAME CHANGERS Hybrid Instruments

"Characterisation and monitoring using in-ground assets"

www.gamechangers.technology/challenge/Characterisation_and_monitoring_using_in-ground_assets

The concept: Blind-tube radiometric probe

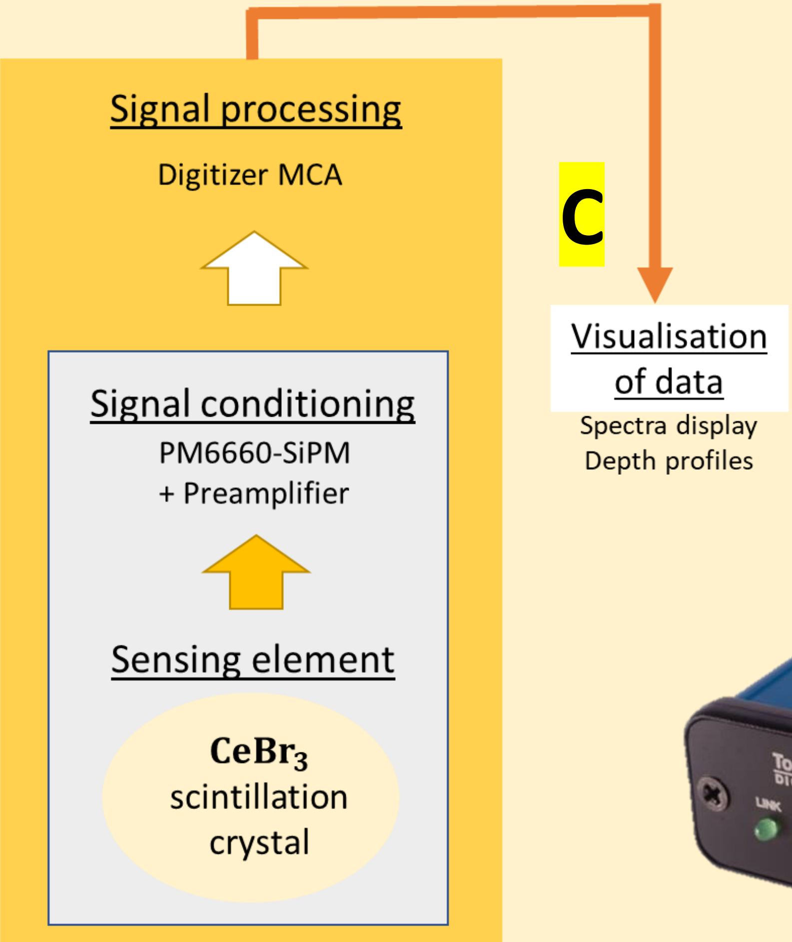

Ø10 mm x 9 mm $CeBr_3$ Detector:

- ✓ Good gamma-ray detection efficiency
- ✓ Good energy resolution 4% @ 662 keV
- ✓ High count-rate capability τ=17 ns
- ✓ High radiation hardness <100 kGy

Unit commercialised by Scionix (Netherlands)

Unit commercialised by BrightSpec NV

TOPAZ-SiPM Digital MCA:

- ✓ Compact full-featured MCA
- ✓ Compatible with dimensions of typical blind-tubes
- ✓ 5V low-ripple, low-noise supply
- ✓ Powered from laptop vis USB cable

The concept: Blind-tube radiometric probe

Signal processing

Digitizer MCA

Signal conditioning

PM6660-SiPM
+ Preamplifier

Sensing element

$CeBr_3$ scintillation crystal

C

Visualisation of data

Spectra display
Depth profiles

- Prototype:

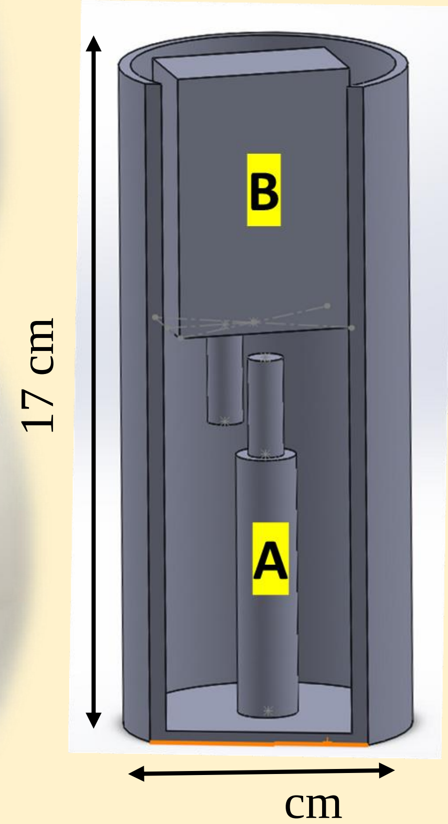

The blind-tube test bed

- Calibration set-up replicates as close as practical the existing in-ground blind-tubes.
- Preform quantitative measurements specific to sample geometry of the field of measurement.
- For more complex scenarios calibrations will be held via Monte Carlo simulations.

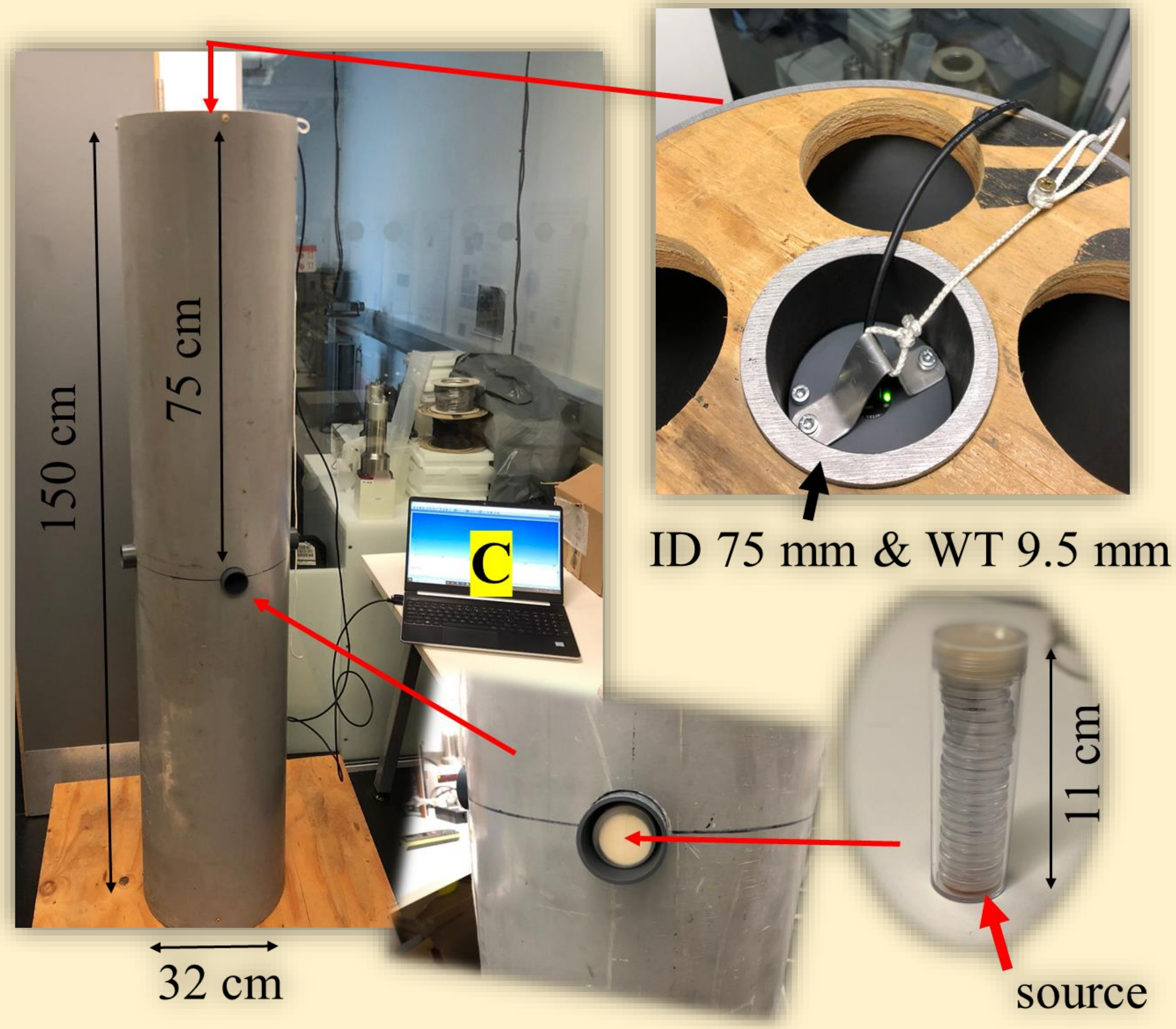

Laboratory experiments

5 V

Power supply

HV-supply C10940
+ Voltage divider
Hamamatsu E-10679-50
+ Ø 14 PMT
Hamamatsu R9880-110
+ Ø10x10mm CeBr3 crystal

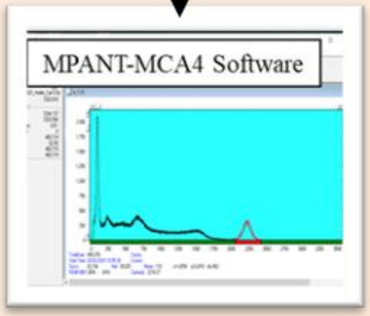

Gamma detection system used in the experiments

- Gamma detection performance:

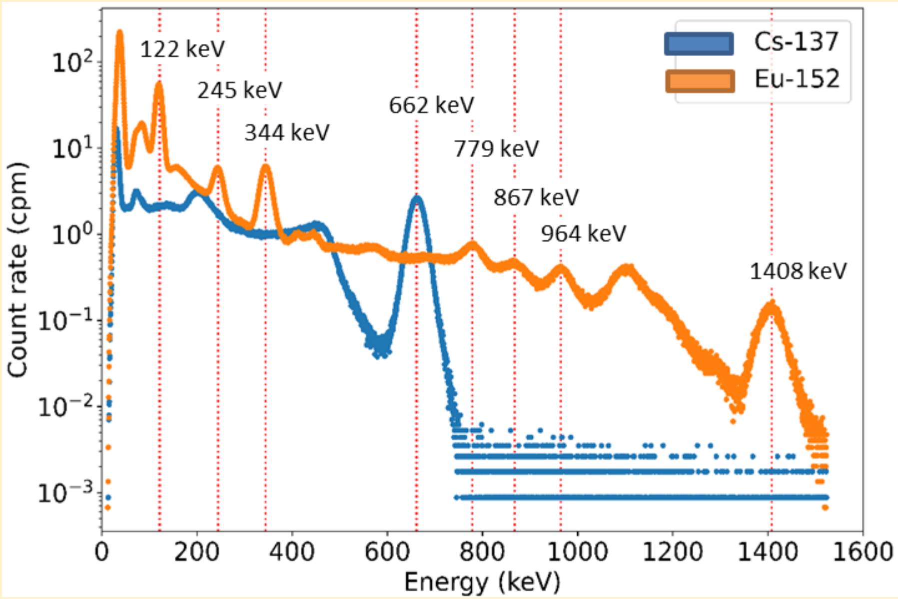

Energy Resolution
5.2% @ 662 keV

Photopeak Efficiency
0.002% @ 662 keV

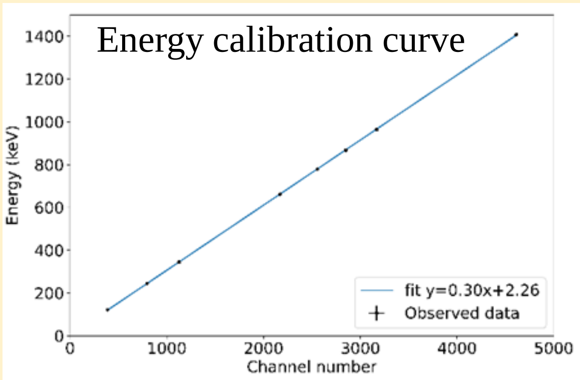

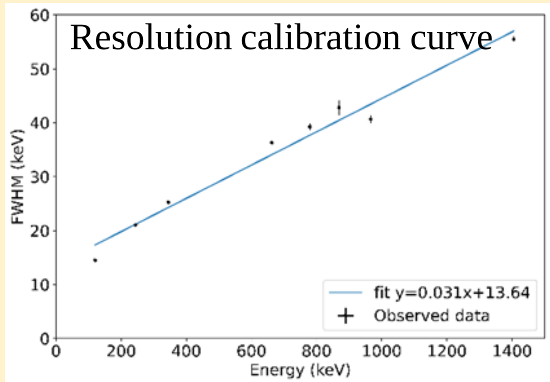

Laboratory experiments

- ^{137}Cs + ^{90}Sr assessment in blind-tubes:

- Generic scenario: **radiometric logging probe** is deployed at a fixed depth central in a **metallic blind-tube.**

A) **^{137}Cs** present in the ground surrounding the blind-tube: energetic gamma-rays from radioactive decay are detectable.

B) **^{90}Sr/^{90}Y** present in the ground surrounding the blind-tube but close to the wall: bremsstrahlung photons detectable from deceleration of the decay energetic beta particles in the steel material.

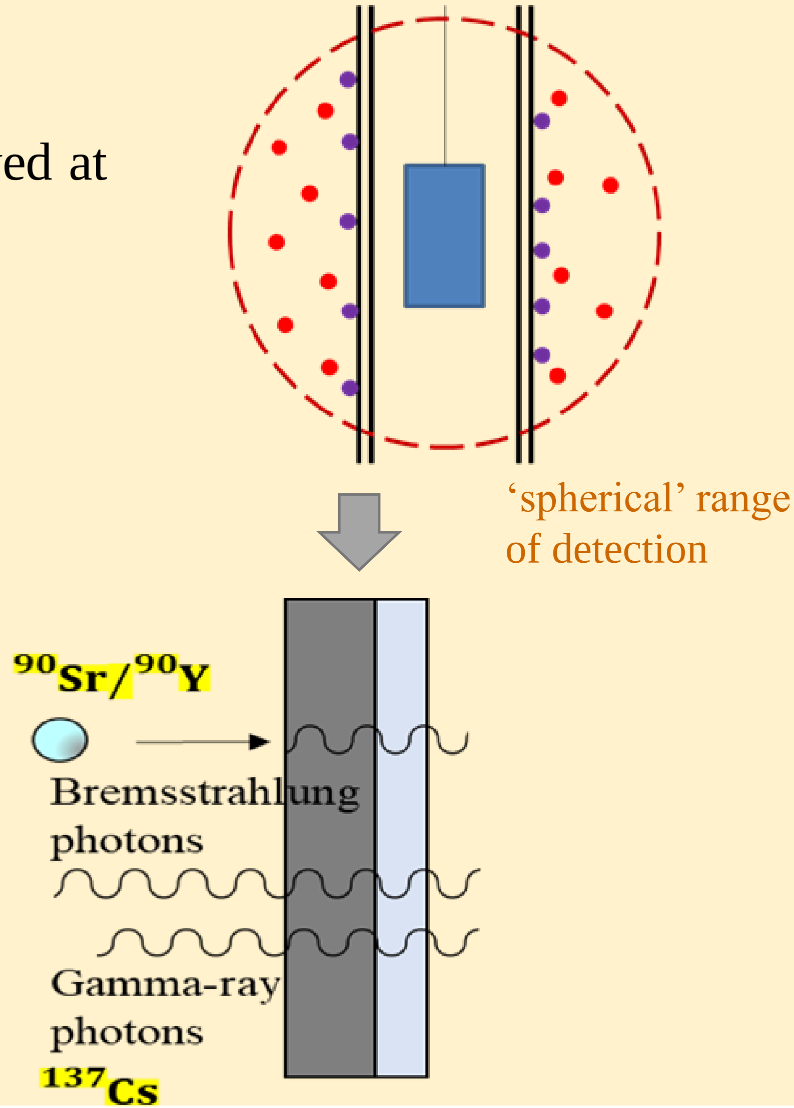

Ref. Wilson *et al.* (1998) Spectral Shape Analysis for Contaminant Logging at the Hanford Site

Laboratory experiments

- ^{137}Cs + ^{90}Sr assessment in blind-tubes: dual-mode performance

Experiment 1:

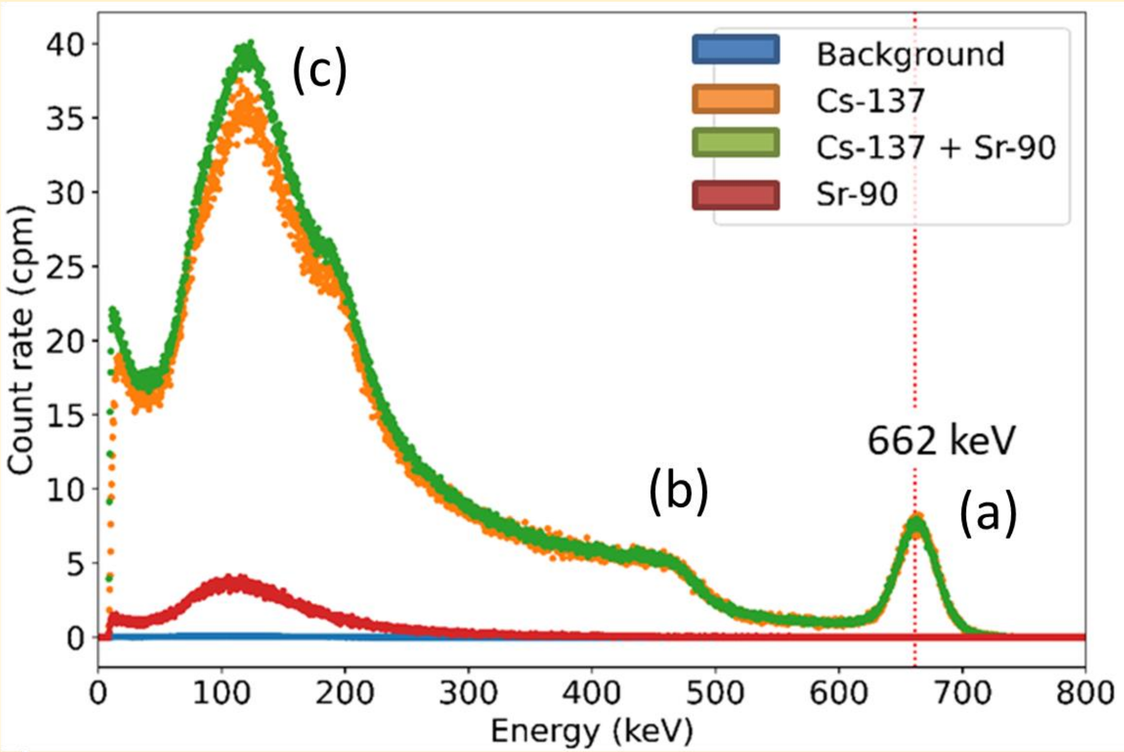

Point sources:
^{137}Cs (304 keV)
^{90}Sr/^{90}Y (370 keV)

Simplified scenario

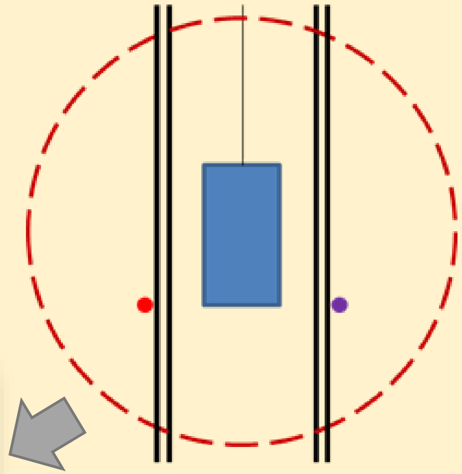

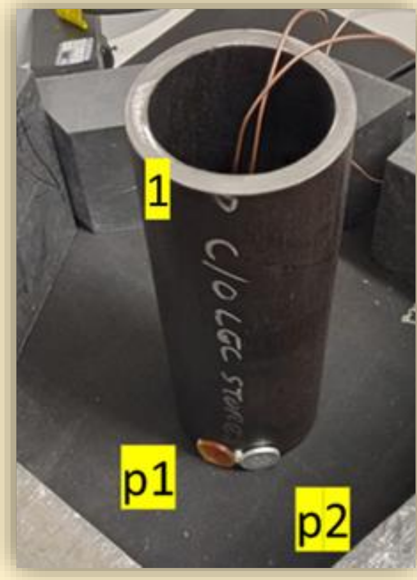

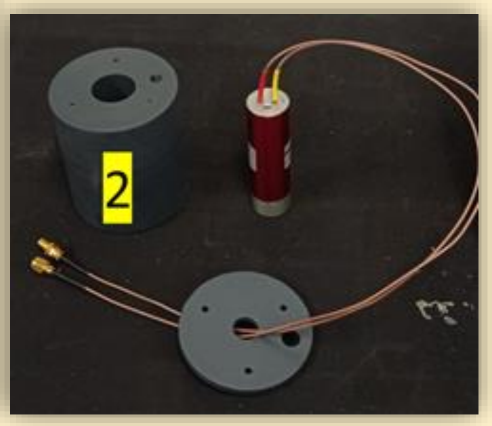

- Intense beta exposure act to degrade the spectrum from ^{137}Cs.

Laboratory experiments

- ^{137}Cs + ^{90}Sr assessment in blind-tubes: dual-mode performance

Experiment 2:

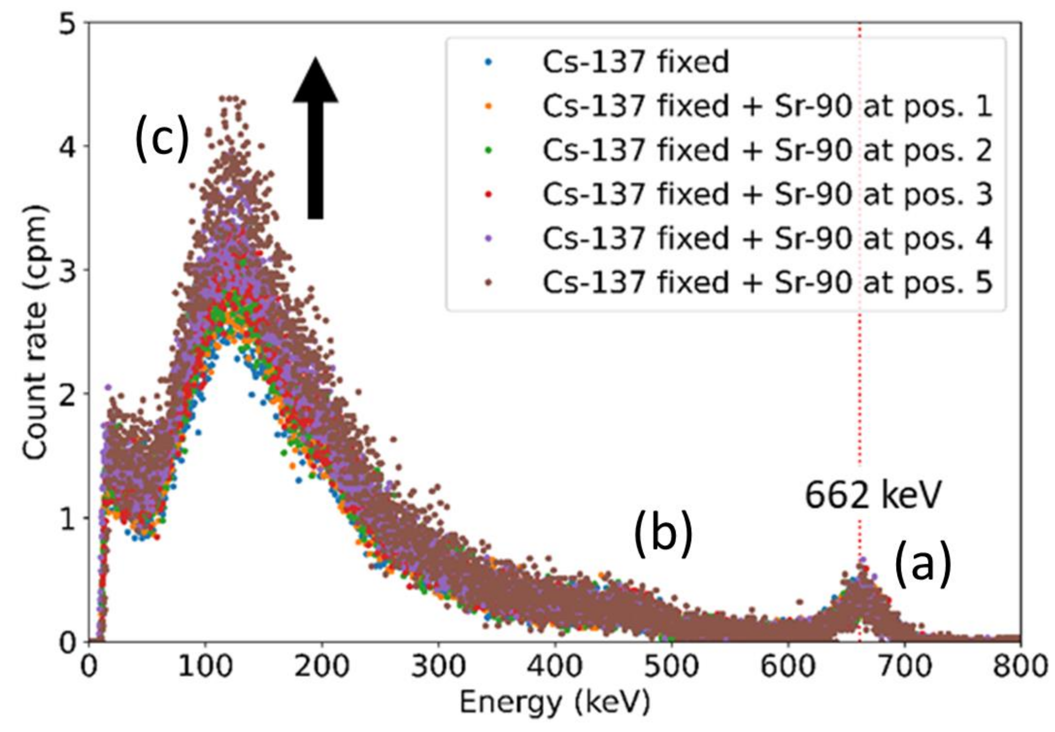

Point sources:
^{137}**Cs** (304 keV)
^{90}**Sr/**^{90}**Y** (370 keV)

<u>Simplified scenario</u>

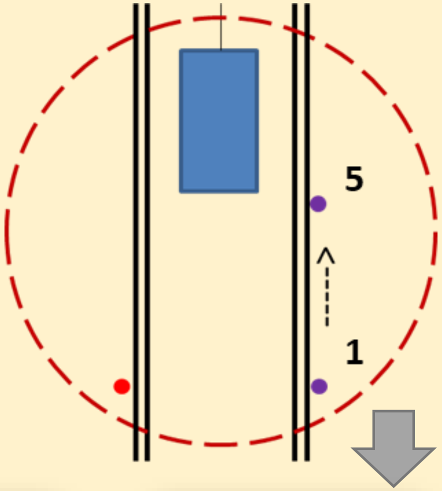

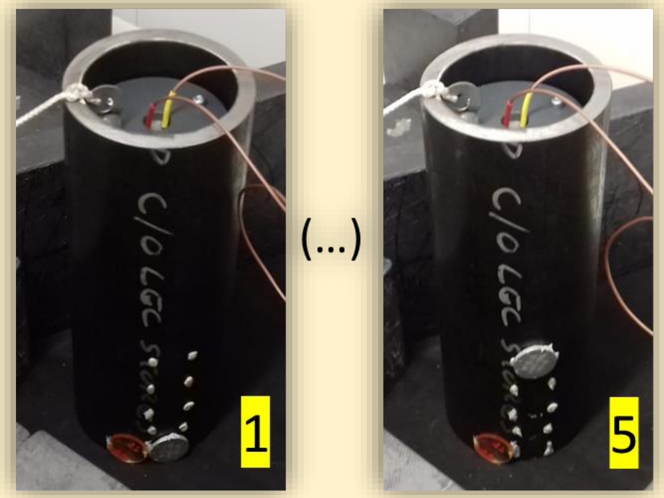

- Gradual increase of counts in (c) region.

Conclusion & Future work

- CeBr3 + Topaz SiPM Digital MCA system presents a promising solution for characterisation of underground sources, addressing challenging site constraints.
- Experiments suggest excellent detector energy resolution and response linearity.
- Detection of ^{137}Cs + ^{90}Sr in a blind-tube successfully addressed for a simplified scenario.

Further investigations are underway to

- enable a wider diversity of scenarios to be considered
- including the study of dual-mode detection limitations,
- and to calibrate the system in the blind-tube test pit arrangement replicating the in-ground blind-tubes.
- And investigate complex scenarios, as different ground composition and source distributions, via Monte Carlo simulations.

TRANSCEND

Transformative Science and Engineering for Nuclear Decommissioning

Soraia Elísio (s.elisio@lancaster.ac.uk);
Malcolm J. Joyce (m.joyce@lancaster.ac.uk);
James Graham (james.graham@uknnl.com);
Barrie Greenhalgh (barrie.greenhalgh@sellafieldsites.com)

GAME CHANGERS

Characterisation and monitoring using in-ground assets

Frank Cave (frank@hybridinstruments.com)
Alex Grievson (a.j.grievson@lancaster.ac.uk)
Aliyu Bala (aliyu@hybridinstruments.com)

Thank you

Poster “Advanced Blind-tube Instrument for Characterisation of Underground Sources”

Lancaster University | NATIONAL NUCLEAR LABORATORY | Sellafield Ltd | GAME CHANGERS | Hybrid Instruments

Alpha, Beta and Gamma dosimetry effects on spent fuel dissolution

By Angus Siberry,
University of Bristol

Modelling Spent fuel dissolution

Source term for radiolytic species → Incorporate into **1D Chemical reaction and diffusion models**

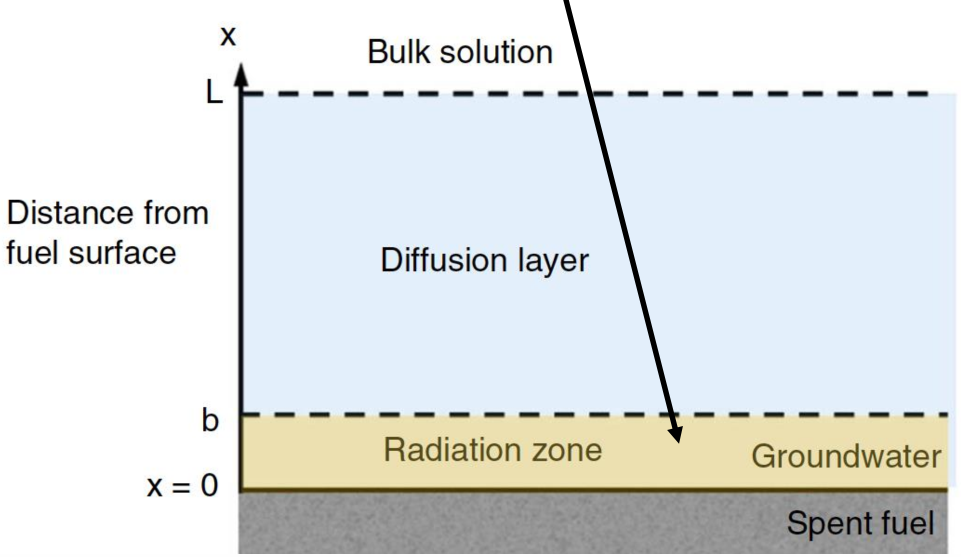

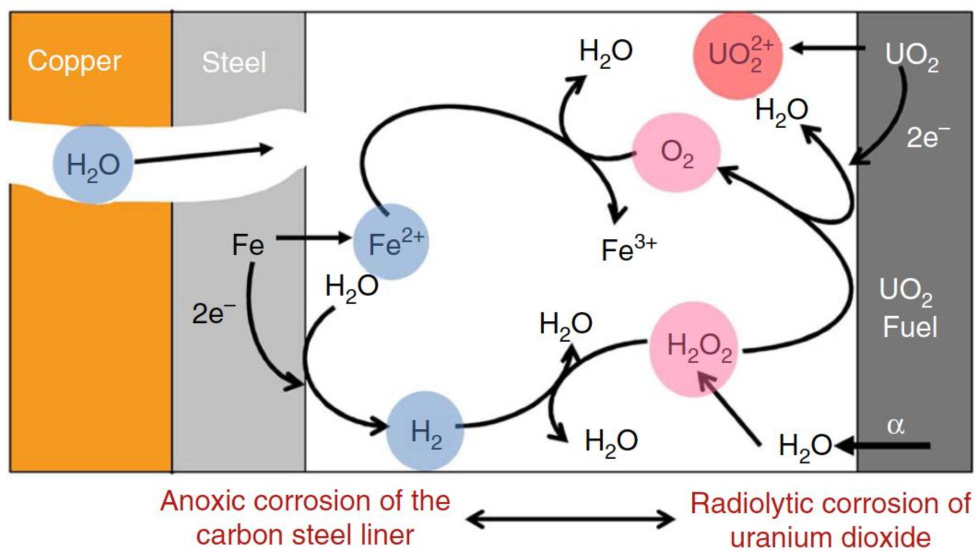

[1] Liu, Nazhen, et al. *Corrosion* 75.3 (2019): 302-308.

Dose rates

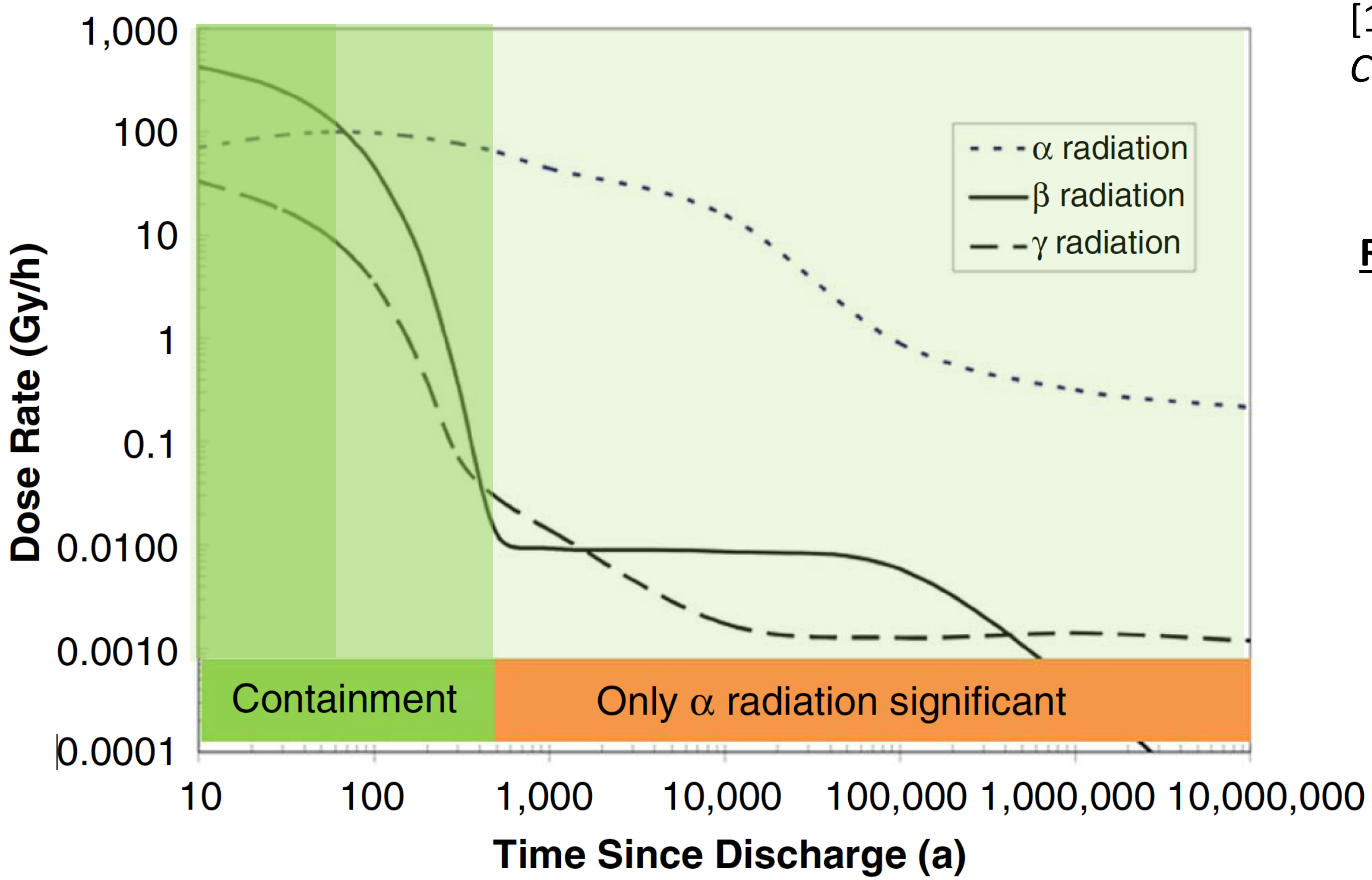

[1] Liu, Nazhen, et al. *Corrosion* 75.3 (2019): 302-308.

<u>Relevant radiation fields</u>

α,β,γ

α,β

α

TRANSCEND

Transformative Science and Engineering for Nuclear Decommissioning

Interaction with water

Interim Wet storage

α,β,γ	α,β

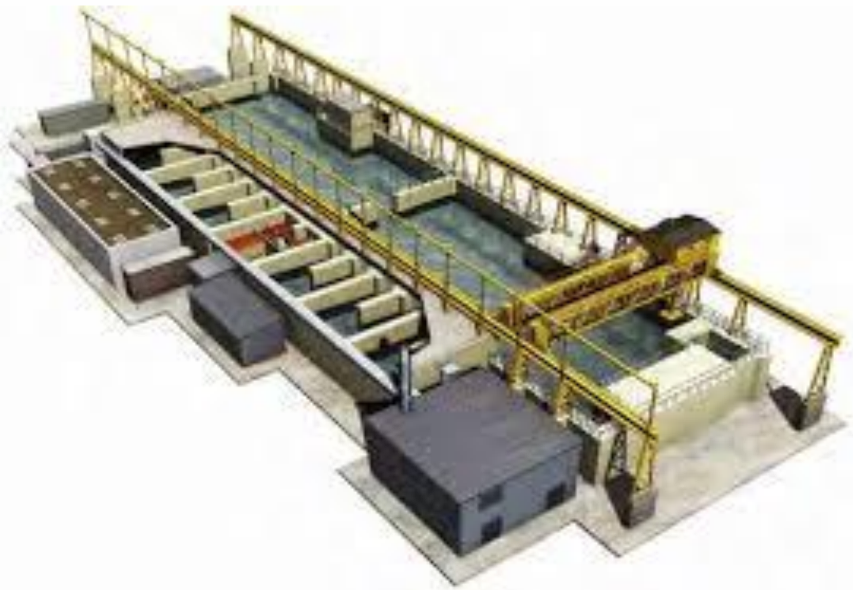

Geological Disposal Facility (GDF)

α

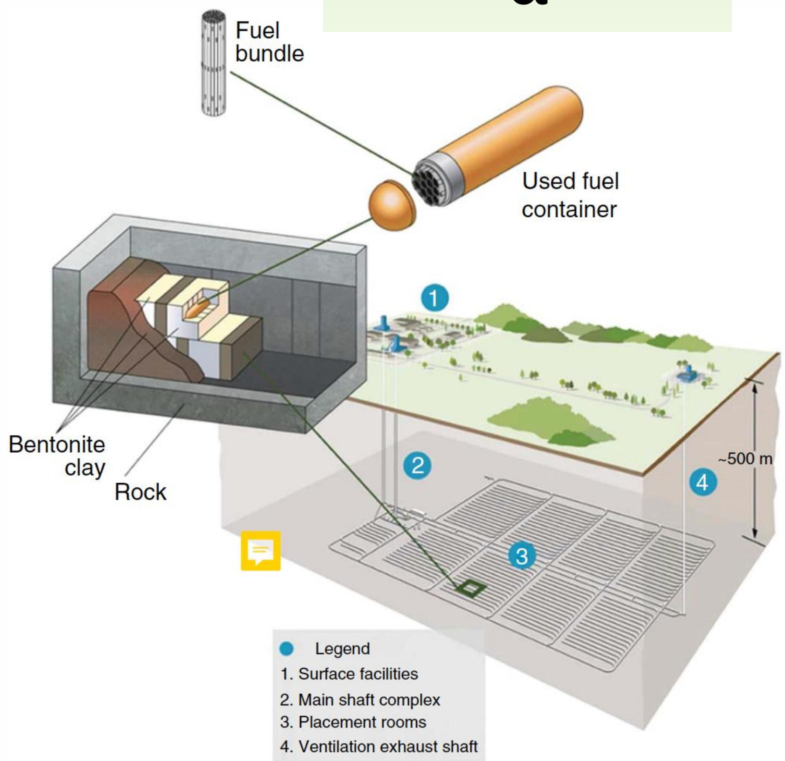

Sellafield Ltd

University of BRISTOL

NATIONAL NUCLEAR LABORATORY

α - modelling

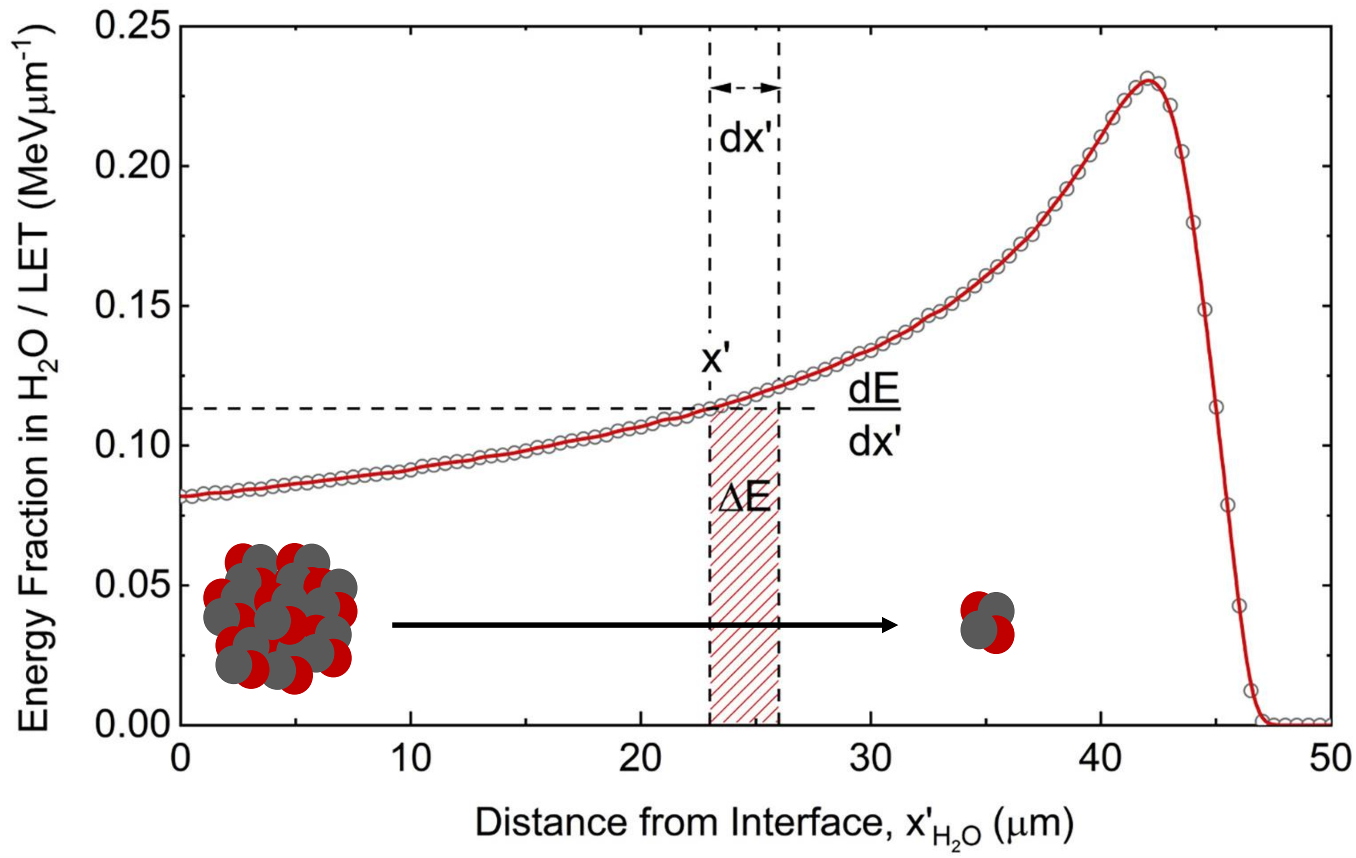

- High Linear Energy Transfer
- Leaves a penumbra of chemical events in its path
- Travels (nominally) in straight lines

α

[2] Siberry, Angus, et al. *Radiation Physics and Chem* (2021): Volume 182.

α – modelling of spent fuel/water interface

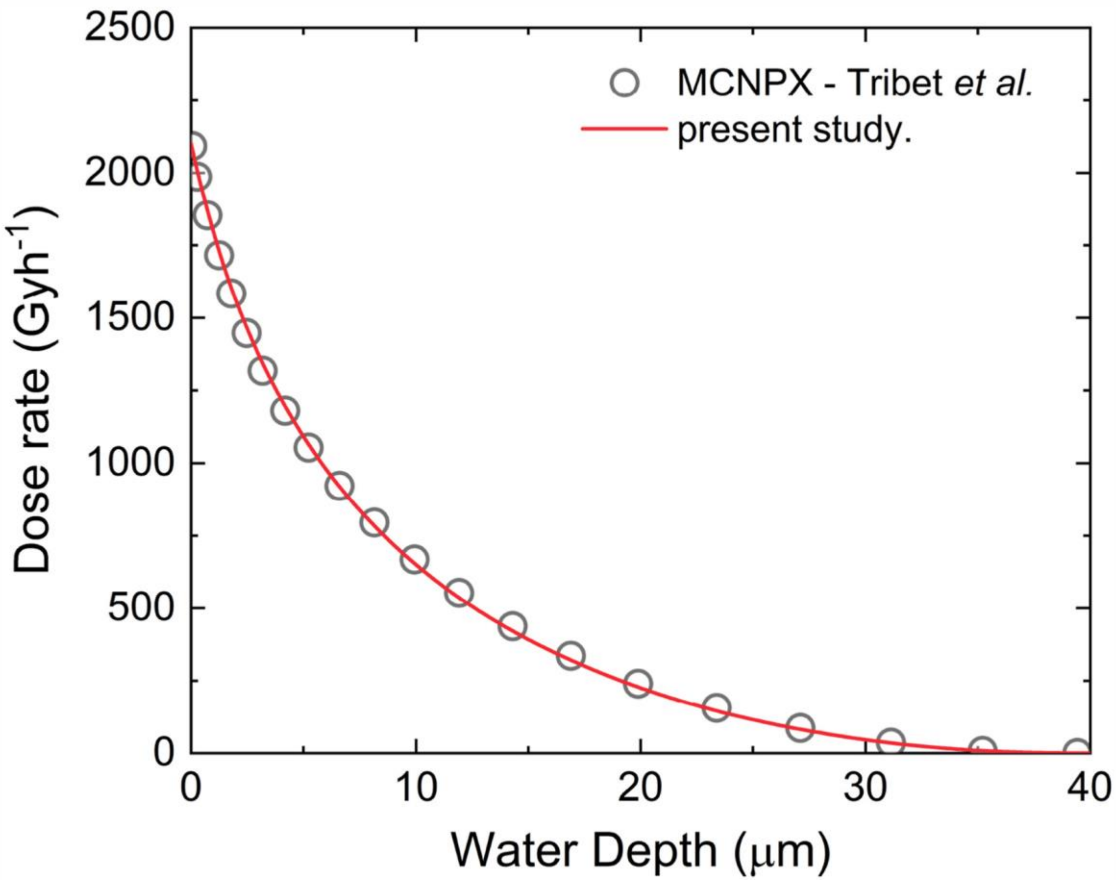

- High dose rates at interface
- Decay curve of energy deposition
- Max penetration in water < **100 μm**

α

[3] Siberry, Angus, et al. *Radiation Physics and Chem* (2021): Volume 188.

TRANSCEND

Transformative Science and Engineering for Nuclear Decommissioning

β - modelling

α,β

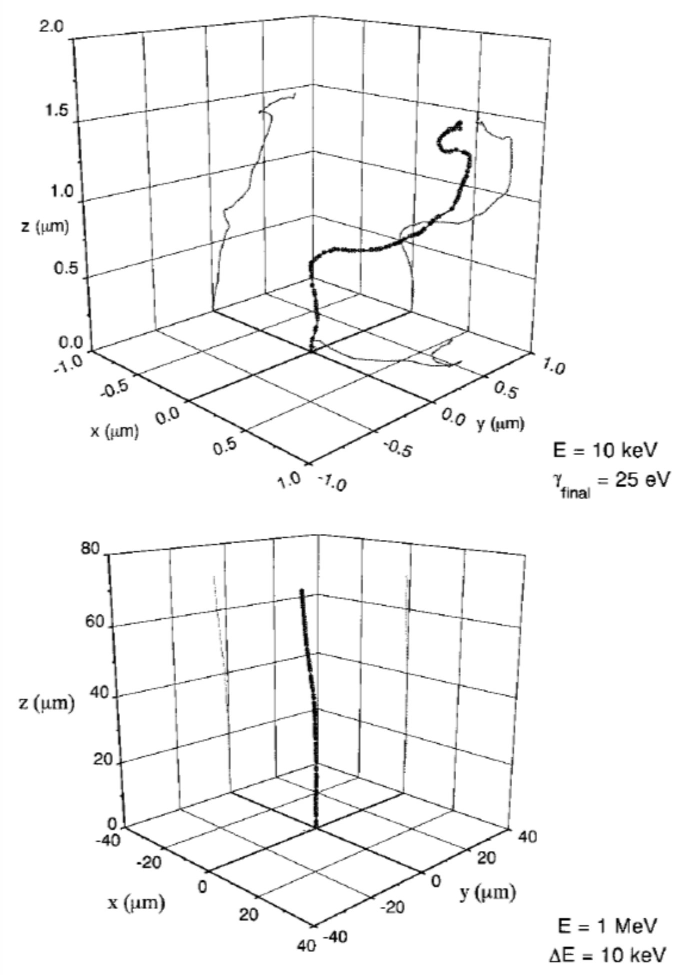

- **Low** Linear Energy Transfer
- Leaves **spurs** of chemical events in its path
- Travels in straight lines above 10 keV [4]

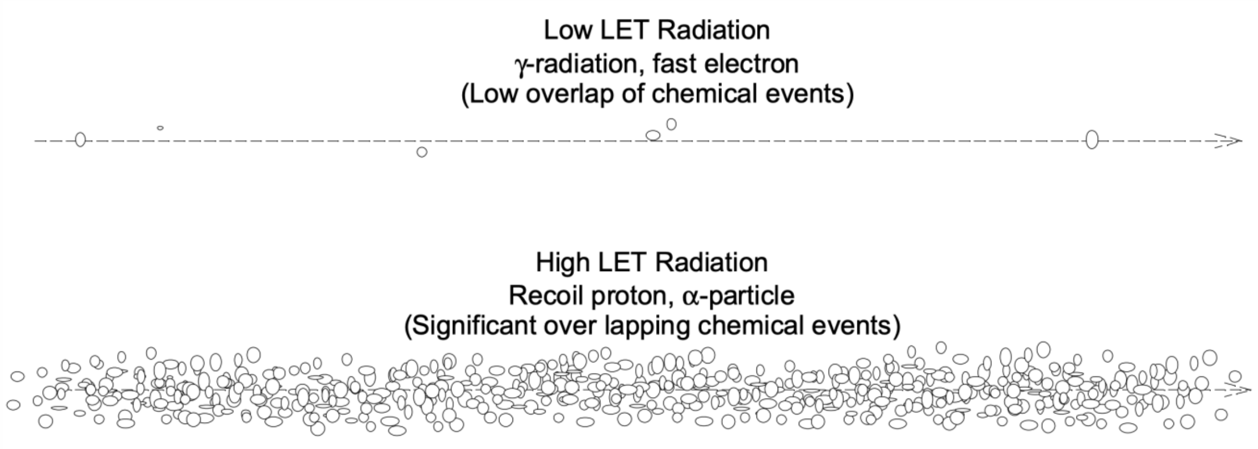

[8] Elliot, A.J., & Bartels, D.M. (2009). (AECL--153-127160-450-001). Canada

[4] Pimblott, Simon M et al. *The Journal of Physical Chemistry* 100.20 (1996): 8595-8606

Sellafield Ltd University of BRISTOL NATIONAL NUCLEAR LABORATORY

Transformative Science and Engineering for Nuclear Decommissioning

β – modelling

α,β

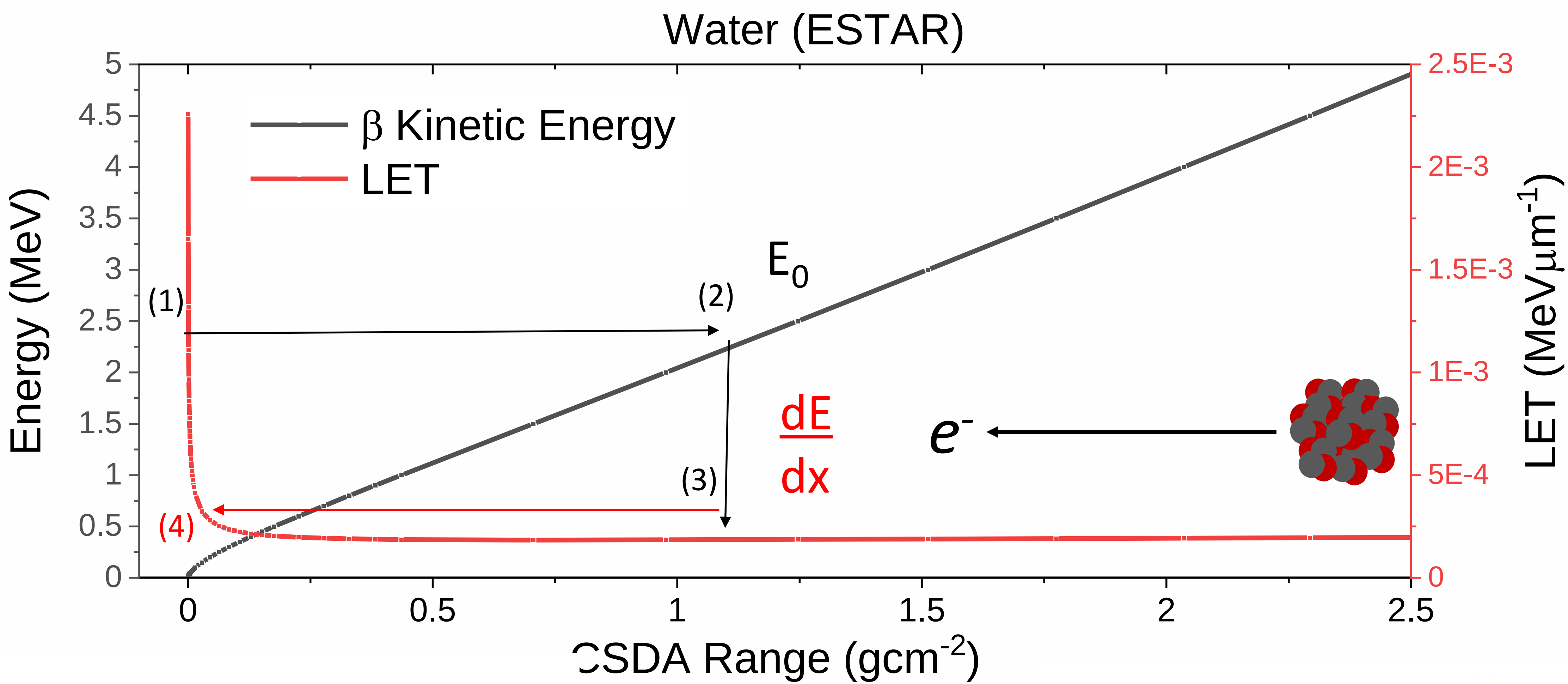

α,β

Modelling spent fuel / water interface (β)

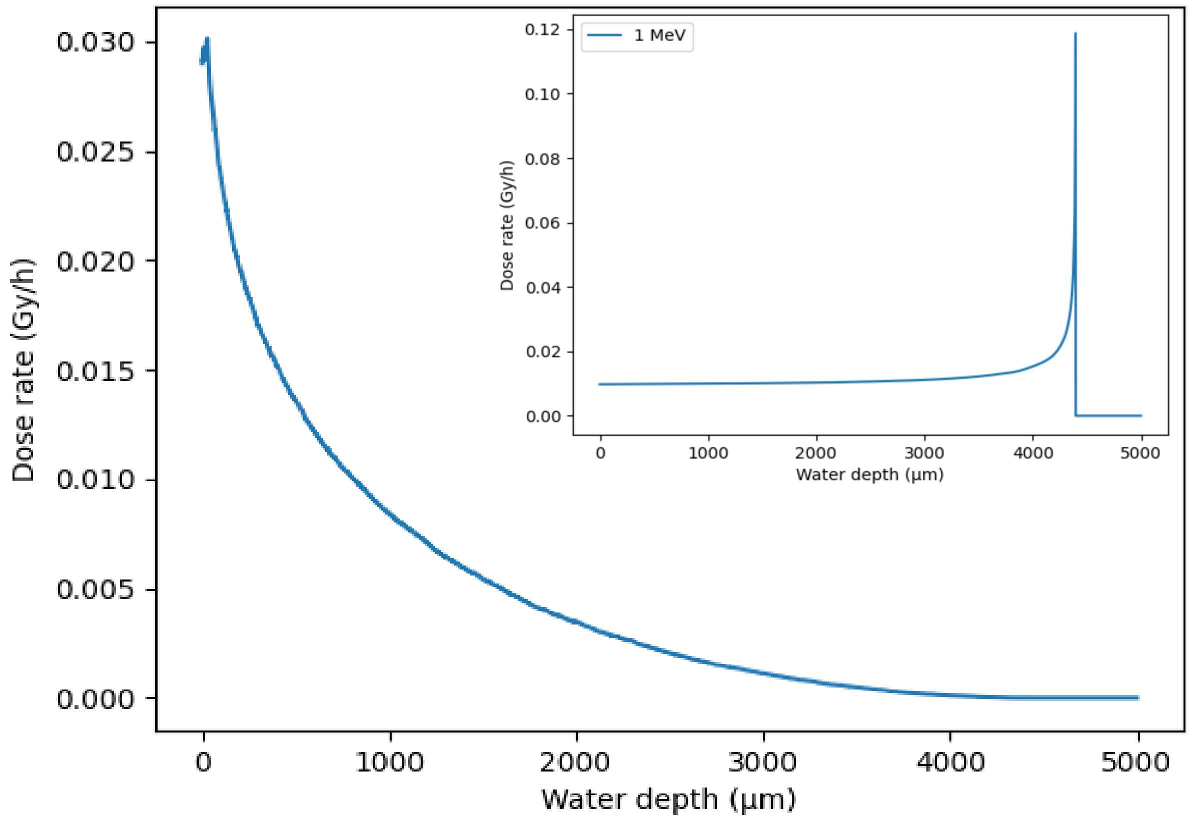

- High dose rates at interface
- Decay curve of energy deposition
- Likely penetration in water < **1 cm**

γ – modelling

α,β,γ

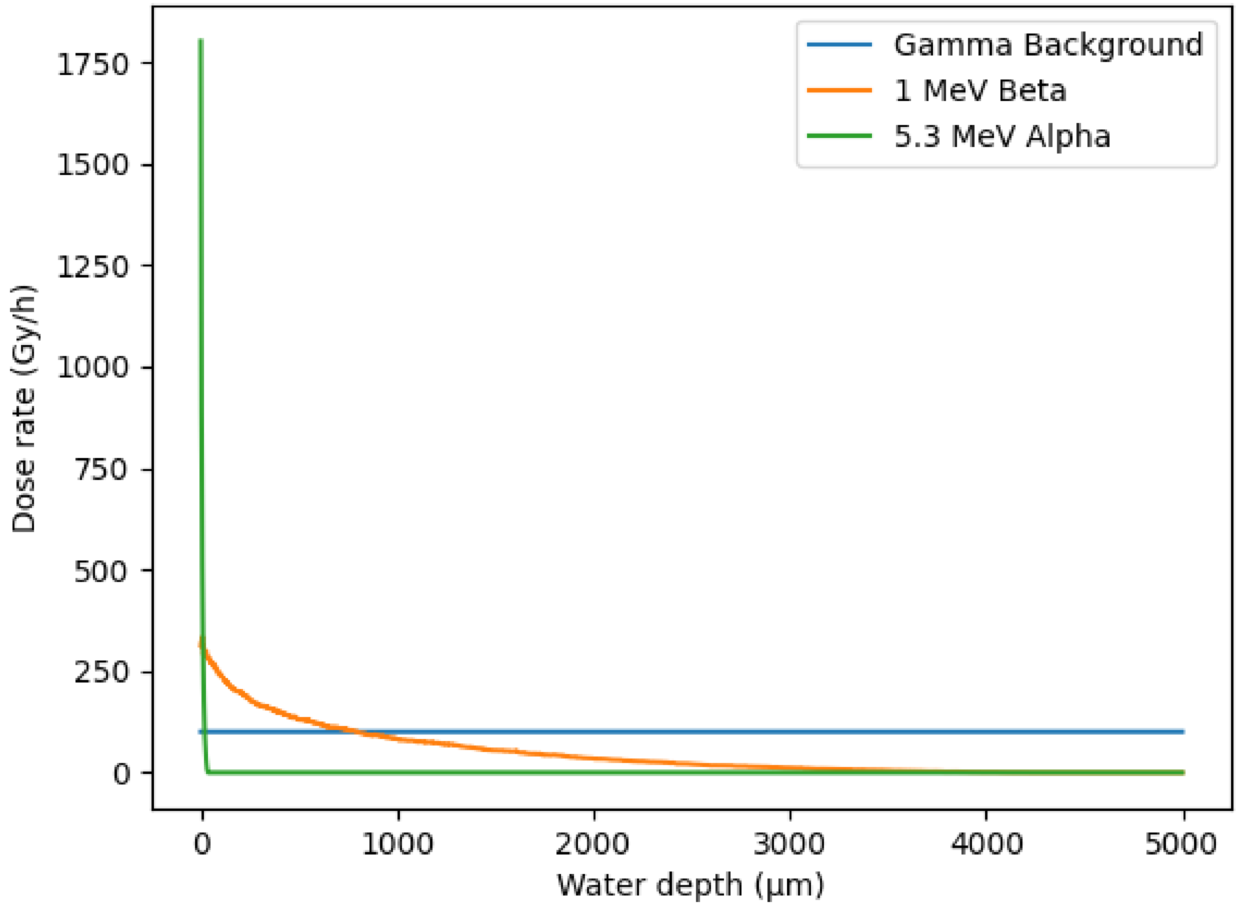

- Likely penetration in water **> 1m**
- **γ lengthscale** >> Diffusion layer **width**
- Background values used as **constant**

TRANSCEND

Transformative Science and Engineering for Nuclear Decommissioning

Dose rates

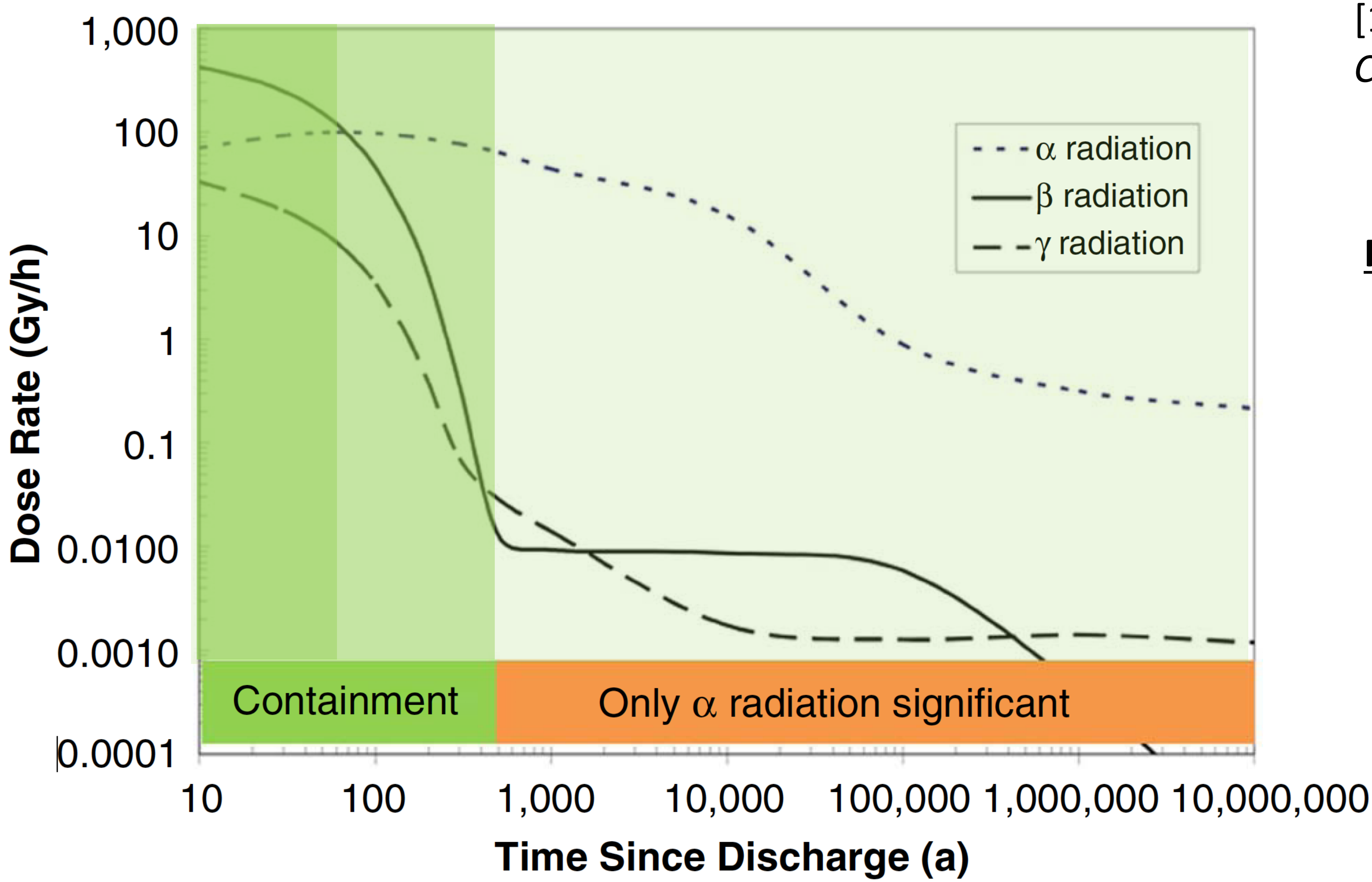

[1] Liu, Nazhen, et al. *Corrosion* 75.3 (2019): 302-308.

Relevant radiation fields

α,β,γ

α,β

α

Sellafield Ltd

University of BRISTOL

NATIONAL NUCLEAR LABORATORY

Transformative Science and Engineering for Nuclear Decommissioning

Interaction with water

Interim Wet storage

α,β,γ	α,β

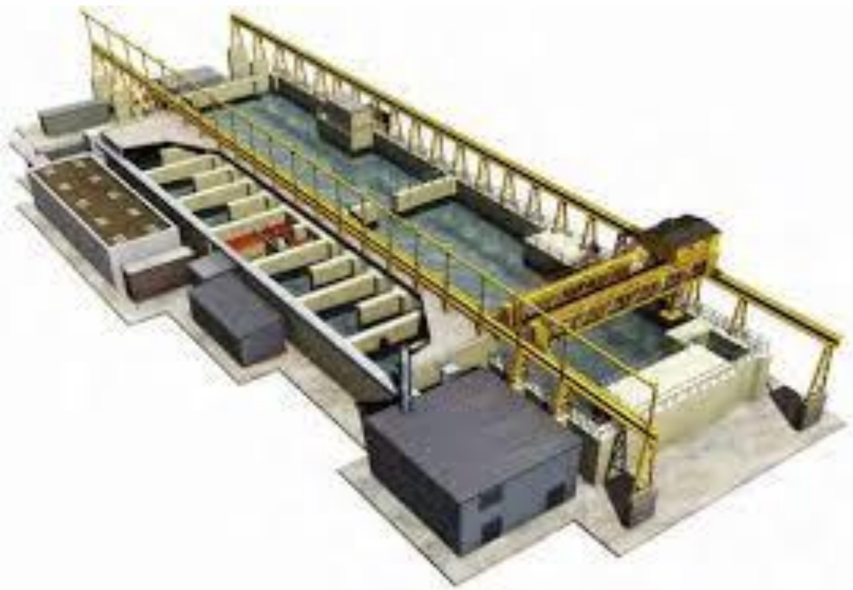

Geological Disposal Facility (GDF)

α

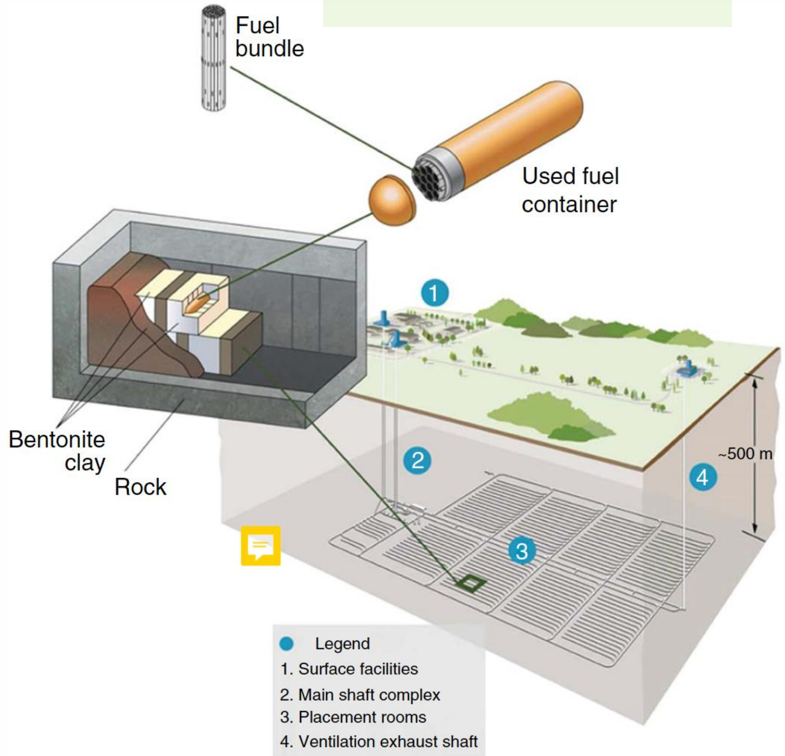

Radiolysis

α,β,γ

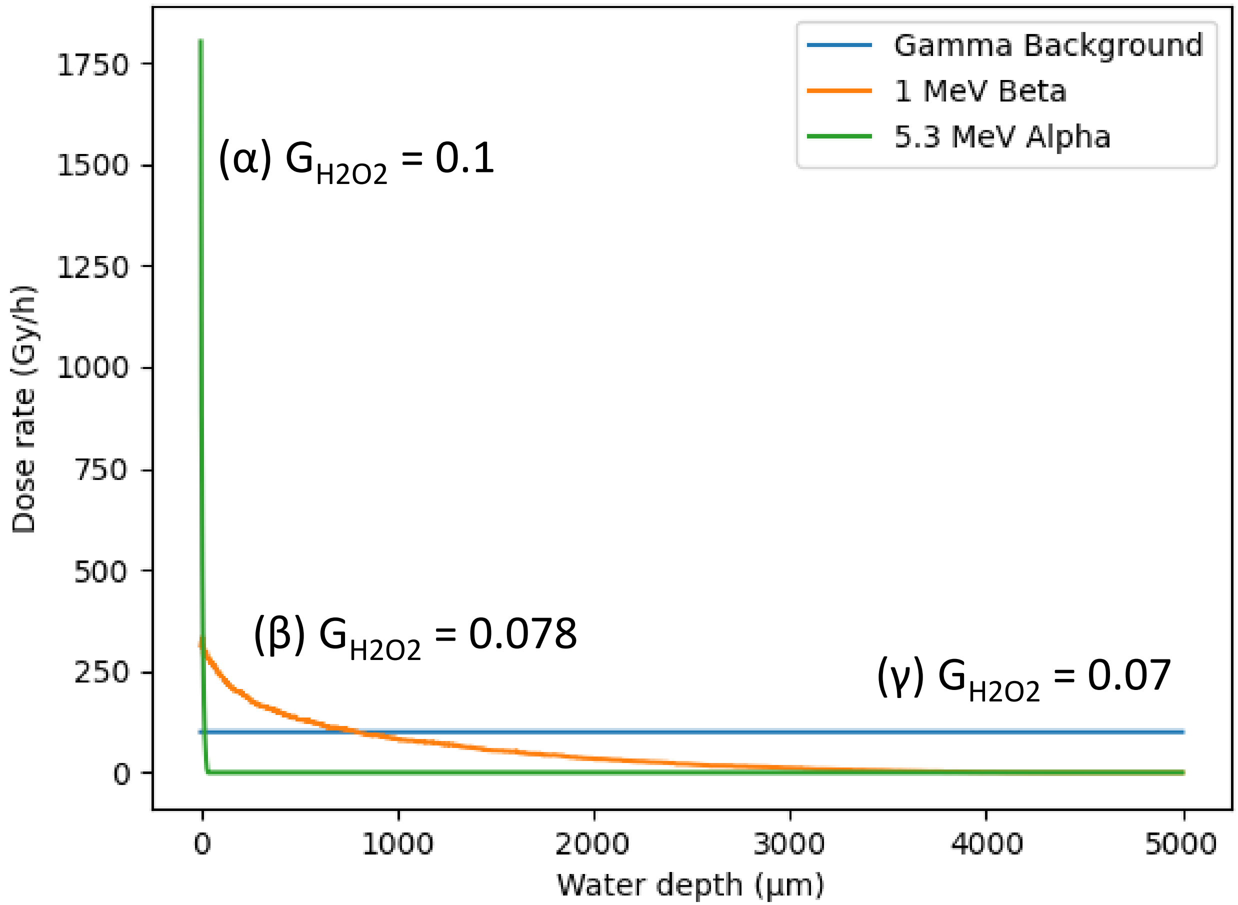

- G – value determines the radiolytic yield per unit energy deposited in water.
- It is radiation-type dependant and in units eV^{-1}
- G = 1 is 1 molecule produced per 100 eV energy deposited

([5-7]Pastina and Laverne 2001, Kohan et al (2013), Mustaree et al (2014))

Transformative Science and Engineering for Nuclear Decommissioning

Radiolysis

α,β,γ

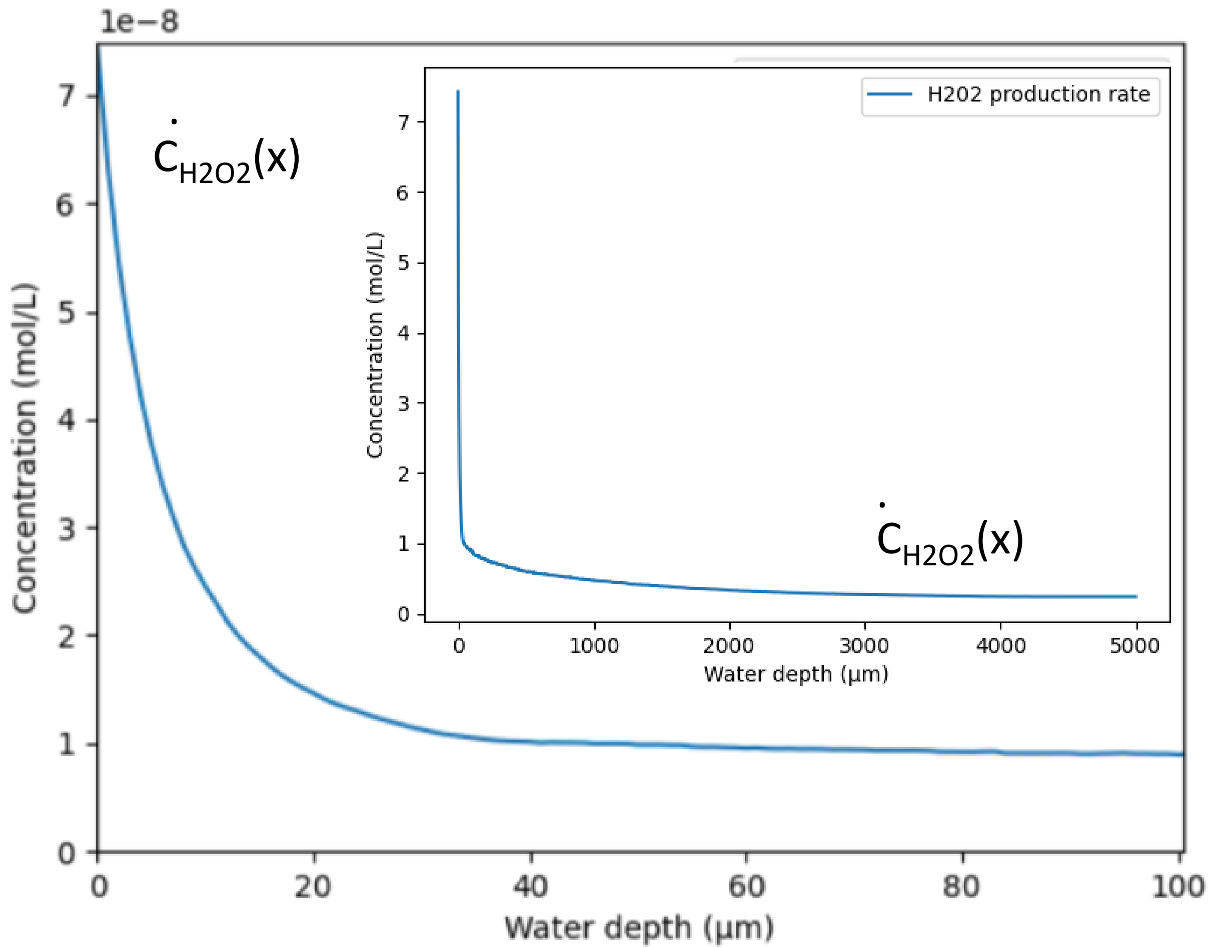

- Scaling dose rate curved by G – value and combining curves provides a **source term**, $C_{H2O2}(x)$
- All radiolytic species will produce different source terms due to variation in g-value and ratios of these values between radiation type

Transformative Science and Engineering for Nuclear Decommissioning

Modelling Spent fuel dissolution

Source term for radiolytic species → <u>Incorporate into **1D Chemical reaction and diffusion models**</u>

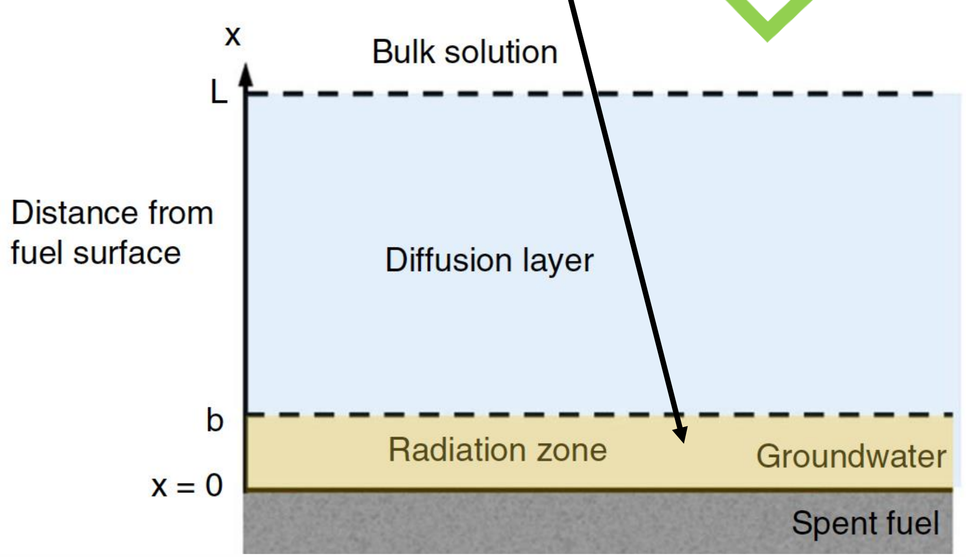

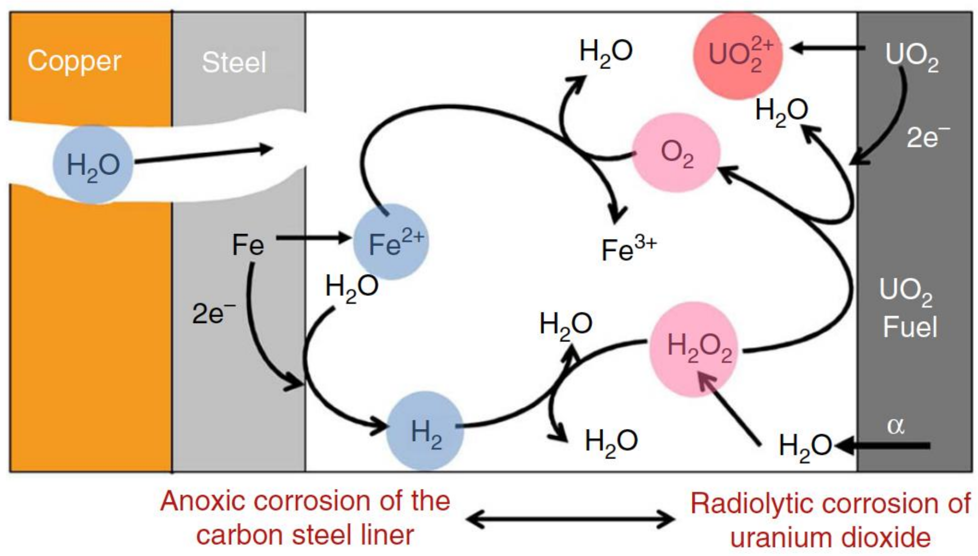

[1] Liu, Nazhen, et al. *Corrosion* 75.3 (2019): 302-308.

Sellafield Ltd

University of BRISTOL

NATIONAL NUCLEAR LABORATORY

1D Diffusion and reaction model

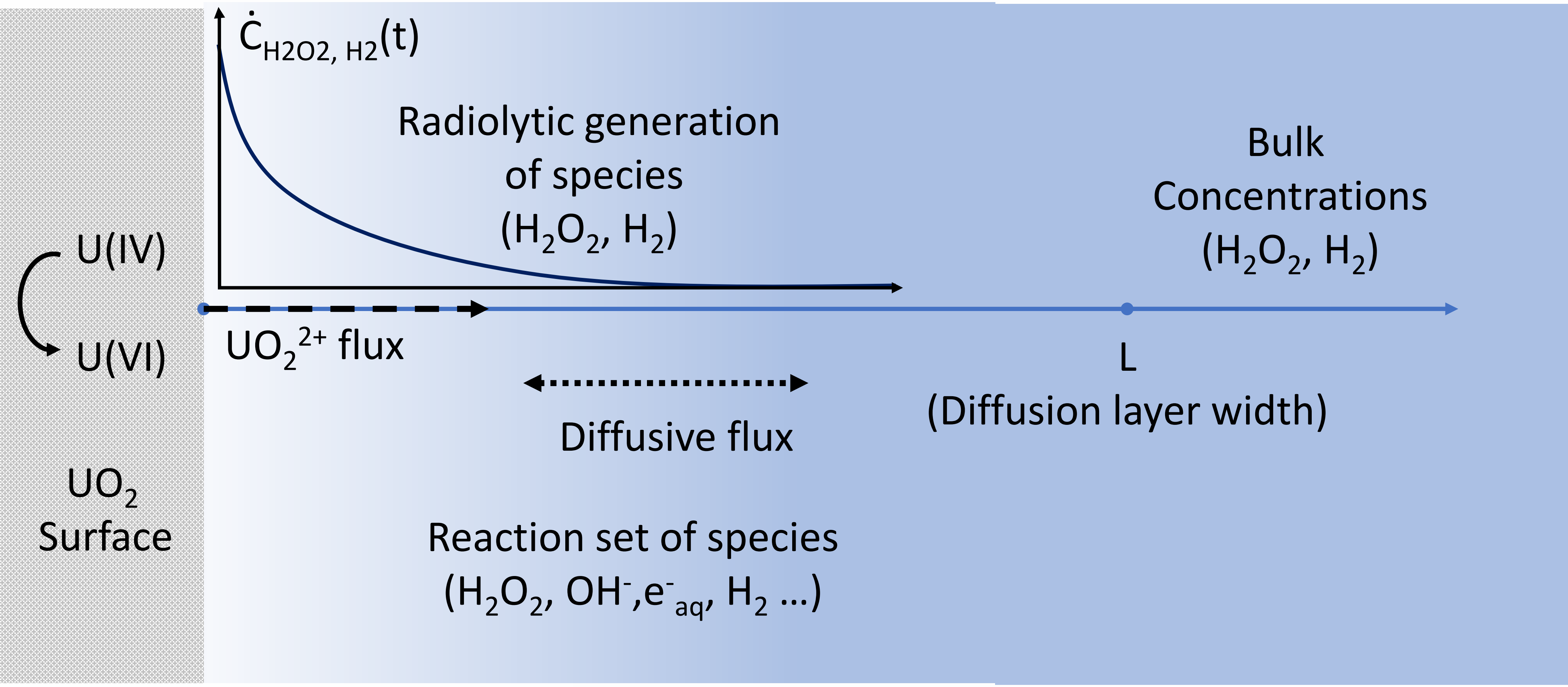

UO_2 dissolution rates (COMSOL)

- Using **COMSOL 1D chemical reaction and diffusion model** [1]
- Import combine source term from **α,β,γ – dose rates**
- Flux magnitude **0.45 +/- 0.1 nmol $m^{-2}s^{-1}$**, approximately 10x that of **Wu et al (2014)**
- **GDF** disposal conditions

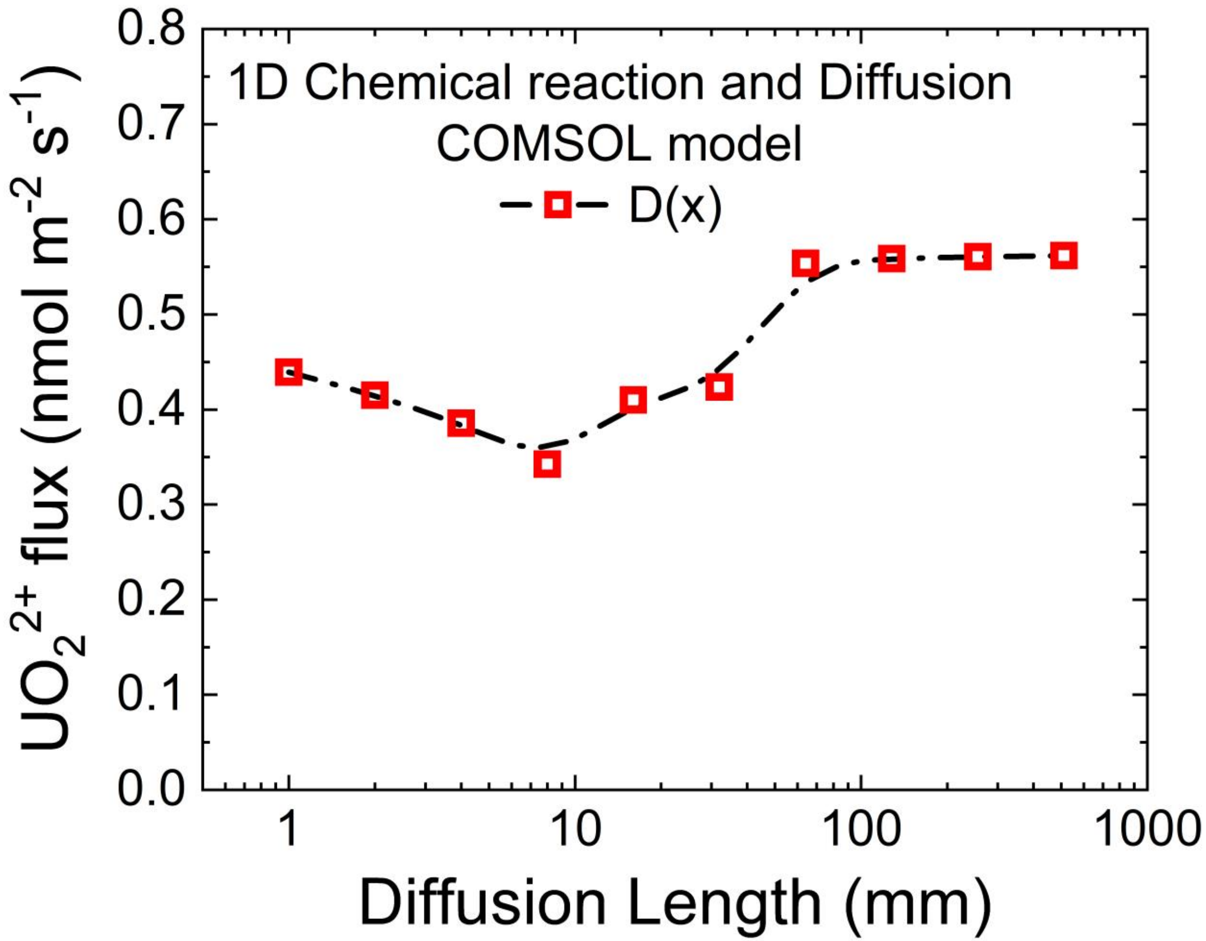

What next – 3D Spherical model

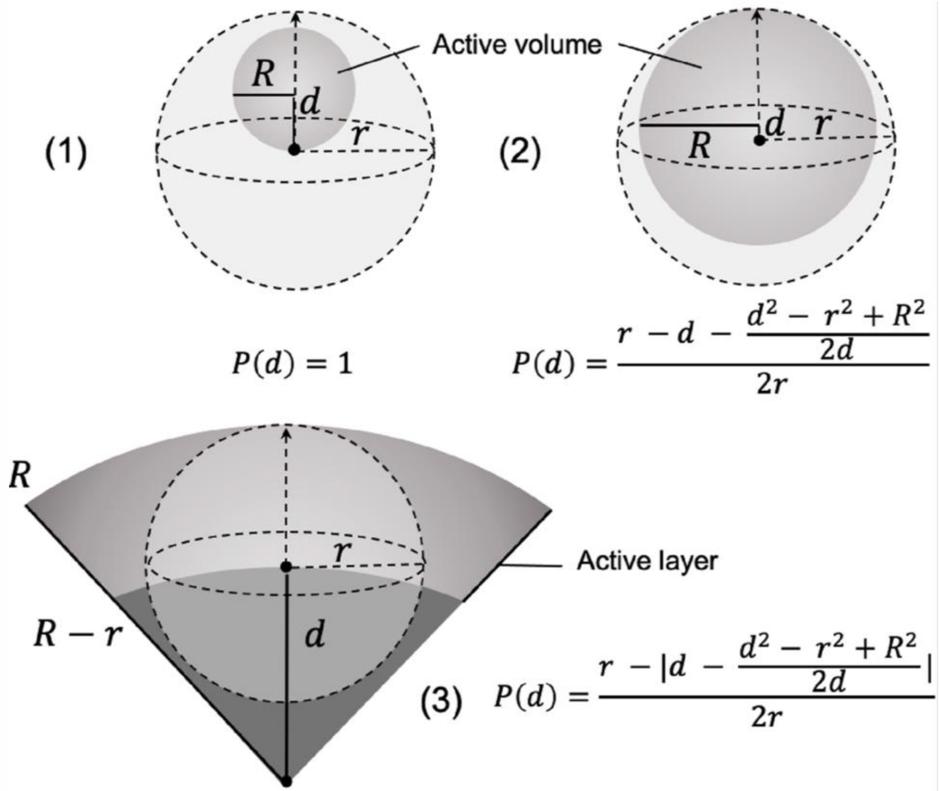

- Extrapolate model into **3-Dimensions**
- Incorporate **geometrical model** for radiolysis source term
- **Time resolved radius changes** to create a feedback loop to code to edit source term
- Replicate dissolution, H_2 and H_2O_2 generation from **suspended sludges** of **spent fuel in fuel pond storage**

What next - Full Reaction set

- Include **all possible reactions** and species created during radiolysis of water
- Reaction set devised **by Elliot and Bartels** [8]
- Import into 1D chemical reaction and diffusion model to get full picture

Number	Reaction
R2	$e_{aq}^- + e_{aq}^- + (2\ H_2O) \rightarrow H_2 + 2\ OH^-$
R3	$H + H \rightarrow H_2$
R4	$OH + OH \rightarrow H_2O_2$
R5	$e_{aq}^- + H\ (+ H_2O) \rightarrow H_2 + OH^-$
R6	$e_{aq}^- + OH \rightarrow OH^-$
R7	$H + OH \rightarrow H_2O$
R8	$e_{aq}^- + H_2O_2 \rightarrow OH + OH^-$
R9	$e_{aq}^- + O_2 \rightarrow O_2^-$
R10	$e_{aq}^- + O_2^-\ (+ H_2O) \rightarrow H_2O_2 + 2\ OH^-$
R11	$e_{aq}^- + HO_2 \rightarrow HO_2^-$
R12	$H + H_2O_2 \rightarrow OH + H_2O$
R13	$H + O_2 \rightarrow HO_2$
R14	$H + HO_2 \rightarrow H_2O_2$
R14a	$H + HO_2 \rightarrow 2\ OH$
R15	$H + O_2^- \rightarrow HO_2^-$
R16	$OH + H_2O_2 \rightarrow HO_2 + H_2O$
R17	$OH + O_2^- \rightarrow (HO_3^-) \rightarrow O_2 + OH^-$
R18	$OH + HO_2 \rightarrow (H_2O_3) \rightarrow O_2 + H_2O$
R19	$HO_2 + HO_2 \rightarrow H_2O_2 + O_2$
R20	$O_2^- + HO_2\ (+ H_2O) \rightarrow H_2O_2 + O_2 + OH^-$
R21	$O_2^- + O_2^-\ (+ 2\ H_2O) \rightarrow H_2O_2 + O_2 + 2\ OH^-$
R22	$H_2O_2 \rightarrow ½\ O_2 + H_2O$
R22a	$H_2O_2 \rightarrow 2\ OH$

Acknowledgements:

Supervisor: Ross Springell

Industrial Supervisors:

NNL – David Hambley
Sellafield – Anna Adamska

Thank you

as14659@Bristol.ac.uk

COMSOL Dissolution Modelling

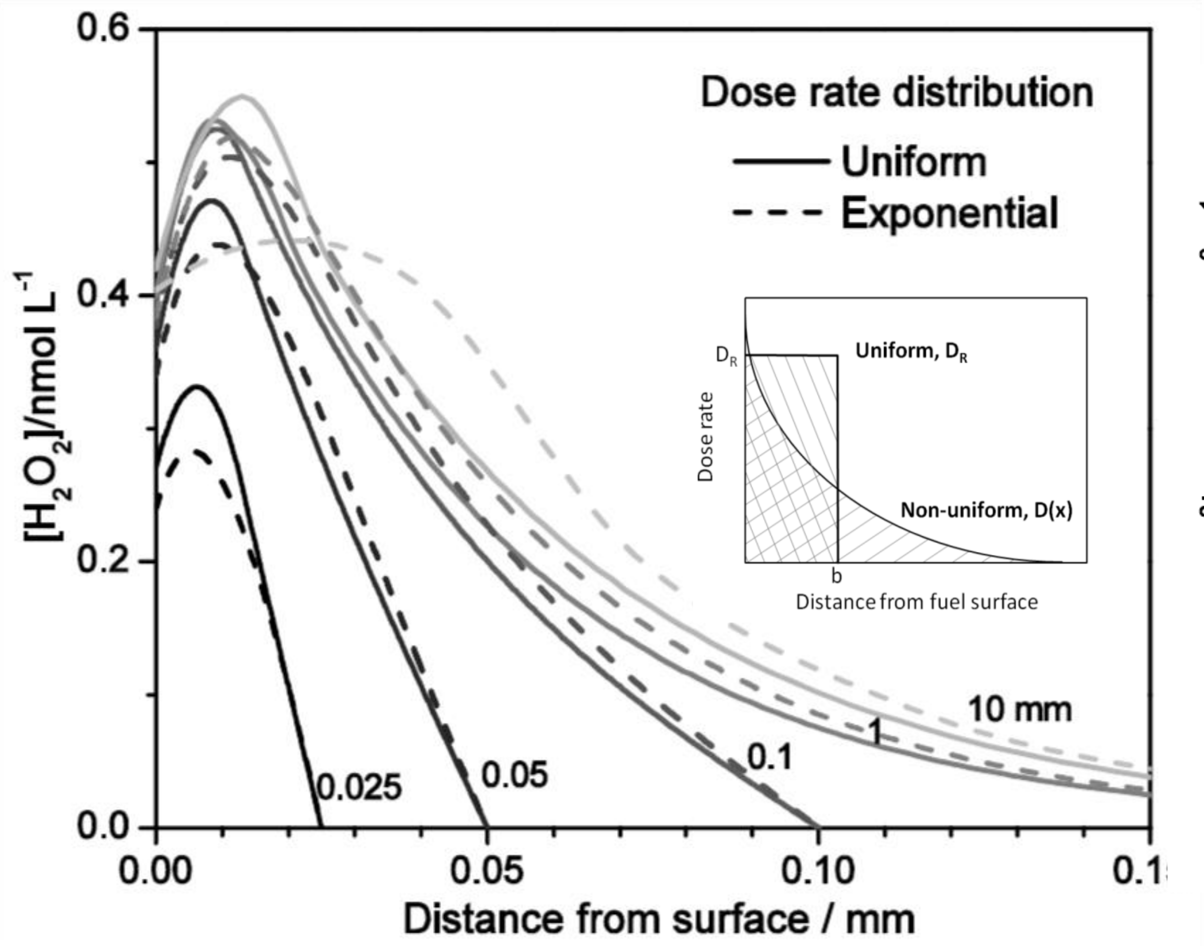

[8] Wu, Linda, (2014)

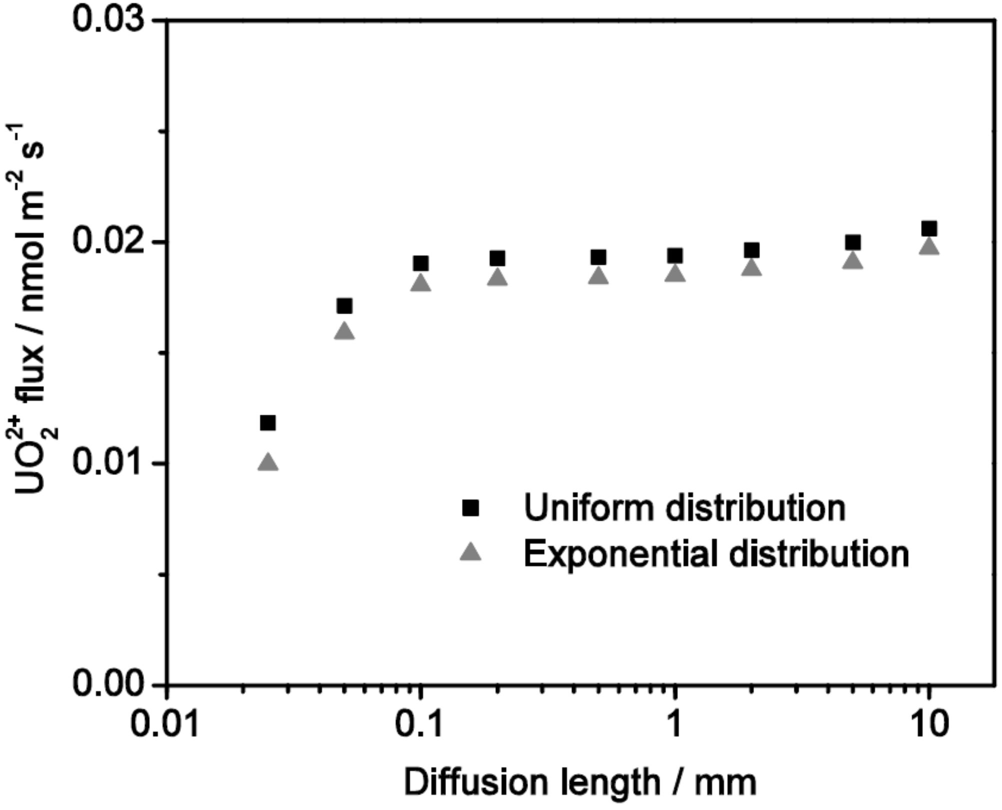

TRANSCEND

Transformative Science and Engineering for Nuclear Decommissioning

DFT Investigation of the Properties of Plutonium Dioxide Nanoparticles

William Neilson, Lancaster University

w.neilson@lancaster.ac.uk

Supervisor: Dr Samuel T. Murphy

TRANSCEND Annual Meeting 2021

11th Nov 2021

Energy

For a Low Carbon Future

Work to date

The intrinsic defect chemistry of $PuO_{2\pm x}$

- The defect chemistry is dominated by oxygen vacancies and interstitials.
- Hyper-stoichiometry found to be unfavourable

Phys. Chem. Chem. Phys., 2021, 23, 4544-4554

The accommodation and impact of Am in $(Pu,Am)O_{2\pm x}$

- Am accommodated in either the +III or +IV oxidation state.
- The impact of the +III oxidation state is to increase the concentration of holes from the valence band, increasing conductivity.

J. Phys. Chem. C, 2021, 125, 28, 15560–15568

The accommodation He in $PuO_{2\pm x}$ and the role of Am.

- The interstitial site is the favoured accommodation site for He.
- As the material ages, and Am accumulates, the oxygen vacancy is promoted as the accommodation site.

Front. Chem. - Solid State Chemistry, In review

The Defect Analysis Package, defap.py

INTRODUCTION

Do the results of studies that investigate bulk PuO_2 represent samples of PuO_2 that have a high surface to volume ratio?
What are the properties of these samples?

Aim and motivation:

- Here, we address these questions by, for the first time, simulating PuO_2 nanoparticles (NPs) using density functional theory (DFT).
- Using a computational approach, we can probe NPs properties. In addition to investigating the local and electronic structure, a computational approach should enable us to make predictions about the aging characteristics of the material by modelling defects and the interaction of the NPs with the surrounding environment (e.g. water) in future work.
- This question is posed as some facilities store PuO_2 as a powder, further a number of nuclear legacy sites, Pu has been found to migrate in subsurface environments in the form of nano-sized PuO_2 colloids.

Methods

Wulff construction

The equilibrium shape of the PuO_2 crystal can be predicted by performing a Wulff construction, where a crystal is constructed such that the surface energy is minimised.

To perform the construction, the surface energies of the low-index surfaces of PuO_2 need to be found and supplied; the low-index (111), (110) and (100) PuO_2 surfaces are illustrated below.

Wulff constructions have predicted a PuO_2 crystal entirely composed of (111) facets.

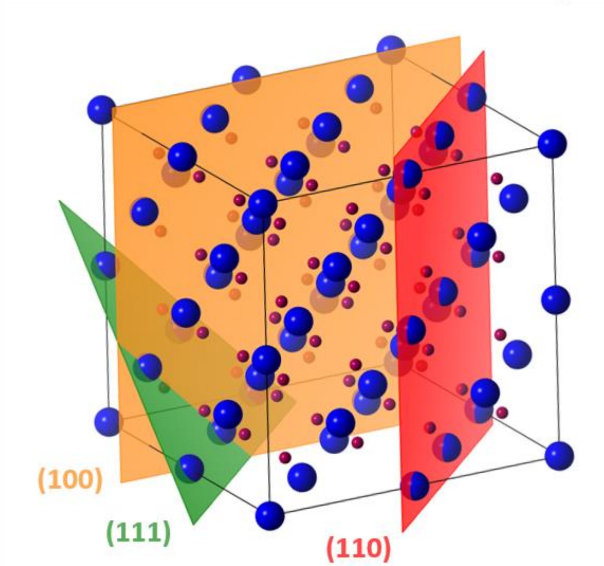

J. Phys. Chem. C 2019, 123, 1, 356–366

Methods

Wulff construction

The initial NP structures were constructed from expansions of the $Fm\bar{3}m$ PuO_2 unit cell, cleaved at the O-terminated (111) surface, creating NPs octahedral in shape.

Two NPs are constructed using this method: $Pu_{44}O_{80}$ and $Pu_{85}O_{160}$, which have a diameter of ~ 1.6 or ~ 2.2 nm.

NPs with a stoichiometric composition are constructed by removing four or five of the corner Pu atoms in $Pu_{44}O_{80}$ and $Pu_{85}O_{160}$, respectively.

These stoichiometric NPs, depicted in the figure, right, now have O-terminated (100) facets at the corners where Pu has been removed.

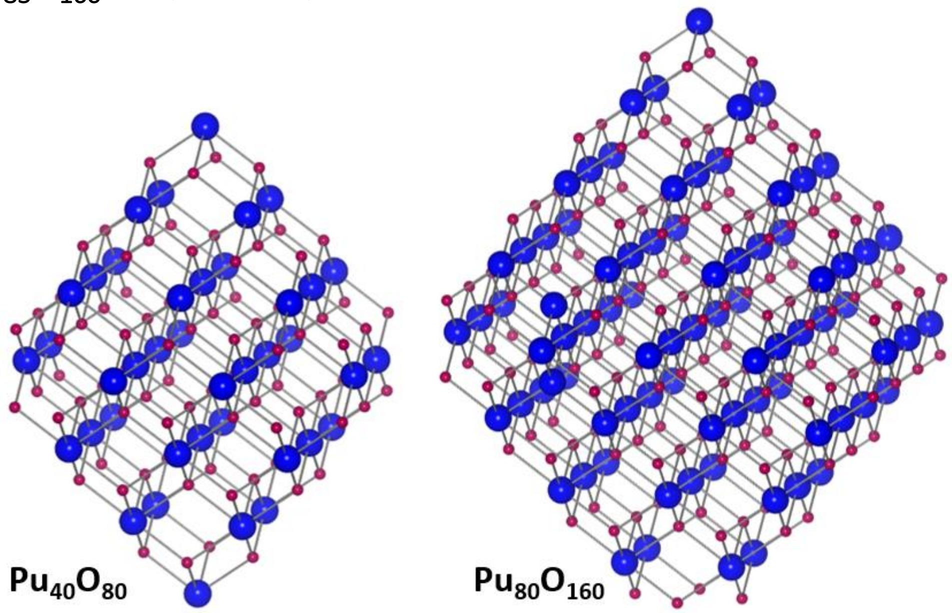

Methods

Computational details

VASP, with PBEsol + *U*

U = varied, J = 0 eV

The cut-off energy for the planewave basis set was 400 eV with reciprocal space summations performed at the Γ-point.

The influence of spin-orbit interaction (SOI) is considered in all simulations.

The minimum distance between the periodically repeating NPs is set at 1.5 nm.

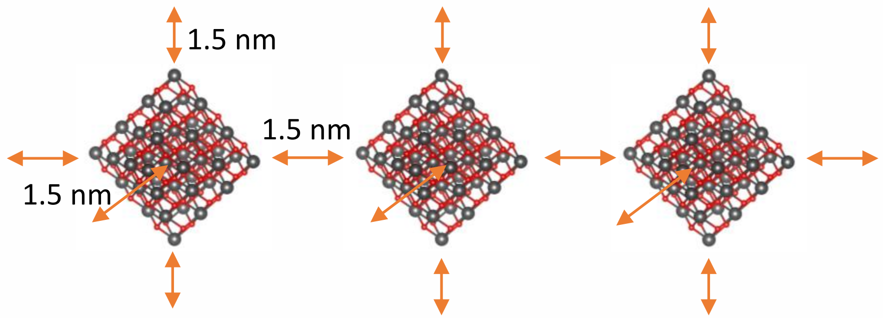

Results

Magnetism

- Using the $Pu_{44}O_{80}$ NP and PBEsol + U (U = 6 eV), we have found that DFT predicts that the longitudinal 3k antiferromagnetic (AFM) configuration remains the ground state when PuO_2 is in NP form.
- The longitudinal 3k AFM structure is maintained in the NP, albeit with some distortion in the direction of the surface Pu atoms magnetic moment.
- The fully-coordinated Pu atoms experience only very small distortion and effectively behave as bulk, longitudinal 3k AFM PuO_2.

Magnetic Configuration		Energy (eV per atom)	Relative energy (eV per atom)
Diamagnetic		-11.75	0.231
Antiferromagnetic			
Longitudinal	1k	-11.97	0.0146
	3k	-11.98	0.0

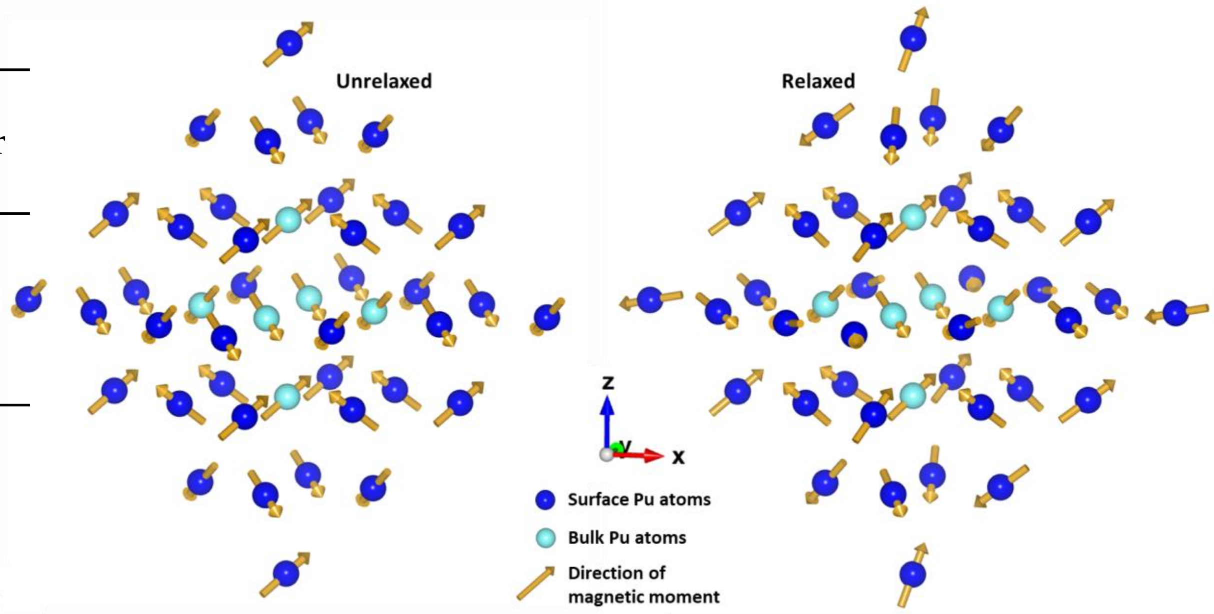

Results

Density of States

- The main characteristics of the DOS at U = 6 eV are retained between NPs of any size and bulk PuO_2: Pu(f) and O(p) bands do not hybridise.
- The NPs contain under-coordinated Pu and O ions that produce defective states in the DOS.
- O sites at the valence band and Pu sites at conduction band narrow the bandgap.
- The effect is reduced with increasing NP size.

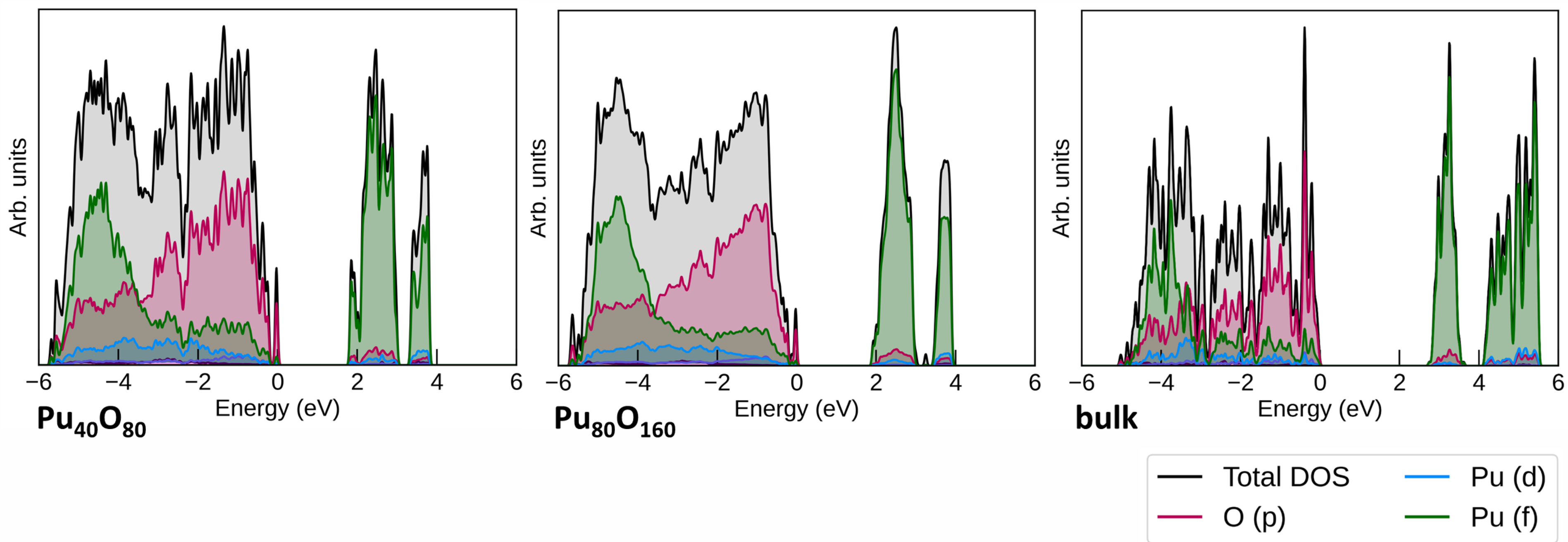

Results

Surface Structure

Formation energy of nanoparticle:

$$E_f = \frac{1}{n}E(Pu_nO_m) - E\left(Pu_{(s)}\right) - \frac{m}{n}E\left(O_{(g)}\right)$$

$E\left(O_{(g)}\right)$: Real gas temperature dependence

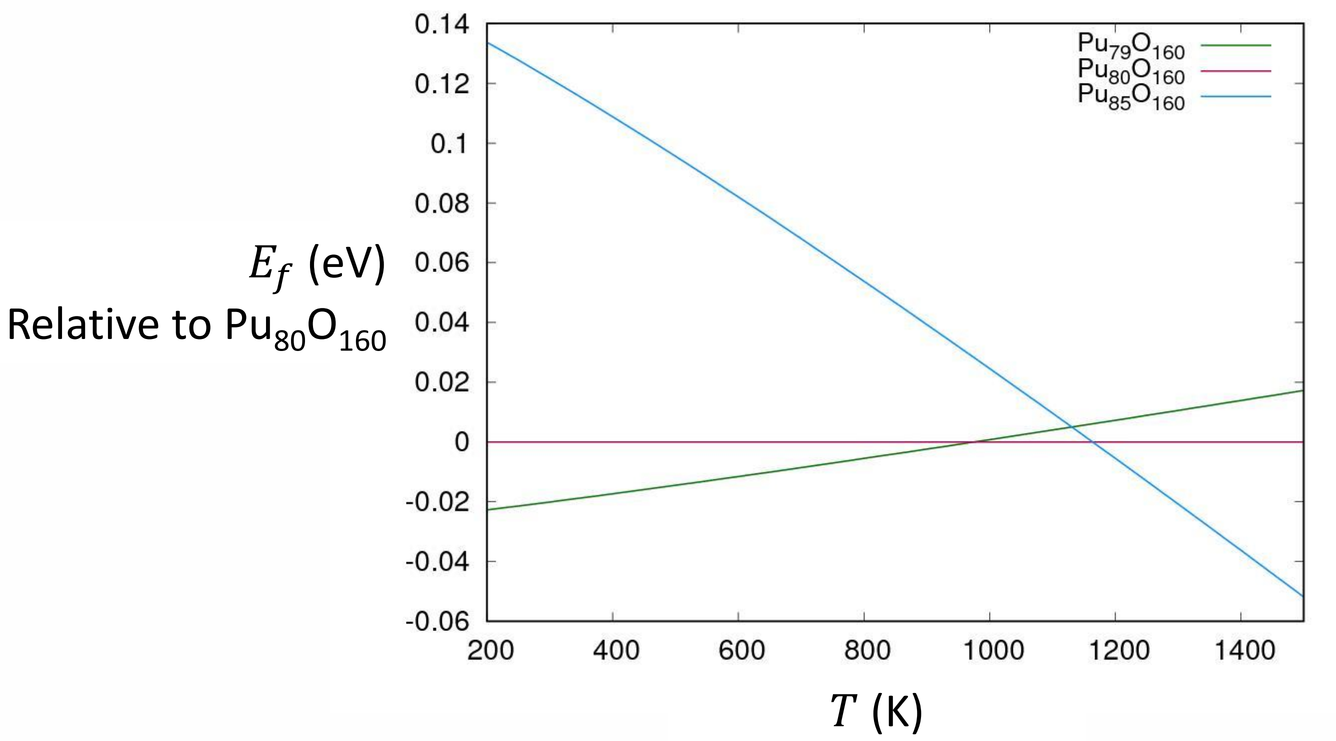

- NPs O-terminated (100) facets favourable at temperatures of interest.

Results

Oxidation state and bond length

- The NPs contain under-coordinated Pu and O atoms, due to their surface structure.
- Bader charge analysis is performed to analyse the DFT prediction of charge distribution.
- We find that, rather than reducing the surface and edge Pu atoms, it is predicted the reduced charge is 'smeared' throughout the particle, such that there is a clear prevailing Pu(IV) oxidation state.
- The exception to this is the corner atoms (1 atom in $Pu_{80}O_{160}$) which is predicted to be reduced to Pu(III). These atoms have a very low coordination number (CN) of 4.

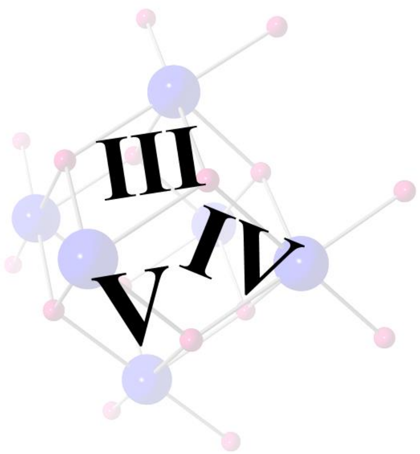

$Pu_{80}O_{160}$	Bulk	2.38-2.51
	Surface and Edge	2.35-2.49
	Corner	1.89
PuO_2		2.51
Pu_2O_3		1.97

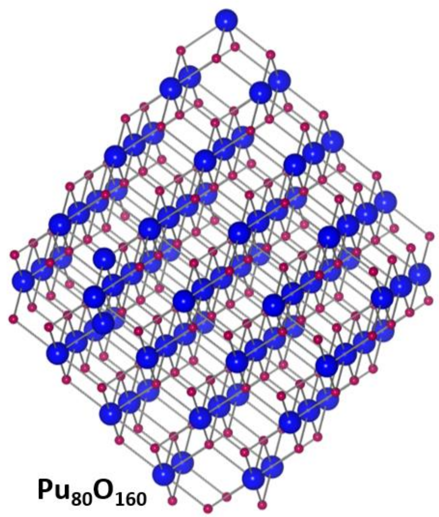

Results

Oxidation state and bond length (continued)

We can explain the result by looking at the Pu-O interaction in the first coordination sphere. Our DFT simulations point to the following:

- The 'bulk' Pu atoms, with CN of 8, have Pu-O bonds of 2.27 – 2.31 Å.
- Surface Pu atoms, with CN of 7, have Pu-O bonds of 2.28 – 2.34 Å.
  - Interestingly, this means that the O atoms that reside on the surface of the particle and are bonded to three Pu ions are not found to have a shortened bond length.
- Pu atoms found on the edges of the NP, with CN of 6, have Pu-O bonds of 2.16 – 2.38 Å.

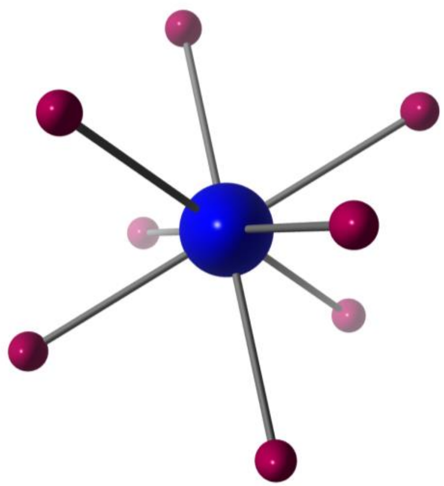

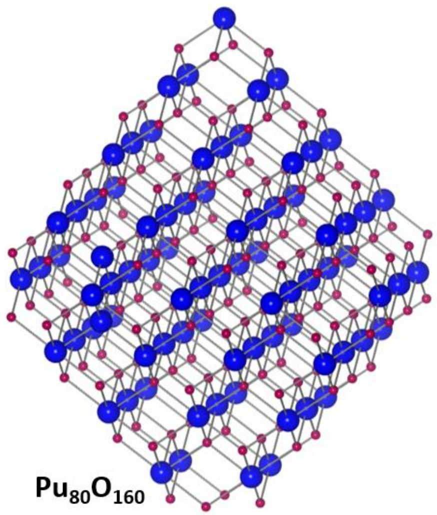

Results

Oxidation state and bond length (continued)

We can explain the result by looking at the Pu-O interaction in the first coordination sphere. Our DFT simulations point to the following:

- The ‘bulk’ Pu atoms, with CN of 8, have Pu-O bonds of 2.27 – 2.31 Å.
- Surface Pu atoms, with CN of 7, have Pu-O bonds of 2.28 – 2.34 Å.
  - Interestingly, this means that the O atoms that reside on the surface of the particle and are bonded to three Pu ions are not found to have a shortened bond length.
- Pu atoms found on the edges of the NP, with CN of 6, have Pu-O bonds of 2.16 – 2.38 Å.

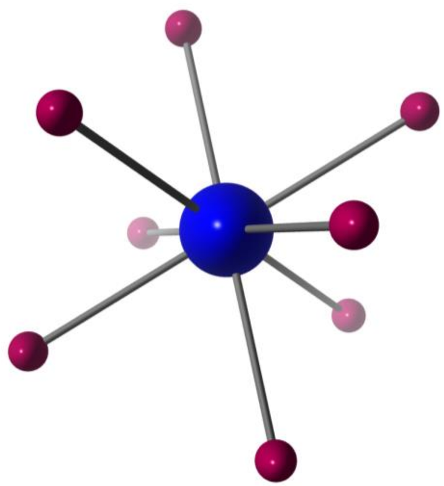

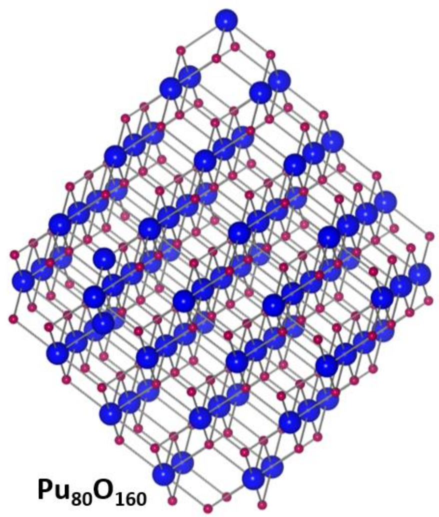

Discussion

- The under-coordinated Pu atoms at the surface are not reduced, instead the charge from fully coordinated Pu atoms is distributed by shortening their Pu-O bond length.
- Pu (V) not present in ‘pure’ NP; charge and bond length analysis confirm.
- Changes to the Pu-O bond length occur, but in an ‘orderly‘ fashion that, together with the other results, points to NPs with bulk-like PuO_2 character.
- The next step would be to introduce water to the model and observe it’s effect.

TRANSCEND

Transformative Science and Engineering for Nuclear Decommissioning

Acknowledgements

- Dr Helen Steele
- Lancaster University
- The High End Computing facility at Lancaster University.

Thank you

w.neilson@lancaster.ac.uk

Transformative Science and Engineering for Nuclear Decommissioning

Off-Gas Emissions From Vitrification of Nuclear Waste

Alex Stone, Sheffield Hallam University

Supervisory / Advisory Team: P. A. Bingham, D. McKendrick, S. Morgan, A. Holloway, A. Nabok

Transcend Theme Meeting 2020

14/11/2021
Transcend Annual Meeting
2021

For a Low Carbon Future

Transformative Science and Engineering for Nuclear Decommissioning

The Problem

- The UK has 133,000 m^3 of radioactive waste in storage and an estimated 4,420,000 m^3 arising in the future[1]
- A majority of this waste is from (or will arise from) site decommissioning and legacy (e.g. Sellafield, Magnox)
- Vitrification has been considered as a waste treatment technique for ILW as is already in use for HLW. This involves the heating of waste to high temperatures up to 1400°C which may volatilise some of the components of the waste[2]

1. NDA. (2020). *The 2019 Inventory*. NDA Department for Business, Energy and Industrial Strategy. https://ukinventory.nda.gov.uk/the-2019-inventory/2019-uk-data/
2. Caurant, D. (2009). *Glasses, glass-ceramics and ceramics for immobilization of highly radioactive nuclear wastes*. Nova Science Publishers, Inc.

Waste Survey

- ILW can be particularly problematic because it encompasses a wide range of materials
- High volume wastes of ILW classification:
  - Some Plutonium Contaminated Material (PCM)
  - SIXEP Sand/Clinoptilolite ion exchange material
  - Corroded Magnox Sludge (supplied by NNL/SL)

The Project

Develop technologies for real time emission monitoring

Establish techniques for reduction of emissions from melts

Create an off-gas system for measuring emissions and trial previous steps

Scale up and apply to industrial size vitrification tanks

Gaseous Components of interest

- Radionuclides (^{137}Cs, ^{129}I, ^{36}Cl, ^{99}Tc, ^{106}Ru, Pu)
  - Toxic to humans and the environment
  - Can accumulate in wildlife
  - Potential for contaminating groundwater
  - Non-active analogues can be used
- Organics (Dioxins, Furans, VOCs)
  - (Can be) Toxic to humans
  - Accelerates ozone decay
  - Produced from PVC and Wood decomposition
- CO, NOx, SO_2, O_2, H_2O

Exp... edure

- Gas is extracted ... nstant flowrate bubbling throug... te nitric acid or sodium hydroxi...
- Analysis of the ... ne flowrate gives a known average ...

3. Kim, D., & Kruger, A. A. (2018). Volatile species of technetium and rhenium during waste vitrification. Journal of Non-Crystalline Solids, 481(October 2017), 41–50. https://doi.org/10.1016/j.jnoncrysol.2017.10.013

Waste Loaded Glasses

Borosilicate (1400°C)

Magnesium Aluminosilicate (1400 °C)

Mixture Windscale (1150 °C)

SIXEP Sludge

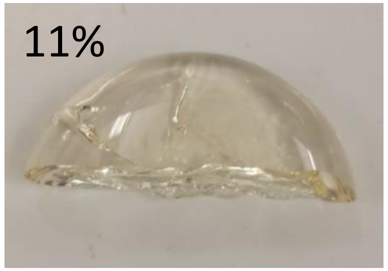

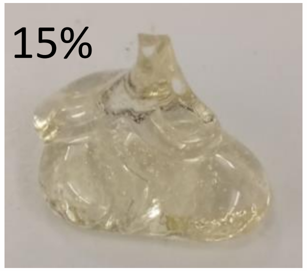

Clinoptilolite/Sand Mixture

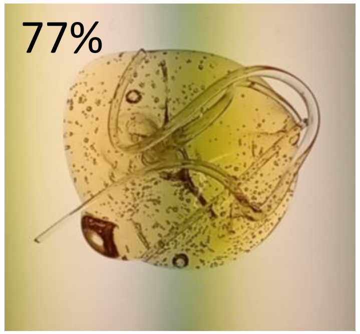

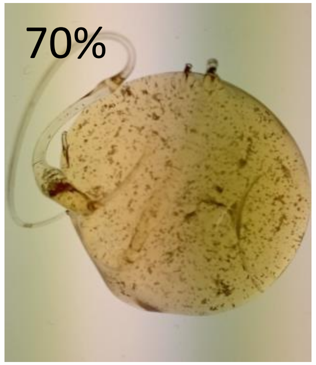

Waste Loading is indicated in the top left of the image and was selected to maximise WL for each glass. 2 hour melting time.

4. Cassingham, N. J., Corkhill, C. L., Stennett, M. C., Hand, R. J., & Hyatt, N. C. (2016). Alteration layer formation of Ca- and Zn-oxide bearing alkali borosilicate glasses for immobilisation of UK high level waste: A vapour hydration study. Journal of Nuclear Materials, 479, 639–646. https://doi.org/10.1016/j.jnucmat.2016.06.009

Waste Loaded Glasses

- Clinoptilolite/Sand Mixture Waste Loading 30 - 80wt% incorporated in MW (2hr melting time, 1150°C)

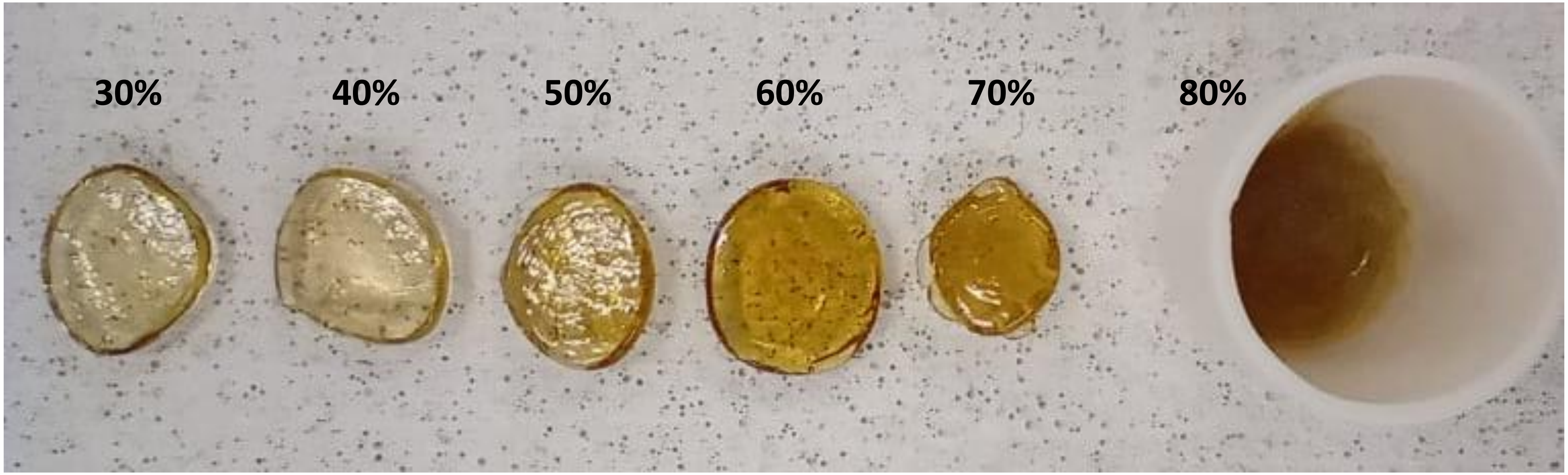

SiO_2	CaO	Al_2O_3	Fe_2O_3	K_2O	MgO
77.60%	4.10%	13.11%	1.47%	2.66%	1.06%

XRF Results from Clinoptilolite raw material

Uncertainty Experiments

- Water evaporation for collection of total mass

(Impinger mass change – Blank moisture) / crucible mass change x 100 = Mass Capture (%)

  - Average of 93% mass capture over 3 tests

- Glass hosted caesium capture stability
  - MW glass host, 1 wt% target Cs_2O in glass added as Cs_2CO_3
  - Mass loss of caesium was found to be 1.39% by collection in HNO_3/H_2O_2 with a standard deviation of 0.115% and error of +/- 0.066% over 3 tests

Capture Stability	Mass Loss	Standard Error	Standard Deviation
H_2O	93%	2.86	4.96
Cs	1.39%	0.066	0.115

Thermogravimetric Analysis

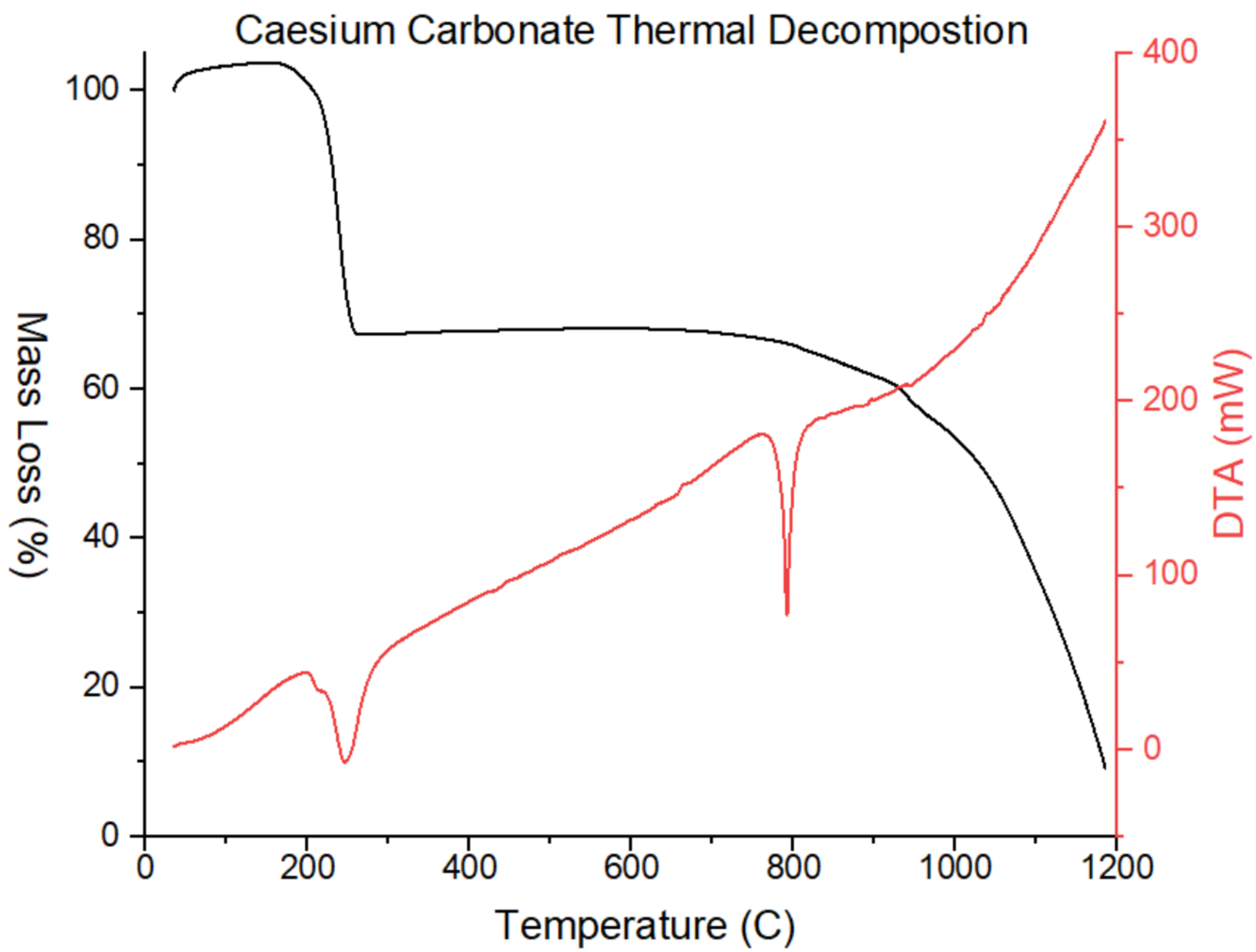

Tubing Depositions

- During monitoring of caesium containing materials small amounts of white deposits were found to present on the ‘hot’ tubing
- XRD of the deposit showed the material is likely to be boron hydroxide $B(OH)_3$ or another boron containing compound

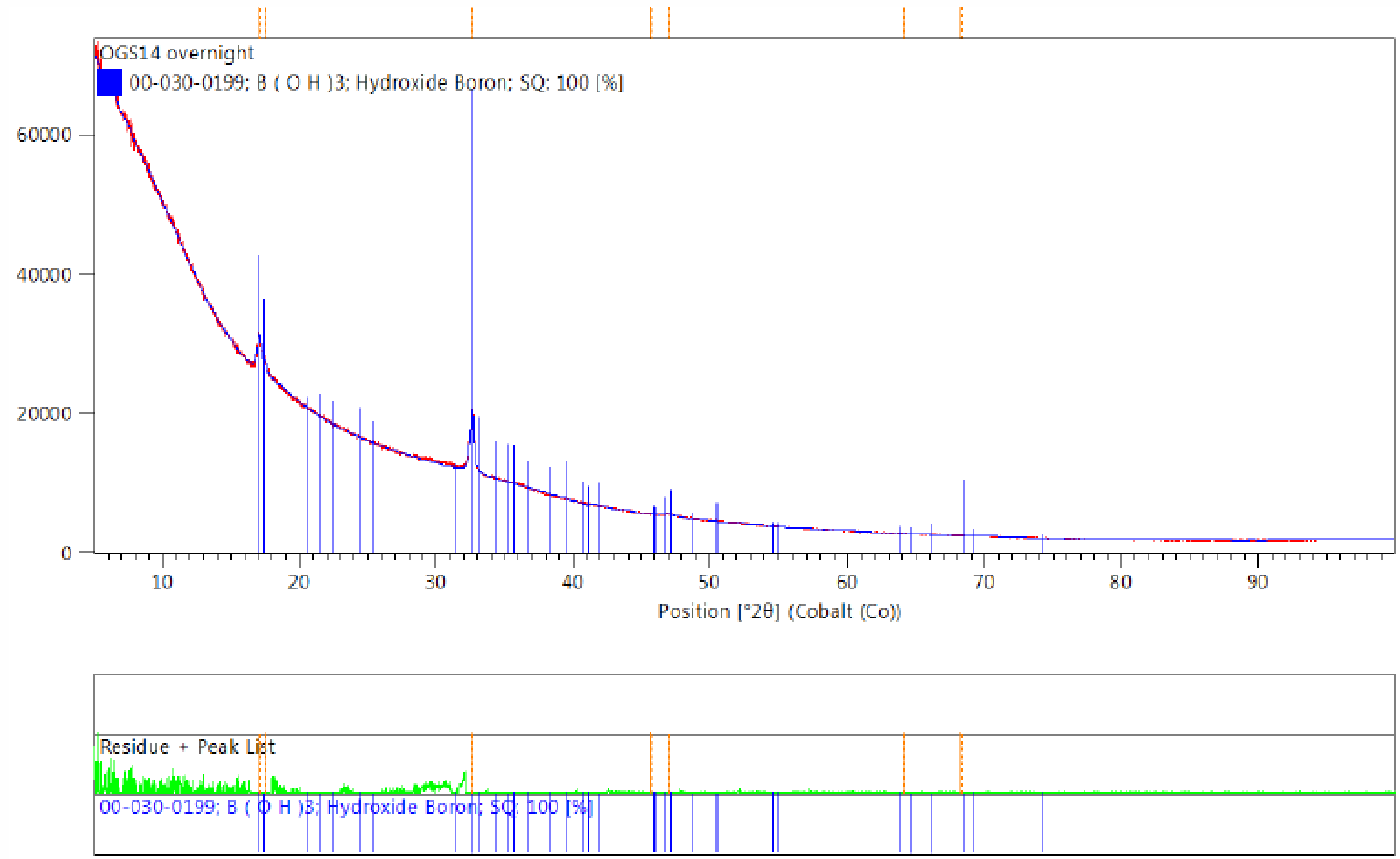

Chloride Volatilisation

	0wt% Chloride MW Glass (Blank) (ppm)			1wt% Chloride MW Glass (ppm)			2wt% Chloride MW Glass (ppm)		
	Cl	B	Na	Cl	B	Na	Cl	B	Na
Impinger Set 1 (0.7M HNO_3)	7	1	5	87	3	2	115	-	-
Impinger Set 2 (0.1M NaOH)	1	0	N/A	20	1	N/A	65	3	N/A
Tube Washes	5	0	2	144	11	107	312	-	-
Total	14	1	7	251	15	109	492	-	-

Conclusion and Future Work

- Capture stability and uncertainty experiments complete
- Waste loaded glasses compiled for Sand/Clino and CMS
- Real time monitoring (technology survey complete)
- Future waste/glass modifications to reduce emissions
  - Eg. WL, Melting Temperature, Graphite, ZnO, carbonates -> Oxides
- Capture and monitoring of other halides (F, Br, I), metals and organics

Raman gas probe. One of the real time analysis systems most promising for the target analytes.

References

1. NDA. (2020). *The 2019 Inventory*. NDA Department for Business, Energy and Industrial Strategy. https://ukinventory.nda.gov.uk/the-2019-inventory/2019-uk-data/

2. Caurant, D. (2009). *Glasses, glass-ceramics and ceramics for immobilization of highly radioactive nuclear wastes*. Nova Science Publishers, Inc.

3. Kim, D., & Kruger, A. A. (2018). Volatile species of technetium and rhenium during waste vitrification. Journal of Non-Crystalline Solids, 481(October 2017), 41–50. https://doi.org/10.1016/j.jnoncrysol.2017.10.013

4. Cassingham, N. J., Corkhill, C. L., Stennett, M. C., Hand, R. J., & Hyatt, N. C. (2016). Alteration layer formation of Ca- and Zn-oxide bearing alkali borosilicate glasses for immobilisation of UK high level waste: A vapour hydration study. Journal of Nuclear Materials, 479, 639–646. https://doi.org/10.1016/j.jnucmat.2016.06.009

Thank you

alex.h.stone@student.shu.ac.uk

Transformative Science and Engineering for Nuclear Decommissioning

In-situ Corrosion Test of Stress Corrosion Cracking using a Novel Small Punch Test Design

Kuo Yuan, University of Bristol

Ronald Clark, National Nuclear Laboratory

Mahmoud Mostafavi, University of Bristol

11th November 2021

Transcend Theme 3 Meeting

Background

Research topic : Development of micromechanical testing methods for spent AGR cladding to examine effects of sensitisation and stress corrosion cracking (SCC)

Aim: To develop a new small punch test setup for AGR cladding with surrogate material (thermally sensitised 304 stainless steel) that can initiate SCC of stainless steel in a short period time for DIC (Digital image correlation) observation

Fig. 1. Spent fuel pond at Sellafield[1]

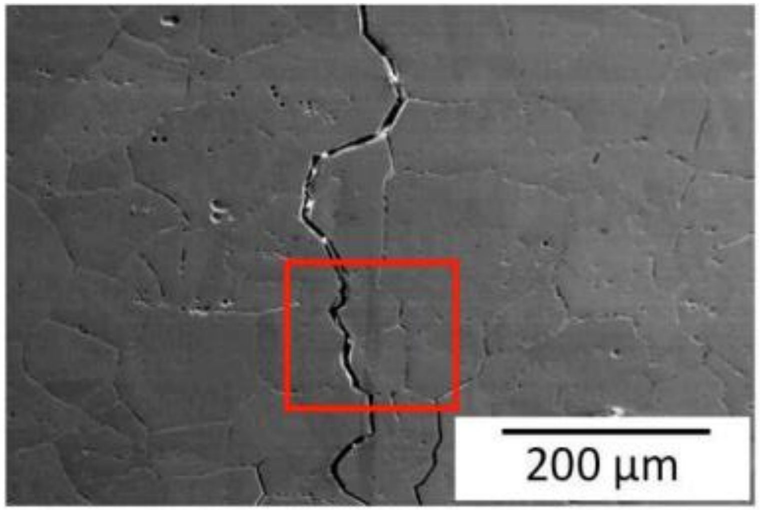

Fig. 2. SEM image of a stress corrosion crack; the crack initiation site is highlighted [2]

Background: Small Punch Test

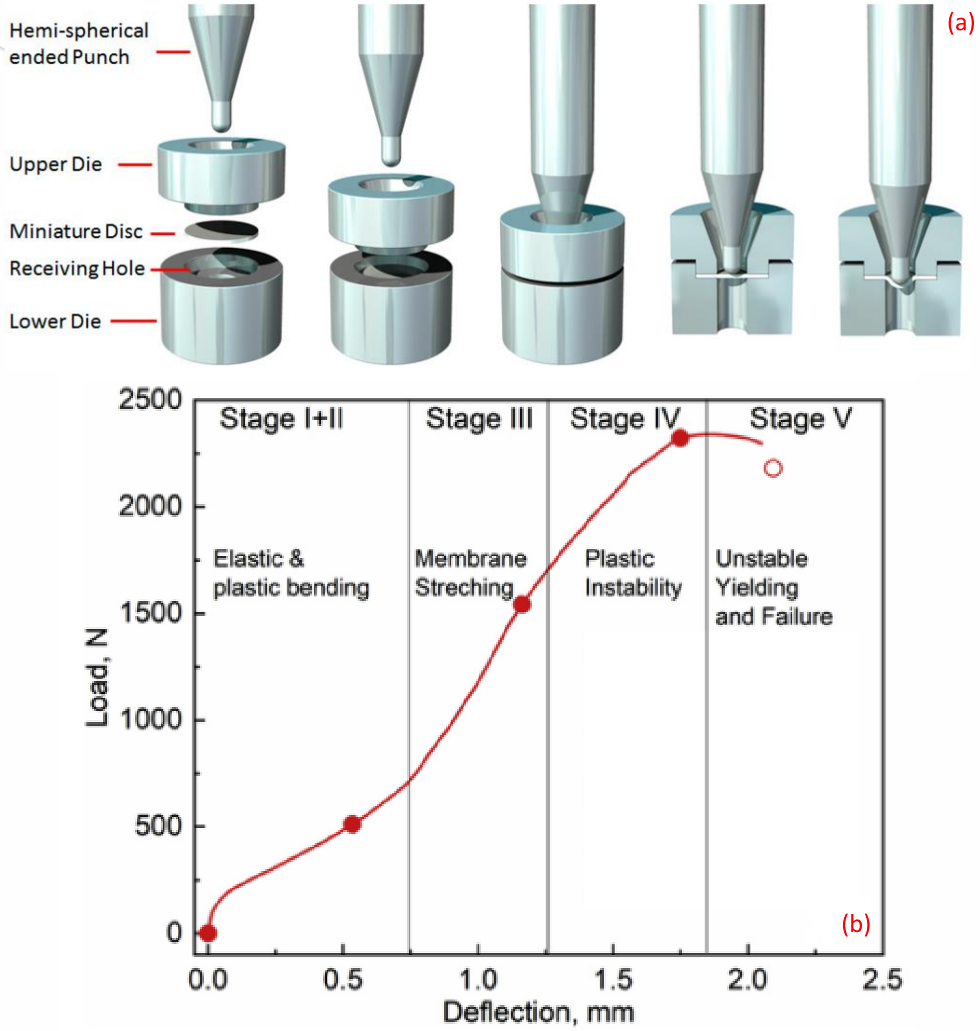

Fig. 3. (a) Schematic of SPT [3] and (b) a typical load vs deflection graph of SPT[4]

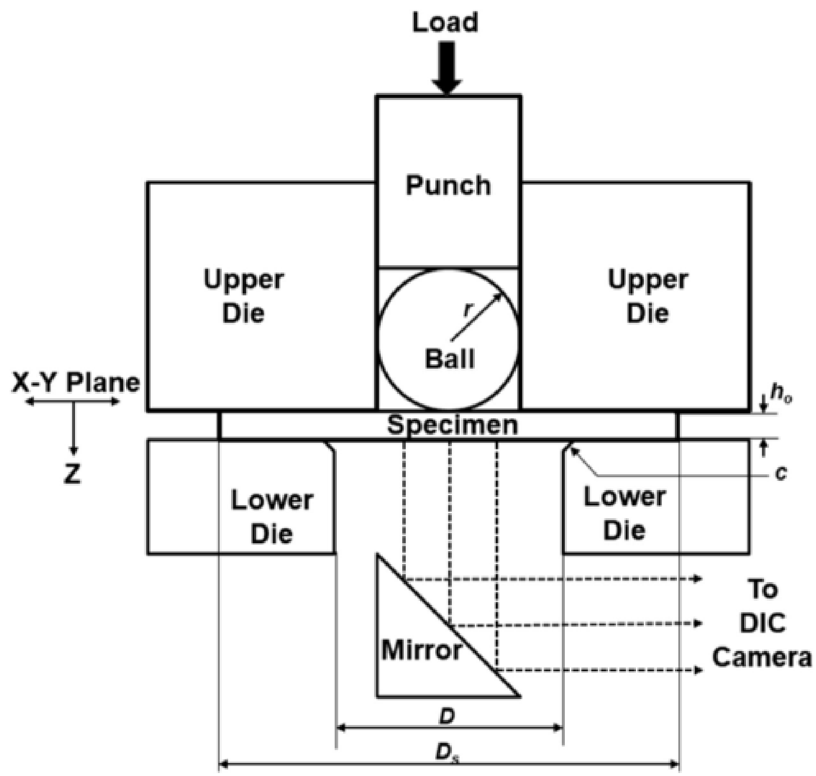

Fig. 4. The small punch test rig with a mirror to accommodate DIC[4]

- SPT only requires a small piece of material, so it is ideal for nuclear materials
- DIC can be implemented to monitor the deformation of the sample
- The environmental condition can also be introduced

New Design

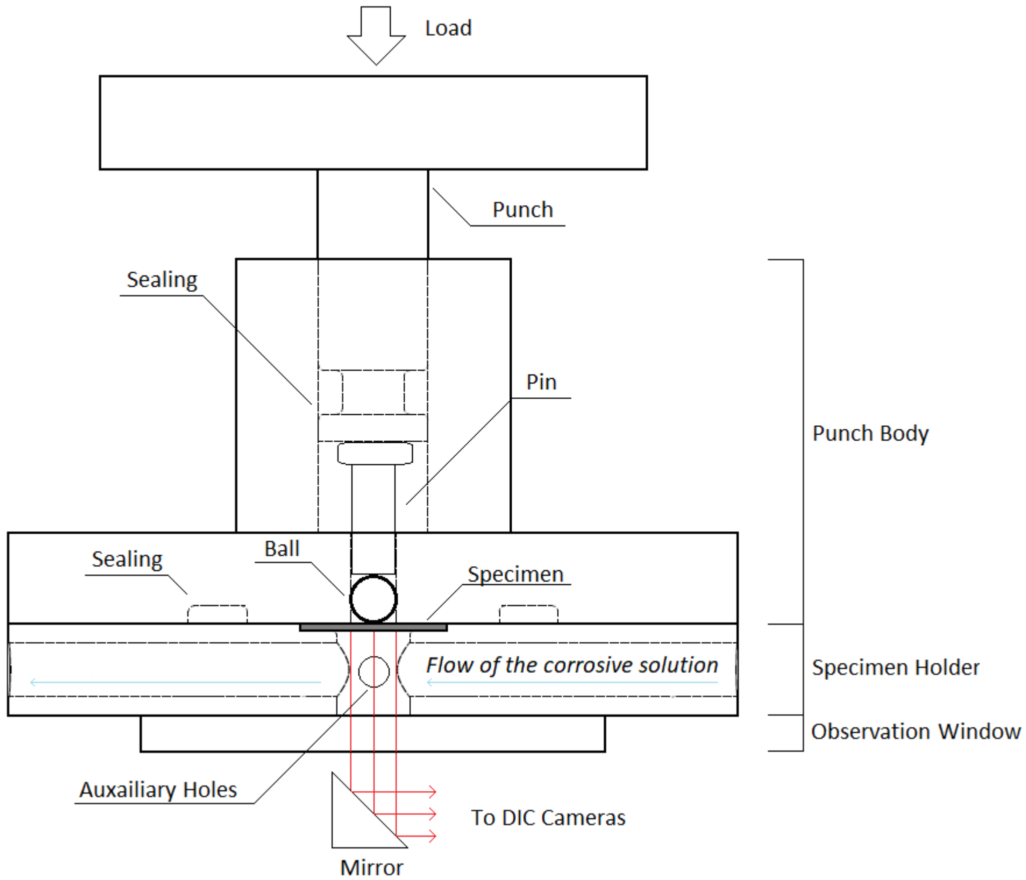

Fig. 5. Schematic of the new SPT design

Instead of applying the corrosive solution on the specimen [5] or submerged the whole rig into the solution [6], the new design allow a flow of corrosive solution to contact the sample to accelerate the initiation of cracking

- A ceramic ball (ø2.5 mm)
- A stainless steel pin (M2.5*8 mm)
- Disk specimen (ø8 mm* 0.5 mm)
- Sealed with O-rings around the punch and between the punch body and the specimen holder
- A window is placed below the specimen holder for DIC observation
- Two auxiliary holes for thermocouples or electrodes to connect to a potentiostat.

New Design

Fig. 6. Image of the small punch test assembly

Testing Setup: loading machine

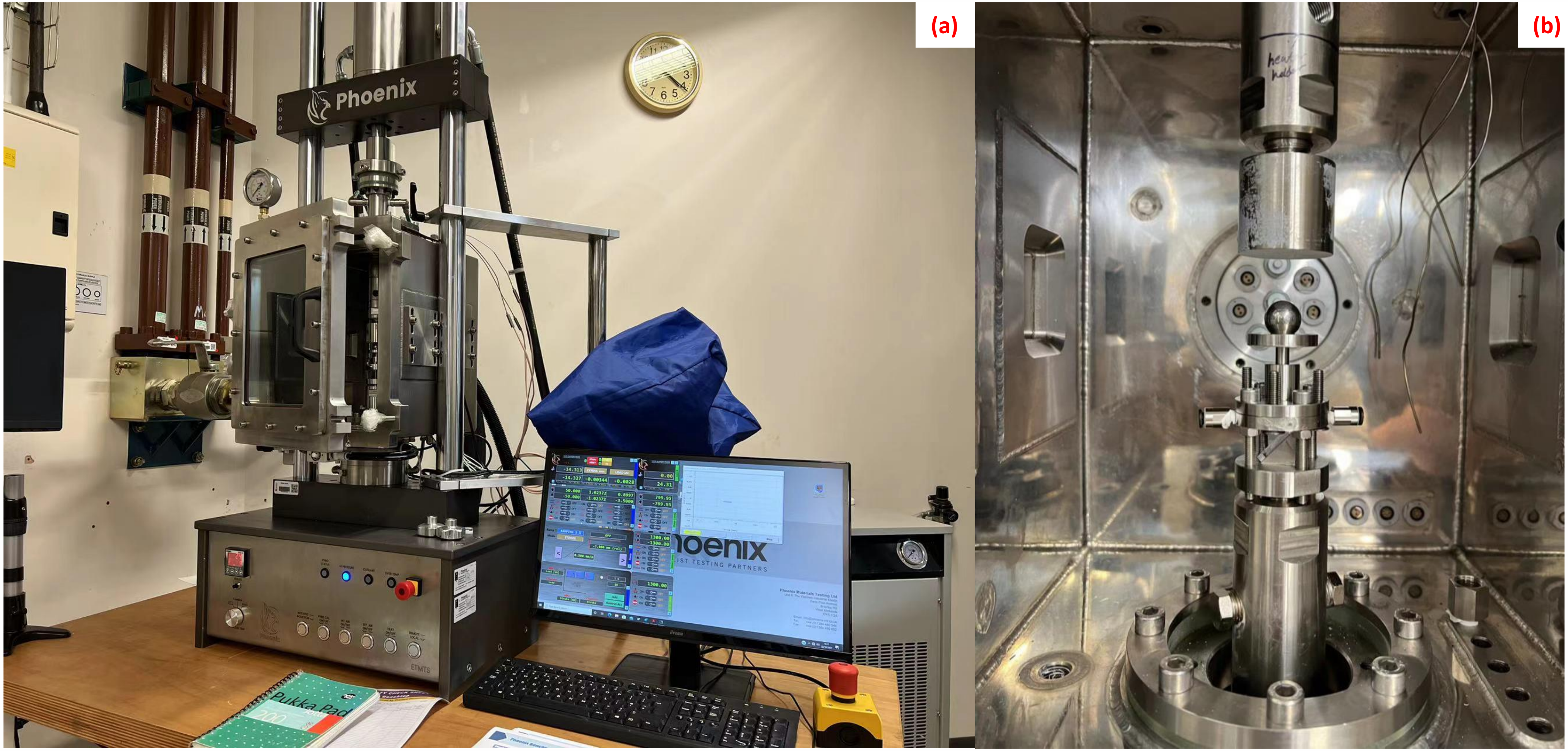

Fig. 7. (a) Phoenix testing machine and (b) the rig in the testing chamber

Testing Setup: Loop

The corrosive solution is heated in the heating bath (bottom left) and extracted by a small pump (centre of the image, powered by a DC supply to the left) to the SPT rig and circulated back to the heater to form a circulation. The tube to the rig is wrapped with insulating materials.

Fig. 8. The circulation system of the corrosion SPT

Corrosive solution

Fig. 9. Self loading tensile sample

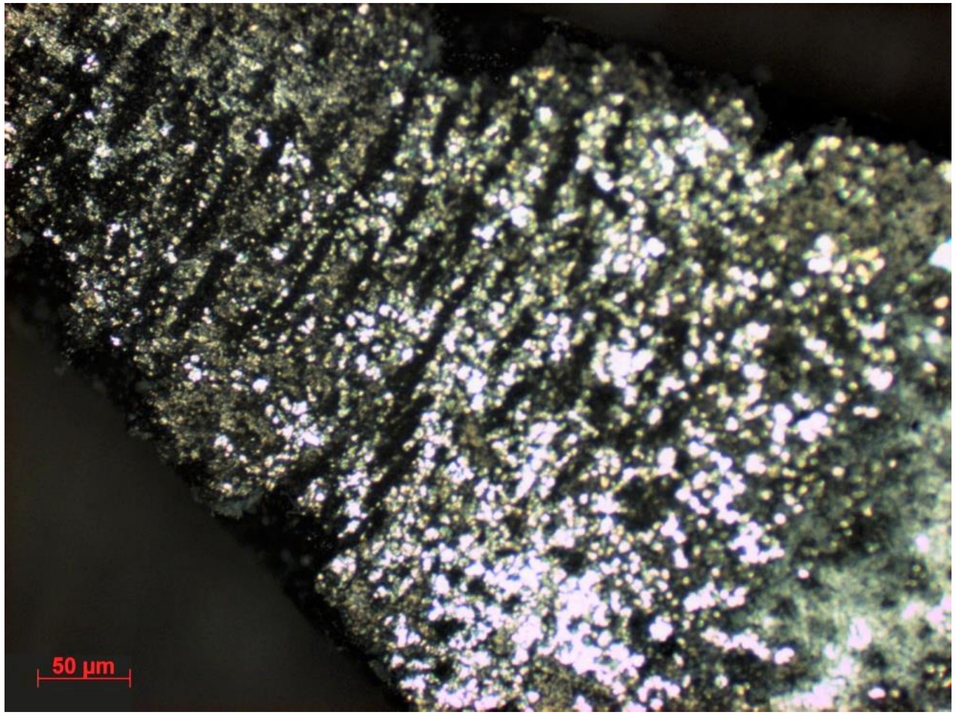

Fig. 10. Stress corrosion cracks on the surface of the sample

Trial experiment: Thermally sensitised (ageing at 600 °C for 50 hours) 304 stainless steel tensile samples were loaded to yield and placed in 1000 ppm sodium thiosulphate solution with 2 drops 37% HCl solution [7],[8] and heated to 80 °C. SCCs successfully developed in 7 hours.

Small Punch Tests:Trial

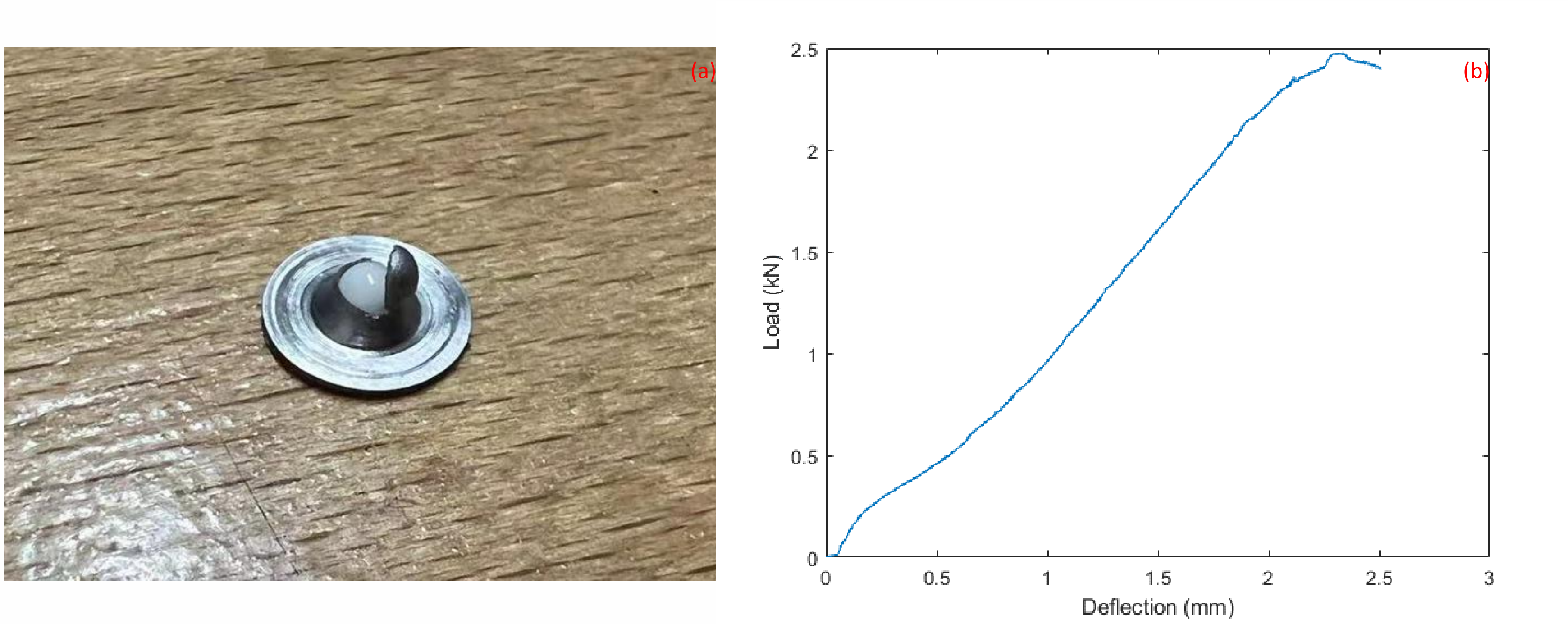

Fig. 11. (a) SPT failed sample and (b) load and deflection graph of a trial test

A few trial tests were carried out under displacement control to find the ultimate load of failure was ~2.5 kN, and for the next corrosion SPT, a load of 1.5 kN was chosen to avoid plastic instability.

Small Punch Tests: Corrosion test

Fig. 12. Corrosion SPT setup

One thermally sensitised (ageing at 600 °C for 50 hours) 304 stainless steel specimen was loaded at 1.5 kN for 6.5 hours, and 395 ppm sodium thiosulphate solution [7] (milder solution to avoid pitting and potential damage to the equipment) was heated to 80 °C (60 °C at the specimen) and pumped in the loop to accelerate corrosion.

Small Punch Tests: Corrosion test

Fig. 13. Corrosion SPT sample

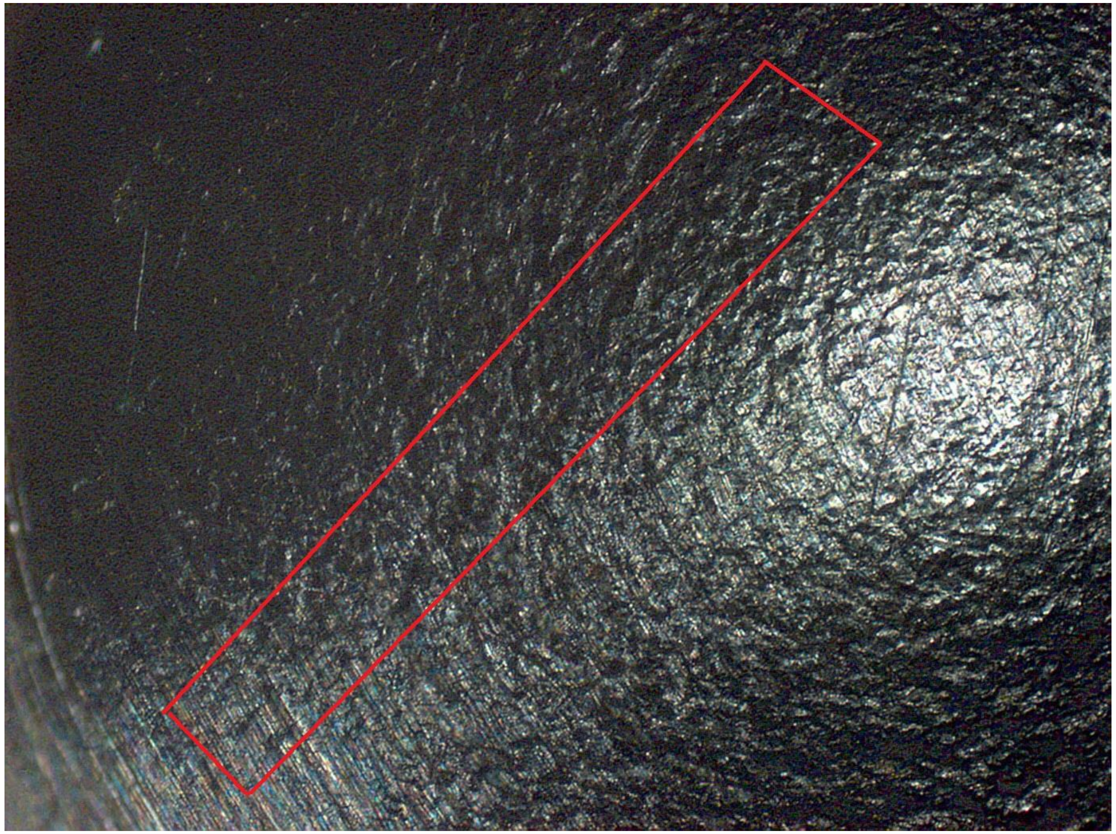

Fig. 14. A crack on the surface of the sample

After 6.5 hours of loading, one large but shallow crack was observed under the microscope.

Small Punch Tests: Comparison

Fig. 15. SPT sample without the solution

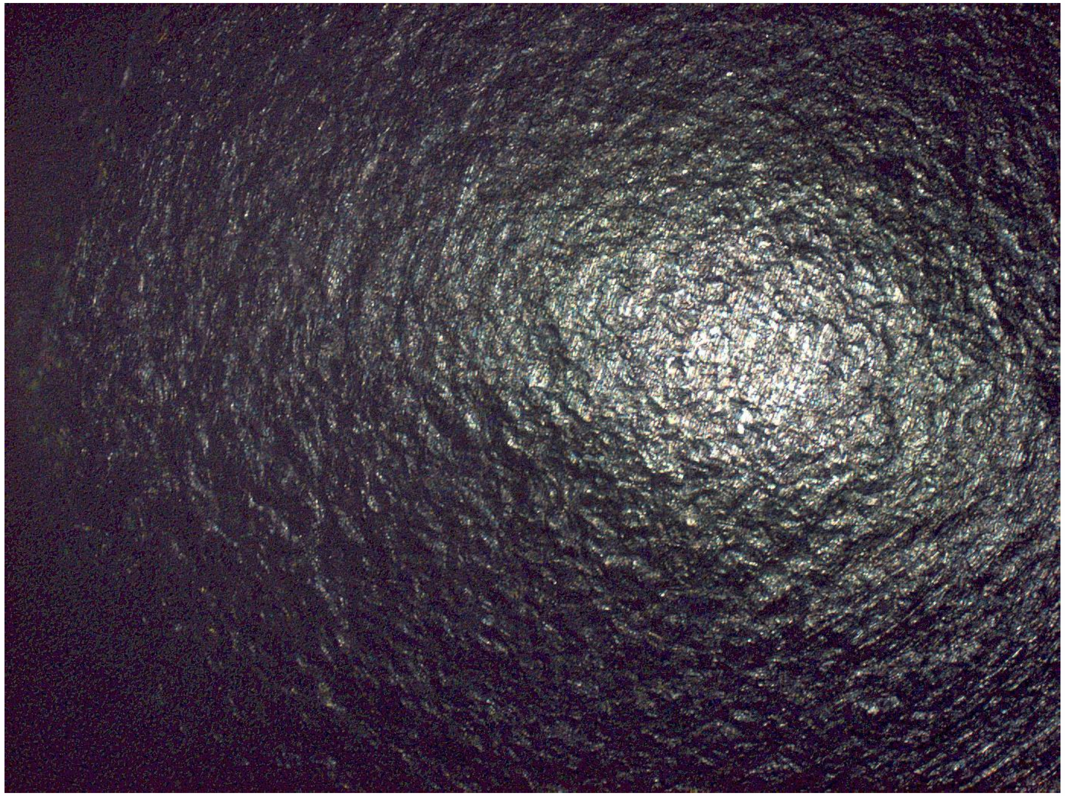

Fig. 16. Surface of the SPT sample without the solution

To compare the effect of the solution, a specimen was tested under the same loading condition and period but without the solution. No crack was observed on the surface.

Conclusions and Plans

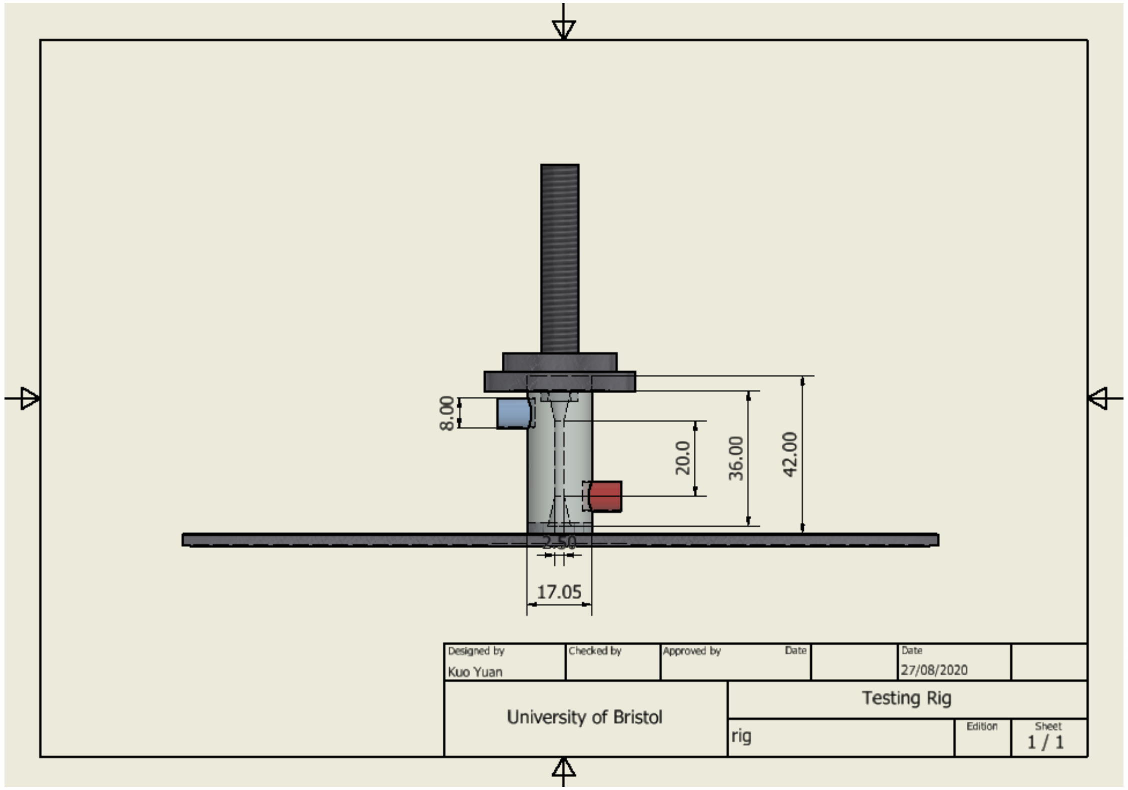

Fig. 17. Schematic of the tensile rig for corrosion test under the synchrotron light source

SCC successfully initiated and observed in the corrosive solution under a constant load using the new SPT setup.

- The tested sample will be better study under the SEM.
- More tests will be done to find the relationship between the size and number of cracks with the combination of loading and solution concentration.
- DIC will be added to the system to monitor the cracks in real time.
- Similar corrosion tests under synchrotron light source is proposed to compare surface SCC and 3D behaviours of SCC.

TRANSCEND

Transformative Science and Engineering for Nuclear Decommissioning

References:

[1] GOV, UK (2017), *Sellafield Ltd. Annual Review of Performance 2016/17*, https://www.gov.uk/government/publications/annual-review-of-performance-201617/annual-review-of-performance-201617 (Accessed 01/11/2021)

[2]Stratulat, A., Duff, J., Marrow, J. (2014), Grain boundary structure and intergranular stress corrosion crack initiation in high temperature water of a thermally sensitised austenitic stainless steel, observed in situ, *Corrosion Science*, 85, 428-435

[3] R. Lancaster, G. Davies, H. Illsley, S. Jeffs, and G. Baxter, "Structural Integrity of an Electron Beam Melted Titanium Alloy," Materials , vol. 9, no. 6. 2016.

[4] V. D. Vijayanand *et al.*, "A novel methodology for estimating tensile properties in a small punch test employing in-situ DIC based deflection mapping," *J. Nucl. Mater.*, p. 152260, 2020, doi: 10.1016/j.jnucmat.2020.152260.

[5] J. Isselin, A. Kai, K. Sakaguchi, and T. Shoji, "Assessment of the effects of cold work on crack initiation in a light water environment using the small-punch test," Metall. Mater. Trans. A Phys. Metall. Mater. Sci., vol. 39 A, no. 5, pp. 1099–1108, 2008, doi: 10.1007/s11661-008-9492-7.

[6] T. Bai and K. Guan, "Evaluation of stress corrosion cracking susceptibility of nanocrystallized stainless steel 304L welded joint by small punch test," Mater. Des., vol. 52, pp. 849–860, 2013, doi: 10.1016/j.matdes.2013.06.019.

[7] S. Moore et al., "Observation of stress corrosion cracking using real-time in situ high-speed atomic force microscopy and correlative techniques," npj Mater. Degrad., vol. 5, no. 1, p. 3, 2021, doi: 10.1038/s41529-020-00149-y.

[8] G. O. H. Whillock, B. J. Hands, T. P. Majchrowski, and D. I. Hambley, "Investigation of thermally sensitised stainless steels as analogues for spent AGR fuel cladding to test a corrosion inhibitor for intergranular stress corrosion cracking," J. Nucl. Mater., 2018, doi: 10.1016/j.jnucmat.2017.10.017.

Thank you

k.yuan@bristol.ac.uk

University of BRISTOL

NATIONAL NUCLEAR LABORATORY